

*Dissertation*

**On magnetic compass orientation in coral reef fish larvae and  
On the sensitivity to polarized light in birds**

von der Fakultät für Mathematik und Naturwissenschaften  
der Carl von Ossietzky Universität Oldenburg  
zur Erlangung des Grades und Titels eines  
Doktors der Naturwissenschaften (Dr. rer. nat.)  
angenommene Dissertation von Herrn

**Michael Peter Georg Bottesch, Diplom Biologe**

geboren am 24.08.1984 in Landshut

Erstgutachter: Prof. Dr. Henrik Mouritsen

Zweitgutachter: Prof. Dr. Michael Winklhofer

Tag der Disputation: 25. August 2021

# Contents

<b>Summary</b> .....	<b>5</b>
<b>Zusammenfassung</b> .....	<b>8</b>
<b>1. Introduction to vertebrate orientation behavior</b> .....	<b>12</b>
1.1. Bird migration .....	12
1.2. Dispersal and natal homing in coral reef fish larvae .....	13
1.3. Strategies in orientation behavior .....	14
1.3.1. Orientation and Navigation .....	15
1.4. Compass orientation .....	19
1.4.1. Sun compass orientation .....	20
1.4.2. Star compass orientation.....	22
1.4.3. Magnetic compass orientation .....	24
1.4.4. Calibration of celestial and magnetic compasses in birds .....	30
1.5. Aims of my Ph.D. thesis .....	34
<b>2. Magnetic compass orientation in coral reef fish larvae</b> .....	<b>36</b>
2.1. Experimental procedures.....	40
<b>3. Orientation by skylight polarization patterns</b> .....	<b>46</b>
3.1. Polarized light in nature and its biological use .....	46
3.2. Sensory basis for polarized light sensitivity .....	49
3.3. The question of polarized light sensitivity in birds .....	51
3.4. Are retinal ganglion cells encoding the e-vector of linearly polarized light in birds?.....	56
3.4.1. Multi-electrode recordings from retinal ganglion cells .....	56
3.4.2. Methods of the experiments of Schneider and Dreyer et al. (2014, unpublished), replicated in the experiments of Dr. Arndt Meyer and me .....	58
3.4.3. Results of the experiments of Schneider and Dreyer et al. (2014, unpublished) .....	65
3.4.4. Methods and results of the follow-up experiments of Dr. Arndt Meyer and me.....	68
3.4.5. Concluding remarks.....	93
3.5. Seen in a different light - No evidence for polarization vision in songbirds in a novel behavioral approach.....	97
3.5.1. Introduction .....	98
3.5.2. Material and Methods.....	100

3.5.3. Results.....	110
3.5.4. Discussion.....	124
<b>4. Conclusions and Outlook .....</b>	<b>128</b>
4.1. Closing the lid – A novel optical property of the third eye lid in birds and its implications for a potential polarization sensor .....	132
<b>5. Own contributions.....</b>	<b>135</b>
<b>6. References .....</b>	<b>137</b>
<b>Appendix .....</b>	<b>160</b>
<b>Curriculum Vitae.....</b>	<b>165</b>
<b>Danksagung .....</b>	<b>169</b>
<b>Erklärung gemäß § 11 der Promotionsordnung .....</b>	<b>171</b>

## Summary

Every year billions of vertebrates travel over considerable distances to find the best habitat for development, breeding or overwintering. Using all their senses for orientation they find their destination with often surprising acuity. The ecological settings in which vertebrates, e.g. coral reef fish larvae and migratory songbirds, extract directional information for their journeys differ strongly. Nevertheless, research over the past decades demonstrated that a set of common orientation mechanisms seemed to govern local movement patterns as well as long-distance migration across vertebrate groups in very similar ways.

In this thesis, I presented a comprehensive overview on the theories on orientation and on the compasses and map senses used in vertebrate orientation. My own experiments aimed to provide new insights on the compass systems used by two vertebrate species with very distinctive orientational needs - migratory songbirds and coral reef fish larvae.

Coral reef fish larvae have previously been shown to distinguish site-specific odors, as well as visual and auditory cues that enable them to pinpoint their natal reef after weeks of dispersal. In the Capricorn bunker reef group (Great Barrier Reef, Australia), ocean currents can drift the pelagic larvae over tens of kilometers. At these distances from home, long-scaled compass cues are needed to return to the vicinity of a reef. At daytime, the sun and sun-related cues can provide reliable directional information. At night, the reef fish larvae need continuous directional information as well. The most reliable directional reference at night is the geomagnetic field. Colleagues and I studied whether settlement-stage coral reef fish *Ostorhynchus doederleini* larvae have the sensory capability of using a geomagnetic compass. In orientation bowls without access to any celestial cues, the tested larvae were able to maintain their directional headings at night comparable to their daytime orientation, but in the presence of the geomagnetic field at night only. Upon an experimental turn of the magnetic field's horizontal component, the same sample of larvae changed their orientation according to the changed magnetic north. These results demonstrated for the first time that coral reef fish larvae can orient by a magnetic compass at night which might help them to return to their natal reef.

A major part of my PhD thesis was dedicated to the question whether polarized light sensitivity in birds exists. A vast body of behavioral data on the influence of skylight polarization patterns on directional choices of migratory birds has been published over the last decades.

Nevertheless, this sensory capability is still strongly debated because classical behavioral tests were prone to biases by light reflection artifacts. Furthermore, anatomical evidence for a receptive mechanism has not been found in birds and all well-controlled studies on avian polarization sensitivity in laboratory-based discrimination tasks revealed negative evidence. I used two separate approaches aiming to prove polarization sensitivity in birds:

In a first approach, former colleagues of mine found that a subset of retinal ganglion cells in chicken responded bimodally to 360° turns of a polarizer in extracellular recordings from the ganglion cell layer of dissected retinal pieces. Inevitably occurring light intensity changes upon the rotation of a polarizer were carefully measured and intentionally included in the stimulation protocol as a control against light reflection artifacts. Conservative post-recording analysis criteria were set to vigorously remove false-positive responses from the data. The described study resulted in several strong indicators for true polarization sensitivity and allowed a high level of confidence in the validity of the data.

After tuition by the original authors, I was able to replicate these results with my colleague Dr. Arndt Meyer using the identical setup as the original authors. Additionally, we extended the light intensity measurements, and we visualized the structural integrity of the retinal pieces after recording, with a focus on the potential for photoreceptor outer segment tilt. Our follow-up experiments uncovered i) potentially critical sources of artificially introduced light intensity changes much stronger than originally controlled for, and ii) strong photoreceptor outer segment tilt at the recording sites caused by structural damage to the tissue that could theoretically allow for artificial polarization sensitivity by transverse dichroism in vertebrate photoreceptors. Based on these results and some indicators from more unsystematic experiments, alternative explanations to the above-stated indicators for polarization sensitivity from the original study could be given that were, however, not based on natural polarization sensitivity. In conclusion, the recorded cell responses might either originate from ganglion cells that encode the e-vector of incident polarized light, or might be caused by a number of potential artifacts caused by unwanted light reflections, loss of the shielding function of the pigment epithelium, photoreceptor tilt and/or impaired functionality of the retinal circuits, or all of the above. However, our experiments did put the “minimum bar” for control procedures up very high that should be met by any future study that claimed evidence for polarization sensitivity in birds.

In a second approach, I established and used a behavioral setup to investigate polarization vision in birds in our lab that was not prone to light intensity artifacts. Using modified LCD monitor screens, I subjected three songbird species in a virtual arena to moving gratings that evoked optomotor responses in luminance contrast. Furthermore, I presented birds with a looming stimulus that mimicked a fast approaching object to trigger escape behavior in the tested birds. After removal of the front polarizers of the LCD monitor screens, the stimuli were presented in polarization contrast, i.e. the stimuli were only visible to subjects with a polarization sensitive visual system, but invisible to the unaided human eye. If birds would possess a polarization sensitive visual system, I would have expected comparable responses to the two stimuli when presented in luminance contrast and in polarization contrast. As a result, I found strong and stable responses to both stimuli in luminance contrast, but no responses (looming stimulus) or no responses that were above a measured baseline of head activity (moving gratings) when presented in polarization contrast upon the removal of the front polarizers of the screens. Therefore, neither the stabilization of visual flow (optomotor responses to moving gratings) nor object recognition (escape behavior as a response to a looming stimulus) can be linked to the birds' potential capability of perceiving polarized light. The most viable interpretation of my results was that the tested songbirds did not possess polarization vision, and most probably do not possess polarization sensitivity at all.

To conclude, my PhD thesis revealed novel findings in the major compass systems of two vertebrate groups. In coral reef fish, I demonstrated that *O. doederleini* larvae possess a magnetic compass that might help them return to their natal reefs. In my main projects, I described why an invasive electrophysiological approach was unfit to unequivocally demonstrate polarization sensitivity in domestic chicken and in three songbird species, I was able to experimentally suggest the inability of birds to detect polarized light information.

In the outlook of this thesis, I will present a so far undescribed novel optical property of the third eye lid in birds, the nictitating membrane. During my PhD, I discovered that the nictitating membrane in birds was highly birefringent and would modify the vibrational properties of polarized light in a complex manner. I will elaborate the potential implications of my discovery for a completely novel view on the potential polarized light sensitivity in birds, which I would like to subject to experimental investigation in my future scientific career.

## Zusammenfassung

Jahr für Jahr überwinden Milliarden Wirbeltiere beachtliche Entfernungen, um das optimale Habitat für ihre Entwicklung, zur Jungenaufzucht oder Überwinterung zu finden. Mit Hilfe all ihrer Sinne finden sie ihr Ziel mit bisweilen beeindruckender Zielgenauigkeit. Die ökologischen Rahmenbedingungen, in denen Wirbeltiere, wie zum Beispiel Korallenriffische und Zugvögel, Informationen über ihre Zielrichtung extrahieren, unterscheiden sich stark. Nichts desto trotz zeigte die Forschung der vergangenen Jahrzehnte, dass ein gemeinsamer Grundstock an Orientierungsmechanismen sowohl bei lokalen Bewegungsmustern, wie auch bei Migration über weite Strecken, eine übergeordnete Rolle für verschiedenste Wirbeltiergruppen auf sehr ähnliche Weise spielt.

In dieser Doktorarbeit präsentiere ich eine allgemeinverständliche Zusammenfassung über die Orientierungstheorien und über die Kompass- und die Kartensinne, die von Wirbeltieren zur Orientierung verwendet werden. Meine eigenen Experimente zielten darauf ab, neue Erkenntnisse über die Kompasssysteme von zwei Wirbeltiergruppen mit sehr unterschiedlichen Orientierungsbedürfnissen zu liefern, nämlich die von Zugvögeln und von Korallenriffischlarven.

In früheren Studien wurde bereits gezeigt, dass Korallenriffische ortsspezifische Gerüche und visuelle sowie auch auditorische Hinweise unterscheiden können, die ihnen nach mehrwöchiger Verbreitungsphase dabei helfen können, ihr Heimatriff zu identifizieren. In Capricornia, einer Riffgruppe im Great Barrier Reef, Australien, vermögen die Strömungen des Ozeans die pelagischen Larven über ein Mehrfaches von 10 Kilometern fortzutragen. Angesichts dieser Entfernungen vom Heimatriff sind Orientierungshilfen von Nöten, die auch über weitere Distanzen verlässlich sind, um in die Nähe eines Riffes zurückzukehren. Am Tag kann die Sonne, sowie von der Sonne abhängige Richtungsweiser, zuverlässige Richtungsinformation liefern. Doch auch nachts benötigen die Korallenriffischlarven durchgehenden Zugang zu Richtungsinformationen. Die zuverlässigste Quelle für Richtungsinformationen bei Nacht ist das Erdmagnetfeld. Meine Kollegen und ich untersuchten, ob Korallenriffischlarven der Art *Ostorhynchus doederleini*, die sich im Stadium der Wiederansiedlung befanden, die sensorische Fähigkeit besaßen, das Erdmagnetfeld als Kompass zu nutzen. In Orientierungsschalen bei Nacht waren die getesteten Larven in der Lage, sich ausschließlich mit Hilfe des Erdmagnetfeldes für vergleichbare Richtungen zu entscheiden wie zuvor am Tag.



Sobald die horizontale Komponente des Erdmagnetfeldes in einem experimentellen Ansatz gedreht wurde, orientierte sich die getestete Gruppe von Larven in Übereinstimmung zum experimentellen neuen Norden um. Mit diesen Ergebnissen konnten wir als Erste zeigen, dass sich Korallenriffische mit Hilfe eines geomagnetischen Kompasses bei Nacht orientieren können. Dies könnte sie dabei unterstützen, zu Ihrem Heimatriff zurückzukehren.

Der Hauptteil meiner Doktorarbeit war der Frage gewidmet, ob die Sensitivität für polarisiertes Licht in Vögeln existiert. In den vergangenen Jahrzehnten wurden zahlreiche Verhaltensstudien über den Einfluss von polarisierten Reflektionsmustern des Himmels auf das Orientierungsverhalten von Zugvögeln veröffentlicht. Nichtsdestotrotz steht diese sensorische Fähigkeit nach wie vor unter hitziger Debatte, da die klassischen Verhaltenstests einer Ergebnisverzerrung durch Lichtreflektionsartefakte ausgeliefert waren. Des Weiteren wurde noch kein anatomischer Nachweis für einen Rezeptionsmechanismus in Vögeln erbracht und alle Studien über die Sensitivität für polarisiertes Licht, die Entscheidungsparadigmen als Grundlage für ihre Untersuchungen hatten und die unter Laborbedingungen gute Kontrollen gegen den Einfluss von Reflektionsartefakten berücksichtigten, lieferten negative Ergebnisse.

In meiner Doktorarbeit verwendete ich zwei unterschiedliche Ansätze, die darauf abzielten, die Sensitivität für polarisiertes Licht in Vögeln nachzuweisen:

In einem ersten Ansatz fanden ehemalige Kollegen von mir heraus, dass eine Teilmenge von retinalen Ganglienzellen von Hühnern mit einer bimodalen Antwort auf 360° Drehungen eines Polarisationsfilters reagierten, wenn meine Kollegen extrazelluläre Antworten auf Ebene der Ganglienzellschicht in Hühnerretinapräparaten ableiteten. Die unvermeidbaren Lichtintensitätsunterschiede beim Rotieren eines Polarisationsfilters wurden aufmerksam gemessen und gezielt in die Stimulationsabfolge integriert, um gegen Lichtreflektionsartefakte zu kontrollieren. Konservative Kriterien zur Analyse der abgeleiteten Daten wurden festgelegt, um sicherzustellen, dass falsch-positive Antworten aus dem Datensatz rigoros entfernt werden konnten. Die beschriebene Studie resultierte in mehreren starken Indikatoren für wahre Polarisations sensitivität und die Ergebnisse erlaubten ein hohes Maß an Zuversicht in die Validität der erhobenen Daten. Nachdem ich von den Autoren der Originalstudie in die Methode eingewiesen wurde, war ich dazu fähig, deren Ergebnisse zusammen mit meinem Kollegen Dr. Arndt Meyer im identischen Versuchsaufbau zu replizieren. Zusätzlich dazu führten wir erweiterte Lichtmessungen durch und fanden einen Versuchsansatz, um die

strukturelle Integrität der Retinapräparate zu visualisieren, mit Fokus auf die Möglichkeit von zur Seite geknickten Außensegmenten der Photorezeptoren. Unsere Folgeexperimente zeigten auf, dass i) es potentiell kritische Quellen künstlich eingebrachter Lichtintensitätsänderungen gab, die sehr viel größer sein könnten als die, für die in der Originalstudie kontrolliert wurde, und dass ii) stark abgeknickte Photorezeptoraußensegmente an den Ableitstellen nachgewiesen werden konnten, die durch strukturellen Schaden am Gewebe entstanden waren und theoretisch eine künstliche Polarisations sensitivität hervorrufen könnten, bedingt durch transversalen Dichroismus, welcher in Photorezeptoren von Wirbeltieren auftritt. Auf Grundlage von diesen Ergebnissen und einigen weiteren Indikatoren aus eher unsystematischen Zusatzexperimenten konnten alternative Erklärungen zu all den obengenannten Indikatoren für Polarisations sensitivität aus der Originalstudie aufgeführt werden, welche allerdings nicht einer natürlichen Polarisations sensitivität zu Grunde lagen. Zusammenfassend ließ sich festhalten, dass die von uns und von den Autoren der Originalstudie abgeleiteten Zellantworten sowohl von Ganglienzellen stammen könnten, die die Achse des elektrischen Feldvektors (e-vector) von polarisiertem Licht codierten, als auch von einer Anzahl an potenziellen Artefakten herrühren könnten, die durch unerwünschte Lichtreflektionen, durch Verlust der Abschirmfunktion des Pigmentepithels, durch seitliches Abknicken der Photorezeptoraußensegmente und/oder durch beeinträchtigte Funktionalität der retinalen Schaltkreise, oder all der eben genannten zusammen, verursacht worden sein könnte. Nichtsdestotrotz konnten unsere Experimente ein gewisses Mindestmaß an Kontrollprozeduren in physiologischen Versuchsansätzen ansetzen, welche in zukünftigen Studien berücksichtigt werden sollten, falls diese auf einen Beweis für Polarisations sensitivität in Vögeln abzielten.

In einem zweiten Ansatz konnte ich einen neuen Versuchsaufbau für Verhaltensversuche in meiner Arbeitsgruppe etablieren und nutzen, um das Polarisationssehen bei Vögeln zu untersuchen, ohne die typische Anfälligkeit für Reflektionsartefakte in Kauf nehmen zu müssen. Indem ich modifizierte LCD Monitore benutzte, konnte ich drei Singvogelarten in einer virtuellen Arena rotierenden Streifenmustern aussetzen, welche virtuell um die Individuen herum rotierten und optomotorische Folgereflexe auslösten, wenn sie in Luminanzkontrast präsentiert wurden. Des Weiteren präsentierte ich den Vögeln einen sich annähernden Stimulus, der ein sich schnell näherndes Objekt nachahmte, um in den getesteten Vögeln einen Fluchtreflex auszulösen. Entfernte man die vordere Polarisationsfolie von den

Monitoren, wurden die Reize in Polarisationskontrast präsentiert, was bedeutete, dass diese Reize nur für Subjekte mit einem polarisationssensitiven Sehsystem sichtbar waren. Für das menschliche Auge waren die Stimuli ohne Hilfsmittel unsichtbar. Würden Vögel ein polarisationssensitives Sehsystem besitzen, dann hätte ich vergleichbare Antworten auf beide Stimuli sowohl im Luminanz- als auch im Polarisationskontrast erwartet. Als ein Ergebnis konnte ich starke und stabile Antworten auf beide Stimuli im Luminanzkontrast hervorrufen, jedoch keine Antworten (im sich annähernden Stimulus) oder keine Antworten, die über das ermittelte Maß der Spontanaktivität von Kopfbewegungen hinaus gingen (rotierende Streifenmuster), sobald die Stimuli nach dem Entfernen der vorderen Polarisationsfolien von den Monitoren im Polarisationskontrast präsentiert worden waren. Daraus ließ sich schließen, dass weder die Stabilisierung von optischem Fluss (optomotorische Folgereflexe) noch Objekterkennung (Fluchreflexe als Antwort auf sich rasch nähernde Objekte) mit einer potenziellen Fähigkeit von Vögeln in Verbindung gebracht werden konnten, polarisiertes Licht wahrzunehmen. Die wahrscheinlichste Interpretation meiner Ergebnisse war, dass die getesteten Vögel kein Polarisationssehen besaßen, und dass sie möglicherweise generell keine Sensitivität für polarisiertes Licht besaßen.

Zusammenfassend lässt sich festhalten, dass ich durch meine Doktorarbeit neue Erkenntnisse zu den wichtigsten Kompasssystemen von zwei Wirbeltiergruppen aufzeigen konnte. Ich konnte nachweisen, dass Korallenriffischlarven einen Magnetkompass besitzen, der ihnen bei der Rückkehr zu ihrem Heimatriff behilflich sein könnte. Ich konnte beschreiben, warum sich eine invasive elektrophysiologische Methode als möglicherweise ungeeignet herausstellte, um Polarisations sensitivität in Hühnern nachzuweisen. Und zuletzt konnte ich in drei Singvogelarten auf experimentelle Weise die These unterstützen, dass Vögel nicht dazu fähig sein könnten, polarisiertes Licht wahrzunehmen.

Im Ausblickteil dieser Doktorarbeit werde ich eine bisher unbeschriebene, neuartige optische Eigenschaft des dritten Augenlides in Vögeln, der Nickhaut, präsentieren. Ich entdeckte, dass die Nickhaut von Vögeln hochgradig doppelbrechende Eigenschaften besitzt und auf komplexe Weise die Schwingungseigenschaften von polarisiertem Licht beeinflussen kann. Ich werde die mögliche Auswirkung meiner Entdeckung auf eine von Grund auf neue Sichtweise auf die mögliche Polarisations sensitivität bei Vögeln aufzeigen, welche ich in meiner weiteren wissenschaftlichen Laufbahn gerne experimentell untermauern würde.

## **1. Introduction to vertebrate orientation behavior**

Among the most fascinating phenomena in animal behavior are the astonishing migratory patterns exhibited by many vertebrate species (e.g. Putman et al., 2014; Putman et al., 2015; Wittemyer et al. 2007; Holland et al., 2006; Mouritsen, 2018). Vertebrates inhabit a vast variety of ecosystems to which the individual lineages have evolved countless adaptations in e.g. phenotype, physiology, sensory capabilities, diet, predatory strategies and life history traits (Liem and Walker, 2001; Begon et al., 2005). The evolutionary progress of these adaptations is a rat race against ecological pressures such as predation risk, competition for limited resources, but also (seasonally) unfavorable environmental conditions (Begon et al., 2005). Migrating, dispersing and homing species can minimize some of these ecological pressures in order to gain the highest fitness benefits for themselves and their offspring (Berthold, 2001). Among the evolutionary driving factors for dispersal are the benefits of colonization of new suitable habitats and the fitness-positive exchange with genetically distinct partners (Greenwood, 2010; Berthold 2001; Newton 2008). Homing on the other hand, i.e. the retention or returning to natal sites at reproduction stage, bares the evolutionary advantages of a stable gene pool with predispositions for the local ecological challenges (Greenwood and Harvey, 1982; Begon et al., 2005; Newton, 2008).

Spectacular observations of seasonal migration, dispersal and homing have been made for all lineages within the vertebrate order. Pacific salmon return to their natal river after reaching maturity in the open ocean thousands of kilometers away (Putman et al., 2014). Turtles spend up to 5-30 years in the open ocean (Putman et al., 2015). For reproduction, they go on a journey back to the exact same beach where they saw the first light of day as newborns (Putman et al., 2015). Herds of elephants travel long distances across unfavorable environments to find bodies of water or isolated patches of food with astonishing precision (Wittemyer et al. 2007). Big brown bats (*Eptesicus fuscus*) were found to travel huge distances in nocturnal foraging flights that resemble the capabilities of birds in terms of precision and the use of orientation strategy (Holland et al., 2006).

### **1.1. Bird migration**

The incredible journeys of the solitary traveling bar-tailed godwits (*Limosa lapponica baueri*) take them to and from their breeding grounds in Alaska and their wintering grounds in the New Zealand archipelago every year which includes over 10.000 kilometers of non-stop flight

across the Pacific Ocean (Gill et al., 2014). In comparison, moderate European climate allows for sub-populations of partial migrants, indicating balanced fitness benefits for migrants and residents (Berthold, 2001; Begon et al., 2005). Obligate migrants like a population of Linnets (*Carduelis cannabina*) on the remote island of Helgoland in the Northern Sea, must migrate due to high levels of competition for scarce resources in hard winters on the small island (Förschler et al., 2010). Like many other migratory songbird species, they show a high site fidelity to their breeding grounds and travel at night, mostly without the contact to and guidance of experienced conspecifics, even in their first year (Berthold, 2001; Newton, 2008). It is astonishing how birds with brains weighing only a few grams accomplish this high level of migratory precision every year. During my PhD, I had the great opportunity to work in one of the world's leading groups in the study of the neurosensory basis of bird migration with a strong focus on geomagnetic orientation. Over the years, the members of this group have published outstanding contributions to the field and throughout this thesis, I tried to acknowledge as many of these outstanding studies in their specific context as possible, ranging from compass orientation behavior, calibration processes with celestial cues, sensory limits of a magnetic compass and the neurosensory pathways underlying magnetic orientation with a bandwidth of methodology ranging from diverse classic behavioral essays to techniques considering neuroanatomy, biochemistry, molecular biology, immunohistochemistry, modern imaging techniques and genetics. If some of these outstanding studies should remain unmentioned throughout my thesis, it was merely due to conceptual limitations and the scope of this thesis.

## **1.2. Dispersal and natal homing in coral reef fish larvae**

Life in a coral reef is a daily battle for survival. Food, resources and shelter are highly limited and specializations for narrow ecological niches are common in reef dwelling species. Most coral reef fish exhibit larval dispersal which might have evolved in order to reduce the high predatory pressure on planktonic early larval stages inside the reef (Kingsford et al., 2002; Leis et al., 2011). Outside the reef, the larvae develop at the fate of ocean currents (Jones et al., 2009) at first, but turn into active swimmers soon (Fischer and Leis, 2009) which enables them to cope with the current drift (Leis et al. 2007). Oriented swimming of the pelagic larvae can determine the level of connectivity among populations and habitats in otherwise benthic species during adulthood (Kingsford et al., 2002; Jones et al., 2009; Leis et al., 2011). At the end of their pelagic phase after days to weeks, larvae must settle at a reef among conspecifics

in the coral burrows (Kaufman et al., 1992). Gerlach et al. (2007) suggested that kin recognition mechanisms might positively influence the aggression levels and the outcome of rivalry for resources, e.g. rivalry for the best protected sites deeper inside the coral labyrinths. This might additionally be in favor of orientation mechanisms that bring the larvae back home to their natal reef for settlement among kin.

It is now known that the time of spawning has a great effect on larval survival rate and their fitness throughout life (Shima et al., 2018). Settlement of the larvae must be synchronized with the moon phase, because in nights around a full moon, predatory pressure is highest due to bright light conditions. On the other hand, larvae arriving at a new moon have the best survival chances (Shima et al., 2018). Interestingly, the data collected by Shima and colleagues (2018) show that larvae arriving at the first quarter after a full moon had bigger body size than other arrivals, which suggests that these fish might have actively prolonged their pre-settlement larval phase, in order to avoid the risks of a full moon arrival (Shima et al., 2018). As a consequence, these fish are bigger and stronger than others, so their chances in territorial fights and competition about mates would be comparably optimal (Shima et al., 2018).

In summary, not only settling at the right time, but also at the right reef can be beneficial, if not vital to fitness. Larval fish can exhibit self-recruitment mechanisms that include behavioral adaptations to facilitate retention near the natal reef (Sponaugle et al, 2002). If retention in the vicinity of a reef (Paris and Cowen, 2004) is not possible, successful homing must include fine orientation capabilities at larger distances (Mouritsen et al., 2013; Bottesch et al., 2016; O'Connor and Muheim, 2017) and imprinting on sound, sight and smell from the home reef at shorter ranges (Leis and Carson-Ewart, 2003; Gerlach et al., 2007; Leis et al., 2011).

### **1.3. Strategies in orientation behavior**

What sensory, physiological and behavioral mechanisms underlie such astonishing behaviors that enable these species to move decisively over astonishing distances across oceans and land, with an impeccable degree of precision? Griffin (1952) categorized three different types of orientation, three principle tools so to say that an animal could employ to reach a goal in familiar and unfamiliar surroundings: (1) piloting along memorized landmarks, orientation using (2) a compass to determine and maintain directions, and (3) a map to determine current location and distance with respect to the goal (Griffin, 1952).

### **1.3.1. Orientation and Navigation**

An arbitrary series of memorized landmarks can suffice for an animal to travel on familiar routes. This has been phrased “Type I” orientation or piloting by Griffin (1952). This basic form of orientation can be achieved by memorizing a sequence of coastline features, mountain ranges, bodies of water, patches of vegetation or other visual, physical and chemical signposts between home and a certain goal (Griffin, 1952). To travel outside familiar routes however, an animal needs navigational skills that are based on a map and a compass: A map to determine the current position and distance with respect to the goal/home, and a compass to provide a directional reference for maintaining a straight goal/home-ward bearing in familiar and unfamiliar surroundings. Employing both a compass and a map simultaneously has been termed true navigation (type III, Griffin 1952). Only with such an ability, animals are able to correct for unpredictable drift by environmental forces during migration and to compensate for natural and experimental displacement (Perdeck, 1958; Figure 1). This is the most complex form of orientation and it is widely believed that this capability comes with experience (for reviews see e.g. Holland 2014; Chernetsov, 2016; Mouritsen, 2018).

#### Mosaic maps

Learning the spatial relationship between a few landmarks can suffice to orient in the sense of a map, defined as a mosaic map (Wallraff, 1974; reviewed in Gagliardo, 2013). For example, hummingbirds on foraging trips learn the spatial relation between a visited food source and nearby landmarks (Pritchard et al., 2016). Experimental modification of the apparent distance between these landmarks changes the calculated location of the food source and thereby the site at which the hummingbird will search for the food source (Pritchard et al., 2016). In comparable manner, a landmark-based map can function for distances outside familiar terrain, if sensory contact to these landmarks is granted or can be extrapolated. Such landmarks can be geographical formations like coastlines or mountain ranges, patches of distinct woodlands or bodies of water (for review see Holland 2014). More controversially debated signposts in the context of landmark-based map cues are local gravitational (Larkin and Keeton, 1978; Blaser et al., 2013, 2014) and characteristic regional infrasound profiles (Hagstrum 2000, 2001, 2013), amongst others (for review see Chernetsov, 2016).

## Grid-/Gradient maps

A grid- or gradient-like distribution of one or more environmental cues can provide constant positional information across borders of familiar areas (Figure 1). A one-coordinate gradient (Figure 1, axis A or B) can indicate the current distance to or the relative location of a familiar goal by comparison between the momentarily perceived dilution/values of the gradient and the learned or inherited dilution/values at the goal (Holland 2014; Figure 1, axis A or B). A bi-coordinate gradient map (Figure 1, axis A and B) on the other hand, can provide exact and even globally distributed positional information on longitudinal and latitudinal location and distance with respect to the goal (Figure 1). The best studied grid- or gradient maps in vertebrate species are the olfactory and the geomagnetic maps (reviewed in e.g. Wallraff 2003; Wiltschko and Wiltschko, 2007; Lohmann et al., 2007; Gagliardo, 2013; Mouritsen 2015; Mouritsen, 2018).

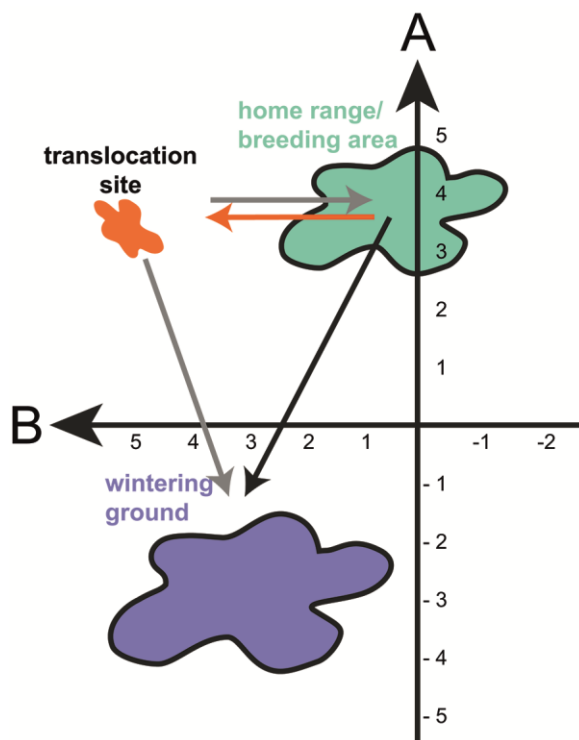


**Figure 1: Scheme of one-coordinate and bi-coordinate gradient maps in animal navigation.**

The gradient-like distribution of only one environmental cue (A or B) can provide longitudinal or latitudinal information, respectively. Distances parallel to this axis can be used in a one-coordinate map sense (Lohmann et al., 2007), e.g. after experimental translocation from the home range in parallel to the gradient B (orange arrow). A bi-coordinate orientation system uses multimodal environmental cues (A+B) that provide positional information that could be used in migratory directions relative to the overlapping gradients (black arrow). Modified after Holland 2014.

### *The magnetic map:*

The Earth can be considered as a big bar magnet. Streams of liquid iron oxides in the outer Earth's core are charged particles in motion that induce a magnetic field. This so called 'Geodynamo' is sustained through high energetic convection, favored by low thermal conductivity in the outer Earth's core, and responsible for the earth magnetic field for at least



3.5 billion years (Konôpková et al., 2016). The resulting magnetic field lines form an angle with the Earth's surface, called magnetic inclination. An inclination angle of  $90^\circ$  defines the magnetic poles (Figure 2, A). The inclination angle decreases gradually to  $0^\circ$  at the magnetic equator, being parallel to the earth surface (Figure 2, A). The geomagnetic field strength reaches values of  $\sim 60$  Micro Tesla ( $\mu\text{T}$ ) at the magnetic poles, gradually going down to  $\sim 30 \mu\text{T}$  at the magnetic equator (Figure 2, A and B). Therefore, the magnetic field provides a global gradient in field strength and inclination which can indicate information on latitudinal position.

The determination of longitudinal position by geomagnetic information would involve the magnetic declination, i.e. the angular discrepancy between magnetic and geographic poles at a certain longitude. This has been considered rather unrealistic for reasons of the irregularity and slowness of this gradient in most parts of the globe. However, there is recent evidence

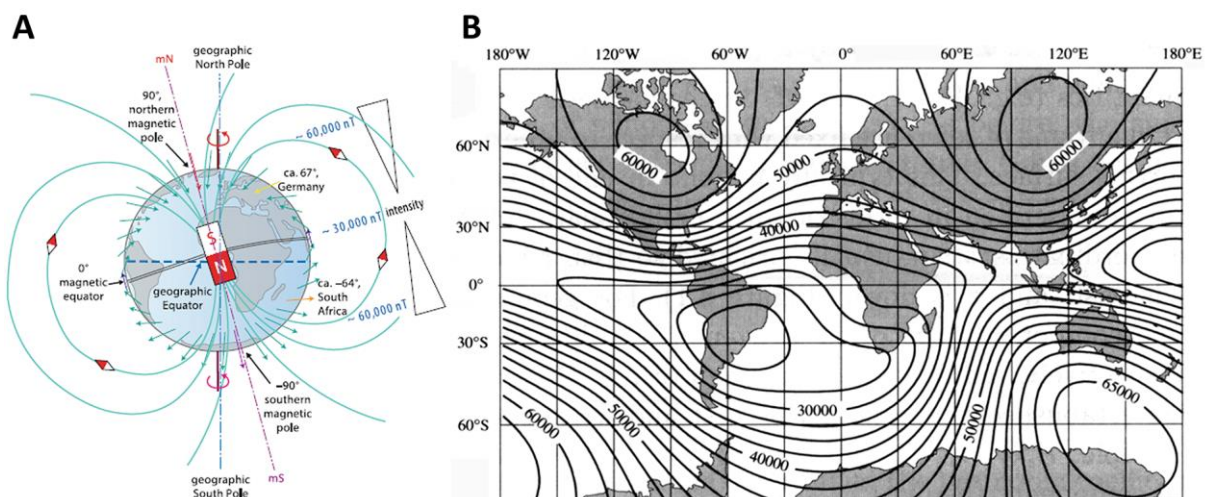


**Figure 2: The geomagnetic field.** The Earth can be regarded a big magnet. Movement of iron-rich compounds in the outer core cause an electromagnetic field. A) The magnetic field lines span the Earth by exiting at the magnetic South pole and reentering at the magnetic North pole. Note that the location of the poles is in motion and diverges from the geographic poles. The magnetic inclination angle (B) and the magnetic field strength decrease gradually from the poles to the equator. A) From Mouritsen, 2013. B) From [www.ngdc.noaa.gov/geomag](http://www.ngdc.noaa.gov/geomag).

that adults of at least some bird species (Chernetsov et al., 2017; but see Chernetsov et al., 2020) alter their migratory directional choices according to a minute experimental change in declination of only a few degrees, which would correspond to a 1000 km E-W translocation in nature (Chernetsov et al., 2017). Based on this fascinating result, there is first evidence that animals could potentially employ a bi-coordinate map sense exclusively based on magnetic map information (Mouritsen, 2018; Chernetsov et al., 2017; but see Chernetsov et al., 2020). On the other hand, a one-coordinate magnetic map could be sufficient in terms of navigation for animals that make additional use of Y-axis orientation, i.e. orientation along coastlines or

other geographic formations (Ferguson and Landreth, 1966). Sea turtles for example imprint on the magnetic field intensity of their natal beach (Brothers and Lohmann, 2015). The return journey could be accomplished by following a coastline towards the gradually converging magnetic field parameters until the imprinted and the currently perceived intensities match (Lohmann et al., 1999, 2004, 2007; Brothers and Lohmann, 2015; see Figure 2, B).

However, temporal and local irregularities in the magnetic field can influence the reliability of magnetic information in navigational tasks. Daily fluctuations around “regular” local field values occur due to continental drift, solar storms, local differences in convection, stream circulation and density of molten iron streams in the outer earth core (Konôpková et al., 2016). Fluctuations around the “normal” magnetic field values around roughly  $\pm 100$  Nanotesla (nT; Skiles, 1985) have to be taken into account in terms of navigational precision, which accounts for a distance uncertainty of  $\sim 30$  km (using the following calculations: pole to equator = 30.000 nT / 10.000 km =  $\sim 3$  nT/km). These daily fluctuations would not cause a serious problem for determining position in the long-distance phase for migratory birds, spanning up to 10.000 kilometers between home and goal. However, homing coral reef fish larvae are potentially drifted only around  $\sim 30$  kilometers away from their intended goal, which lies well within daily geomagnetic field fluctuations. Therefore, the magnetic field gradient could be highly unreliable in terms of map information in this context. In general, the use of magnetic map information on scales shorter than 30 km must be considered unrealistic for now (Mouritsen, 2018; but see Komolkin et al., 2017).

#### *The olfactory map:*

Odor gradients possess their strength as a map cue at shorter distances - as opposed to the magnetic gradient map - when odor plumes carried by wind or currents still form sharp gradients extending the borders of familiar areas (Wallraff and Andreae, 2000; Gagliardo, 2013; Holland, 2014; see Figure 1). However, geographic obstacles or meteorological events like storms can cause severe turbulences in wind or current flow, so after a certain terrain-/weather-dependent distance, the concentration of a chemical cue might be too weak to still carry reliable olfactory map information (Leis et al., 2011; Gagliardo, 2013). As opposed to this argument, geographic formations can form actual flow channels carrying the prominent scents over huge distances (Atema, 1988; Papi, 1972; Grimes and Kingsford, 1996; Gagliardo, 2013; Holland, 2014).

### *Combination of both map cues:*

Vigorous debates about the predominance of one of these two map senses has affected the bird research community for decades. Since I did not touch this subject experimentally in my PhD thesis, I refrain from taking sides in this argument, except for stating that both suggested map senses have their limitations at intermediate distances between 10 - 100 km. At shorter ranges, integration of multiple cues for landmark-based navigation and mosaic map navigation might be key to pinpoint the goal, which would include olfactory cues (Papi et al., 1971, 1972; Gagliardo, 2013) as well as potential geomagnetic, gravitational and infrasonic signposts (Chernetsov, 2016). Odors are believed to be rather locally distributed and that their reliability drops fast at intermediate distances. At longer distances, the slow gradient of the geomagnetic field can serve gradient map-based navigation (Gagliardo et al., 2006), but at intermediate ranges the geomagnetic field is least reliable as well due to daily fluctuations (Skiles, 1985; Mouritsen, 2018). At these intermediate distances, individual experience with present site-specific cues must be considered the most determining factor for the choice of respective cues, i.e. olfactory or magnetic cue choice. A set of experiments performed by Wiltschko and Wiltschko (1988a, 1989) suggested that the animal's experience with respective map cues could potentially be responsible for diverging outcomes of past studies. Two groups of homing pigeons were either raised in a wind-exposed loft or in a loft shielded from wind-borne information, respectively, but both groups of birds had access to the natural magnetic field. Displaced in absence of odors and released thereafter, only the birds raised in the wind-exposed loft were unable to home. Indirect but elegant, this study suggested an experience-weighted use of either magnetic or olfactory information for orientation (Wiltschko and Wiltschko, 1988a, 1989).

### **1.4. Compass orientation**

The ability of extracting directional information towards a specific goal in familiar and unfamiliar environments is termed compass orientation (Type II orientation, Griffin 1952). Any fixed and dynamic directional reference can serve as a compass cue. Visual, olfactory, auditory or any other sensory type of landmark can provide a relative directional reference with respect to a known goal. When the goal was outside familiar territories and sensory contact to known landmarks was not granted, several apparent celestial compass cues, i.e. the sun and the stars, can provide global directional reference during the day and night. Additionally, sun-related information like horizon glow, intensity gradients and predictable spectral distributions are

forming reliable directional cues at the time around dusk and dawn (Coemans et al., 1994a). Furthermore, skylight polarization patterns are most prominent at twilight (Wehner, 2001) and are suspected to aid the orientation in birds (for review see Åkesson, 2014; Muheim, 2011, but see chapter 3.3 in this thesis) and many other vertebrate and invertebrate species (see chapter 3.1 and 3.2. in this thesis). Detailed information about the physical basis and biological use of skylight polarization patterns, and the sensory prerequisites needed to detect them can be found in chapter 3.1 and 3.2. in this thesis.

#### Compass orientation towards an unknown goal:

On their first autumn migration, a genetically inherited, species-specific compass direction (Berthold et al., 1991, 1992; Helbig, 1996) can help migrating birds to determine goal-ward directions and maintain a straight bearing into this direction even over longer distances. Additionally, an inherited internal clock and intrinsic flight distance measuring have been suggested to explain species-specific en route turns in migratory direction at determined waypoints (Berthold, 1991; Gwinner, 1996). This was termed a “clock and compass” mechanism (e.g. Mouritsen, 1998; Mouritsen, 2018). Surprisingly, pied flycatchers (*Ficedula hypoleuca*) tested in their first migratory season in orientation funnels performed the proper orientation turn only upon experiencing a gradual adjustment of the geomagnetic field strength as would be perceived en route (Beck, 1984; Beck and Wiltschko, 1988; Weindler et al., 1995). Therefore, inherited sensory landmarks like magnetic map values might play an additional role in compass orientation towards an unknown goal (Heyers et al., 2017).

#### **1.4.1. Sun compass orientation**

A sun compass can literally be found in all vertebrate species tested for orientation so far (e.g. fish: Goodyear and Ferguson, 1969; amphibians: Ferguson et al., 1968; reptiles: DeRosa and Taylor, 1978; birds: Kramer, 1952; mammals: Fluharty et al., 1976). This widespread orientation tool seems to be the most important modality during daytime orientation across vertebrates (for review see Able, 1980; Deutschlander et al., 1999; Chernetsov, 2015). The relevant cue in sun compass orientation is the sun’s azimuth, i.e. the geographic angle of the sun with respect to the horizontal plane (reviewed in Able, 1991; Gould, 1998; Figure 3), the sun’s elevation is ignored (Kramer, 1953; Schmidt-Koenig, 1961). This is believed to account for all vertebrate taxa (Able, 1991).

When the sun was used to keep a directed bearing in longer-distance travels, the sun's azimuth and its apparent movement across the sky have to be compensated with respect to

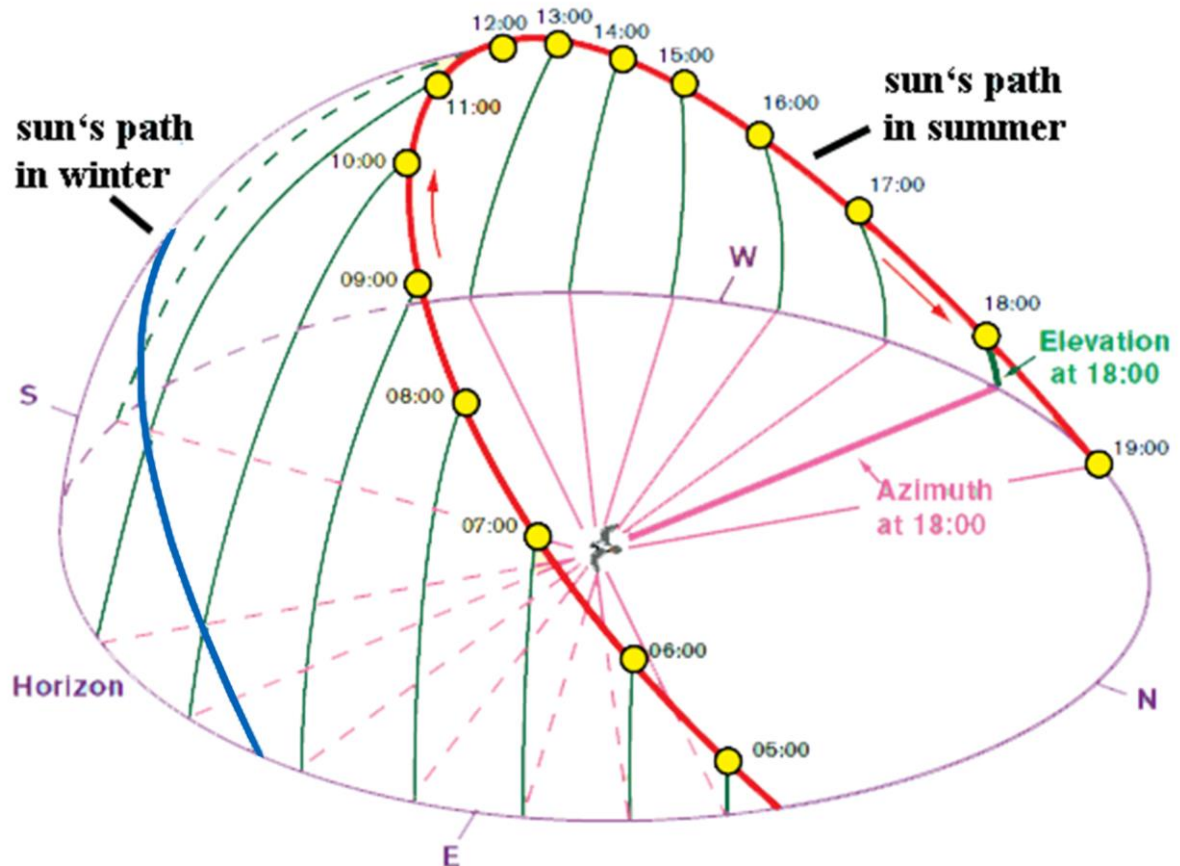


**Figure 3: The sun's azimuth at different times of day and latitudes.** Sun disk elevation changes drastically at different times of the year and different latitudes. In summer, the sun's elevation at 40°N latitude in June is equivalent to 35°N latitude in May, a month earlier (red line). The difference between summer and winter are depicted by the red and blue lines. The azimuth on the other hand is almost not affected by season and location. Note the much faster azimuth movement at the time around noon as compared to dusk and dawn. Modified from Gould, 1998.

the time of day in reference to the animal's internal clock (Kramer, 1952; Schmidt-Koenig, 1958; Hoffmann, 1953; Schmidt-Koenig, 1961; Wiltschko et al., 1976; Figure 3). After an experimental clock-shift, birds misinterpreted the geographic position of the sun disk accordingly (Hoffmann, 1953; Schmidt-Koenig, 1961). Even an artificial sun disk (light bulb) for experimental manipulations of the sun's path was effective in influencing the sun compass orientation of several vertebrate species, e.g. songbirds (*Sylvia atricapilla*; Viehman 1982), coral reef fish larvae (*O. doederleini*; Mouritsen et al., 2013), sea turtle (*Chrysemys picta*; DeRosa and Taylor, 1978), land turtles (*Emydoidea blandingii*; Krenz et al., 2018).

In preparation for chapter 3 in this thesis, I like to emphasize on the fact that not the natural appearance of the sun disc, but merely an artificial source of light (light bulb) sufficed in the

just mentioned clock-shift experiments to influence the directed movement of caged animals. Before continuing to read, ask yourself the following question: How could the outcome of an experiment for the orientation capabilities of such visually guided animals be influenced, when the visual surroundings in an ideal experimental setup could be set to be completely homogeneous, except for a purposely introduced, faint light gradient providing slightly brighter and darker areas in this setup (see chapter 3.3 in this thesis)?

#### **1.4.2. Star compass orientation**

During the night, the stars can provide reliable compass information to the observer after learning to associate prominent star constellations with geographic directions in the following way: To the stationary observer on the ground, the earth's revolving around its tilted orbital axis infers the impression that the stars rotate around the earth (Figure 4). The angular velocity of stars close to the celestial equator is highest, while star constellations close to the Earth's rotation axis appear to move slowest, thus indicating the center of apparent rotation, i.e. the geographic poles (Figure 4). Polaris in the constellation of *Ursa Minor* lies very close to this celestial North Pole and can be used as the celestial compass reference for geographic North (Figure 4).

The by far best studied vertebrates for star compass orientation are night-migratory songbirds. Early observations in behavioral experiments revealed the potential importance of the stars for orientation, because directional choices of the tested birds were less clear when the stars were not visible (Kramer 1949; Sauer 1957). A series of following studies suggested that birds might possess an inherited representation of star constellations and that they were able to perform true star navigation, i.e. determine latitudinal position by the stars (Sauer, 1957, 1961; Sauer and Sauer, 1960, Sauer and Emlen, 1971). However, this hypothesis was soon discarded because the sensory and cognitive capacities that would be necessary were considered unrealistic (Kramer 1957, Pennycuick 1960, Wallraff 1960, Adler 1963).

From the 1960s-70s, Emlen performed well-controlled studies with indigo buntings (*Passerina cyanea*) under a planetarium sky. He was able to hand-raise birds under the influence of experimental star presentations, he was able to manipulate the star constellations around which the projected night sky rotated, to switch off chosen star constellations, to set the projected planetarium sky to be stationary or to be rotating in the opposite direction (Emlen 1967a, 1967b, 1969, 1970, 1972, 1975). The insights from these studies gave rise to most of

the knowledge we have today about star compass orientation. In fact, all following studies supported the results from Emlen's work (e.g. Wiltschko, 1987; Mouritsen and Larson, 2001;

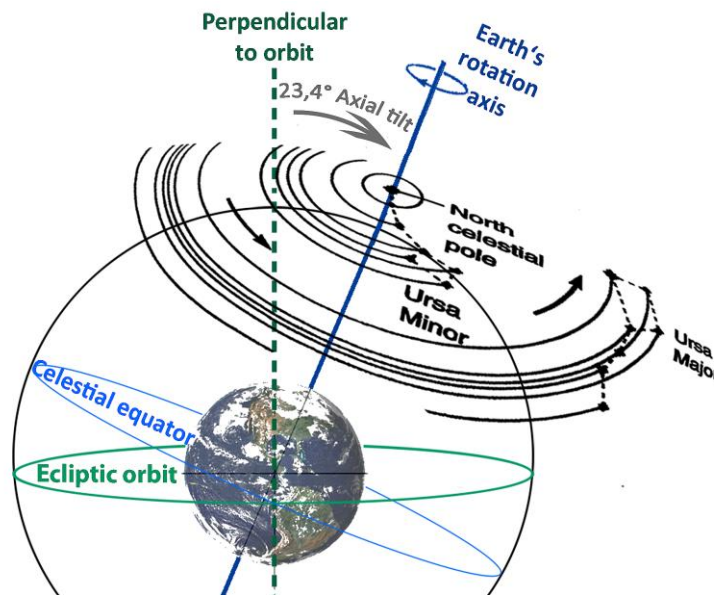


**Figure 4: Apparent rotation of the starry sky.** The Earth orbits in an ecliptic path around the sun with an axial tilt of  $23,4^\circ$ . The rotation of the earth around its north-south axis results in an apparent rotation of the celestial sphere around this axis, including the stars, planets and other celestial bodies. The angular speed of polar- and circumpolar star constellations is slowest, while constellations closer to the celestial equator (e.g. *Ursa Major*) appear to rotate faster. The center of rotation in the northern hemisphere, currently the star Polaris in the *Ursa Minor* constellation, indicates geographic north. Modified after [www.scienceblogs.com](http://www.scienceblogs.com).

Michalik et al, 2013, Pakhomov et al., 2017): The star compass, like the sun compass, has to be learned and it is not based on an inherited internal projection of the night sky (also confirmed by Mouritsen and Larson, 2001). In contrast to the sun compass, the movement of particular star constellations does not need to be linked to an internal clock. A study on the time-independent star compass of European robins (*Erithacus rubecula*) independently confirmed Emlen's findings in experiments under the natural starry sky (Pakhomov et al., 2017). The apparent center of celestial rotation is the important reference cue and has to be observed during a sensitive period in early development to learn the indicated geographic pole-ward direction (Emlen, 1970, 1972; Able and Able, 1995a, 1996; Michalik et al., 2013; Figure 4). Michalik et al. (2013) provided evidence that this learning phase must last at least 7 days in young European robins (*E. rubecula*; Michalik et al., 2013). In an operant conditioning approach, Alert et al. (2015a) demonstrated that pigeons can learn the principle of finding the rotational center of an arbitrary rotating dot pattern (Alert et al., 2015a). Their results suggest that birds could (a) potentially perceive the very slow rotation itself, if other visual pathways than the frontal visual field and the accessory optic system, e.g. the lateral visual field, were involved (reviewed in Alert et al., 2015a) or (b) rather use a "snapshot strategy" to recognize and mentally rotated objects or pattern (reviewed in Alert et al., 2015a).



### 1.4.3. Magnetic compass orientation

In early observations, Merkel and Fromme (1958) noted that European robins (*Erithacus rubecula*) showed directed orientation behavior even in the absence of any visual cues (Merkel and Fromme 1958). This led to the first assumptions that these migrants might use another global directional cue aside of the sun and the stars. Soon, the first indirect evidence for the role of geomagnetic information in this “non-visual task” (Merkel and Fromme, 1958) was revealed by steel shielding of the experimental chamber, which critically reduced the natural geomagnetic field strength and in turn successfully impaired the orientation capabilities of the tested birds (Fromme 1961). In 1968, Wiltschko built the first Helmholtz coil system around orientation cages, a device that allowed for experimental manipulation of the ambient static magnetic field, which in turn allowed him to demonstrate the first direct evidence for a magnetic compass in the European robin (*Erithacus rubecula*; Wiltschko, 1968). Soon after, Wiltschko & Wiltschko (1972) elegantly proved that the magnetic field is used as a unipolar

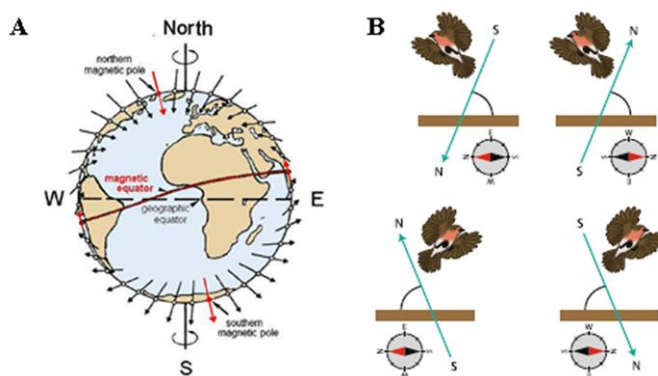


**Figure 5: The avian magnetic compass is an inclination compass.** (A) The geomagnetic field lines form an intersection angle with the Earth surface. The arrows indicate the local magnetic vectors with their lengths proportional to the intensity of the local field. The magnetic poles and the magnetic equator are marked in red. (B) Birds have been demonstrated to be unable to detect the polarity of the magnetic field (left versus right, in top and bottom rows, respectively). When the magnetic field vector was experimentally flipped vertically (top versus bottom, in left and right column,

respectively), the tested birds oriented into the opposite direction. Note that with a vertical flip, the horizontal component does not change its polarity, as depicted in the little compass needles at the bottom of each sketch. As a consequence, birds interpret the steeper intersection angle between the Earth surface and the magnetic inclination as polewards (Wiltschko, 1976). A) After Wiltschko and Wiltschko, 1995. B) From Mouritsen, 2013.

inclination compass in birds (Figure 5). This became evident by a 180° flip in the directional choices of birds tested under the influence of an experimental vertical flip of the magnetic inclination (Wiltschko & Wiltschko 1972; Figure 5). Birds can only deduce the axial directions of geomagnetic pole-wards vs. equator-wards by following the inclination angle but cannot deduce the polarity of the field (Wiltschko & Wiltschko 1972; Lefeldt et al., 2014; Schwarze et al., 2016b; Mouritsen, 2018; Figure 5).

As opposed to the celestial compasses introduced in chapter 1.2.1. and chapter 1.2.2. in this thesis, the magnetic compass does not have to be learned, but instead a genetically inherited,



species-specific direction relative to their geomagnetic compass helps migratory birds to determine and maintain their seasonally appropriate migratory direction (Wiltschko and Gwinner, 1974; Berthold et al., 1992; Wiltschko and Wiltschko, 1995c; Helbig, 1996). Since then, behavioral responses to external magnetic fields have been reported in many species across vertebrate groups, e.g. turtles (Lohmann, 1991), fish (Quinn, 1980), mole rats (Burda et al., 1990), amphibians and salamanders (Phillips and Borland, 1992a). Colleagues and I found that even coral reef fish *O. doederleini* larvae use a geomagnetic compass that might help them return to their natal reef at night (Bottesch et al., 2016; chapter 2 in this thesis). Our results were followed shortly by the publication of a study that suggested geomagnetic compass orientation in coral reef fish *Chromis atripectoralis* larvae during daytime as well (O'Connor and Muheim, 2017). A particularly pressing gap in migration research is the missing conclusive evidence for the sensory bases of magnetoreception.

#### Sensory basis of magnetoreception

It is astonishing that for almost every vertebrate lineage a different set of hypotheses for a potential magnetoreception mechanism exists (see below; for reviews see e.g. Deutschlander et al., 1999; Kirschvink et al., 2001; Holland, 2014; Hore and Mouritsen, 2016; Mouritsen 2018). This non-unified abundance of theories is further complicated by the notion that - at least in birds - the sensory basis for the magnetic map sense (Wiltschko and Wiltschko, 2013; Kishkinev et al., 2013; Heyers et al., 2017; Pakhomov et al., 2018; Kobylkov et al., 2020) and the magnetic compass sense (e.g. Heyers et al., 2007; Zapka et al., 2009; Wu et al., 2020) might be provided by different sensory modalities (Wiltschko and Wiltschko, 2007; Gould, 2008; O'Neil, 2013; Chernetsov, 2016; Mouritsen, 2018; Chernetsov et al., 2020), as described in the following paragraphs. Nevertheless, especially in the last decade, modern interdisciplinary techniques in biology revealed and will continue to reveal interesting findings to take our understanding of the sensory basis of magnetoreception forward. Three currently prevailing, main hypotheses on magnetoreception in vertebrates exist: a radical pair-based light-dependent mechanism, an iron mineral-based mechanism and an electric induction mechanism.

#### *Radical pair-based mechanism of avian magnetoreception:*

In birds, a strong experimental framework of published research supports the theory of visually mediated geomagnetic compass information (for review see Ritz et al., 2000, 2004;

Wiltschko et al, 2010; Hore and Mouritsen, 2016; Mouritsen, 2018). Summarized in short: The magnetic compass of birds is wavelength dependent, i.e. dependent on short-wavelength light (Wiltschko et al., 1993; Wiltschko et al., 2010). Geomagnetic information is detected in both eyes of migratory songbirds (Zapka et al., 2009; Hein et al., 2010; Hein et al., 2011) and processed to a specific region in the visual Wulst that receives input via the thalamofugal visual pathway (*Cluster N*; Heyers et al., 2007; Zapka et al., 2009; Heyers et al., 2010; Zapka et al., 2010; Mouritsen et al., 2016; Mouritsen, 2018).

In 1978, Schulten et al. first formulated the theory of a light-dependent radical-pair mechanism (Schulten et al., 1978) that currently prevails as the primary model for the avian magnetic compass (Ritz et al., 2000; Wiltschko and Wiltschko, 2007; Ritz et al., 2010; Hore and Mouritsen, 2016; Mouritsen, 2018). To fully comprehend this model, interdisciplinary knowledge of at least quantum chemistry, biophysics, molecular biology and photoexcitation cascades in vertebrate photoreceptors are necessary, which were elegantly put into context in comprehensive reviews by Hore and Mouritsen (2016) and by Mouritsen (2018). Since my own work presented in this thesis did not focus on details of the sensory basis of magnetoreception, I summarize this theory in as few words as possible: Electron transfer in photosensitive molecules can lead to the light-induced formation of radical pairs (Hore and Mouritsen, 2016). The unpaired electrons in the radical pair possess magnetic moment that can interact with each other in e.g. hyperfine interactions, which can affect the interconversion rate of allowed quantum states of unpaired electron spin in the two radicals, i.e. singlet state (parallel spin) of triplet state (anti-parallel spin; Hore and Mouritsen, 2016). The direction of a static external magnetic field with respect to the orientation of a photosensitive molecule forming these radical pairs, can influence the proportion of the spin states over time (Hore and Mouritsen, 2016). Visual processing of geomagnetic information would involve a spin-selective reaction of interaction partners, i.e. a processing pathway that is dependent on whether the unpaired electrons in a light-induced radical pair were either in singlet state or triplet state (Hore and Mouritsen, 2016). In other words, the direction of the static geomagnetic field could in theory influence the product yield of a light-induced chemical reaction (Hore and Mouritsen, 2016). On the other hand, oscillating electromagnetic fields would mask the influence of a static geomagnetic field on the spin state of unpaired electrons in a radical pair. Radiofrequency electromagnetic fields indeed have a disruptive effect in experiments on the orientation capabilities of birds (Ritz et al., 2004; Ritz et al., 2009; Engels

et al, 2014; Kavokin et al, 2014; Schwarze et al., 2016a; Hiscock et al., 2017; Pakhomov et al., 2017; Kobylkov et al., 2019).

The most promising candidates as primary receptor molecules in the eyes of birds are cryptochromes (Ritz et al. 2000; Liedvogel et al., 2007; Niessner et al., 2011; Niessner et al., 2016; Bolte et al., 2016; Guenther et al., 2018; Wu et al., 2020). Cryptochromes are blue-light sensitive (Ritz et al. 2000; Liedvogel et al., 2007; Niessner et al., 2011), which matches the experimental observations of wavelength dependency of the avian geomagnetic compass (Wiltschko et al., 1993; Wiltschko et al., 2010). Cryptochromes are expressed in the retina of birds (Mouritsen et al., 2004; Liedvogel et al., 2007; Niessner et al., 2011; Niessner et al., 2016; Bolte et al., 2016; Guenther et al., 2018; Wu et al., 2020) and do not possess a primary visual function but are typically involved in the circadian clock. The currently most promising magnetoreceptor molecule is Cryptochrome 4 (CRY 4), which is the only splice variant of the known cryptochromes that does not exhibit seasonal expression patterns (Guenther et al., 2018). CRY 4 is localized in the avian double cones (Guenther et al., 2018; Wu et al., 2020) and binds flavin adenine dinucleotide (FAD), which is known to form long-lived radical pairs upon photoexcitation (Ritz et al. 2000; Liedvogel et al., 2007; Hore and Mouritsen, 2016; Mouritsen, 2018; Wu et al., 2020).

*An iron mineral-based mechanism of avian magnetoreception:*

For long, an iron mineral-based mechanism of magnetoreception located in the upper beak of birds (Fleissner et al., 2003) has been considered a mutually exclusive alternative to a visually mediated mechanism (Wiltschko and Wiltschko, 2013). Ferro- and paramagnetic compounds connected to the nervous system have been proposed to underlie the mediation of geomagnetic information in many vertebrate species (Fleissner et al., 2003; Winklhofer and Kirschvink, 2010; Naisbett-Jones et al., 2020; for reviews see Shaw, 2015; Mouritsen, 2018). In birds, experiments with strong magnets or magnetic pulses which would be able to re-magnetize iron-mineral compounds but would have no effect on a radical pair-based mechanism, were in fact successful in deflecting the orientation of experienced birds accordingly (Wiltschko et al., 2009; but see the paragraph below). While the notion of microscopic “compass needles” that translate geomagnetic information to the nervous system might appear very appealing, it bears major experimental constraints for unambiguous proof: The Earth magnetic field pervades most tissues, and iron-rich magnetic compounds are not rare in cells throughout the body of birds (Treiber et al., 2012; Lauwers et al., 2013).

Furthermore, Treiber et al. (2012) found that the iron-rich particles in the upper beak of birds (long believed to be avian magnetoreceptors; Fleissner et al., 2003) were not connected to nerve endings, but instead were macrophages. Additionally, the location of these compounds was highly inconsistent among animals of the same species (Edelman et al., 2015), another argument against a role of these iron-mineral compounds (Fleissner et al., 2003) as the avian magnetic compass sensor (Mouritsen, 2018).

#### *Synergy of the two hypotheses in birds:*

The upper beak in birds is innervated by the ophthalmic branch of the trigeminal nerve (Heyers et al., 2010; Kobylkov et al., 2020) which is necessary for determining location by a magnetic map sense (Heyers et al., 2010; Zapka et al., 2010; Kishkinev et al., 2013; Heyers et al., 2017; Pakhomov et al., 2018; Kobylkov et al., 2020), but not magnetic compass orientation (Zapka et al., 2009; Pakhomov et al., 2018). Dissection of the trigeminal nerve resulted in the inability of birds to compensate for experimental displacements (Heyers et al., 2017), while compass orientation remained unaffected (Pakhomov et al., 2018). It crystallized in the last decade of research that at least in birds the magnetic compass (visual) and the magnetic map (trigeminal) were provided by two distinct sensory systems (for reviews see Wiltschko and Wiltschko, 2007; Mouritsen, 2018). The before-mentioned magnetic pulsing experiments (Wiltschko et al., 2009) had an influence on the orientation behavior of experienced adult birds but did not affect the orientation of inexperienced juvenile birds (Wiltschko et al., 2009). The latter are believed to not possess a magnetic map sense yet, so probably the deflection of orientation behavior after pulsing had an unintended effect on a potentially iron mineral-based map sense in the adults, while the potentially visually mediated magnetic compass might have remained unaffected by pulsing in young birds (Hore & Mouritsen, 2016; Mouritsen, 2018).

#### An electric induction mechanism for magnetoreception in elasmobranch vertebrates

A different hypothesis for magnetoreception concerns elasmobranch fish only. The ampullae of Lorenzini, the electric sense organs in elasmobranchs can be seen as electric conductors and might function as magnetoreceptors in sharks, skates and rays in the following theoretical way (Kalmijn, 1981; Paulin, 1995; Molteno and Kennedy, 2009): Moving electrically conductive tubes or rings - the ampullae of Lorenzini - through a static magnetic field could induce current in their electrosensory organ. The strength of electric induction could be direction-selective

for external magnetic fields that run perpendicular with the longitudinal plane of the tube. A shark swimming through water could keep a constant bearing relative to the geomagnetic field by tuning the strength of electromagnetic induction in the electric sense organ to match specific compass directions (Molteno and Kennedy, 2009). Unfortunately, so far no directly behavioral evidence exists to support the electric induction hypothesis (Mouritsen, 2013; Mouritsen, 2018), but studies with bar magnets attached to the head of elasmobranchs resulted in disorientated behavior which shed doubt on this hypothesis (Hodson, 2000; Kirshvink et al., 2001; Walker et al., 2003; but see Molteno and Kennedy, 2009) and favored an iron mineral-based mechanism for magnetoreception as described in the section above. Although speculative, it could be possible that like in birds, parallel processing of map (iron mineral-based) and compass (electric induction) information by two sensory modalities might occur in elasmobranchs, but evidence for that would be needed in the future.

To conclude, the mechanism(s) of vertebrate magnetoreception is (are) not easily unraveled. The evolution of magnetic sensors might have taken place several times independently. Therefore, a variety of analogously evolved sensor types might exist that function differently (Lohmann and Lohmann, 1993; Thalau et al., 2006) and may have differentiated from different tissues (Semm et al., 1980; Demaine and Semm, 1985; Phillips and Borland, 1992b). A recent study identified a new trigeminal brain pathway that is potentially transmitting magnetic map information to multisensory integration centers (Kobylkov et al., 2020). Knowledge of such central nervous relays might help to identify the integration of and the neuronal projections from multimodal magnetoreceptive sensory systems. More evidence is certainly needed from truly multidisciplinary approaches involving ethology as well as e.g. spin chemistry, quantum physics, biochemistry, genetics, neuroanatomy and so on in the next decades (proposed by Hore & Mouritsen, 2016; Mouritsen, 2018) and more well-documented evidence is needed from additional vertebrate species as model animals. The brains of zebra fish (*Danio rerio*) are small and nearly transparent, which facilitates the application of many modern techniques like *in vivo* Ca<sup>+</sup>-imaging and screening for neuronal activity markers upon magnetic stimulation (Myklatun et al., 2018). Strong behavioral evidence exists for a magnetic map sense and magnetic imprinting in partly marine fish (Putman et al., 2013, 2014, 2020). 40 years ago, evidence for magnetic compass orientation has been demonstrated in salmon fry (Quinn, 1980). Now, there is first evidence for the use of a geomagnetic compass in coral reef fish larvae (Bottesch et al., 2016; summarized in chapter 2 in this thesis).

#### **1.4.4. Calibration of celestial and magnetic compasses in birds**

Birds breeding in the arctic polar circle face steep magnetic inclination angles and particularly high temporal variation of the magnetic field due to daily fluctuations (Skiles, 1985). As a result, the almost vertical magnetic field vector in the arctic polar circle (Figure 2) might not contain any meaningful directional information for birds due to sensory limitations (Lefeldt et al., 2015). Following a magnetic loxodrome orientation, i.e. orientation along magnetic field strength isolines (Imboden and Imboden, 1972; Gudmundsson and Alerstam, 1998; compare Figure 2, B), was reported as the most probable in-flight mechanism for free-flying Eurasian birds (Åkesson and Bianco, 2017). At high latitudes however, orientation along magnetic isolines would result in birds circling around the polar circle (Åkesson et al., 2001; compare Figure 2, B). The opposite is true at the magnetic equator, where the magnetic inclination is close to parallel to the earth surface (see Figure 2). Consequently, the geomagnetic field might contain only ambivalent, axial directional information for the unipolar inclination compass in birds (Schwarze et al., 2016b). Birds migrating across the Polar- and/or equatorial regions seem obliged to use celestial compasses for geographic reference in addition to their innate magnetic compass. Furthermore, a certain flexibility in the prioritized use of one compass system or the others (i.e. magnetic or celestial) must exist, depending on their reliability and availability (Muheim et al., 2003; Åkesson and Bianco, 2017).

##### Compass calibration in experienced adult birds

North American migrants face a particularly high magnetic declination, i.e. a high directional discrepancy between magnetic and geographic North. Additionally, the declination changes rapidly during longitudinal movement. Frequent calibration of the diverging magnetic and geographic information appears to be necessary and it crystallized that celestial compasses calibrate the magnetic compass in North American birds (Able and Able, 1996, 1997; Cochran et al., 2004; Muheim et al., 2006).

For European birds on the other hand, geographic and magnetic deviations are rarely as big, and a hierarchical calibration order of compass systems has been proposed (e.g. Witschko and Witschko, 1975a+b; Muheim et al., 2006; but see Chernetsov et al., 2011). In most - but not all - European bird species tested so far, the geomagnetic information seemed to calibrate celestial compasses (Bingman, 1987; Witschko and Witschko, 1990; but see Chernetsov et al., 2011; Guinchi et al., 2015; Åkesson, et al., 2015). Many contradicting results have been raised over the last decades, which led to opposing conclusions of the predominant compass

cue. It is however important to note, following the comprehensive arguments published in Pakhomov et al. (2017), that (1) many of the contradicting observations might emerge from differences in experimental design. There exists no established unified testing paradigm across research groups. Experimental setups differ for example in the viewing angle of the celestial sphere granted to the tested birds or the exposure time to the cue conflict before testing (Muheim et al., 2009; Moore and Phillips, 1988; but Wiltschko and Wiltschko, 1974; Sandberg, 1991; Able and Able, 1995b). (2) The experimental cue conflict situation in some orientation experiments might be too unnatural, since deviations of 90°, as used in most cue-conflict experiments, do not occur in nature regularly (Able and Able, 1993). Therefore, orientation behavior in funnel experiments under such unnatural conditions does not necessarily imply that the bird would behave accordingly in the wild (Pakhomov et al., 2017). (3) The migratory decisions made by a bird in the wild can be influenced by a wide variety of environmental factors and the bird's individual experience with them. Therefore, a rather flexible combination of environmental cues used by different individuals based on experience could benefit migratory success more than to rely merely on one potentially erratic calibration cue in a stiff hierarchical manner (Able and Able, 1993; Able and Able, 1996; Mouritsen, 2015). Pakhomov et al. (2017) reasonably argued that (4) middle-distance migrants like most European songbirds could in theory afford greater deviations from their programmed route to compensate for later in the next leg of migration than long-distance migrants. Additionally, experienced birds can rely on true navigation skills (chapter 1.1.1 in this thesis), which enables them to compensate for navigational errors en route. In summary, the take-off direction of an experienced bird – which is the main aspect of migration tested in cue-conflict experiments in orientation funnels – might not be as important to the migrant as believed, given that exploratory deviations from the ideal route could easily be compensated for later. In that sense, it is very plausible that a bird might chose a very rough estimate of the correct migratory take-off direction - especially in conflicting cue situations - and once aloft explore the ideal wind channels, travel height, geographic formations to follow, and so on. To conclude these thoughts, many more cue-conflict experiments with free-flying birds (e.g. Cochran et al., 2004; Chernetsov et al., 2011; Akesson and Bianco, 2017) are needed to unravel cue-weighting processes in experienced birds.

### Compass calibration in inexperienced juvenile birds

Calibration processes between information from the independent celestial and magnetic compass systems used by experienced birds take place on a frequent and flexible basis (Able and Able, 1995a, 1996; Cochran et al., 2004; Muheim et al., 2006; Liu and Chernetsov, 2012). However, inexperienced juvenile birds prior to their first migration are believed to possess a rather fixed compass hierarchy to determine the genetically inherited migratory direction (Able and Able, 1990a, 1990b; Bingman, 1984; Wiltschko and Wiltschko, 1988b; Able and Able, 1997). On their first migration they cannot rely on experience-based weighing mechanisms and most probably not on map information (Chernetsov et al., 2011; Mouritsen, 2018; Chernetsov et al., 2020). Therefore, they need to establish functioning compasses including a determined calibration mode prior to their first migration. The celestial compasses have to be learned (see chapter 1.2.1 and 1.2.2.) and for the development of a functional star compass in particular, a sensitive learning period during ontogeny has been suggested, after which the star compass and the calibration process of the magnetic compass were believed to be fixed (Emlen, 1970, 1972; Michalik et al., 2013). Ample evidence has been provided for the calibration of the magnetic compass upon celestial rotation during early development (under artificial starry skies: e.g. Wiltschko et al., 1987; Able and Able, 1990a; Michalik et al., 2013; natural presentation of the sky: e.g. Able and Bingman, 1987; Able and Able 1990b, 1990c), and ample evidence exists for no calibration of celestial compasses by magnetic information (Bingman, 1984; Wiltschko and Wiltschko, 1988b; Able and Able, 1997). Colleagues and I (Alert et al., 2015b) found that juvenile European robins (*Erithacus rubecula*) that did not experience any celestial rotation or only non-sense artificial star compass cues before the onset of their first migration, their magnetic compass would be defective or mis-calibrated (Alert et al., 2015b).

This study has been published in an international journal (*Scientific Reports*). I did not contribute to the design and carry-out of the experiments, but only assisted in hand-raising a part of the birds tested in these experiments. Therefore, I refer the reader to the published full text version of the paper (Alert et al., 2015b) and only shortly summarize this study here: We hand-raised European robin (*E. rubecula*) nestlings to very precisely control the perceived environmental cues during early life. After birds were self-sufficient, artificial celestial information was experimentally put into conflict with natural geomagnetic information



throughout the early development (Figure 6, A). During the first autumn migratory season, a mis-calibration of the magnetic compass by artificial, nonsense celestial cues during early life

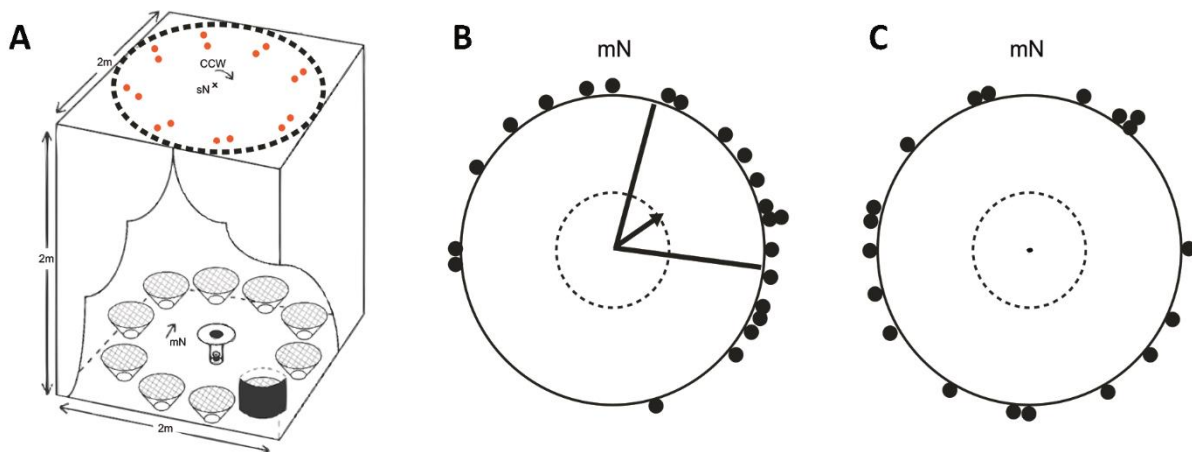


**Figure 6: Recalibration of the magnetic compass in birds that were granted access to natural celestial cues prior to their spring migratory season.** A) Sketch of the experimental star test chambers setup. Birds were placed in funnels positioned in a circle in the nights during the pre-migratory phase in early life. Each bird experienced a different direction of the center of rotation but had continuous access to the natural geomagnetic field. During the birds' first autumn migratory season, they were unable to show a species-specific south-westerly orientation in the star test chambers (data not shown). B) Half the group was kept in an outdoor aviary prior to the following spring migration with full access to celestial cues and the geomagnetic information. These birds oriented towards their species-specific direction in magnetic huts in the presence of geomagnetic information only during the following spring migratory season. They seem to have re-calibrated their compass systems to establish a functional magnetic compass. C) Birds that were kept indoors over the winter and therefore had no experience with meaningful celestial cues remained unable to establish a functioning magnetic compass. A) Modified after Michalik et al., 2013; B) and C) Modified after Alert et al., 2015b.

appeared to have led to disoriented birds in the magnetic field during nightly tests in *Emlen* funnels in magnetic huts. In the following period of late winter and early spring, these birds with a mis-calibrated magnetic compass were separated into two groups: birds were either (1) continuously kept in a windowless room indoors, or (2) transferred to outdoor aviaries granting them full access to natural celestial cues. In the following spring migratory season, the birds were asked to orient according to magnetic information in the magnetic huts in absence of celestial cues at night. The birds in the aviary group were now able to show species-specific spring migratory direction towards the north-east according to their magnetic compass (Figure 6, B), while the indoor group remained disoriented as in the preceding autumn (Figure 6, C). This results provided the novel finding that birds raised indoors with no access or access to artificial nonsense celestial cues were able to establish a functional magnetic compass later in life, extending the sensitive period for celestial compass learning beyond the first autumn, which has traditionally been considered its limit (Emlen, 1970, 1972; Able and Able, 1995a, 1996; Michalik, 2013).

## 1.5. Aims of my Ph.D. thesis

In my PhD thesis, I studied mechanisms of compass orientation involving celestial and magnetic cues in different vertebrates on the behavioral and neurophysiological level. I aimed to answer two major questions:

### ***(1) Do coral reef fish larvae use a magnetic compass to orient at night?***

Many model animals have been demonstrated to perceive the geomagnetic field, but the location and identity of the sensor(s) for this remarkable capability are still heatedly debated. Colleagues and I investigated the potential capability of coral reef fish larvae to orient according to geomagnetic compass information at night. This capability bears the possibility of a precise orientation system in this species and might help in the longer-distance phase of their natal homing. Therefore, colleagues and I tested freshly settled larvae of the cardinal fish species *Ostorhynchus doederleini* at a reef located in the Great Barrier Reef, Australia. The facilities of the One Tree Island research station offered the possibility of experiments in a natural geomagnetic field vastly undisturbed by anthropogenic noise. Because visual guidance of orientation by celestial cues during the day could influence the outcome of our magnetic experiments, we set up our experiments in a cleared basement storage room at night, which also allowed for exclusion of any other light sources. We were able to test magnetic compass orientation using Helmholtz coil systems under normal and changed magnetic field conditions at night, in absence of any other orientation cues. This study has already been published in a high-ranking international journal (Bottesch et al., 2016, *Current Biology*).

### ***(2) Do birds perceive polarized light information?***

Among the most pressing gaps in bird migration research is the missing unequivocal evidence for sensitivity to and the use of skylight polarization patterns in birds. Behavioral experiments in the past led to controversial and ambiguous data because of the uncertain influence of reflection- and light intensity artifacts on some results. Therefore, the major aim of my PhD thesis was dedicated to find approaches enabling me to answer the question whether polarization sensitivity exists in birds. I used two independent approaches to tackle the problem from different angles: In electrophysiological recordings from the retinal ganglion cells in chicken, a colleague and I investigated the validity of promising cell responses collected by former colleagues in electrophysiological extracellular recordings from the retinal ganglion

cell layer in domestic chicken as a response to polarized light stimulation. In their experiments, a subset of ganglion cells in the birds' retina appeared to encode the e-vector of polarized light. If validated by my additional investigations, such evidence would directly demonstrate the sensory capability of the avian visual system to process polarized light information. After tuition by the original authors, a colleague and I replicated the original study and conducted a series of additional control experiments that were necessary to exclude any alternative explanations for the observed bimodal cell responses to a 360° turn of a polarizer in retinal ganglion cells. These control experiments included the investigation of photoreceptor tilt at the recording sites, which could lead to artificial polarization sensitivity in the photoreceptor outer segments due to transverse dichroism in vertebrate photoreceptors. For this approach, we needed to find a structural fixation method to conserve the tissue as close to the recording condition as possible and thereafter visualize the immunohistochemically stained opsins in cone outer segments on a confocal laser scanning microscope (CLSM).

In a second, behavioral approach, I designed and performed experiments with the aim to demonstrate polarization vision in songbirds. Using LCD monitor screens, I was able to present selected stimuli to three songbird species that triggered strong behavioral responses in the tested birds, i.e. optomotor responses and escape behavior. Upon removal of the front polarizing sheets of the LCD monitor screens, these stimuli were presented in polarization contrast which is in turn was only visible to animals that possess the sensory basis to detect polarized light. Consequently, comparably strong behavioral responses to the stimuli presented on manipulated and intact LCD monitor screens would provide strong evidence for polarization vision and directly indicate the necessarily underlying sensory prerequisites for polarization sensitivity in birds.

## 2. Magnetic compass orientation in coral reef fish larvae

The following results of my colleagues' and my work on coral reef fish larvae at One Tree Island Research Station, Capricorn Bunker Reef Group, Great Barrier Reef, Australia, have already been published in a high-ranking international journal (Bottesch et al., 2016, *Current Biology*) and have been presented at international conferences (e.g. *ASAB Winter Meeting*, London; *Behaviour 2017*, Estoril). In several internal revision sessions with all co-authors (namely Prof. Dr. Gabriele Gerlach, Maurits Halbach, Andreas Bally, Prof. Dr. Michael J Kingsford and Prof. Dr. Henrik Mouritsen), the manuscript was polished for the optimal wording and comprehension. Rewording here would not benefit the presentation of our study. Therefore, I recite the published full-text version of our work (Bottesch et al., 2016).

Many coral reef fish larvae spend days to months in the open ocean before settlement on coral reefs (Brothers et al., 1983). Early in development, larvae have limited swimming capabilities (Fischer et al., 2000) and will therefore be greatly affected by currents. This can potentially result in dispersal distances of tens of kilometers (Gerlach et al., 2007). Nevertheless, up to 60 % of surviving larvae have been shown to return to their natal reefs (Gerlach et al., 2007). To home, the larvae must develop strong swimming capabilities and appropriate orientation mechanisms. Most late-stage larval reef fish can, after being passively drifted for days to weeks, swim strongly (Fischer et al., 2000), and *Ostorhynchus doederleini* larvae have been shown to use chemotaxis to identify their natal reef once in its vicinity (Gerlach et al., 2007) and a sun compass for longer distance orientation (Mouritsen et al., 2013) during the day. But how do they orient at night? Here, we show that newly settled fish caught at One Tree Island (OTI) at the Capricorn Bunker Reef Group (Great Barrier Reef) can use geomagnetic compass information to keep a southeast heading. This behavior might help them return to their natal reef in the absence of any celestial cues at night.

Over the years, DNA microsatellites have shown that up to 60% of freshly settled *O. doederleini* at OTI could be assigned to the adult population of OTI with a probability of 85% and that the adult populations of the four different reefs located only 4 to 20 km apart within the Capricorn Bunker Reef group can be separated genetically (Gerlach et al., 2007). These observations indicate strong and persistent larval homing. A hydrodynamic model of the predominant tidal and ocean currents prevailing at the Capricorn Bunker Reef Group suggests dispersal distances of up to 50 kilometers towards a north-northwest direction after 8 days

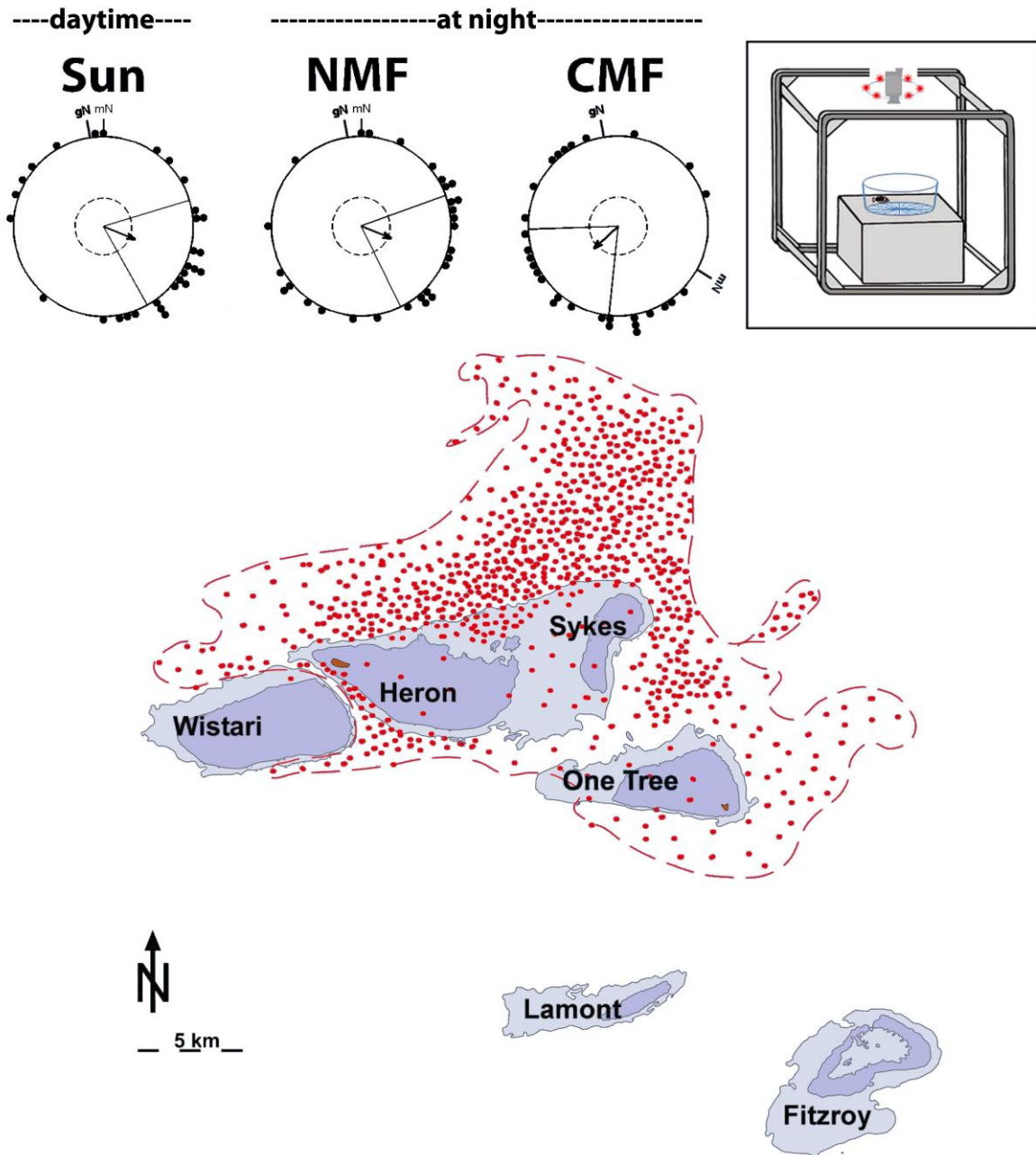


**Figure 7: Settlement-stage cardinal fish *O. doederleini* can use a magnetic compass to home.** Center: A hydrodynamic model of the tidal and NNV drift currents prevailing at Capricorn Bunker Reef Group, Australia illustrates the expected distribution of passively dispersing particles (red dots) 8 days after release from the One Tree Reef (modified after Gerlach et al., 2007). Settlement-stage *O. doederleini* were individually tested in an orientation bowl. For sun compass experiments during the day, the fish were tested under clear sunny skies. At night, the fish were placed inside the 99% homogenous center of a Helmholtz coil (Insert, top right). The headings of the fish were recorded by an overhead infrared video camera. The polar plots at the top of the figure show the spontaneous compass orientation of the fish under clear skies during the day (Sun), and at night in the absence of any celestial cues in the natural magnetic field (NMF) and in a magnetic field turned 120° clockwise (CMF). Each dot at the circle periphery indicates the mean orientation based on 3-5 tests of one individual fish in the given condition. Arrows indicate the group mean vectors. Lines flanking the group mean vector indicate the 95% confidence intervals for the group mean direction. The length of the vector,  $r$ , is calculated by vector addition and serves as the statistical measure of directedness. The dashed circles indicate the radius of the group mean vector needed for significance according to the Rayleigh Test for  $p < 0.05$ ,  $p < 0.01$ ,  $p < 0.001$ , respectively. From Bottesch et al., 2016.

(Figure 7, center; Gerlach et al., 2007). To counter this drift current direction and successfully home to their natal site, reef fish larvae have to be able to use compass information from the environment during both the day and the night. Mouritsen et al. (2013) reported data from sun compass experiments and demonstrated that settling and newly settled *O. doederleini* show a significant directional preference towards the south-southeast in orientation experiments during the day. In two consecutive years (2014 and 2015), we were able to replicate these data (Figure 7, Sun). Under clear skies, the group mean orientation of newly-settled fish was directed significantly towards the southeast (Figure 7, Sun; mean direction:  $112^\circ$ ,  $r = 0.382$ ,  $n = 30$ ,  $p = 0.011$ , Rayleigh test). These results confirm that a celestial compass is used for orientation in this cardinal fish species during the day. But how do they orient during the night when the sun is not available?

During the night, a star compass and a geomagnetic field compass are known to provide stable information for orientation in well-studied migratory species such as birds (Wiltschko and Wiltschko, 1995c; Mouritsen, 2015). But the stars are often unavailable to a larval fish in the open ocean because of overcast weather and/or water surface turbulences. In contrast, the geomagnetic field potentially provides a constant source for directional information available on all nights.

We therefore tested the spontaneous orientation responses of freshly settled *O. doederleini* during the night inside Helmholtz coils, which allowed us to manipulate the properties of the geomagnetic field in the absence of any celestial cues (Figure 7, top right insert box). In the unchanged, natural geomagnetic field (NMF, mean of measurements:  $B = 50607 \pm 166$  nT [Standard Deviation (SD)],  $D = 9^\circ$ ,  $I = -52.96 \pm 0.25^\circ$ [SD]), the group mean orientation of the fish was significantly oriented towards southeast (NMF mean direction:  $112^\circ$ ,  $r = 0.363$ ,  $n = 29$ ,  $p = 0.021$ , Rayleigh test; Figure 7, NMF), which is almost identical to the headings of the simultaneously caught settlers tested during the day for their sun compass orientation (Mardia-Watson-Wheeler (multi-sample):  $W = 0.693$ ,  $p = 0.707$ ; see Figure 7, compare Sun vs. NMF). These results indicate that *O. doederleini* are capable of orienting in the appropriate SE direction during the night, even when celestial orientation cues such as the sun and the stars are unavailable.

To test whether the fish used the available magnetic compass cues to keep the appropriate SE orientation, we experimentally turned magnetic north 120 degrees clockwise while we kept the magnetic field intensity and inclination angle identical to One Tree Island NMF values

(changed magnetic field [CMF], mean of measurements:  $B = 50691 \pm 210$  nT [SD],  $D = 129 \pm 0.78^\circ$ ,  $I = -52.96 \pm 0.23^\circ$  [SD]). When the fish were tested in the CMF, they turned their orientation  $115^\circ$  clockwise (CMF mean direction:  $227^\circ$ ,  $r = 0.367$ ,  $n = 29$ ,  $p = 0.019$ ; Figure 7, CMF) compared to their mean orientation in the unchanged geomagnetic field. The orientation of the fish in the CMF was significantly different from the orientation of the same fish in the NMF (Mardia-Watson-Wheeler test:  $W = 9.673$ ;  $p = 0.008$ ; and the 95% confidence intervals for the mean direction in the NMF and CMF groups did not overlap; see Figure 7, compare NMF vs. CMF). Furthermore, the orientation direction in the CMF corresponded well to the expected  $120^\circ$  clockwise change compared to the NMF (the 95% confidence interval broadly includes a  $120^\circ$  clockwise change; Figure 7, compare NMF and CMF).

We conclude that *O. doederleini* can use geomagnetic compass information for their directional choices at night and note that the observed SE directional swimming would help to counter the long-distance NNW drift predominant at the Capricorn Bunker Reef Group (Gerlach et al., 2007). We also suggest a two-phase orientation mechanism in dispersing reef fish larvae: first an innate compass mechanism based on global cues, e.g. geomagnetic information and celestial cues, in the long-distance navigation phase for swimming into the proper direction followed by a homing process to identify the natal reef based on more local cues such as odors, sounds and/or landmarks (Gerlach et al., 2007; Mouritsen et al., 2013; Wiltschko and Wiltschko, 1995c; Mouritsen, 2015). One prediction from this hypothesis of an 'innate adaptive homing orientation' is that fish larvae dispersed from islands with differently directed predominant currents should spontaneously orient in different compass directions that would maximize the probability of returning to the natal reef. This prediction should be tested in the future and is already supported by in situ diver observations suggesting that the orientation of the coral reef fish *Chromis atripectoralis* differed regionally (Leis et al., 2015). Although orientation and homing using the geomagnetic field is well known in birds (Wiltschko and Wiltschko, 1995c; Mouritsen, 2015) and sea turtles (Putman et al., 2011), and empirical evidence of geomagnetic imprinting has been found in salmon (Putman et al., 2013; Putman et al., 2020), studies on magnetic compass orientation in fish larvae are still scarce (Quinn et al., 1980, but see O'Connor and Muheim, 2017); our study demonstrates that reef fish larvae can use a magnetic compass to orient at night.

Soon after our publication, a study by O'Connor and Muheim (2017) demonstrated that coral reef fish *Chromis atripectoralis* larvae can use a geomagnetic compass during daytime

(O'Connor and Muheim, 2017). Future studies on coral reef fish larvae could focus on the sensory mechanism underlying larval magnetoreception and could investigate the potential similarities or differences to the unipolar inclination compass of birds and other vertebrates.

## **2.1. Experimental procedures**

All experiments in this study were conducted between 2013 and 2015 at One Tree Island (23.51 S, 152.09 E), in the Capricorn Bunker Reef Group in the southern Great Barrier Reef, Australia (Figure 7, center). A total of 42 cardinal fish *Ostorhynchus doederleini* larvae were tested in these experiments (see details in supplemental Table S1-S2 in the published version of the study (Bottesch et al., 2016), notice that many fish were tested both in the sun compass and the magnetic compass experiments).

Although it is known that reef fish larvae can change their behavior profoundly in the time around settlement, Mouritsen et al. (2013) already showed that there is no difference in the orientation behavior between pre-settlement *O. doederleini* caught in crest nets and *O. doederleini* settlers caught on patch reefs a few hours after their arrival at the reef (Mouritsen et al., 2013). Due to this knowledge and our experience with low catch rates with crest nets or light traps, we decided to collect newly settled *O. doederleini* at artificial patch reefs inside the lagoon early every morning. Pre-settled fish enter the reef during the night (Kingsford, 2001), so our study animals were caught only a few hours after their arrival at the reef. Experimental fish were kept in individual home aquaria (30 x 15 x 15 cm) supplied with oxygenated, fresh seawater and coral rubble. Temperature was kept constant around  $29 \pm 2$  °C. Fish were fed *Artemia sp.* and fresh plankton, ad libitum. The *O. doederleini* measured 10-14 mm at the start of the tests and 12-15 mm at the end of the experiments. To reduce any potential effects of developmentally induced changes in orientation behavior in our data, we tested all fish in a short as possible period of time after capture.

The sun compass experiments were conducted in January-February 2014 and 2015 at the same location on the island and using the same protocol as in Mouritsen et al. (2013): Individual fish were tested in orientation bowls allowing the fish a good view of the sky all the way down to the horizon. They were only tested under clear sunny skies between 8:00 and 11:00 in the morning when the sun is positioned clearly in the east and between 14:00 and 17:00 in the afternoon when the sun is positioned clearly in the west during this time of the year. The bowl was placed on a levelled wooden platform on which a sundial of black lines



was drawn in 22.5-degree segments relative to magnetic North (Mouritsen et al., 2013). A finer angular resolution for recording fish position does not make sense given the size of the fish and the size of the bowl, but with 40 directions recorded, this resolution is more than sufficient to record the fish's preferred direction (Mouritsen et al., 2013). Each fish was tested separately. A given sun compass test was performed as follows (Mouritsen et al., 2013): The fish was transferred from its home aquarium in the wet lab to the testing bowl on the beach with a small plastic jar. It was carefully released into the middle of the bowl. After ca. 60 sec of acclimation, its geographic position relative to the center of the bowl was recorded in 30 sec intervals for the next 20 min (Mouritsen et al., 2013). The observer simply noted down, which of the black lines in the sun dial was closest to the head of the fish.

As in our earlier experiments (Mouritsen et al., 2013), the fish spent the vast majority of their time hovering somewhere near the edge of the bowl. The fish position relative to the center of the bowl was used as the directional measure rather than their heading, since they can move no further in any given direction once it reaches the edge of the bowl (Mouritsen et al., 2013). Most of our fish clearly showed a preferred direction by either hovering fairly stationary or by slowly swimming back-and-forth along the edge of the bowl around their preferred direction, or by moving away and quickly returning to the edge near the preferred direction (Mouritsen et al., 2013). This behavior confirms that position in the bowl relative to the center of the bowl is the most relevant orientation measure [S1]. A description of the circular statistical analysis follows below in the respective paragraphs.

The observer sat on a stool next to the bowl. As in Mouritsen et al. (2013), the observer systematically rotated position relative to the bowl (N, E, S, or W) between tests. It was shown in Mouritsen et al. (2013) that the observer had no significant effect on the directional choices of the fish. At the end of the test, the fish was transferred back to its holding tank. Between tests, the bowl was cleaned and the water in the test bowl was replaced by fresh and filtered OTI reef sea water. The raw data for the sun compass tests can be found in supplemental Table S1 in the published version of the study (Bottesch et al., 2016).

The magnetic compass experiments in this study were conducted in January-February 2013, 2014 and 2015. For the magnetic compass experiments, the local magnetic field values at One Tree Island were obtained by the Geoscience Australia online AGRF Calculations ([www.ga.gov.au](http://www.ga.gov.au)) (Main Field Intensity = 50851 nT; Declination = 9°, Inclination = -52.93) and

measured daily with a Meda<sup>®</sup> 3-axis hand-held magnetometer at several locations on the island (Mean of measurements: Main Field Intensity = 50797 ± 51 nT [SD]; Declination = 9 °; Inclination = -53.10 ± 0.12 ° [SD]). Two independently working sets of Helmholtz Coils (each of the Helmholtz coils were single-wound, 1-axis, ~ 1 m diameter) were used. The two Helmholtz coil sets (see Fig. 1, insert box, one Helmholtz coil set consists of two single coils) were set up 5 m apart and visually separated in a windowless, wooden room. Visual cues, e.g. the moon and the stars can therefore be excluded as directional cues during our experiments. All light sources from the equipment were covered and electronic devices were placed as far as possible from the setup to exclude phototaxis, electromagnetic disturbances and other potential artifacts. The magnetic compass experiments were conducted in darkness, but not in complete darkness, since some leftover diffuse stray light from various natural and artificial sources could not be completely screened. All ceiling lights were switched off 2 hours before testing. Handling of the fish was performed under dim red light from head torches.

The experimental magnetic fields (NMF and CMF condition, respectively) were generated by sending current through the two independent sets of Helmholtz coils independently using two Kepco<sup>®</sup> Bipolar Operational Power Supplies (BOP 50 – 4M), one for each set of Helmholtz coils. We carefully measured that the induced currents in one set of coils did not alter the applied magnetic field values of the other set of coils 5 meters away. In the changed magnetic field condition (CMF), a declination of +129° (CW) was generated without substantially altering the main field intensity (50691 ± 210 nT [SD]) and the inclination (-52.96 ± 0.23 ° [SD]) of the local magnetic field vector. In the unchanged normal magnetic field condition (NMF), the same amount of current as in the CMF experiments was sent through resistors instead of through the coils. This served both as control for putative noise (from the power supplies) and temperature artifacts as well as a control condition testing whether the fish could orient in their typical SE direction at night without access to celestial cues.

As mentioned above, the magnetic orientation experiments were only done at night. Half an hour after sunset, the fish were transferred in the dark from their home aquaria into small bowls in the 99% homogenous center of a set of Helmholtz coils where they were acclimatized to their new magnetic environment for at least 50 minutes as a safety measure because our experience from bird orientation studies suggests that it may take longer for animals to realize that a magnetic field has changed than it would take them to realize that the position of the

sun has changed. Within the experimental magnetic field, a single fish at a time was transferred into a clear plastic circular bowl (17 cm diameter and 6 cm water depth) at the top of the 99% homogeneous region within the given Helmholtz coil set. The orientation of the fish was monitored by videotaping them using an overhead infrared video camera (infrared diodes: 960 nm wavelength and invisible for the fish) (Figure 7, insert box). However, before we started to record magnetic orientation data for a given fish, we allowed the fish to acclimate to the testing bowl for 5-15 minutes. The vast majority of the tested *O. doederleini* did not show signs of stress (inactivity or monotonous circling) after 5-15 min acclimatization in the new environment. This stands in contrast to other species, such as some Pomacentrids, which were not behaving well in the setup during earlier preliminary sun compass experiments (*P. coelestis* were stressed and completely inactive).

The infrared video camera was aligned with magnetic north, so we could easily assign a magnetic compass direction to the fish's position with respect to the center of the bowl. One test lasted 20 minutes during which we noted the position of the fish 40 times, one data point every 30 seconds. We chose this paradigm because it has been successfully used in the previous sun compass experiments (Mouritsen et al., 2013) and thus ensures comparability of sun and magnetic compass test results, and because preliminary tests from the previous years suggested that, in the vast majority of cases, no significant change in the orientation occurred depending on whether 10, 20, or 30 minutes of behavior was observed. The 20 minutes is a good compromise between sufficient statistical power on the one hand and time-efficiency on the other.

After each magnetic testing session, the testing bowl was also carefully rinsed with fresh and filtered sea water as in the sun compass experiments to exclude that e.g. olfactory cues could be transferred from one tested animal to the next.

We pseudo-randomized the order of the treatments so that all fish were tested in both sets of coils, evenly often in both conditions (NMF and CMF), at different times of the night and equally spread across the whole testing period. Due to serious time pressure to conduct our experiments in each season, we were not able to intersperse the order of the NMF and CMF treatments on a trial-by-trial basis for every individual, but we made sure that an equal amount of fish were tested in CMF first or NMF first, respectively (for full details, see supplemental data Tables S1-S2 in the published version of the study; Bottesch et al., 2016).

Both sets of coils were alternately used for NMF and CMF exposure, changing every 2-3 days. With these paradigms, we tried to ensure, as good as logistically possible on this isolated island, that any putative coil effects, learning effects, and/or sequential correlation could not affect the main results and conclusions of our work.

The evaluation of the raw data was done blinded and in the same way as described in (Mouritsen et al., 2013). Thus, all evaluation procedures were pre-determined (i.e. not modified/biased post-hoc). The analysis was performed in three consecutive steps. During each of these steps, mean angles were calculated according to conventional methods of circular statistics using the Rayleigh test as described in Batschelet (1981) and used in multiple previous studies, i.e. the mean vector was calculated by adding unweighted unit vectors pointing in each of the recorded mean directions divided by the number of tests with the given individual or by the number of individual fish tested, respectively (Batschelet, 1981; Wiltschko and Wiltschko, 1978; Wiltschko et al., 1993; Leis and Carson-Ewart, 2003; Zapka et al., 2009; Hein et al., 2010; Hein et al., 2011; Mouritsen et al., 2013b; Berenshtein et al., 2014; Engels et al., 2014; Schwarze et al., 2016). First, we calculated the mean direction of each individual test based on the 40 directions collected for a given fish during one 20 min testing period. To allow for assessment of both intra- and inter-individual variance, each of the fish was tested at least 3 times in the NMF condition and at least 3 times in the CMF condition (for exact details see Table S2 in the published version of the study; Bottesch et al., 2016). It is known from the vast literature on orientation tests with migratory birds that repeated tests are needed to determine the intended mean orientation direction of an individual animal with reasonable accuracy (e.g. Wiltschko and Wiltschko, 1978; Wiltschko et al., 1993; Zapka et al., 2009; Hein et al., 2010; Hein et al., 2011; Engels et al., 2014; Schwarze et al., 2016). Furthermore, by using average directions based on repeated tests of the same individuals, the number of experimental animals can also be significantly reduced, which is an important ethical consideration in modern biology. We used the Rayleigh test to gain an indication of the consistency of the orientation in the individual tests. For the purpose of calculation, we treated the repeated measures as independent (even though they are not) and used the very conservative  $p < 0.001$  level as an arbitrary threshold for inclusion in the further analyses. The few less consistently oriented individual tests were considered random and were excluded from further analyses (for details see Table S2A in the published version of the study; Bottesch et al., 2016). Second, the individual mean direction was calculated for each individual based

on the mean directions observed in the 3-5 tests with that individual. Third, the group mean vector shown in the circular diagrams in Figure 7 was calculated based on the mean orientations of the individual fishes tested in the NMF and CMF conditions, respectively. We required that the mean orientation vector of a given individual in both of the magnetic conditions exceeded a minimum cut-off  $r$ -value of 0.2. Fish with an individual mean vector shorter than the 0.2 cut-off  $r$ -value were considered too inconsistent in their orientation choices and were therefore excluded from the calculation of the group mean vector (for details see Table S2B in the published version of the study; Bottesch et al., 2016). The reasoning for this additional exclusion threshold is that when an individual mean vector based on only 3-5 tests per individual results in an  $r$ -value below 0.2, the calculated direction is essentially meaningless (random) and the inclusion of such unreliable directions could potentially mask the orientation capabilities of the reliably oriented individuals on the group level. All statistical procedures used here are very similar to the standard procedures used elsewhere in studies of animal orientation behavior (e.g. Batschelet, 1981; Wiltschko and Wiltschko, 1978; Wiltschko et al., 1993; Leis and Carson-Ewart, 2003; Zapka et al., 2009; Hein et al., 2010; Hein et al., 2011; Mouritsen et al., 2013b; Berenshtein et al., 2014; Engels et al., 2014; Schwarze et al., 2016) and are identical to the methods used in our previous study of sun compass orientation in the same fish species at the same location (see Mouritsen et al., 2013). For full details on the individual tests, their sequence, and the mean orientations of all our tested fish, see Tables S1-S2 in the published version of the study; Bottesch et al., 2016).

### **3. Orientation by skylight polarization patterns**

The time around sunset has been demonstrated to play a crucial role in the compass calibration processes in birds (e.g. Moore, 1978; Sandberg, 1991, Cochran et al., 2004; Muheim et al., 2007). In the twilight period, when the sun (see chapter 1.2.1. in this thesis) has set below the horizon, but the first bright stars (see chapter 1.2.2. in this thesis) are not yet visible, sun-related secondary cues could be used for geographic reference. Horizon glow, hemispheric intensity gradients, the spectral composition of the sky (Coemans et al., 1994a) and skylight polarization patterns (Wehner, 1976) have been suggested (for review see Muheim, 2011) and would provide very reliable information at the time around dusk and dawn.

In this chapter, I give a detailed overview on the fascinating, but polarizing sensory mystery of sensitivity to polarized light in birds. After a description of the physical phenomenon of light polarization, and an overview of its biological use in nature (chapter 3.1. in this thesis), I will present the necessary sensory prerequisites for its perception in vertebrates (chapter 3.2. in this thesis). It is then necessary to review the different approaches used so far to demonstrate polarization sensitivity in birds (chapter 3.3. in this thesis) and to clarify the experimental pitfalls responsible for the - in my opinion - persistently unanswered question whether polarized light sensitivity in birds exists (chapter 3.3. in this thesis).

Using two distinct approaches during my PhD, I was not able to deliver a conclusive answer to the question whether birds were sensitive to polarized light (chapter 3.4. and chapter 3.5. in this thesis). If anything, my studies made it more doubtful that birds possess this sensory capability.

#### **3.1. Polarized light in nature and its biological use**

Light is a quantum mechanical phenomenon. Photons - the quantum amount of light energy - propagate through space in the form of an electromagnetic wave with certain frequencies, i.e. with a certain wavelength. These different wavelengths can be used by most animals to distinguish colors (Gegenfurtner and Kiper, 2003). Chromophores localized in retinal photoreceptors are specialized to maximally absorb light energy of discrete wavelength ranges. All the colors humans can distinguish are based on three different types of chromophores, i.e. three discrete channels for color vision (blue, green and red; Gegenfurtner and Kiper, 2003). Now imagine the color vision capabilities of mantis shrimp (e.g.

*Odontodactylus scyllarus*) that possess up to 12 such discrete channels (Cronin et al., 2001) or the tetra-chromatic visual system of birds extending into the UV as a discrete color channel (Rajchard, 2009). Besides color perception at the limits of our imagination, the polarization of light can be used as an additional form of vision in some invertebrate animals (e.g. mantis shrimp: Marshall et al., 2007; Chiou et al., 2008, 2012; cuttlefish: Temple et al., 2012; for review see Marshall and Cronin, 2014), but is completely indistinguishable for the eyes of others (e.g. humans).



**Figure 8: The polarization of light in nature.** Light scattered in the atmosphere (A) or reflected from smooth and dielectric surfaces (B) becomes linearly polarized. Note that the degree of polarization, i.e. the percentage of e-vectors in a ray of light propagating in the same plane, depends on the angle of scattering (maximum degree at  $90^\circ$ ; A) and refraction (maximum degree at Brewster angle,  $56^\circ$ ; B). The plane of polarization is perpendicular to the reflective/scattering surface. C: A photograph depicting the polarization of light in a natural scenery through a polarizing filter oriented in two perpendicular orientations (yellow double-arrows in C and D). Note that light polarized perpendicularly to the transmission axis of the polarizing filter (reflected polarized light off the water surface in C, bottom half; scattered polarized atmospheric light in D, top half; compare C and D) is not reaching the camera lens. A) and B) from Wehner, 2001.

Light emitted from the sun is unpolarized, i.e. the vibrational planes (electric vectors, e-vectors) of the photons in a discrete ray of light propagate with stochastic distribution (Figure 8, A, top left). When such a random distribution of e-vectors was biased towards one particular plane, the light is called partially linearly polarized. In nature, linear polarization of light is caused by scattering and reflection off dielectric and smooth surfaces, such as atmospheric gases (Wehner, 1976; Figure 8, A; natural example given in Figure 8, C vs. D, compare top halves), water (Horváth, 2014; Figure 8, B; natural example given in Figure 8, C vs. D, compare bottom halves), metals, glass, and basically all smooth surfaces, like stones, leafs and tree branches (Horváth and Hegedüs, 2014). The plane of emitted linear polarization is in parallel to the emitting surface (Wehner, 1976; Horváth, 2014). The proportion of photons vibrating with the same e-vector orientation in a beam of light is defined as the degree of linear

polarization, i.e. 0% is unpolarized light, and 100% is fully linearly polarized light. The maximal degree of linear polarization is achieved upon scattering in a 90° angle (Figure 8, A, C, D) and upon reflection in an angle of 54° (Brewster angle; Born and Wolf, 1999; Figure 8, B, C, D).

The detection of linearly polarized light has been suggested to be used (1) by various groups across the animal kingdom, e.g. dung beetles (reviewed in Dacke, 2014), ants, bees and wasps (reviewed in Zeil et al., 2014), fruit flies, crickets and butterflies (reviewed in Heinze, 2014), aquatic insects like dragonflies (reviewed in Horváth and Csabai, 2014), crustaceans like crabs and shrimp (reviewed in Marshall and Cronin, 2014), cephalopods like cuttlefish and octopus (reviewed in Shashar, 2014), bony fish (reviewed in Roberts, 2014), amphibians like newts, salamanders, frogs and toads (reviewed in Meyer-Rochow, 2014a), reptiles like lizards, marine turtles, some crocodylian species and snakes (reviewed in Meyer-Rochow, 2014b) and birds like pigeons and diverse songbird species (reviewed in Åkesson, 2014) and (2) in numerous behavioral tasks, e.g. for improving object contrast (Lin and Yemelyanov, 2006), signaling (Cronin and Marshall, 2011), camouflage and camouflage breaking (Jordan et al., 2012; Shashar et al., 2000) and orientation (underwater: Waterman, 2006; on land: Wehner, 1976; reviewed in Horváth and Varjú, 2004). In terms of geographic orientation on land, atmospheric scattering of sun light provides a reliable pattern of linear polarization in the celestial sphere (Wehner, 1976; Figure 9). The degree of polarization gradually rises towards its maximum at a scattering angle of 90° between the observer and the sun (compare Figure 9, A and B). When the sun disk is close to the horizon at sunset or sunrise, a band with a maximum degree of linear polarization is bisecting the celestial sphere in the north-south axis (Figure 9). At all times, the e-vector propagates perpendicular to the plane between the sun and the observer (Figure 9, A and B, blue dashed lines). Therefore, the e-vectors in the band of maximum polarization run parallel to geographic north-south axis at dusk and dawn in this simplified example (Figure 9, B, blue dashed line). Behavioral experiments indicated the use of skylight polarization patterns in orientation in virtually all the polarization sensitive groups named above (for review see Horváth and Varjú, 2004). For the vertebrate groups however, the validity of some results originating in behavioral studies has been questioned due to potentially introduced light artifacts (more detail in chapter 3.3. in this thesis), especially in amphibians (Horváth and Varjú, 2004, pp. 317–323) and in birds (Coemans et al., 1990, 1994; Muheim, 2011). Furthermore, in most vertebrate groups, a hypothesis but no prove of a retinal sensor system has been demonstrated.



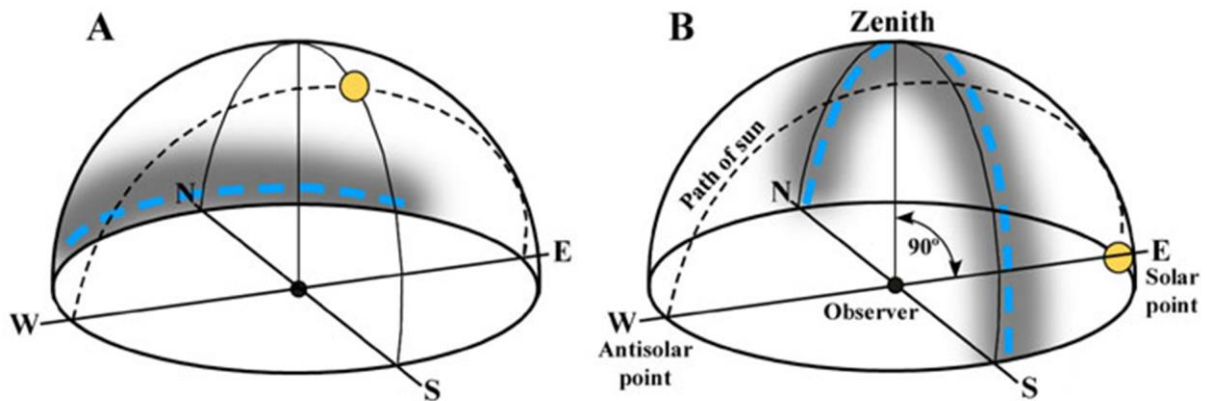


**Figure 9: The band of maximum polarization at different times of day.** Atmospheric reflections of sun light are polarized with a preferred e-vector orientation perpendicular to the plane observer - atmospheric molecules – sun. A band with maximal degree of polarization originates in a  $90^\circ$  scattering angle (dark gray band in A and B). The blue dashed lines in A) and B) show the orientation of the e-vectors within the strongly polarized band. At sunrise/sunset (B), the band of maximum polarization intersects the horizon in the North-South axis. Modified after Wellington 1974; Wehner 1976.

### 3.2. Sensory basis for polarized light sensitivity

The sensitivity to linearly polarized light of any visual system is founded on dichroic absorption in highly aligned chromophores (Snyder and Laughlin, 1975). Chromophores are the photosensitive molecules in photoreceptors in the eyes of vertebrates and invertebrates. Dichroism is the differential absorption of incoming light depending on the plane of polarization. E-vectors that are in parallel to the axis of highly aligned chromophores are absorbed maximally, whereas perpendicular e-vectors are absorbed minimally (Wehner, 1976). If all or most of the chromophores in one photoreceptor cell are aligned in parallel to each other, the cell is differentially excited by different e-vectors of linearly polarized light, i.e. the cell can be polarization sensitive (Wehner, 1976).

In rhabdomeric photoreceptors of insects and crustaceans, the axial alignment of the photosensitive molecules inside microvilli, combined with the aligned arrangement of microvilli inside the photoreceptor cells result in high dichroic ratios (Snyder, 1973). This is the well-documented basis for insect and crustacean polarization sensitivity (for review see Marshall and Cronin, 2014), even though little is known yet about the cellular processes of membrane anchoring.

In vertebrates on the other hand, the dichroic ratios of photoreceptors are typically low due to the rotational freedom and lateral diffusion of visual pigments in the fluid outer segment membranes (Hargrave, 2001; Figure 10, A and B) that are stacked perpendicularly to the incoming light (Wehner, 1976; Figure 10, A and B). A stochastic distribution of molecule

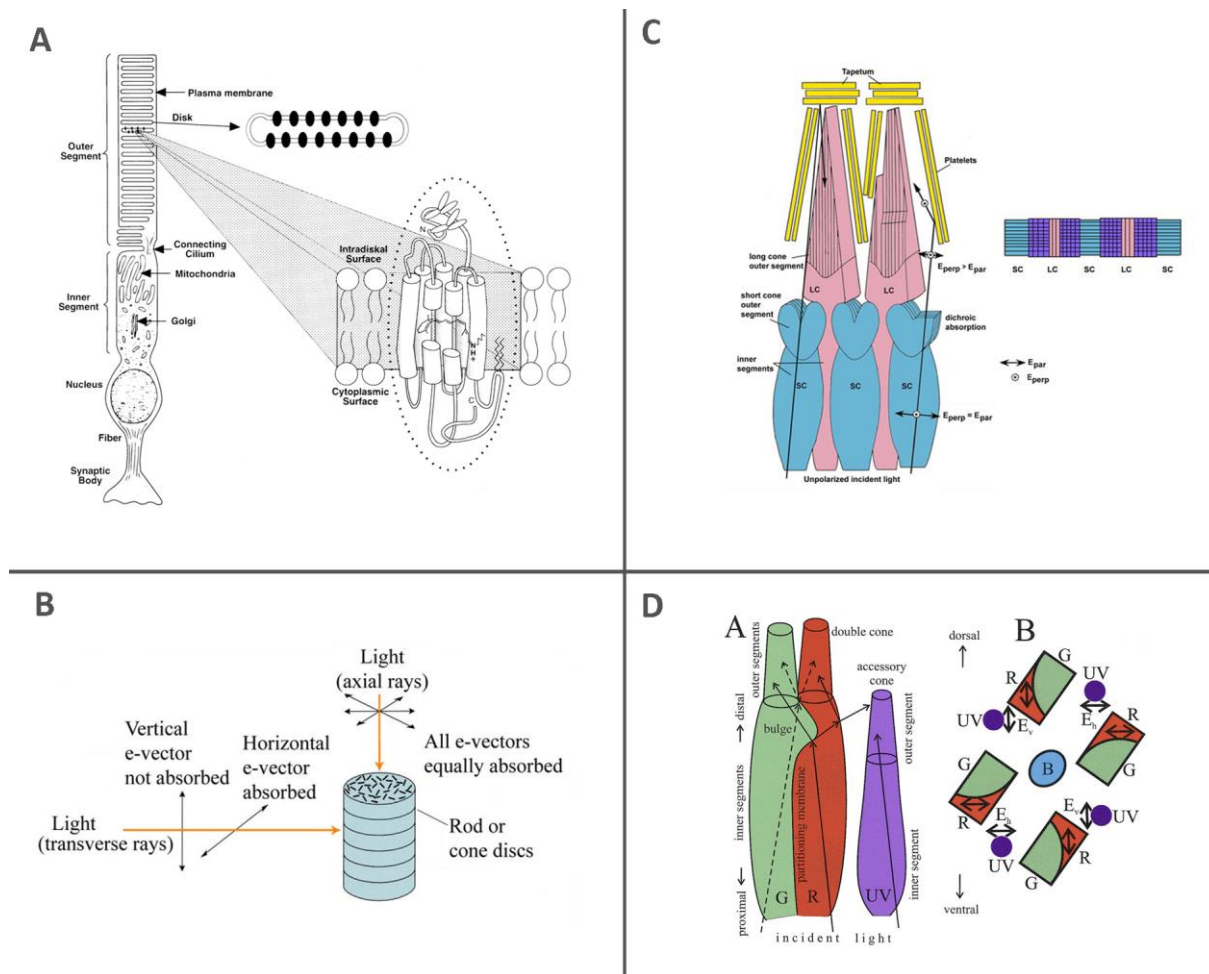


**Figure 10: The sensory bases of vertebrate polarization sensitivity.** A) Scheme of a rod photoreceptor. The disk membranes in the outer segments of vertebrate photoreceptors are stacked on top of each other and are highly in parallel to each other. The visual pigment is bound by transmembrane protein complexes and oriented in parallel to the membrane (blowup in A). B) Scheme of polarized light entering the disks axially or transversely. Due to a rotational freedom of the (rhod)opsins bound to the membranes, axially incoming light is equally absorbed irrespective of its e-vector orientation or degree of polarization. However, transversely entering rays of polarized light can be differentially absorbed. C) Specialized photoreceptor outer segments in the photoreceptors of bay anchovy (*Anchoa mitchilli*) have been reported to have their disc membranes stacked in an upright orientation, i.e. they are oriented transversely to the incident light (depicted in red and blue). Two types of photoreceptors, long cones (depicted in red) and short cones (depicted in blue), possess orthogonally arranged disc membranes, providing a structural basis for polarization contrast sensitivity in some anchovy species. Insert to the right: schematic top view onto the long axis of photoreceptors. D) In rainbow trout, the interstitial membrane that separates the primary and accessory cone in double cones forms a pronounced tilt. One hypothesis on polarization sensitivity in this species suggests the internal reflection of polarized light onto an adjacent UV cone (black arrows). The transverse orientation of incoming light would then provide the basis of polarized light sensitivity (see B). A) From Hargrave, 2001. B) After Bradbury and Vehrencamp, 2011. C) After Novales Flamarique and Hárosi, 2002. D) After Novales Flamarique et al., 1998.

orientation inside the membranes leads to indifferent light absorption regardless of the e-vector orientation of incoming light (Figure 10, B). However, the outer segment membranes are stacked highly parallel to each other, so light entering transversely to the long axis of the photoreceptor outer segment can result in dichroic absorption to a certain degree (Roberts et al., 2004; Figure 10, B). In specialized cones in the retina of some anchovy species, such a high

degree of chromophore alignment has been found in outer segments that are not orientated axially, but longitudinally to the incoming light (Novales Flamarique and Hárosi, 2002; Figure 10, C). Furthermore, a study revealed a higher than expected axial dichroic ratio in goldfish double cones (Roberts and Needham 2007). Highly ordered oligomeric arrays in the membranes of vertebrate photoreceptors might provide a basis for this high axial dichroism as a principle mechanism of polarization sensitivity in vertebrates (Kroeger et al 2003). A further hypothesis in fish includes internal reflections off platelets in the photoreceptor cells that transversely reflect the light back onto the outer segment (Novales Flamarique and Hárosi, 2002; Figure 10, C). In amphibians, axial dichroism in photoreceptors has been found outside the eye, in the pineal organ (Taylor and Adler, 1978). In birds, a hypothesis originally proposed for goldfish polarization sensitivity is the most prominent at the current time. In double cone photoreceptors which are the most abundant photoreceptors in birds (Kram et al., 2010), the shared membrane separating primary and accessory cone describes a prominent tilt which has been hypothesized to potentially reflect polarized light transversely onto the accessory cone or onto adjacent UV cones (Novales Flamarique et al., 1998; Figure 10, D). Electrophysiological recordings in goldfish were successful to demonstrate that such a sensory basis for polarization sensitivity - by complex response interactions of UV cones and double cones – might be possible (Ramsden, et al., 2008; Hawryshyn, 2010). However, several experimental approaches in fish were unsuccessful to demonstrate any behavioral response, including the presentation of dynamic polarization contrast in a foraging task and object avoidance (Pignatelli et al., 2011), and feeding in reduced versus enhanced polarized UV-light environment (Browman et al., 2006). In object discrimination tasks on the other hand, fish were successfully trained to polarization stimuli (Mussi et al. 2005). It appears that the ecological context and the type of stimulus presented might be crucial to demonstrate polarization sensitivity in an animal on the behavior level.

### **3.3. The question of polarized light sensitivity in birds**

*“False facts are highly injurious to the progress of science, for they often endure long; but false views, if supported by some evidence, do little harm, for everyone takes salutary pleasure in proving their falseness: and when this is done, one path towards error is closed and the road to truth is often at the same time opened”*

Darwin, 1871

The research on polarization sensitivity in birds had a very peculiar history. In 1950, Kramer observed that starlings continued to show oriented behavior in orientation cages when the sun was occluded from vision, but patches of blue sky were visible. Therefore, he assumed that skylight polarization patterns may assist bird orientation (Kramer, 1950). Two years later, Montgomery and Heinemann (1952) performed the first direct experiment on polarization sensitivity in homing pigeons. However, in an operant conditioning paradigm their birds could not be trained to distinguish a rewarded plane of polarization from the unrewarded perpendicular axis. With these results, the theory of polarized light sensitivity in bird was off the table for long.

Over 20 years later, Kreithen & Keeton (1974) and Delius et al. (1976) developed rather sophisticated approaches to test polarization sensitivity in pigeons. Kreithen & Keeton (1974) used negative reinforcement to increase the heart rate of their tested subjects whenever a rotating stimulus was presented. Trained successfully with a rotating cross-hair, the stimulus was replaced by a rotating polarizer in experimental trials. The heart rate was significantly increased in some of their pigeons (Kreithen and Keeton, 1974). Delius et al. (1976) found that pigeons could choose the correct lever in a skinner box associated with the e-vector orientation of linearly polarized overhead illumination. In the second part of this study, the authors found b-wave modulations in electroretinograms (ERG) from the pigeon eye that depended on the experimentally rotated incident e-vector orientation. Consequently, these positive findings - indicative of polarization sensitivity in pigeons - stimulated a train of orientation experiments with migratory birds in the following decades (see further below).

However, Coemans et al. (1990 and 1994b) replicated the behavioral experiments of Montgomery and Heinemann (1952) and Delius et al. (1976). They verified the negative results of the former and effectively demonstrated that the pigeon's choices in Delius et al. (1976) originated from light reflection artifacts, i.e. the choices of the birds were based on unintentionally introduced light gradients, caused by differential reflection of polarized light from walls that were perpendicular or parallel to the e-vector orientation, respectively. Note that comparable effect of artificial light gradients could probably account for the results indicating a polarization-dependency of magnetoreception in Muheim et al. (2016), who used a setup with similar reflective properties as the Skinner box used in Delius et al. (1976). In the same manner, Coemans et al. (1994b) suggested that Kreithen and Keeton (1974) may have conditioned their pigeons to an artificial intensity flicker caused by differential reflections of

polarized light, rather than by the rotation of the polarizer itself. Furthermore, Vos Hzn et al. (1995) replicated the ERG recordings from the pigeon eye (Delius et al., 1976), but carefully controlled for reflection artifacts during stimulation and applied quantitative statistical analysis of the retrieved wave forms. They found no evidence for polarization sensitivity in pigeons (Vos Hzn et al., 1995). Indeed, the authors were able to replicate the results of Delius et al. (1976) only when they intentionally introduced an artificial light intensity change (Vos Hzn et al., 1995).

More recently, Greenwood et al. (2003) was able to train migratory starlings and non-migratory quail to discriminate objects that differed in luminance contrast for a food reward. However, objects contrasted by different e-vector orientations were indistinguishable to the same birds (Greenwood et al., 2003). Comparable negative results were raised by Melgar et al. (2015) when they asked Zebra fishes to discriminate objects that were presented in polarization contrast on manipulated LCD monitor screens (Melgar et al., 2015).

To conclude, all well-controlled conditioning experiments conducted so far (Coemans et al., 1990, 1994b; Vos Hzn et al., 1995; Greenwood et al., 2003; Melgar et al., 2015) revealed negative results regarding polarization sensitivity in birds. But how about behavioral studies investigating the role of skylight polarization patterns in bird orientation?

In 1982, Able performed the first orientation experiment with migratory white-throated sparrows (*Zonotrichia albicollis*) in *Emlen* funnels, granting the sparrows a view of the sky only through linear polarizers (Able, 1982). When he altered the natural e-vector orientation of skylight polarization by rotating the linear polarizers, the birds changed their orientation accordingly (Able, 1982). Identical results were reported in further North American species in the following years (Moore, 1986; Able, 1989; Able and Able, 1995b). It is noteworthy at this point that these North American migrants possess a natural migratory direction along the geographic North-South axis and accordingly, in parallel to the (experimental) e-vector axis. However, blackcaps (*Sylvia atricapilla*; Helbig and Wiltschko, 1989) and European robins (*E. rubecula*; Helbig, 1991) showed similar directional choices as observed in North American species alongside the experimentally manipulated e-vector axis. These European birds usually show a species-specific migratory orientation towards the south-west, i.e. a compass course that is relative to the e-vector axis, not in parallel to it would have been expected (Helbig and Wiltschko, 1989). This “polaritactic” axial orientation response alongside the e-vector in orientation cage experiments is highly unnatural for European birds (Helbig and Wiltschko,

1989) and probably a result of light artifacts (Coemans et al., 1994b; for review see Muheim, 2011; but see Able 1989). Since polarized light in funnel-shaped cages is strongly reflected off the surfaces parallel to the e-vector and weakly reflected off perpendicular surfaces (Figure 12, A), a double light intensity gradient results inside orientation cages which might serve as a directional cue to the birds. Birds are highly phototactic and even unnatural visual cues can mis-calibrate natural compass systems (see chapter 1.2.1 and chapter 1.2.4. in this thesis). The behavioral responses in the aforementioned North American species (Able, 1982; Moore 1986; Able, 1989; Able and Able, 1995b) cannot be referred unambiguously to the plane of polarization any longer due to the fact that orientation according to potentially introduced light gradients, i.e. along the e-vector axis, coincided with the birds' migratory direction with respect to the natural polarization patterns, i.e. north-south along the e-vector axis.

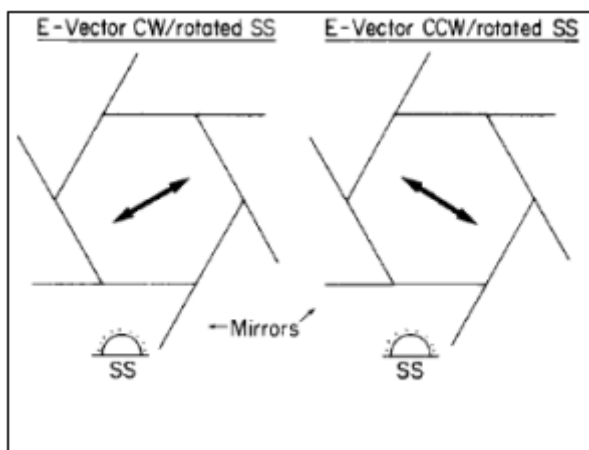


**Figure 11: Hexagonal orientation cage with mirror deflector panels.** The band of maximum polarization can be mimicked by equipping vertically aligned polarizers at two opposite cage walls and horizontally aligned polarizers on the other 4. Vertical e-vectors are hereby intersection the horizon at an axis that can be determined by the experimenter. Furthermore, deflector panels on every window were equipped with mirrors to deflect the apparent azimuth of the sun (SS). After Moore and Phillips, 1988.

In 1988, Moore and Phillips developed a rather elaborate setup for their study in yellow-rumped warblers (*Dendroica coronate*; Moore and Phillips, 1988). Using a hexagonal cage with transparent walls they were able to deflect the position of the sun at dusk by mirrors, and simultaneously polarize the incoming light through the side walls (Moore and Phillips, 1988; Figure 11). This setup enabled them to mimic the band of maximum polarization close to the horizon by equipping opposing walls with vertically or horizontally aligned polarizers (Figure 11). As a result, Moore and Phillips (1988) observed a bimodal distribution of orientation choices along the mimicked band of maximal polarization, i.e. along the experimental N-S axis. But, in each case of a hexagonal cage setup (Moore and Phillips, 1988; Muheim et al., 2007, 2009; Figure 11), the floor and ceiling would strongly reflect horizontally polarized light (Figure 12, B). Therefore, a comparable double light gradient as in orientation funnels could have

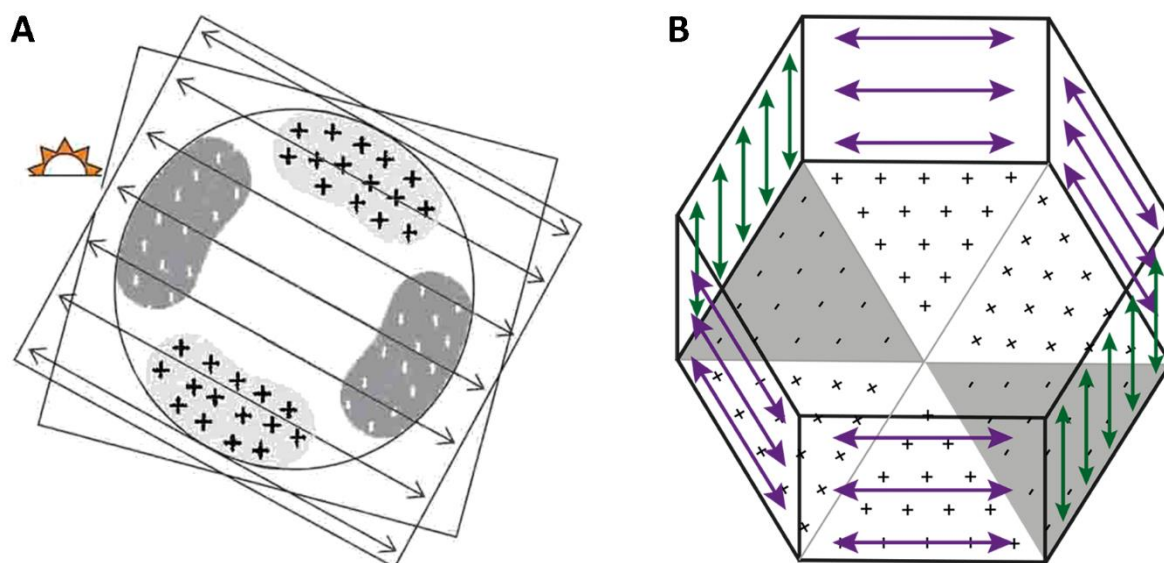


**Figure 12: Linear polarizers cause light intensity gradients inside experimental setups.** A) Sketch illustrating light reflections of polarized light in *Emlen* funnels. Reflections are strongest (indicated by bright patches with plus signs) at the sloping funnel walls in parallel to the e-vector axis of a linear polarizer placed on top of the funnel (indicated by double arrows). Reflections are weakest (indicated by dark gray patches with minus signs) at the sloping funnel walls perpendicular to the e-vector axis of a linear polarizer. Light intensity gradients (starting at the depicted sun's position in the sketch: dark-bright-dark-bright-dark) result inside the funnel, with opposite sides of the funnel having identical light reflection properties (axial distribution). Depolarizing the skylight before polarization may even enhance the homogeneity of this light intensity artifact. B) Illustration of the same effect in hexagonal orientation cages. Horizontally polarized light is reflected strongest off the cage floor and ceiling (indicated by bright patches with plus signs), generating persistent light gradients inside the cage comparable to A). A) Modified and corrected after Muheim, 2011. B) Own illustration, adapted after Moore and Phillips, 1988.

resulted, i.e. the brightest points perpendicular to the provided plane of polarization for the orientation task (Figure 12, B).

Elegant solutions to the light artifact problem were studies that refrained from an experimental manipulation of polarization patterns, but instead denied the access to this particular property of the celestial sphere by using depolarizers (Helbig, 1990; Able and Able, 1993; Wiltschko and Munro, 1995). Day-migrating Yellow-faced Honeyeaters (*Lichenostomus chrysops*; Munro and Wiltschko, 1995) for example, were able to orient without view of the sun under partially overcast skies, but when the authors depolarized the sky, the birds became disoriented on group level (Munro and Wiltschko, 1995). However, the absence of polarized light cues and the inability of birds to orient in this line of experiments provides merely indirect evidence and could be coincidental.

In conclusion, the use of skylight polarization patterns for sunset orientation and for calibration of compass systems in birds remains unclear. The controversy of results from

laboratory-based and behavioral experiments, and the potential role of secondary cues in the latter leave reason to question this sensory capability down to its mere existence.

### **3.4. Are retinal ganglion cells encoding the e-vector of linearly polarized light in birds?**

Direct evidence for retinal modulation of polarized light information in the bird's eye is strongly needed.

The avian retina, as in the vertebrate visual system in general (Masland, 2001), consists of a highly complex network of specialized circuits that process the visual information from the outside world to higher brain areas. In the avian retina, six specialized photoreceptor types were found, each containing a unique chromophore type (opsins and rhodopsins) with distinct spectral sensitivity and a unique oil droplet type to additionally spectrally filter the incoming light: rods (scotopic vision, 500-510 nm), UV cones (370 or 410 nm), blue cones (450 nm), green cones (510), red cones (570 nm) and double cones (570 nm; Hunt, 2009). Visual information at the photoreceptor layer is picked up by bipolar cells and projected to retinal ganglion cells (Masland, 2001). All information to higher brain areas leaves the retina in the form of action potentials produced at the axon hillocks of retinal ganglion cells (Sanes and Masland, 2015). At this point, the incoming visual information has already been separated and pre-processed by specialized retinal pathways into visual modalities as complex as luminance contrast, spectral contrast, visual flow, object segregation, local movement of objects and movement direction (Vaney et al., 2012; Sanes and Masland, 2015). This channeling is mainly accomplished by (a) specialized wiring between distinct types of ganglion cells, bipolar cells and photoreceptors, by (b) modulatory input of horizontal cells on the photoreceptor graded potentials, and by (c) modulatory input of different types of amacrine cells on the activity of ganglion cells (Vaney et al., 2012). If the e-vector of polarized light was one additional visual modality in bird vision, it must be detected by specialized, polarization-sensitive photoreceptors, must be encoded through specialized retinal wiring and the signal must pass through retinal ganglion cells on the way to higher visual brain areas (Masland, 2001; Sanes and Masland, 2015).

#### **3.4.1. Multi-electrode recordings from retinal ganglion cells**

We do not know if and how the e-vector of polarized light was detected in avian photoreceptor cells and by which photoreceptor type(s) exactly (see chapter 3.2. in this



thesis). Furthermore, no information on specialized retinal pathways or wiring regarding polarization sensitivity in the literature on birds exists. But if the avian visual system was sensitive to polarized light, we should be able to detect pre-processed and channeled signals in form of retinal ganglion cell responses. Therefore, Nils-Lasse Schneider and David Dreyer (Schneider and Dreyer et al., 2014, unpublished) used multi-electrode extracellular recordings from the retinal ganglion cell layer in whole mounted retinal pieces of domestic chicken (*Gallus gallus*). This enabled them to simultaneously record from up to 99 neurons in the retinal ganglion cell layer upon stimulation with linearly polarized light. As described below they used a well-controlled light stimulation protocol to exclude light intensity artifacts and a conservative post-processing data analysis to exclude false-positive responses from their data as good as possible. I will summarize the methods and results of their study below in detail. They successfully recorded from retinal ganglion cells that selectively responded with a bimodal response to 360° rotations of the e-vector, as would be expected from polarization sensitive cells.

During a few months of training by Dr. Dreyer, co-author of the original study (Schneider and Dreyer et al., 2014, unpublished), I learned to perform the retinal dissections, the script-based protocols for light stimulation using Matlab®, the electrophysiological recordings including controls, the data acquisition, and the analysis of cell responses. After this training, I was able to successfully replicate the experiments with Dr. Arndt Meyer. Due to the fact, that our replication experiments and our additional experiments - if not explicitly stated differently in the text - were based on and logically dependent on the exact experimental protocol used by Schneider and Dreyer et al. (2014, unpublished), I will present the methods used by the original authors and Dr. Arndt Meyer and me in great detail. I would like to acknowledge, that large parts of chapter 3.4.2. *Extracellular recordings and light stimulation* and chapter 3.4.2. *Data analysis of rotational stimuli* were adapted from the unpublished manuscript (Schneider and Dreyer et al., 2014, unpublished). I took part in the internal revision process and in wording during the rebuttal attempt in close collaboration with the original authors, Dr. Arndt Meyer and Prof. Dr. Henrik Mouritsen. Using alternative wording here would not be beneficial for clarity, in my opinion.

### **3.4.2. Methods of the experiments of Schneider and Dreyer et al. (2014, unpublished), replicated in the experiments of Dr. Arndt Meyer and me**

#### Retinal preparation

Under dim red light inside a light-tight room, 1 to 42 days old domestic chicken (*Gallus gallus*) of both sexes (4 to 90 days old in my experiments) were sacrificed by decapitation after being dark-adapted for 2 to 4 hours (1-4 hours in our experiments). Retinal pieces were dissected and flat-mounted in a bath chamber with glass floor (Figure 13) in the following way: The eyeballs were removed from the skull by opening the orbital bones and carefully cutting the eye muscles, the optic nerve and conjunctive tissue with fine surgical tools made of stainless steel. Using a sharp and cleansed razor blade, the frontal hemisphere of the eye was cut away along the “equatorial line” of the eyeball. First, the posterior hemisphere was carefully freed of the vitreous body using a pair of tweezers and thereafter, it was cut into three pieces with a razor blade in the following manner: the first incision was made close to and in parallel to an imaginary line drawn by the extended base of the *Pecten oculi*. The second incision was made to cut away the *Pecten oculi*, which was discarded thereafter, resulting in a ventronasal retinal piece and a temporal half of the eye cup. The third incision was placed to divide the temporal half of the eye cup into a ventrotemporal and a dorsotemporal retinal piece.

In advance to these dissecting procedures, a solution of precisely mixed ions was prepared for replacing extracellular fluid losses and restoring chemical balances (Ringer’s solution, after Stett et al., 2000: 100 mM NaCl, 30 mM NaHCO<sub>3</sub>, 50 mM Glucose, 6 mM KCL, 2 mM MgSO<sub>4</sub>, 1 mM CaCl and 1 mM NaH<sub>2</sub>PO<sub>4</sub> in bi-distilled water, pH adjusted to 7.4, with the modification that 0.27 mM acetylsalicylic acid was added). Additionally, an agarose pad was prepared that would carry the dissected retinal pieces during recordings in the bath chamber. The agarose pad was prepared by dissolving 4% Agar Agar in modified Ringer’s solution (same recipe as above, but without addition of the Glucose, because chiral saccharides like Glucose can possess polarization-active optical properties), heating the solution above boiling point 3 times in a microwave, thereafter draining it into a glass form spaced by object trays (thickness of glass form 1-1.5 mm) for cooling, and then cut into small (~1.5 cm width x 2 cm length) pads with a thickness of 1-1.5 mm to carry the retinal pieces in the bath chamber during recording as described below.

The following steps were very delicate, very critical and not always worked as desired: To obtain an isolated retinal piece with the pigment epithelium still attached separated from the

sclera, a small piece of single layered cellulose tissue was placed on top of each retinal piece and was gently attached to the ganglion cell side by allowing the cellulose tissue to soak with residual vitreous fluid or by applying a drop of Ringer's solution from the tip of a fine brush. After a few seconds of adhesion – duration determined by experience alone – the connection between the cellulose tissue and the retina would be strong enough to allow us to slowly pull the tissue from the sclera containing the isolated retina with pigment epithelium attached. In many attempts, at the time of removal the tissue was still too wet to pull the retina with it. A retry of the above steps was never successful and the retinal piece had to be discarded. Drying out for a few seconds too long would adhere the retina to the cellulose tissue too strong for easy separation of retinal piece and cellulose tissue in the next step. In many attempts, the retina would not separate from the sclera without tearing, would come off completely without the pigment epithelium, or as in many even worse attempts, patches of pigment epithelium came off attached to the retina, but surrounding patches remained attached to the sclera, visibly tearing and stretching the whole retinal tissue upon removal. The retinal pieces were only used for stimulation and recordings, if the preceding and the following preparation steps resulted in a retinal piece with largely attached pigment epithelium and if smooth procedures were noted. These decisions were made by the best possible judgment of the experimenters and care was taken that only neat-appearing retinal pieces were considered for further processing. However, it is important to note here that the true dimension of mechanical stress and microscopic tissue damage during each preparation attempt remained largely undeterminable. In many cases, Dr. Arndt Meyer and I noticed that the pigment epithelium would visibly detach later in the bath chamber during the course of a recording session.

The successfully isolated retina pieces, still attached to the cellulose tissue, were transferred into a small glass pan filled with Ringer's solution, carefully released at the edges from the cellulose tissue with a fine brush and – once free floating – maneuvered on top of a previously prepared agarose pad by using a fine brush and draining the Ringer's solution slowly from the small glass pan with a pipette. Precautions were taken to avoid touching the photoreceptor side of the retinal piece. However, touching and manipulating the edges of the retinal pieces were unavoidable, so we did our best to limit contact only to the edges.

Sitting on the agarose pad with the ganglion cell layer facing towards the incident light as in the natural situation (Figure 13), the isolated retina piece was transferred into a bath chamber, was covered with a frame of filter paper weighed down by a small (2 cm in length) rhomboidal

frame of stainless steel to keep the retina in place, and was supplied with oxygenated and heated (37°; heating system: Multichannel systems, Germany, TC02) Ringer's solution by perfusion of the bath chamber with a customized pumping system (pump: Ismatec, Germany;

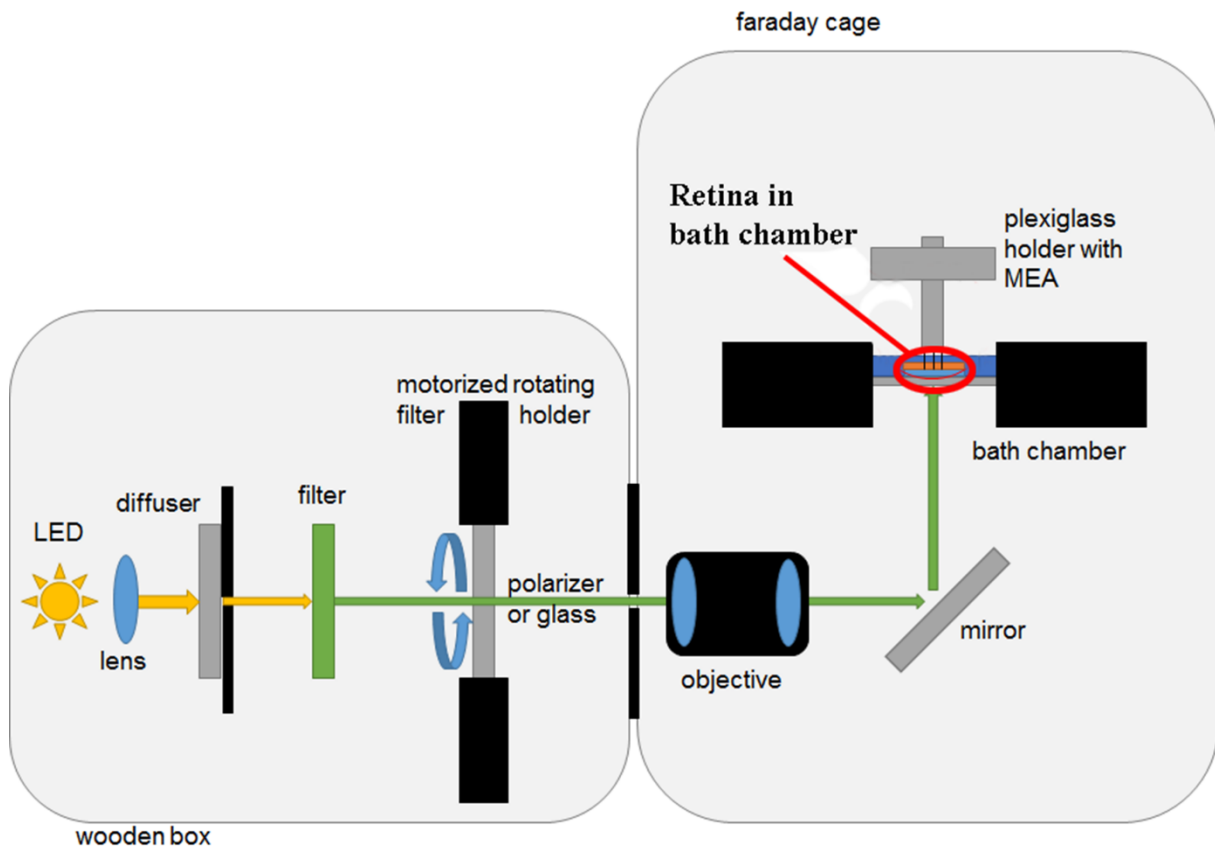


**Figure 13: Sketch of the experimental setup for extracellular multi-electrode recordings from avian retinal ganglion cells.** A dissected retinal piece was flat-mounted in a bath chamber with a glass floor (top right). The ganglion cell layer faced downwards, the attached pigment epithelium faced towards the micro electrode array mounted on a micromanipulator (top right). The 10x10 electrode array was lowered into the retinal tissue until the isolated electrode tips recorded extracellular potentials from the ganglion cells. Broadband white light from a LED diode (bottom left) was bundled by a convex lens and sent through a) a diffuser to fully depolarize the light ray, b) a broad-band green (520-580 nm) spectral filter for maximal excitation of avian double cones, c) a linear polarizing filter mounted in a stepper motor housing, to be able to rotate the e-vector orientation of the polarized light in 360° turns, d) a pinhole aperture to eliminate any potential stray light, e) an objective to adjust focus onto the whole mounted retina, and f) a mirror to redirected the light to the bath chamber and onto the retinal tissue. Sketch received with kind courtesy of Dr. Arndt Meyer.

REGLO Digital MS-2/8) at a perfusion rate of 10 ml/min. Once in this position, the retina was kept in the dark for at least 15 minutes to recover from mechanical and chemical stress before a recording session was initiated.

#### Extracellular recordings and light stimulation

A square (4.2 x 4.2 mm) 10x10 microelectrode array (Blackrock Microsystems, Salt Lake City, UT, USA; 99 electrodes to detect extracellular signals and one electrode used as reference) with sharp silicon electrodes (impedances 200-610 kΩ; 400 μm distance between electrode

tips) was inserted into the retina from the photoreceptor side through the pigment epithelium, down through the retinal network until the electrode tips were in close proximity to ganglion cells (Figure 13). Insertion of the electrode array from this side was done to assure an unobstructed light path as in the natural situation, and to use the shielding effect of the pigment epithelium against possible light reflections off the array mounting (custom-built plexiglass stamp, connected to a manually driven micromanipulator (Leica, Germany; Micromanipulator R)). The recording area was screened with a 6-sided aluminum Faraday cage, separately grounded and placed on vibration-reducing tables inside a 5m x 4m x 2.5m aluminum chamber that screened electromagnetic disturbances from the surroundings (Engels et al., 2014).

The detected signals were amplified and band-pass filtered (250Hz to 7.5 kHz) by the Front End Amplifier (Bionic Technologies), then digitized and stored on a hard disc as a binary Neural Event (.NEV) data file using the Neural signal processor-module and the GUI software Neural Data Acquisition Program v3.2 (Bionic Technologies). The thresholds for spike detection were hand-adjusted above the noise-level on each channel after automatic pre-setting using the “Auto Threshold” option of the software. The system records with a sampling frequency of 30 kHz and a digital step size of 0.49  $\mu\text{V}$ . In case of a supra-threshold event, a timestamp and a fixed window of the channel’s voltage curve (300 ms before and 1300 ms after the event) was stored. A detailed description and review of the recording-system, manufactured by Bionic Technologies (Salt Lake City, UT, USA; nowadays Blackrock Microsystems) is in Guillory and Normann (1999); c.f. Schneider and Dreyer et al. (2014, unpublished). Light stimulation was a full-field (8mm diameter, illuminating the whole retina piece) light spot generated by a LED (Cree Inc., Durham, NC, USA; MC-E CREE) with a light intensity of  $6.4 \times 10^{12}$  photons  $\text{cm}^{-2} \text{s}^{-1}$  (Figure 13). Light was spectrally filtered by a green color filter (Edmund Optics GmbH, Barrington, NJ, USA; VG-9, 500-590 nm) to match the maximum absorption of avian double cones (Figure 13). The chosen light intensity was approximately equivalent to the intensity of green light present at or shortly after sunset. Light was sent through a linearly polarizing filter (Edmund Optics, Barrington, NJ, USA; Ultra Broadband Wire Grid Polarizer, catalogue #68-750) in a custom-built, rotatable mount driven by a stepper motor controller/driver module (Trinamic Motion Control GmbH, Hamburg, Germany; PANdrive PD 013-42 and TMCM-013) through a gear belt (Figure 13). A precision broadband laser mirror (Edmund Optics, Barrington, NJ, USA; catalogue #64-114) was used to direct the polarized light onto the retina

without altering the degree or axis of polarization (Figure 13). The overall configuration resulted in a spot of linearly polarized, broad-spectrum green light with a rotatable e-vector, which was focused onto the retina piece (Figure 13).

At the beginning of each experiment, the multi-electrode array was driven into the retina from the pigment epithelium side very slowly, while the retina was exposed to light flashes (0.3 s duration, 5 s inter-stimulus interval, unpolarized). The first light responses recorded from the retina indicated that the electrode tips were arriving at the level of the ganglion cell layer. Once the estimated optimum of the number of ganglion cells responding to light flashes was reached, the light responses of the ganglion cells to at least 30 flashes were recorded. The same was done after the polarization stimuli at the end of each recording session. The estimated optimum ganglion cell number was different each time, because the ganglion cell layer was not hit by the micro-electrode array at perfect orthogonal angles, probably due to mixed effects of the agarose pad, the flexible array mounting or even a slight floating of the retinal piece in the perfusion stream. The MatLab script for light flash stimulation can be found on the external hard drive linked to this thesis (“Toshiba:\RawData Chapter 3.4\0 MatLab Scripts\MatLabScripts POL Stimulation Michael\VisualThreshold.mat”). An explanatory description to the usage of the Matlab-script can be found here “Toshiba:\RawData Chapter 3.4\Anleitung zur MatLab-gestützten Lichtstimulation und Analyse der MEA Ableitungen”.

After the initial stimulation with light flashes, the retinal piece was light adapted (10-15 mins) to an illumination of linearly polarized green light at a flux-density of  $6.4 \times 10^{12}$  photons/cm<sup>2</sup>/s produced by a static polarizer orientation along one of the following four axes: 0°/180° [up/down], 45°/225°, 90°/270°, or 135°/315°. Following this adaptation time, we rotated the polarizer in 360° turns in 3 seconds. By rotating the polarizer in the optical path, the plane of vibration (polarization axis) of linear polarized light (e-vector) was rotated accordingly. When a polarizer is rotated in 360° turns, bimodal response patterns are expected of cells that encode the e-vector of polarized light due to the assumption that the preferred e-vector axis of polarized light, i.e. the e-vector axis that most strongly excites the underlying visual system, is met two times during one turn.

#### Control experiments in the original study by Schneider and Dreyer et al. (2014, unpublished)

When the polarizer was rotated in 360° turns in 3 s intervals (Figure 14, a), some ganglion cells responded with bimodal firing patterns during one full rotation (Figure 14, c and e). Alternatively, these responses could potentially be caused by an artificial light intensity flicker

caused by differential reflections of the e-vector during the rotation of a polarizer (Coemans et al., 1990; Vos Hzn et al., 1995). Photometric measurements done by Schneider and Dreyer et al. (2014, unpublished) and replicated by Dr. Arndt Meyer and me revealed that even after best-possible alignment of all optical devices in the light path, an e-vector dependent intensity flicker was in fact detectable, ranging from 0.3% up to 1.5% intensity change. As an adequate control stimulus, each full e-vector turn in either direction was intersected by a sinusoidal light

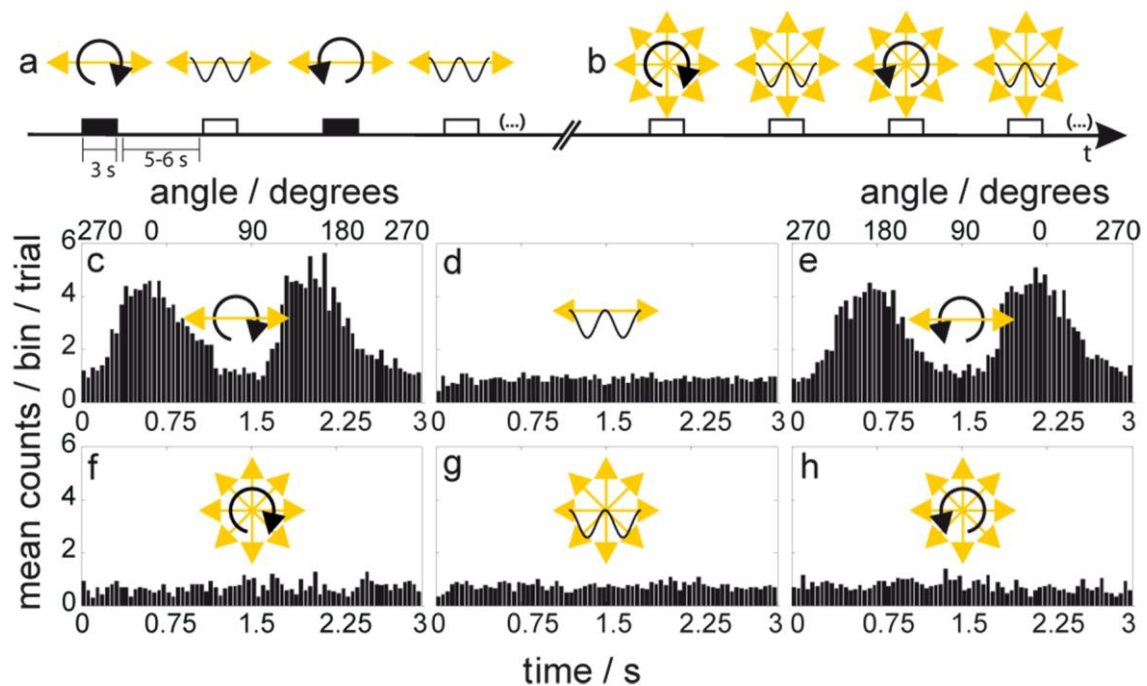


**Figure 14: Experimental stimulation protocol and control measurements for recording e-vector encoding retinal ganglion cells of chicken.** a) The e-vector of polarized light was rotated in  $360^\circ$  turns in 3 seconds, clockwise (CW) and counterclockwise (CCW). Each rotation was followed by a stationary phase of the e-vector and a subsequent sinusoidal intensity change. One recording session included 50 trials, i.e. 50 turns in each direction and 100 intensity sinuses. b) Repeating the same protocol, the polarizer was replaced by a piece of glass to eliminate the possibility of positive cell responses caused by light flicker during a  $360^\circ$  turn of the polarizer. As depicted in c-h, our experiments resulted in some recordings from retinal ganglion cells that responded bimodally to the turn of a polarizer in both directions. This is what has been expected from an e-vector encoding ganglion cell. c+e) During a  $360^\circ$  turn, the preferred axis of polarization sensitive photoreceptors is excited twice, hence the axial firing pattern. d+g) Comparable responses were never observed when the intensity was modulated sinusoidally, or when the polarizer was replaced by a piece of glass (f-h). From Schneider and Dreyer et al., 2014, unpublished.

intensity change in the same time interval as the  $360^\circ$  rotation of a polarizer (Figure 14, a), with an intensity difference set to 2.5% (Figure 14, a).

Thereby, a potential light reflection artifact during a polarizer turn could be simulated in a conservative way using intensity changes much higher than photometrically measured during a polarizer turn. As a second control stimulus, in some recording sessions the polarizer was replaced by a piece of glass (Figure 14, b) to control for potential dust particles casting a dis-

and reappearing shadow on the retinal cells, potentially causing a similar bimodal response upon a 360° turn of a polarizer. Additionally to these controls, the polarization degree and the spectral composition of the light were polarimetrically (optometer: Gigahertz-Optik, Türkenfeld, Germany, Model P-9710) and spectroscopically measured (spectrometer: Ocean optics, Dunedin, FL, USA, USB4000-UV-VIS) to be constant during e-vector rotation. The MatLab script for light stimulation with a turning polarizer can be found on the external hard drive linked to this thesis (“Toshiba:\RawData Chapter 3.4\0 MatLab Scripts\MatLabScripts POL Stimulation Michael\evecturn.mat”). An explanatory description to the usage of the Matlab-script can be found here “Toshiba:\RawData Chapter 3.4\Anleitung zur MatLab-gestützten Lichtstimulation und Analyse der MEA Ableitungen”.

#### Data analysis of rotational stimuli

An automated analysis protocol in five automated steps, custom-written for the Matlab® 2013b environment by Nils-Lasse Schneider, was used for all recorded raw data: (i) All data from electrodes that recorded less than 5 spikes within the 3 s stimulus intervals in over 50% of the stimulus repetitions were disregarded, due to unreliability of cells with so few spikes in further analysis. (ii) Spike times during the 3 s time intervals per trial were converted into angles that corresponded to the respective polarizer orientation angles (e-vector angle) at any given spike time. The starting angle of the respective recording session and the direction of the turn per trial (CW or CCW) were considered in this conversion. For convenient visual comparison, the spike times during a sinusoidal intensity change and during glass turns were converted into angles in the identical manner. Per recorded electrode, these “spike angles” were plotted in raster plots and in peri-stimulus angle histograms (PSAH; depicted in Figure 14, c-h) where spike angles were summed over all trials. (iii) the PSAHs were plotted as a circular diagram, where the number of spikes recorded in each 5° interval was plotted inside a unity circle relative to the highest number of spikes recorded in a single 5° interval in any of the conditions (the length of this bar was defined as 1; Figure 15). Using circular statistics (Rayleigh Test; Batschelet, 1981), the total mean vector of all recorded spikes were calculated by adding up unity vectors in each recorded spike angle. (iv) The mean angle of the spikes recorded in each single trial was calculated. Based on these mean angles, a group mean vector of the means of the individual trials was calculated. (v) Since the plane of the e-vector of linearly polarized light provides axial information, it is expected that ganglion cells that respond to the e-vector orientation of the polarized light should show a 180° bimodal



distribution of spike angles. To test for a 180° bimodally symmetrical distribution, a doubling of the angles should lead to a significantly oriented unimodal distribution in a Rayleigh test (Batschelet, 1981). To give a descriptive example, if the angles of a axial distribution along the axis 45°/225° were doubled, both angles result in the identical value 90° ( $45^\circ * 2 = \underline{90^\circ}$ ;  $225^\circ * 2 = 450^\circ$ ,  $450^\circ - 360^\circ = \underline{90^\circ}$ ) and can be used in a circular statistical test for unimodal distribution in a Rayleigh test (Batschelet, 1981). Two analyses were used, one considered all recorded doubled spike angles in all trials combined, and the other considered the doubled spike angles recorded in each single trial. (vi) Batschelet (1981) provided a correlation table that defines the minimal r-value (length of the resulting vector in circular statistics; Batschelet, 1981) required at a given sample size n (here the number of trials or the number of spike angles per trial, respectively for the two types of analyses) for significance at the  $p < 0.001$  level according to the Rayleigh Test (Batschelet, 1981). Here, a corrected r-value (r-corr) was defined as the difference between the minimum mean vector length required for  $p < 0.001$  and the calculated r-value of doubled spike angles. Values were calculated for the CW (r-corr CW) and CCW (r-corr CCW) rotations separately. If both r-corr CW and r-corr CCW were  $> 0$ , the recorded spike distribution was considered as highly significant bimodal. The MatLab scripts for automated data analysis can be found on the external hard drive linked to this thesis ("Toshiba:\RawData Chapter 3.4\0 MatLab Scripts\Pol\_Analysis\_Michael"). An explanatory description to the usage of the Matlab-script can be found here "Toshiba:\RawData Chapter 3.4\Anleitung zur MatLab-gestützten Lichtstimulation und Analyse der MEA Ableitungen".

### **3.4.3. Results of the experiments of Schneider and Dreyer et al. (2014, unpublished)**

In 22 out of 74 retinas in total, Schneider and Dreyer et al. (2014, unpublished) recorded 49 highly significant bimodal responses of retinal ganglion cells upon the rotation of a polarizer under very strict and conservative analysis criteria.

To sum up their main findings, (1) only a subset of ganglion cells (~3% of all recorded units) appeared to encode the e-vector of polarized light as would be expected from a specialized polarization sensitive circuit in the vertebrate visual system (Masland, 2001; Vaney, 2012; Sanes and Masland, 2015). (2) The ganglion cells never responded bimodally to one of the intensity/glass control experiments (depicted in Figure 14, d and g-h). (3) In each recording session, the e-vector of the linearly polarized light was kept stationary for a defined period of 15-30 minutes before the first rotation, and for the 5 seconds between each of the trials (360° polarizer turn or sinusoidal intensity change; see Figure 14, a). The authors observed that most

of the bimodally responding ganglion cells preferred an e-vector orientation  $\sim 90^\circ$  relative to the static e-vector axis (Figure 15, A-D, top rows). Furthermore, the cell's response was silenced in an immediately following recording session when this stationary e-vector axis was aligned with a cell's preferred firing axis (Figure 15, A-D, bottom rows). This observation was interpreted by the original authors as a cellular adaptation process to the stationary e-vector axis and as indicative of an underlying polarization sensitive retinal network. (4) Typically, there is an observable time lag between a stimulus and a neuronal response when recording from a cell (Sakura et al., 2008; c.f. Schneider and Dreyer et al., 2014, unpublished). Based on this assumption, a slightly delayed spike angle would be expected in CW versus CCW turns of a polarizer. However, the opposite was observed by Schneider and Dreyer et al. (2014, unpublished). When turning the polarizer in CW directions, the cells preferred a slightly "earlier" e-vector axis (smaller spike angles) than in opposing CCW directions (higher angles). This "predictive" or "paradox" response has been previously reported in neurons that encode the e-vector axis in insects (Sakura et al., 2008; Träger and Homberg, 2011; c.f. Schneider and Dreyer et al., 2014, unpublished). (5) The spiking activity of the cells that satisfied the selection

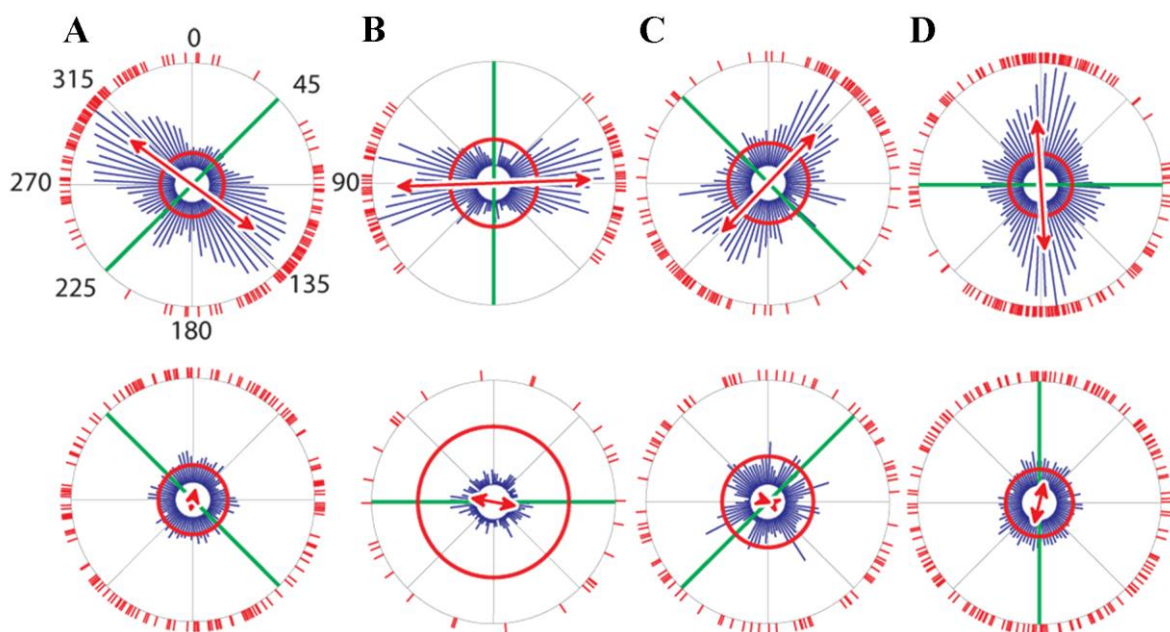


**Figure 15: Responses of polarization-sensitive RGCs can be silenced when the static e-vector axis corresponds to the polarization-sensitive cell's preferred e-vector axis.**

Top row: the bimodal responses of retinal ganglion cells are presented as circular bar diagrams. Our automated data evaluation protocol first correlated the timestamps of all spike events recorded from one unit to the corresponding e-vector orientation at that time. The blue bars depict the total peri-stimulus angle histograms [PSAH] grouped in  $5^\circ$  bins. The short red lines at the circle periphery indicate the preferred axes indicated in each of the individual stimulus trials evoking at least 5 spikes. The green lines indicate the static e-vector axis present between stimuli and during control stimuli and thus the static e-vector axis immediately prior to rotation of the polarizer. Bottom row: represent the silenced responses of the cells in the row above. From Schneider and Dreyer et al., 2014, unpublished.

criteria for significant bimodal responses ( $r\text{-corr} > 0$  in both CW and CCW polarizer turns) appeared to not form a response continuum with the rest of the recorded cells: two normal-like distributions, one on each side of the selection criteria border ( $r\text{-corr} > 0$  in both turn directions), were observed (Schneider and Dreyer et al., 2014, unpublished; Figure 16). Furthermore, the majority of bimodally responding retinal ganglion cells seemed to respond with an on-off response to light-flashes. Consequently, the original authors reasoned that units passing the selection criteria seemed to belong to a separate population of ganglion cells (Schneider and Dreyer et al., 2014, unpublished).

Taken together, the authors found highly significant bimodal responses originating from a small subpopulation of retinal ganglion cells in the chicken retina that must be real responses to the rotating e-vector of the polarized light confirmed by conservative controls against bias by light intensity artifacts and false-positive results.

This appeared to be a well-designed and well-controlled study, providing the first evidence for polarization sensitivity in retinal ganglion cells of birds. However, in the revision process after

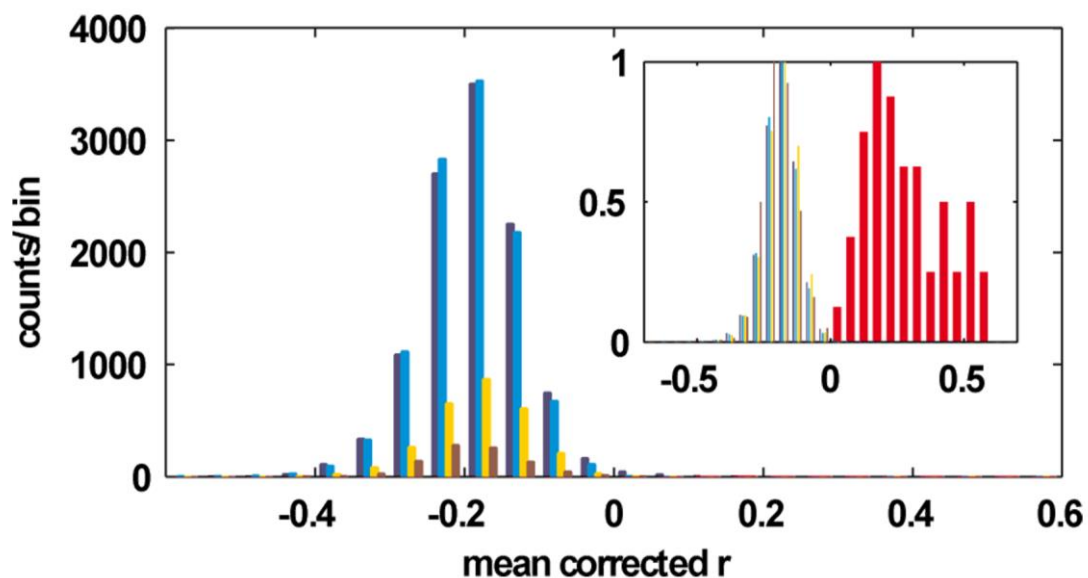


**Figure 16: Bimodally responding ganglion cells appear to belong to a separate subpopulation.** The mean corrected  $r$ -values of all cells recorded from were binned in steps of 0.05: light blue bars: 2.5% sinusoidal intensity changes with a static polarizer present; yellow bars: rotations of the glass; brown bars: 2.5% sinusoidal intensity changes with glass present; dark blue bars: rotations of a polarizer which led to no highly significant bimodal responses; red bars: cells showing highly significant bimodal responses to a rotating polarizer. Insert: the same data normalized relative to the most frequent bin for each condition. From Schneider and Dreyer et al., 2014, unpublished.

the original manuscript was submitted, the reviewers critique focused on one major question: could it be possible that the bimodal responses originated in artificial transverse dichroism caused by artificial lateral tilt of photoreceptors due to damage to the retina during the dissection and recording process?

#### **3.4.4. Methods and results of the follow-up experiments of Dr. Arndt Meyer and me**

At the point when the reviews were received, both original authors had already left the working group, putting me and my colleague Dr. Arndt Meyer in the position to perform some replication experiments in the identical setup to verify the methods and to perform some additional experiments to answer the concerns of the reviewers.

##### (I) Photoreceptor tilt due to structural damage of the tissue could in theory have led to artificial polarization sensitivity due to transverse dichroism in vertebrate photoreceptor outer segments.

In the natural situation, the outer segments of vertebrate photoreceptors are structurally fixed in their upright position by cells of the pigment epithelium. Proliferations of the pigment epithelium invaginate the spaces between outer segments. If the pigment epithelium was torn, photoreceptors might lose this stabilizing element and this in turn might cause photoreceptor outer segments to tilt or tear off. Vertebrate photoreceptors are transversely dichroic due to the parallel stacking of visual pigment contained in the disc membranes of the photoreceptor outer segment (Roberts et al., 2004; Figure 10, A and B). Upon a tilt to the side, incoming light would reach the outer segments transversely. Such a tilt could cause artificial polarization sensitivity which in turn could lead to a bimodal response of ganglion cells upon e-vector rotation.

An experiment was designed to evaluate the possibility of photoreceptor tilt during recordings or as intended in our case, to demonstrate to the reviewers that no tilt was noticeable.

##### *Methods:*

After each recording session using the exact protocol after Schneider and Dreyer et al. (2014, unpublished; see methods section in chapter 3.4.2. in this thesis) we kept the retina in the bath chamber and immediately analyzed whether ganglion cells in this recording responded bimodally to the turn of a polarizer and met all analysis criteria applied by Schneider and Dreyer et al. (2014, unpublished). The raw data of these recordings and analyses can be found on the external hard drive linked to this thesis ("Toshiba:\RawData Chapter 3.4\1 RawData of

MEA recordings”). If so (the corresponding results of the respective analyses can be found on the external hard drive linked to this thesis here “Toshiba:\RawData Chapter 3.4\2 Results from 98 MEA recordings with successful CLSM scans”), we carefully retracted the electrode array, removed the down-weighing frame and drained the bath chamber from Ringer’s solution. Thereafter, we embedded the retina in still-liquid agarose (4% Agar Agar dissolved in Ringer’s Solution) at 40° C inside the bath chamber. Doing so, we were able to conserve the tissue’s current structural state as good as possible while the agarose slowly cooled and hardened and encapsulated the retinal tissue. Next, we carefully removed the agarose-embedded retinal piece from the bath chamber and processed the tissue for immunohistochemical staining of cone outer segments. First, we fixed the tissue in paraformaldehyde (PFA, 4% in phosphate buffer (PB), 4°C) over night. PFA was washed out (3x PB á 10-20 minutes) and unspecific binding sites were blocked with normal donkey serum (DS, 10% in PB + 0.3% Triton X 100 + 0.05% NaN<sub>3</sub> (PB-TA), 24 hours, 4°C). Opsins of short wavelength-sensitive (SWS) cone outer segments were bound to a specific primary antibody (OPN1SW@goat, sc-14363, Santa Cruz, Biotechnology Inc., CA, USA; 1:500 in PB-TA with 1% DS, 3 days, 4°C). After excessive, unbound primary antibody was washed out (3x PB each for 30 minutes), a secondary antibody (Alexa 555 donkey@goat, 1:500 in PB-TA, 3 days, 4°C, dark) was used for fluorescent labeling of the primary antibody that was previously bound to the SWS cone outer segments. After tissue infiltration with TDE (25%-50%-75%-90%-2x96% each for 1 hour), which replaced water in the tissue, increasing the refractive index and therein reducing the refractive difference to the glass in the microscope optics, we were able to take images of the whole-mounted retina with sufficient imaging depth and the necessary resolution on a confocal laser scanning microscope (CLSM; Leica SP2) equipped with a HC PL APO 40x/NA 1.30 Oil immersion objective. The retinal tissue was placed under the CLSM and precisely rotated to the same orientation as during the recordings in the bath chamber of the electrophysiological setup, identified by the marks left by the electrode array. From 12 retinal pieces, we sampled image stacks (2048x2048 px, scan width 375 µm, scan depth 50-100 µm) of photoreceptor outer segments around individually identified electrode holes (98 image stacks in total). The corresponding image scans can be found on the external hard drive linked to this thesis here “Toshiba:\RawData Chapter 3.4\3 Results of the 98 CLSM scans”

To quantify the degree of tilt, to statistically measure the level of alignment of outer segment tilt around single electrodes, and to potentially find any correlation of the preferred bimodal

response axes of the ganglion cells with the tilting axes of the photoreceptor outer segments, we post-processed the image stacks sampled at the confocal microscope in ImageJ/Fiji. To determine the degree of tilt, we classified the side length ratio of overlay ellipsoids fitted around the stained outer segment signals: straight outer segments in upright position would be viewed as an almost round circle in the microscope, i.e. the ratio of the fitted ellipsoid sides would equal roughly 1:1 (no tilt). Ratios higher than 1:3, where one side of the fitted ellipsoid was at least three times longer than the shorter side, was defined as strong tilt. All image stacks were set to north according to the 0°/180° plane of polarization during stimulation. Hereafter, we were able to determine the direction of tilt of each individually stained outer segment. The results of this analysis and a description of how image processing was done can be found on the external hard drive linked to this thesis here “Toshiba:\RawData Chapter 3.4\4 Results of the Outer segment Tilt Analysis”. Using circular statistics, we were able to calculate the mean vector of the overall tilt direction around each electrode hole (Rayleigh test; Batchelet, 1981), and to calculate the r-corr value as a measure of axial significance, i.e. as a measure of the tilt alignment among individual outer segments around one electrode. Comparing the mean vectors and r-corr-values, we correlates tilt direction to the preferred e-vector angle of the recorded ganglion cell and correlated the alignment of tilt with the bimodality of the ganglion cell response.

#### *Results:*

We were able to scan the SWS outer segments in 12 retinal preparations. In each of these preparations, we successfully recorded at least one ganglion cell responding bimodally to the turn of a polarizer. In these 12 retinae, we scanned outer segments around in total 98 electrodes (Table 1). At 25 of these electrodes, bimodal responses in both polarizer rotation directions have been recorded (r-corr CW and r-corr CCW > 0). At 17 electrodes, bimodal responses have been recorded in one direction of polarizer rotation (either r-corr CW > 0 or r-corr CCW > 0). 56 electrode scans were made as reference scans around electrodes with non-bimodally responding ganglion cells (Table 1).



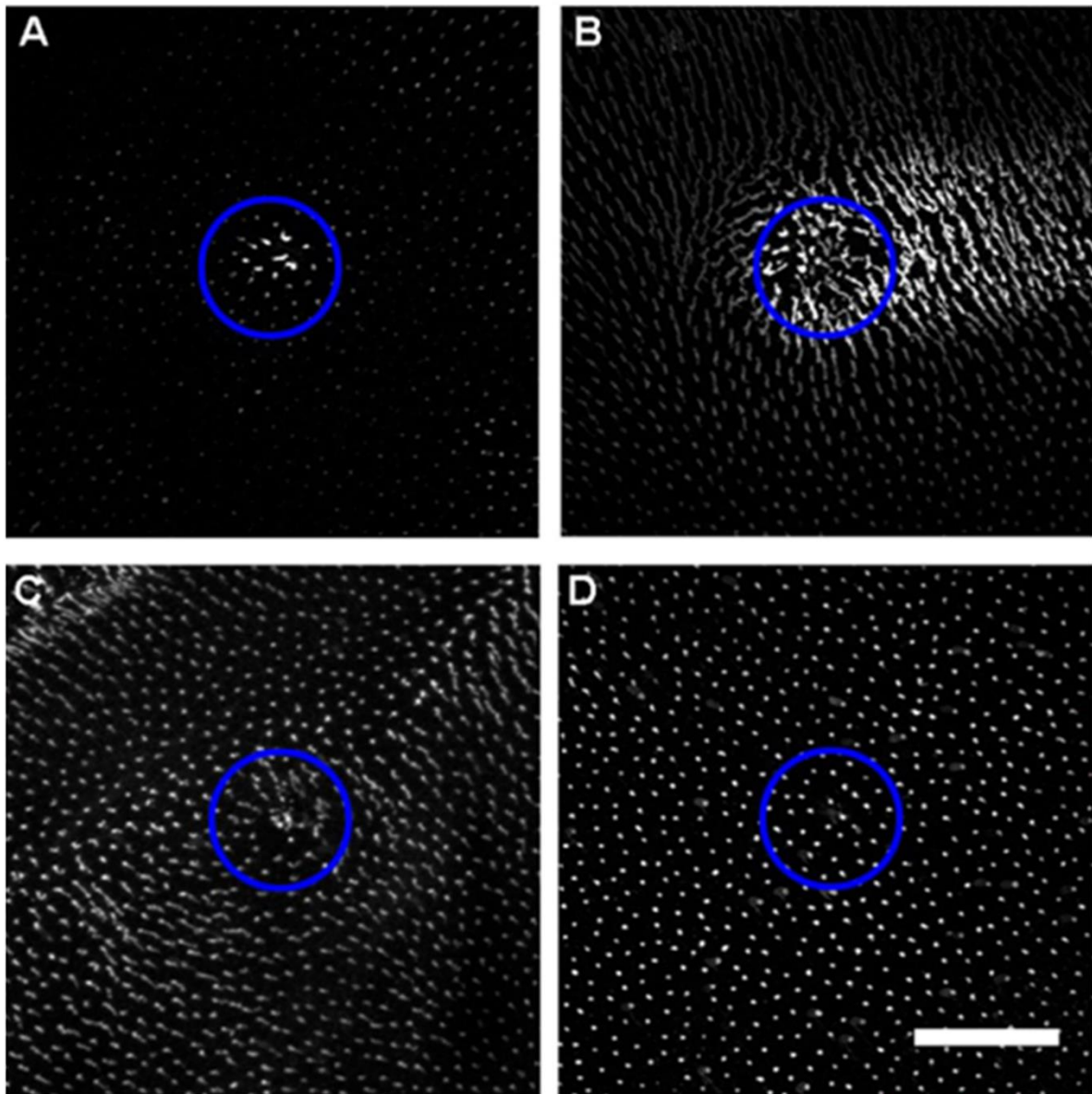


**Figure 17: Opsin stainings in SWS photoreceptor outer segments revealed severe transverse tilt in most, but not all evaluated recordings of ganglion cells that responded bimodally to the turn of a polarizer.** Outer segments that are fully bent to their side can be artificially polarization sensitive due to the transverse dichroism in vertebrate photoreceptors. After we recorded bimodal ganglion cell responses, we embedded the tissue in Agarose (4% in Ringer’s solution) to preserve its structural state and we immunohistochemically stained opsins of short wavelength-sensitive (SWS) cone outer segment (OPN1SW@goat, sc#-14363, Santa Cruz, Biotechnology Inc., CA, USA), labeled with a fluorescent marker (Alexa 555 donkey@goat). As seen in these top view scans (Leica SP2 equipped with a HC PL APO 40x/NA 1.30 Oil immersion objective) around the electrode holes (indicated by blue circles in A-D) of electrodes where significant bimodal ganglion cell responses were recorded, only the outer segments in the electrode holes were bent (A, Electrode 2015-07-17 E094), almost all outer segments were fully tilted but in different angles (B, Electrode 2015-10-13 E010), many outer segments were tilted in a different degree but mostly aligned in parallel (C, Electrode 2015-10-30B E010). D) Almost all outer segments are in an upright position (D, Electrode 2015-07-20 E042). Note that from 25 units in which we recorded bimodal ganglion cell responses upon the rotation of a polarizer, this scan (D) is the only one that did not show severe cases of photoreceptor outer segment shearing, tilt or detachment. Scale bar in right panel for all panels: 100 $\mu$ m. The full record of image stacks sampled from 98 electrodes can be found on the external hard drive linked to this thesis here “Toshiba:\RawData Chapter 3.4\3 Results of the 98 CLSM scans”.

**Table 1: Photoreceptor outer segment tilt in bimodally responding ganglion cells.** A numerical summary table of the electrode IDs, the responses recorded to light flashes before and after stimulation with a rotating polarizer. The summary table contains the preferred mean doubled angles and corrected vector length (r-corr) of responses to CW, CCW and combined responses to the turn of a polarizer. In each row, the number of stained photoreceptor outer segments, the maximum tilt ellipse aspect ration (ER), the percentage of tilted outer segments, their resulting mean doubled angle and its corrected vector length (r-corr tilt) are given for the respective electrode. The complete record of raw data, including the 98 CLSM scans and the results from 98 MEA recordings can be found on the external hard drive linked to this thesis here “Toshiba:\RawData Chapter 3.4” -> folder 3 and 4.

Electrode ID		Responses to Light Flashes		Ganglion cell response characteristics						Tilt properties in CLSM scans				
Date	Electrode	pre-Pol-Stim	post-Pol-Stim	r-corr CW	r-corr CCW	r-corr ombined	preferred angle (combined)	Starting angle (stationary)	SUM	# stained outer segments	maxER	% tilted (ER > 3)	doubled angles (tilt)	r-corr (tilt)
2015-07-20	4	OFF	ON-OFF	0,153	0,171	0,241	322	90	3	778	2,73	0,00	228	0,65432
2015-10-21	9	ON-OFF	ON-OFF	0,209	0,152	0,263	161	0	3	300	3,33	0,33	145	0,56041
2015-07-20	1	ON	ON-OFF	0,121	0,138	0,240	149	0	3	819	3,36	0,37	212	0,33338
2015-07-17	9	ON-OFF	ON-OFF	0,081	0,031	0,112	180	0	3	682	3,71	0,59	148	0,39110
2015-07-20	5	ON-OFF	ON-OFF	0,033	0,002	0,065	321	90	3	777	3,96	0,64	208	0,58821
2015-10-30A	6	ON-OFF	ON-OFF	0,084	0,149	0,073	329	90	3	341	4,02	0,88	122	0,35781
2015-10-30A	8	ON-OFF	ON-OFF	0,261	0,256	0,360	45	90	3	280	4,39	12,86	318	0,36696
2015-10-30A	9	ON-OFF	ON-OFF	0,270	0,338	0,407	44	90	3	176	4,79	19,32	339	0,08832
2015-10-30A	6	OFF	ON-OFF	0,132	0,062	0,060	324	90	3	425	4,92	7,53	49	0,05714
2015-08-19	3	ON-OFF	ON-OFF	0,427	0,364	0,497	49	135	3	253	5,08	7,91	64	0,00218
2015-10-30A	5	OFF	ON-OFF	0,007	0,113	0,063	11	90	3	316	5,14	6,96	246	0,41575
2015-10-30A	7	OFF	OFF	0,146	0,252	0,103	11	90	3	343	5,16	3,21	348	-0,08626
2015-08-19	4	ON-OFF	ON-OFF	0,027	0,048	0,147	45	135	3	347	5,63	5,19	270	-0,07942
2015-10-30A	6	ON-OFF	ON-OFF	0,236	0,350	0,382	33	90	3	249	6,13	21,29	324	0,17984
2015-08-19	2	ON-OFF	ON-OFF	0,452	0,198	0,417	68	135	3	240	6,42	7,08	278	0,09426
2015-05-03	4	ON-OFF	-	0,251	0,001	0,118	10	135	3	889	6,59	4,61	31	0,49682
2015-05-12	6	ON-OFF	ON-OFF	0,128	0,076	0,202	338	90	3	511	6,92	6,65	101	0,27091
2015-09-08	4	OFF	OFF	0,157	0,196	0,261	38	90	3	361	7,82	41,27	309	0,45216
2015-10-30B	1	OFF	OFF	0,145	0,283	0,319	158	0	3	905	8,72	17,24	237	0,62247
2015-10-16	8	ON-OFF	ON-OFF	0,013	0,158	0,166	173	0	3	503	9,68	20,08	209	0,50229
2015-09-08	2	OFF	OFF	0,524	0,396	0,549	30	90	3	290	10,40	52,07	340	0,50059
2015-09-08	3	OFF	OFF	0,341	0,351	0,440	13	90	3	353	10,42	49,29	337	0,60507
2015-09-08	1	OFF	OFF	0,498	0,402	0,520	31	90	3	286	10,92	57,69	324	0,56597
2015-10-13	1	OFF	OFF	0,133	0,144	0,088	45	90	3	1062	21,91	59,60	312	0,71760
2015-05-12	7	ON-OFF	ON-OFF	0,106	0,048	0,169	360	90	3	602	24,52	11,96	110	0,40671
2015-07-20	2	OFF	ON-OFF	0,110	-0,16550	0,041	193	0	2	925	3,66	0,54	181	0,10760
2015-07-20	7	ON-OFF	ON-OFF	-0,08672	0,021	0,071	7	90	2	579	3,82	0,52	177	0,45342
2015-10-30A	5	OFF	ON-OFF	0,104	-0,12669	0,073	320	90	2	344	4,50	3,49	133	0,36085
2015-07-17	9	ON-OFF	ON-OFF	-0,04863	0,338	0,243	204	0	2	658	5,20	13,22	132	0,62609
2015-08-19	7	ON-OFF	ON-OFF	-0,00021	0,154	0,149	76	135	2	454	6,58	23,13	78	0,18009
2015-09-08	5	OFF	ON-OFF	-0,01702	0,097	0,145	19	90	2	407	6,59	25,06	299	0,55848
2015-05-03	9	ON-OFF	-	0,099	-0,18956	0,060	338	45	2	735	7,00	9,12	254	0,25519
2015-10-30A	9	OFF	ON-OFF	-0,00801	0,097	0,148	8	90	2	527	7,24	26,19	282	0,50400
2015-07-20	3	-	ON-OFF	-0,10761	0,107	0,105	13	90	2	826	7,32	8,72	350	0,30525
2015-07-17	9	ON-OFF	ON-OFF	-0,01146	0,155	0,176	166	0	2	745	7,34	22,55	275	0,35954
2015-05-03	9	ON-OFF	-	-0,12123	0,018	0,052	44	135	2	869	7,98	14,15	268	0,40946
2015-05-03	9	OFF	-	0,018	-0,04299	0,049	12	135	2	614	8,00	2,77	289	0,39812
2015-07-20	8	-	ON-OFF	-0,07720	-0,09360	0,017	170	0	1	520	3,20	0,19	191	-0,13711
2015-07-20	7	OFF	ON-OFF	-0,09423	-0,03486	0,051	176	0	1	719	3,43	0,28	306	0,05272
2015-10-30A	8	ON	OFF	0,118	-0,25811	-0,00097	85	90	1	342	5,11	2,63	276	0,15809
2015-05-03	6	OFF	-	-0,15073	0,068	-0,00968	37	135	1	769	5,77	5,20	153	0,26256
2015-07-20	2	OFF	ON-OFF	-0,08979	-0,05997	0,028	348	90	1	966	5,95	14,91	340	0,53038
2015-10-30A	5	OFF	OFF						0	360	2,23	0,00	212	-0,01723
2015-10-30A	6	OFF	ON-OFF						0	381	2,24	0,00	64	-0,08258
2015-10-30B	2	on-OFF	on-OFF						0	843	2,45	0,00	167	0,35383
2015-10-13	1	OFF	OFF						0	718	3,11	0,28	261	0,04622
2015-10-30A	1	on-OFF	ON-OFF						0	429	3,32	0,23	195	0,25606
2015-10-16	2	-	-						0	734	3,51	0,14	324	0,22576
2015-10-30B	5	ON-OFF	ON-OFF						0	1135	3,56	0,70	176	0,04076
2015-10-16	6	ON-OFF	ON						0	587	3,57	0,51	183	0,22261
2015-10-30A	9	on-OFF	ON-OFF						0	352	3,88	2,84	359	0,03374
2015-10-13	9	on-OFF	OFF						0	894	4,01	0,45	295	0,18475
2015-08-19	5	ON-OFF	ON-OFF						0	346	4,09	0,58	178	0,32271



2015-05-12	3	ON	ON-OFF						0	480	4,13	2,08	5	0,24359
2015-10-30B	1	OFF	OFF						0	957	4,20	1,04	247	0,21651
2015-05-03	1	ON	-						0	681	4,28	2,35	18	0,43040
2015-05-03	5	ON	-						0	971	4,64	0,82	196	0,18337
2015-05-03	3	ON-off	-						0	1008	4,66	2,08	9	0,27964
2015-07-17	8	ON-OFF	ON-OFF						0	836	4,84	3,71	111	0,15336
2015-08-19	8	ON-OFF	ON-OFF						0	525	4,94	2,10	168	0,52466
2015-10-16	7	OFF	ON-OFF						0	1028	4,99	0,68	266	0,11591
2015-05-12	7	ON-OFF	ON-OFF						0	464	5,19	7,76	122	0,57646
2015-05-12	4	ON-OFF	ON-OFF						0	580	5,28	10,00	54	0,14201
2015-05-03	2	ON	-						0	1097	5,38	4,10	257	0,07883
2015-05-12	3	-	ON-OFF						0	583	5,78	3,60	203	0,04493
2015-05-03	8	ON-OFF	-						0	872	5,80	9,17	294	0,50833
2015-05-03	5	ON-OFF	-						0	836	6,04	1,08	212	-0,00827
2015-05-03	7	ON-OFF	-						0	824	6,27	3,76	287	-0,04683
2015-05-12	5	ON-OFF	ON-OFF						0	505	6,49	10,30	118	0,16213
2015-05-03	2	ON	-						0	825	6,52	3,52	14	0,45843
2015-10-21	8	ON-OFF	ON-OFF						0	379	6,59	6,86	169	0,45483
2015-05-03	1	ON	-						0	839	6,64	3,93	48	-0,04228
2015-05-03	1	ON	-						0	712	6,68	7,02	34	0,58043
2015-05-12	6	ON-OFF	ON-OFF						0	558	6,86	8,06	175	0,46279
2015-05-12	4	ON-OFF	ON-OFF						0	509	7,04	7,07	16	0,09082
2015-05-12	4	OFF	ON-OFF						0	420	7,38	13,57	69	0,23246
2015-05-03	4	ON	-						0	811	7,62	9,86	101	0,00918
2015-05-03	6	ON-OFF	-						0	911	7,65	9,44	238	0,49118
2015-05-12	2	ON-OFF	ON-OFF						0	491	7,71	7,54	321	0,25916
2015-05-03	7	ON	-						0	714	8,03	19,33	139	0,47279
2015-05-12	3	ON-OFF	ON-OFF						0	558	8,14	6,63	13	0,27068
2015-05-03	8	ON-OFF	-						0	744	8,52	18,95	300	0,46949
2015-05-03	2	ON-OFF	-						0	816	8,79	10,66	29	0,64569
2015-05-12	5	ON-OFF	ON-OFF						0	507	8,95	19,72	50	0,40198
2015-05-12	7	ON-OFF	ON-OFF						0	500	9,06	10,20	193	0,38209
2015-05-12	1	ON-OFF	ON-OFF						0	385	9,30	18,70	317	0,47700
2015-05-12	2	ON-OFF	ON-OFF						0	543	9,35	11,05	356	0,36647
2015-10-16	8	ON-off	ON-off						0	482	9,45	11,41	233	0,46210
2015-05-03	6	ON	-						0	817	9,71	7,96	182	0,33500
2015-05-03	3	ON	-						0	758	9,76	16,23	92	0,32613
2015-05-12	6	ON-OFF	ON-OFF						0	490	10,07	9,80	216	0,09402
2015-05-03	7	ON-OFF	-						0	801	10,35	42,20	303	0,46894
2015-10-21	1	ON-OFF	ON-OFF						0	608	10,50	20,89	44	0,39113
2015-07-17	9	ON-OFF	ON-OFF						0	747	11,54	43,24	103	0,23253
2015-07-08	8	ON-OFF	ON-OFF						0	775	12,67	52,13	36	0,51881
2015-05-12	6	ON-OFF	OFF						0	563	13,36	14,39	62	0,07227
2015-05-12	9	ON-OFF	ON-OFF						0	775	32,82	9,55	25	0,25488
2015-05-12	7	--	-						0	417	40,43	17,99	104	0,26946

As a result of our analysis, we observed strong tilt ( $ER > 3$ ) in at least one outer segment around 94 out of 98 electrode scans (Table 1; examples depicted in Figure 17 A-C). 24 out of 25 of the electrode scans from ganglion cells that showed a bimodal response to the turn of a polarizer exhibited strong outer segment tilt, maximal ellipse ratios in these scans ranging from  $maxER = 3.20$  to up to  $maxER = 24.52$  (Table 1; examples of three of these 25 electrode scans with very different tilting properties are given in Figure 17 A-C). In only 1 out of these 25 electrode scans, outer segments seemed not to be strongly tilted ( $maxER = 2.23$ ; Table 1; Figure 17 D). In the 24 out 25 electrode scans with bimodal ganglion cell responses and strong tilt, the percentage of strongly tilted outer segments ranged from 0.34 % to up to 59.6 % of all outer segments in the respective scan (Table 1; Figure 18, A). In the 17 electrode scans where bimodal tendencies were recorded, i.e. a bimodal response was only observable in one turn

direction of the polarizer), percentage of strongly tilted outer segments ranged from 0.19 % to up to 26.19 % with maximum ellipse ratios ranging from  $\text{maxER} = 3.20$  to up to  $\text{maxER} = 7.24$  (Table 1; Figure 18, A). In the 56 electrode scans where no bimodal response was observable in any turn direction of the polarizer, the percentage of strongly tilted outer segments ranged from 0.14 % to up to 52.13 % with maximum ellipse ratios ranging from  $\text{maxER} = 3.11$  to up to  $\text{maxER} = 40.43$  (Table 1; Figure 18, A). There were only 3 out of these 56 electrode scans in which outer segments appeared not to be strongly tilted ( $\text{maxER}$  values were 2.23, 2.24 and 2.45; Table 1).

To sum up these numbers, we found substantial tilt in all retinal pieces analyzed. We found a high degree of photoreceptor tilt around all but one electrode where bimodal ganglion cell responses had been recorded (24 out of 25 electrodes; Table 1; depicted in Figure 17 A-C). As the reviewers to the original study by Schneider and Dreyer et al., (2014, unpublished) suspected, we did in fact observe tilted, sheared or bent photoreceptor outer segments around electrodes where bimodal ganglion cell responses were recorded in our follow-up experiments. Consequently, artificially introduced transversal dichroism could potentially contribute to or even be responsible for a bimodal ganglion cell response to a turning polarizer. It is however very important to note here, that photoreceptor outer segments around one electrode with bimodal ganglion cell responses appeared not to be tilted nor bent (Figure 17, D). Furthermore, the percentage of strongly tilted photoreceptor outer segments around one electrode neither indicated a bimodal ganglion cell response, nor differed between ganglion cells responding bimodally to the turn of a polarizer and ganglion cells that did not show bimodal responses (Table 1; Figure 18, A).

We considered the possibility that highly aligned photoreceptor tilt could naturally increase a potential effect of transverse dichroism on the ganglion cell response characteristics. We found no evidence for such a phenomenon in our data. The alignment of tilt in each scan, measured as the corrected length of the mean vector angle ( $r\text{-corr tilt}$ ; Rayleigh Test for axial distribution; see chapter 3.4.2. *Data analysis of rotational stimuli*; Table 1), did neither indicate nor differ between bimodally and non-bimodally responding ganglion cells (Figure 18,

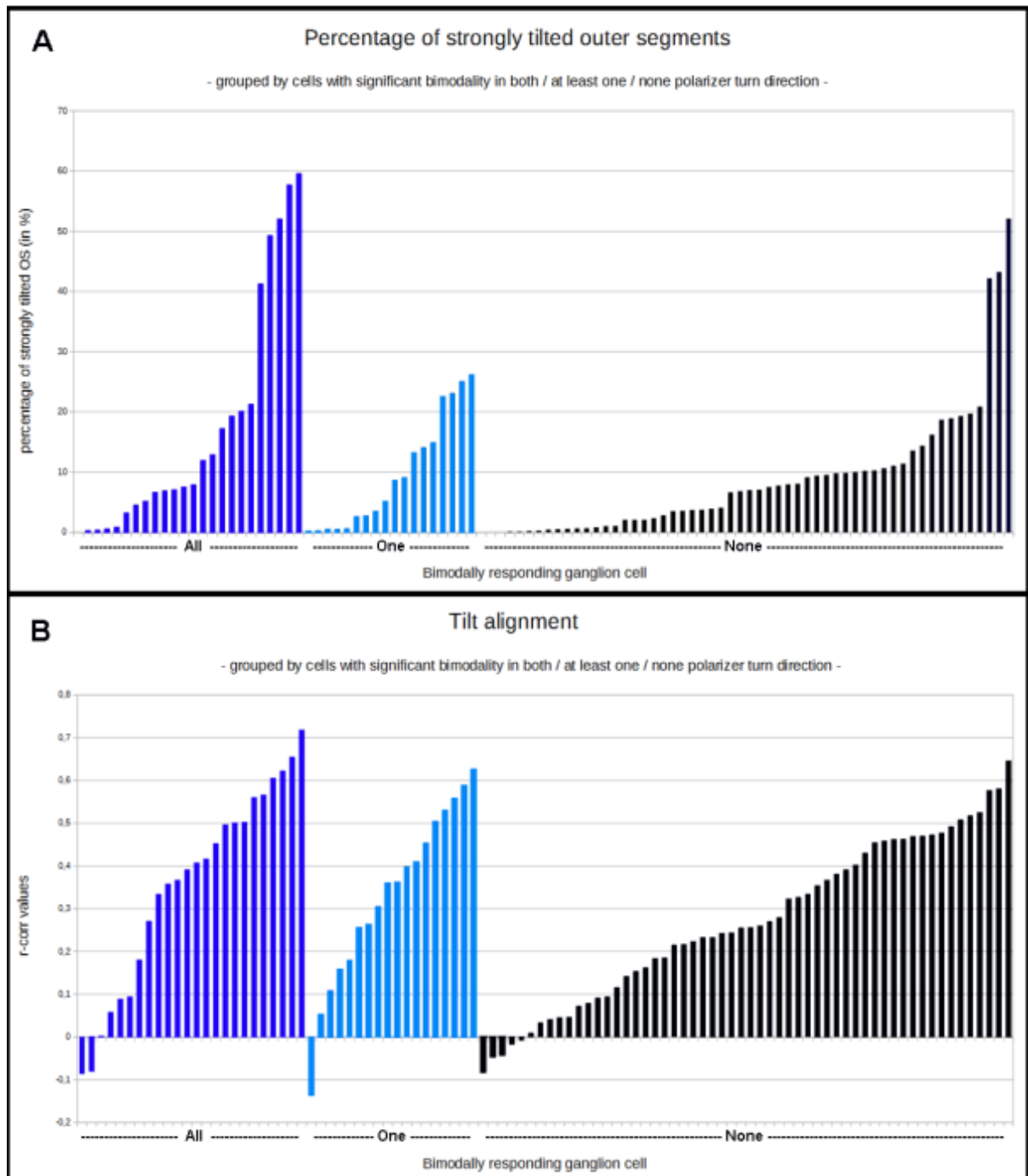


**Figure 18: Neither the percentage of tilted photoreceptors nor the degree of tilt alignment in photoreceptor outer segments could be used as an indicator for the presence nor the absence of a bimodal response in ganglion cells to the turn of a polarizer.** A) The percentage of strongly tilted photoreceptor outer segments (ellipsoid aspect ratio  $ER > 3$ ; see Table 1) was not indicative of a bimodal ganglion cell response. Comparable distribution of low or high percentage was found in ganglion cells that showed significant bimodal responses in both polarizer turn directions (All), in only one polarizer turn direction (One) and in no polarizer turn direction (None). B) The degree of alignment in photoreceptor outer segments was not indicative of a bimodal ganglion cell response. As a measure for alignment, we used the corrected length ( $r\text{-corr}$ ) of the mean doubled angles of the tilting direction of photoreceptor outer segments (Rayleigh Test for axial distribution; see chapter 3.4.2. *Data analysis of rotational stimuli*; Table 1). Positive values ( $r\text{-corr tilt} > 0$ ) indicate a statistically significant axial distribution. The higher the  $r\text{-corr}$  value, the higher the axial alignment of tilt in the scanned photoreceptor outer segments. Comparable distributions of  $r\text{-corr}$  values were found in ganglion cells that showed significant bimodal responses in both polarizer turn directions (All), in only one polarizer turn direction (One) and in no polarizer turn direction (None).

B). Furthermore, no indication for a correlation of the alignment of photoreceptor outer segment tilt (r-corr tilt) with the level of bimodality in the ganglion cell response (r-corr ganglion cell) could be found in our data (Figure 19).

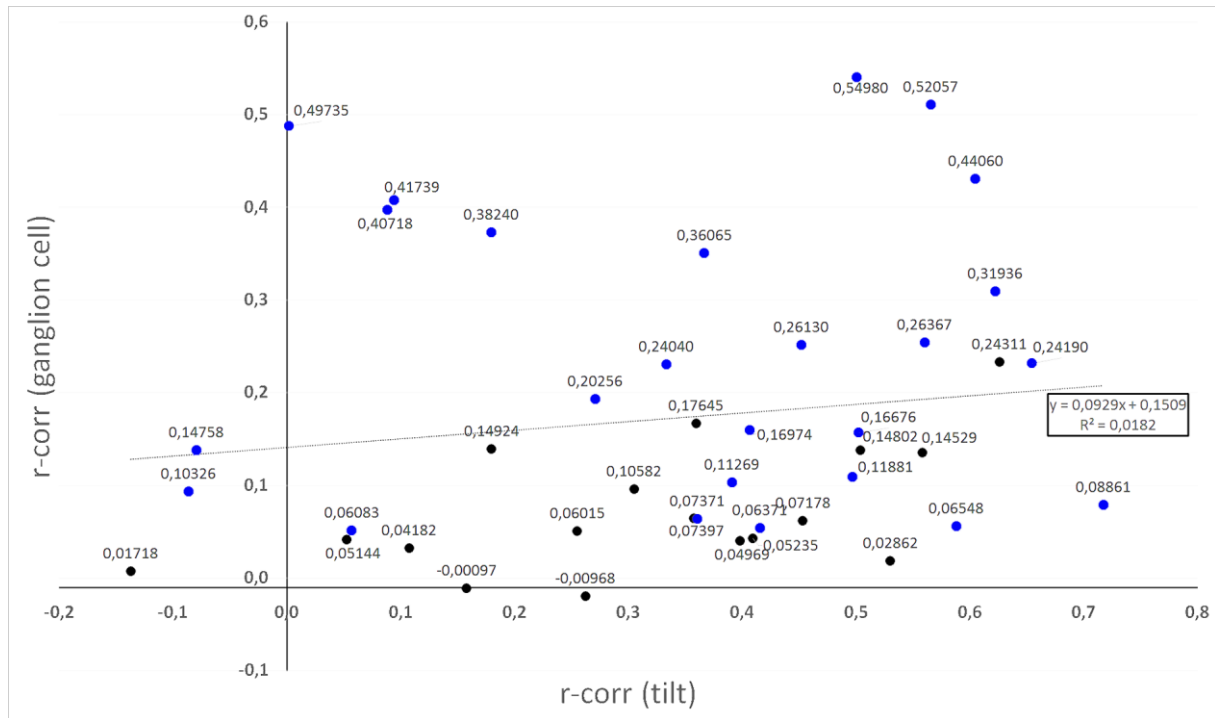


**Figure 19: The degree of tilt alignment in photoreceptor outer segments did not correlate with the degree of bimodality in ganglion cell responses to the turn of a polarizer.** We compared the degree of tilt alignment in photoreceptor outer segments with the statistical level of significance of a bimodal ganglion cell response to the turn of a polarizer, measured as the length of the corrected length (r-corr) of the mean doubled angles, separately for the tilting direction of photoreceptor outer segments (r-corr tilt) and the preferred angle of a ganglion cell response (r-corr ganglion cell; Rayleigh Test for axial distribution; see chapter 3.4.2. *Data analysis of rotational stimuli*; Table 1). The most significantly bimodal ganglion cell responses to the turn of a polarizer (r-corr ganglion cell > 0.4) occurred both when photoreceptor outer segment tilt was highly aligned (r-corr tilt > 0.5) as well as when almost no significant tilt alignment was observed (r-corr tilt < 0.1). The same was observed for ganglion cell responses with less significant axial distributions (r-corr ganglion cell < 0.1). Blue dots: ganglion cells with r-corr > 0 in both polarizer turn directions (Table 1). Black dots: ganglion cells with r-corr > 0 in only one polarizer turn direction (Table 1).

To evaluate, whether the mean axis of outer segment tilt in each scan could be indicative of the associated ganglion cell's bimodal response angle, we used circular statistics to calculate the mean vector and r-corr values of outer segment tilt angles for each of the electrode scans with bimodal ganglion cell responses. Due to the axial character of both the bimodal response in ganglion cells and of the laterally tilted photoreceptor outer segments, an angular deviation of 90° would be the maximum that could be observed. Using circular statistics on the axial values would therefore result in a highly significant distribution, even in completely uncorrelated response-tilt angles. Therefore, we used the doubled angles of the mean tilt

direction for each scan as the basis and subtracted the associated doubled angles of the preferred ganglion cell responses that did show significant bimodal responses to the turn of a polarizer. If transverse dichroism caused by photoreceptor tilt was responsible for bimodal ganglion cells, we should possibly observe a clustering of response angles in a roughly axial distribution in a circular plot (Figure 20, A) and a clustering of response angles plotted against tilting angles with roughly 180° shift in a dot plot (Figure 20, B). We found no evidence for a correlation of the overall tilt angle with the corresponding ganglion cell's response angle.

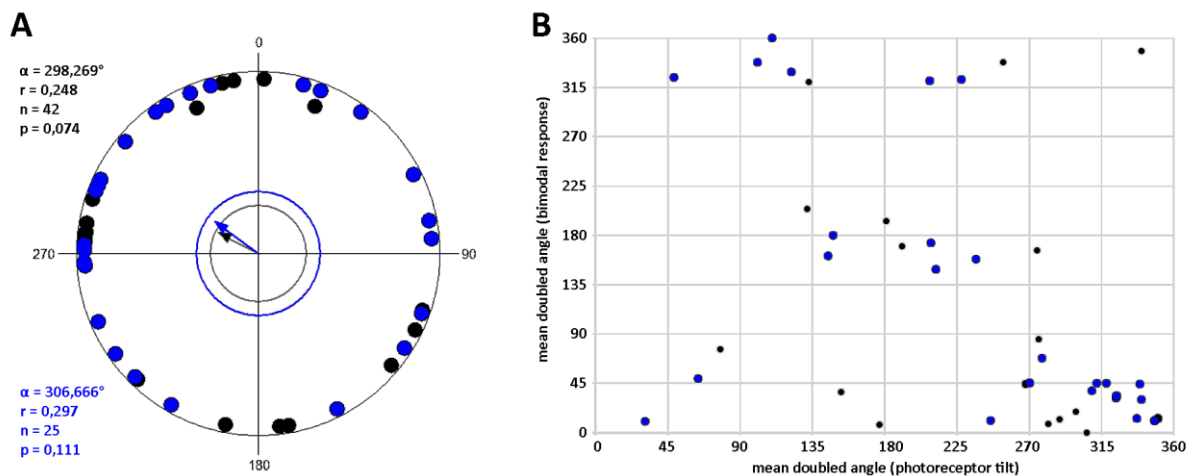


**Figure 20: The cellular response axis and the angle of photoreceptor tilt did not correlate.** Each dot represents a pair of the mean doubled angles from the ganglion cells response to the turn of a polarizer and the corresponding photoreceptor outer segment tilt angle. A) Circular plot of subtracted mean doubled angles. Photoreceptor outer segment tilt angle was set to 0° and each corresponding bimodal ganglion cell response was subtracted. If transverse dichroism caused by photoreceptor tilt was responsible for the angle of bimodal ganglion cell responses, we should observe a significantly axial distribution. We observed random unimodal distributions (Rayleigh Test; Batschelet, 1981). Blue dots: ganglion cells with r-corr > 0 in both polarizer turn directions (Table 1). Black dots: ganglion cells with r-corr > 0 in only one polarizer turn direction (Table 1). B) Dot plot of pairs of mean doubled angles. If transverse dichroism caused by photoreceptor tilt was responsible for the angle of bimodal ganglion cell responses, we should observe a clustering of pairs of response angles and tilting angles with roughly a 180° shift on the x-axis. However, we found no such clustering. Note that all possible angles between 0°+180° (perfect correlation of tilt and response) and 90°+270° (maximal deviation) were represented in this plot. However, the mean angles of bimodal ganglion cell responses (y axis) were not distributed equally, due to the constraint of a dependency on the static e-vector angle during stimulation.

### Conclusion:

The presence of photoreceptor tilt alone cannot give an exclusive explanation for the observed bimodal responses in some cells. The absence of photoreceptor outer segment tilt in one significantly bimodally responding ganglion cell (Figure 17, D) might even suggest proper polarization sensitivity in this cell and - combined with the observations of strong tilt in photoreceptor outer segments of non-bimodally responding ganglion cells - might indicate a coincidental role of tilt in the observed bimodal ganglion cell responses. However, in the

particular scan, some of the inner segments of the photoreceptors were weakly co-stained (see Figure 17 D, light gray staining of inner segments with broader diameter than the outer segments) which were not facing straight upwards as expected but were facing to the side. There is a possibility that this image stack – as well as possibly others – was not scanned completely orthogonally to the photoreceptor layer. If the viewing angle in this scan would be corrected until the depicted inner segments were facing upwards, all the outer segments would appear tilted. However, this reasoning must be considered highly speculative. Nevertheless, in my opinion one exception (1 out of 25 scans) should not be considered the rule.

We found no evidence for correlation in neither the strength (ellipse ratio), the mean angle nor the alignment of photoreceptor tilt (*r*-corr tilt) with the properties of a bimodal response in ganglion cells to the turn of a polarizer (mean angle and *r*-corr ganglion cell). However, it has to be stated here, that the correlation of tilt to cell response has some limitations: we had (a) no specific information on the receptive field of the respective ganglion cells (Chen and Naito, 2009), i.e. which of the scanned photoreceptor outer segments contributed to the cell response (see Figure 17), we assumed that (b) the tilt characteristics of the cone type we stained (i.e. UV cones) were representative of all the cone types in the area, we had (c) no further information on the functional integrity of the neuronal connections between individual outer segments (either tilted or straight) and downstream neurons, i.e. which individual photoreceptor connections were potentially torn off and which ones were tilted but still connected (see Figure 17 and Figure 21 in the next section), and (d) the angular properties of transverse dichroism in avian cone outer segments are unknown. To elucidate the latter, in fish double cone outer segments, the transverse dichroisms has been reported to be not directly coinciding with the transverse axis of the photoreceptor. A rotational freedom seems to be responsible for a tilt of visual pigments in the membranes of cones, allowing angles of up to 20° with respect to the disc membrane stacks (Roberts et al., 2004). In birds, experiments to evaluate such properties have not been published to my knowledge. Consequently, in birds the range of angular mismatch between the long axis of the photoreceptors, documented here as the tilt direction, and the transversal axis of maximum dichroism of linearly polarized light has to be assumed to potentially diverge in a similar way, or more or less, than documented for fish as a representative species for dichroism in vertebrate photoreceptors. In a potential scenario, each photoreceptor might have a differently oriented maximum

transverse absorption axis, which could explain why we cannot document a correlation of the mean vector angles of tilt versus the preferred response angle of the ganglion cell. Additionally, response characteristics varied between recorded ganglion cells, e.g. mixed ON/OFF-responses or ON-responses or OFF-response to light flashes. These response characteristics did change during the experiment in some cells, e.g. from OFF-responses to light flashes in the beginning of a session to ON-OFF-responses to light flashes in the end of a session. A correlation of expected peak response timing (spike angles) with outer segment tilt angles could therefore be biased.

To conclude, there are several uncertainties associated with correlating tilt angle of photoreceptor outer segments and recorded ganglion cell responses angles to polarized light. Nevertheless, I strongly believe that in the mere presence of the lateral tilt of photoreceptor outer segments documented by the experiments of Dr. Arndt Meyer and me, the claim of unambiguous evidence for polarization sensitivity as promoted by the original study (Schneider and Dreyer et al., 2014, unpublished) does not stand.

In addition to this thoroughly tested potential influence of transverse dichroism in tilted photoreceptor outer segments, Dr. Arndt Meyer and I followed a few additional concerns of the reviewers to evaluate further potential sources of unwanted biases in the data. However, we were not able to test the following questions as systematically as the above. Nevertheless, I would like to present some of the results with the remark that the data presented in the following sections are to give a complete picture of potential worst-case scenarios:

(II) E-vector-dependent light intensity changes reflected off the electrode array could in theory differentially stimulate the photoreceptor outer segments through a detached or ruptured pigment epithelium.

The authors of the original study went through great effort to polarimetrically measure possible sources of a light reflection artifact in the light path. This led to the appliance of a 2.5% sinusoidal intensity change control as described above in chapter 3.4.2. However, Schneider and Dreyer et al. (2014, unpublished) did not consider the parts of the electrode array that would be in the light path during stimulation (Figure 21, A+C). The local intensity differences at the electrodes, caused by differential reflections of the e-vector angle upon rotation of the polarizer, were carefully measured by Dr. Arndt Meyer in a simulated scenario. He illuminated the dismantled electrode array with a LED light source (Cree Inc., Durham, NC,

USA; MC-E CREE), placed a linear polarizer (Edmund Optics, Barrington, NJ, USA; Ultra Broadband Wire Grid Polarizer, catalogue #68-750) that was rotated in 720° rotations in between the light source and the electrode array and measured the light intensity at the electrode array with an optometer (Gigahertz-Optik, Türkenfeld, Germany, Model P-9710). Constant light intensity values would be expected if no differential reflection of the e-vector of incident polarized light would occur, and a double sinusoidal curve would be expected if differential reflections did occur at the electrode array. Dr. Arndt Meyers experiment resulted in a double-sinusoidal curve with e-vector-dependent intensity differences peaking around 50% (Figure 21, B). These strong reflection artifacts were mainly caused by the smooth base of the electrode array, that would be shielded by an intact pigment epithelium in the recording situation, but also at the uninsulated electrode tips (Figure 21, A).

Even though the pigment epithelium appeared to be intact in many retinal pieces in the beginning of the recording session (fully described in the methods section in chapter 3.4.2. *retinal preparation*), the pigment epithelium was not intact after many recording sessions, potentially due to mechanical irritation by the super-fusion stream of Ringers solution, preceded by mechanical and chemical stress during tissue preparation, but primarily due to piercing of the electrodes through the retina from the pigment epithelium side (Figure 21, A and C), which in turn led to randomly occurring local detachment of pigment epithelium from the retinal tissue. The visual shielding function of pigment epithelium would in theory not be guaranteed any longer during stimulation with a turning polarizer. Shed-back light off the exposed base of the electrode array could then bias the ganglion cell responses. This was in fact considered a potentially important factor of producing reflection artifacts by Schneider and Dreyer et al. (2014, unpublished).

The strong reflection artifacts were also measured around the uninsulated electrode tips in the light path during a recording session from ganglion cells that might potentially shed e-vector dependent light intensities on to the photoreceptor outer segments. Furthermore, residual retinal tissue and residual pieces of agarose were found alongside the electrode shafts (Figure 21, A), which would be in the light path during stimulation with a turning polarizer. The delicate electrode array was properly rinsed with 70% ethanol for 1-4 hours after each day, by the original authors and by Dr. Arndt Meyer and me. However, some residual debris appeared to stick to the electrodes at arbitrary places (Figure 21, A). Some of these residues were polarization active as depicted in Figure 21, A, i.e. they have optical properties (e.g. chirality,



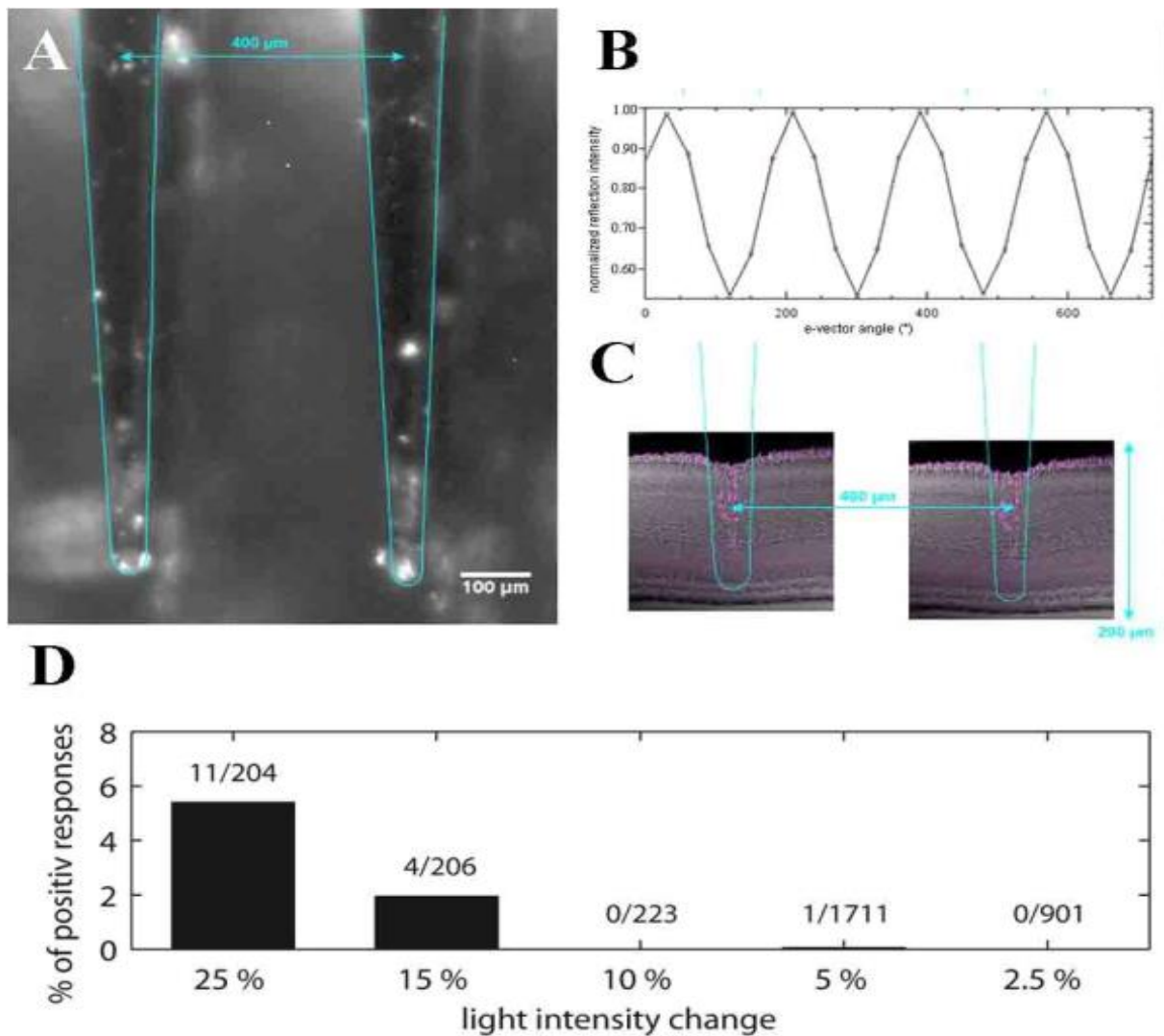


**Figure 21: Evaluation of light intensity artifacts at the electrode array and contrast sensitivity of retinal ganglion cells.** A) Light microscopic image of two adjacent electrode tips in the 10x10 multi-electrode array, viewed through the polarization optics of a light microscope. Seen through two crossed polarizers, the image would be completely dark, if no properties of the e-vector distribution in the light was modified. The brighter tips of the electrodes indicate differential e-vector reflection. Note the bright spots at the electrodes originating from polarization-active residual debris. B) Polarimetric measurements revealed a sinusoidal light intensity change reaching up to 50% intensity difference in polarized light reflected from the electrode array. Measurements were done upon rotating the e-vector orientation of linearly polarized light in discrete steps. C) Transverse vibratome section through the part of the retina where the electrode was located during a recording session (compare to B). The stained photoreceptor outer segments (magenta) illustrate the retinal damage done by the electrode tips that tore and pushed photoreceptor outer segments down into the electrode pit. D) Percentage of ganglion cells that responded to discrete light intensity change contrast steps (Schneider and Dreyer et al., 2014, unpublished). Note that at a contrast as high as 25%, only roughly 5.4% (11/204) of the cells responded, at 15% intensity change only a subset of roughly 1.9% of all stimulated cells responded. A-C) received with kind courtesy of Dr. Arndt Meyer. D) From Schneider and Dreyer et al. (2014, unpublished).

birefringence) that rotate the vibrational axis of incident polarized light. Such particles can either facilitate or diminish an effect of differential reflection originating at the electrodes.

To conclude, we found arbitrarily occurring polarization-active residues in the light path, differential light intensity changes measured at the electrode tips and a potentially missing shielding function of the pigment epithelium that might potentially allow a local back-

shedding effect of differential light intensity changes off the base of the electrode array onto the photoreceptor outer segments during recording from ganglion cells.

Assuming a worst-case scenario, the local disruption of pigment epithelium could in theory lead to bimodal excitation patterns in adjacent photoreceptors that are stimulated by the sinusoidal intensity changes of up to 50% upon rotating a polarizer. It is very important to note here, that the degree of pigment epithelium disruption across the retina can vary drastically due to the unpredictable effect size of the different sources of disruption given above (e.g. electrode holes, super-fusion stream, incisions made during retinal preparation). Therefore, we can assume that such a scenario could potentially occur locally and at arbitrary locations across the retinal piece. Consequently, not all ganglion cells we recorded from would be stimulated with a similar light intensity change and not with the same e-vector distribution, i.e. only a subset of ganglion cells in one recording could in theory respond bimodally where overlapping reflection artifacts add up, while effects cancel each other out for ganglion cells at other locations where the pigment epithelium was intact or polarization active residues diminished the effects.

However, there are more positive arguments that could be raised here to diminish the role of these reflection artifacts all together. One important argument would be that the absence of pigment epithelium does not correlate with the presence of bimodal ganglion cell responses. Across the 98 electrode scans we analyzed for photoreceptor tilt, we found pigment epithelium that appeared to be completely intact in bimodally responding ganglion cells, and on the other hand we found minute local and far-scaled disruption of the pigment epithelium adjacent to both bimodally and non-bimodally responding ganglion cells. However, in my opinion, the same reasoning as in the section above should be applied here: if the potential influence of reflection artifacts cannot be excluded, a claim for unambiguous evidence of polarization sensitivity should not be held up.

(III) Reduced overall retinal health and addressing the additional reviewers' critique that low contrast sensitivity might explain why only a subset of ganglion cells responded bimodally to the turn of a polarizer.

For extracellular recordings at the ganglion cell layer the electrodes needed to be pushed through the photoreceptor cell layer to the proximal part of the retina (Figure 21, C). Therefore, the structural integrity of the photoreceptors and the retinal network might be locally disrupted (Figure 21, C, stained photoreceptor outer segments - depicted in magenta -

were torn and pushed down into the electrode pit). This might lead to a local loss of functionality and reduced overall retinal health. According to this assumption, the authors of the original study (personal communication with Dr. Dreyer) as well as Dr. Arndt Meyer and I observed spreading depression events in virtually all retinal samples recorded from. These rhythmic spiking events are indicators of mechanical, electrical and oxidative stress and cell death in the retina (Van Harreveld, 1978; Nedergaard et al., 1985), spreading like waves across the retina, making it temporarily and repeatedly unresponsive to light stimulation. Furthermore, Schneider and Dreyer et al. (2014, unpublished) reported a high threshold for intensity contrast in their recordings (cells responded to intensity contrast only above 10%; Figure 21, D). I successfully recorded a bimodally responding ganglion cell using the identical stimulation protocol as in Schneider and Dreyer et al. (2014, unpublished), but interspersing the turns of the polarizer with an intensity sinus of 15% contrast, instead of 2.5% contrast. The raw data of these recordings and the analyzed results can be found on the external hard drive linked to this thesis here "Toshiba:\RawData Chapter 3.4\5 Results of additional recordings\Chapter 3.4.4. III". To determine the number of cells recorded from simultaneously, I initially stimulated the retina with light flashes of unpolarized light (500ms flashes, 2s pause interval) prior to the first turn of a polarizer. 65 cells responded to light flashes, i.e. 65 cells were recorded from simultaneously (Figure 22, yellow tipped electrodes). Only 8 of these 65 cells responded to the 15% sinusoidal light intensity change (Figure 22, Insert boxes). 1 of these 8 responded bimodally to the turn of a polarizer in both directions (highly significant bimodal response; Figure 22, Electrode 98), 3 of these 8 cells responded bimodally in one polarizer turn direction (Figure 22, Electrode 99, 90 and 89). None of the other 57 cells showed significant bimodal responses to the 360° rotations of a polarizer. This result may be considered as anecdotal, since I was not able to systematically test a larger quantity of retinae for statistical evaluation of the phenomenon. Nevertheless, this example could suggest that the subset of retinal ganglion cells that responded bimodally to the turn of a polarizer observed by Schneider and Dreyer et al. (2014, unpublished) and by Dr. Arndt Meyer's and me, might be a subset of cells that were still sensitive to intensity contrast at all. Such a notion suggests, that small light intensity changes, i.e. artificial transverse dichroism in some outer segments (i) or/and an artificially introduced reflection artifact (ii), might potentially be detected by the most contrast sensitive cells only. If the overall retinal health condition emits the major part of all potential cells (57 out of 65 cells in the exemplary

experiment presented here), a subset of ganglion cells responding with a bimodal response to the turn of a polarizer cannot be considered as indicative for a specialized a polarization sensitive retinal pathway. Regarding the same logic, my experiment provided an indicator for why not many more cells would have responded to potential artificial light intensity changes. A more systematic approach to address this question might lead to more conclusive, less speculative results.

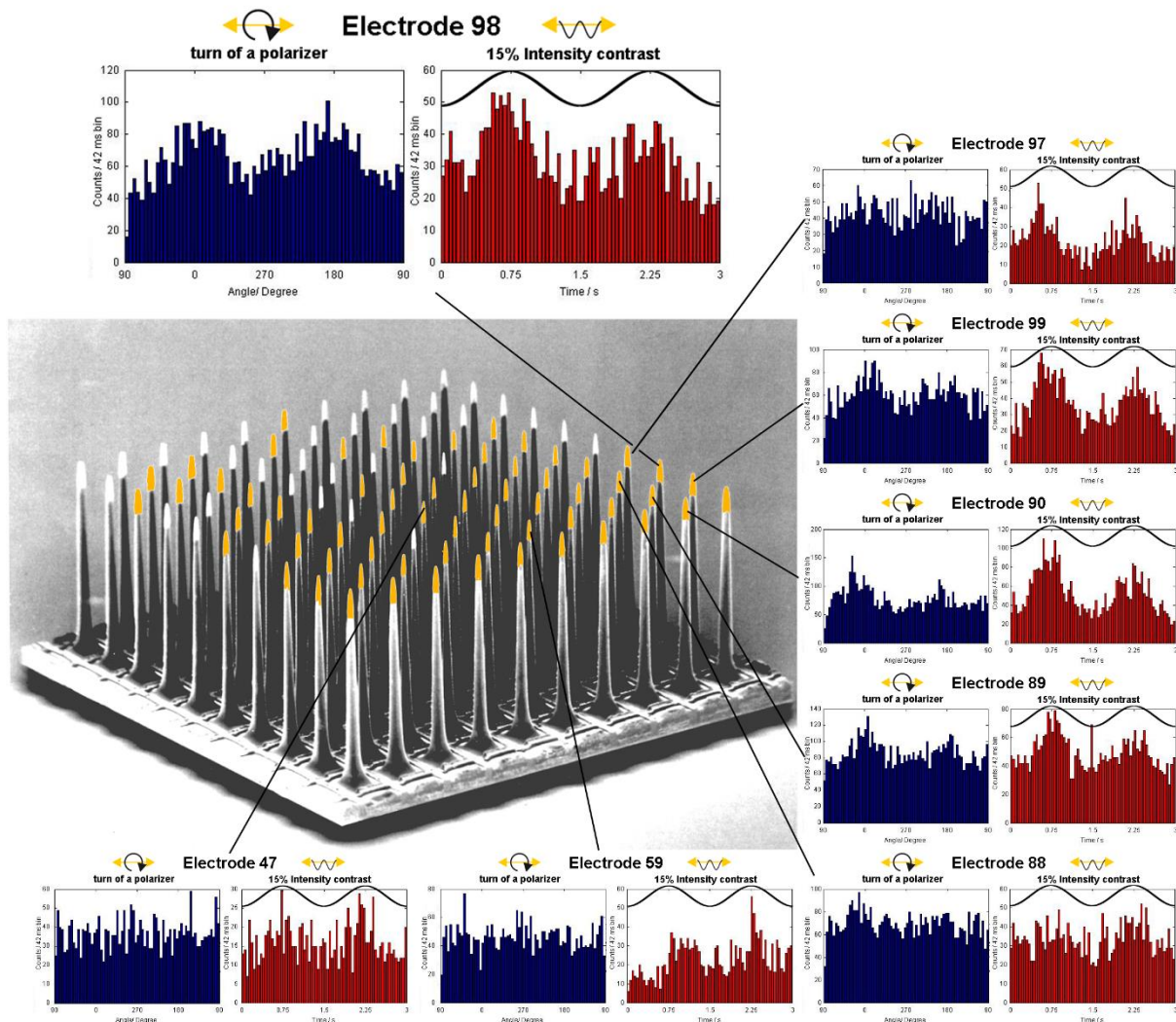


**Figure 22: Low overall contrast sensitivity could explain the low number of bimodally responding cells upon the turn of a polarizer.** In a recording from retinal ganglion cells following the preparation and stimulation protocol of Schneider and Dreyer et al. (2014, unpublished), but with an intensity sinus of 15% contrast instead of 2.5%, only 8 (Electrodes 47, 59, 88, 89, 90, 97, 98 and 99) out of 65 (yellow tipped electrodes in the center scheme of the electrode array) responded significantly bimodal to the intensity sinus with 15% contrast. Among these 8 contrast sensitive cells, 1 cell (electrode 98) responded significantly bimodal to the turn of a polarizer and 3 cells showed clear tendencies towards significant bimodality (Electrode 89, 90 and 99). All other recorded ganglion cells did neither show contrast sensitivity to a 15% intensity sinus nor bimodal responses to the turn of a polarizer.

(IV) Properties of the stimulation protocol used in Schneider and Dreyer et al. (2014, unpublished) might have reduced the number of retinal ganglion cells responding bimodally to the turn of a polarizer.

The constant light stimulation might have negatively affected the responsiveness of the retinal ganglion cells by negative effects on retinal health e.g. photoreceptor bleaching and neurotransmitter depletion. In order to avoid this factor and therein potentially preserve the overall retinal sensitivity, i.e. to stimulate as many cells in the retina as possible, I modified the light stimulation protocol in the following ways: The light was switched off for 4 seconds between one set of trials, turned on for 3 seconds with a stationary e-vector, followed by one trial of polarizer turns in clockwise (CW) and counterclockwise (CCW) directions, respectively, followed by one trial of a sinusoidal 75% light intensity change, each interspersed by 1 second pause duration. The spectral filter was removed to stimulate with broad band white light (~400 - 800  $\mu\text{m}$ ) instead of spectrally narrowed green light (520 - 580  $\mu\text{m}$ ). Light intensity levels were adjusted (measured with a portable spectrometer: Ocean optics, Dunedin, FL, USA, USB4000-UV-VIS) to match intensities used by Schneider and Dreyer et al. (2014, unpublished). The raw data of these recordings and the analyzed results can be found on the external hard drive linked to this thesis here "[Toshiba:\RawData Chapter 3.4\5 Results of additional recordings\Chapter 3.4.4. IV](#)". As a result, 85 cells throughout this recording session responded bimodally to a 75% intensity change (Figure 23, blue tipped electrodes), and 20 of these cells responded bimodally to the turn of a polarizer. 16 of these 20 cells responded bimodally in both turn directions of a polarizer (highly significant bimodal response; Figure 23, blue tipped electrodes), 4 of these 20 cells responded bimodally in one polarizer turn direction. The high number of contrast sensitive cells indicated good overall retinal health in this recording. However, these numbers should not be compared to the numbers in the experiment described in the previous section. Here, I used a very high sinusoidal intensity change to continuously stimulate as many cells as possible, rather than testing for low contrast sensitivity as a control against reflection artefacts. However, the number of bimodally responding ganglion cells to the turn of a polarizer was the highest ever observed in any of our recording sessions. It appears that my attempt to preserve retinal sensitivity by the changes in the stimulation protocol was successful in this recording. Nevertheless, I realize that an alternating contrast setting, i.e. a presentation of either a 2.5% intensity change or a 75% intensity change in every second set of trials, would have been optimal.

This anecdotal result might suggest that some modifications of the stimulation protocol that use full spectrum light to stimulate all photoreceptor types and that avoid bleaching and neurotransmitter depletion by allowing recovery time with lights off between polarizer turns, could enhance the numbers of bimodally responding ganglion cells in recordings. Although speculative, the bleaching and neurotransmitter depletion effect might serve as an explanation for the absence of bimodal responses in some cells with high outer segment tilt and disrupted pigment epithelium. The observation of an adaptation in ganglion cell response to the static e-vector angle in the beginning of the recording sessions and in between polarizer turns (Schneider and Dreyer et al, 2014, unpublished; for details see methods section in 3.4.2.; Figure 14 and 15) could in theory be explained by a bleaching effect that selectively affects the photopigment aligned in parallel to the static e-vector. By bleaching of photopigment parallel to the static e-vector, only the photopigment perpendicular to the static e-vector could contribute to the cell response upon the subsequent rotation of a polarizer (Schneider and Dreyer et al, 2014, unpublished; for details see methods section in 3.4.2.). Consequently, the ganglion cell would respond bimodally to the polarizer turn with a preferred angle  $90^\circ$  to the static e-vector angle (as depicted in Figure 15). However, this is mere speculation and a systematic approach would be useful to prove or disprove this assumption.

The adjacent position of bimodally responding ganglion cells and their location at the edges of the electrode array (Figure 23, blue tipped electrodes) was observed repeatedly. It was very unfortunate, that the attempt to stain the outer segments in this particular retinal piece failed due to some unexpected damage of the retina during processing for scanning in the confocal laser scanning microscope. The adjacent position of bimodally responding ganglion cells (Figure 23, blue tipped electrodes) might be an indicator for true polarization sensitivity. Many natural polarization sensitive visual systems have their specialized photoreceptors arranged in specialized areas in array-like formation, like the dorsal rim area in insects (Labhart, 2016), the midband ommatidia in stomatopod crustaceans (Marshall et al, 2007) or the specialized retinal rows in anchovy teleost fish (Hawryshyn, 2010). On the contrary, the reoccurring adjacent location of bimodally responding ganglion cells at the edges of the electrode array in many independent recordings, i.e. close to the edges of the retinal piece where incisions were made during tissue preparation (for details see the methods section in this chapter *retinal dissection*; Figure 23, blue tipped electrodes), might be a result of photoreceptors that “lean” over the cutting edge of the retinal piece and/or a torn pigment epithelium close to the



incision lines. It remains up to debate which of the two explanations might be true. Based on our isolated findings here in these rather unsystematic experiments, argumentation in the one or the other direction would be highly speculative.

Nevertheless, in addition to the potential influence of photoreceptor tilt (i) and potential local reflection artifacts (ii), it cannot be excluded that the enhanced probability of bimodally responding cells observable at the edges of many retinal pieces could be explained by artificial causes. Therefore, the claim of unambiguous evidence for polarization sensitivity is challenged further.

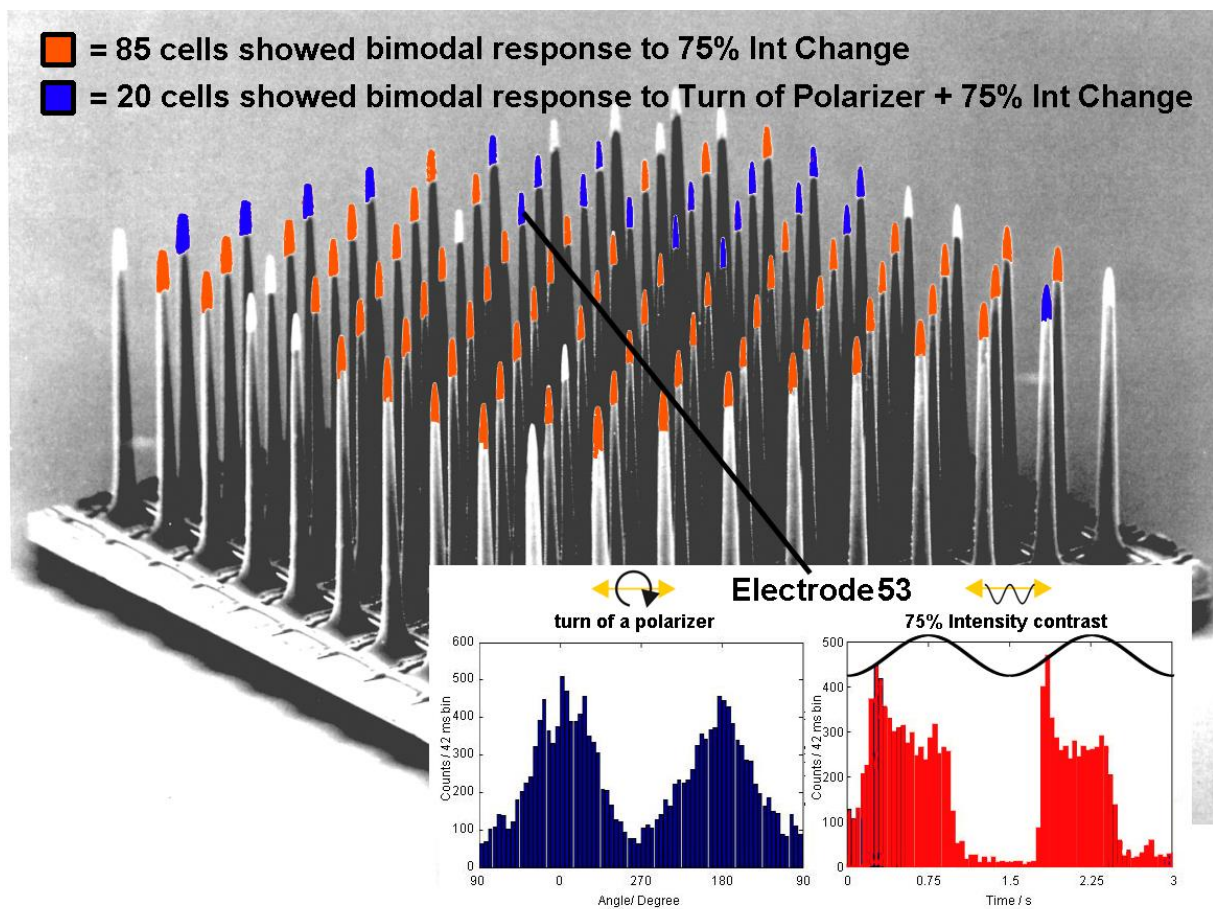


**Figure 23: Increased numbers of bimodally responding cells to the turn of a polarizer by stimulation with broad-spectrum polarized light, interspersed with periods of lights OFF, instead of constant illumination with green light.** In one recording, retinal ganglion cells were enabled to recover from light stimulation between each set of CW- and CCW rotation of the polarizer, followed by an intensity sinus with 75% contrast. Good overall retinal responsiveness was indicated by 85 cells that responded bimodally to the intensity sinus (orange tipped electrodes, red bars in right panel of the insert box). Of these 85 cells, 20 cells responded significantly bimodally to the turn of the polarizer (blue tipped electrodes, blue bars in left panel of the insert box). These high numbers of positive cells in one retinal piece were unexpected in a visual system that was naturally sensitive to polarized light. Note that the bimodal responses to the turn of the polarizer come from electrodes at the edges of the array, and putatively close to the edges of the intact part of the retinal piece close to the incisions made during preparation. The adjacent location of these 20 cells could indicate a specialized area in the retina on one hand, or artificial sensitivity to polarized light due to reflection artifacts and photoreceptor tilt at the edges of the retinal piece on the other hand.

(V) Are the ganglion cell responses recorded by the original authors really part of a separate response continuum?

One of the selection criteria for highly significant bimodality in retinal ganglion cells by the authors of the original study considered only cells with significant bimodal responses in both directions (CW and CCW) and when combined (i.e. bimodal significance in three modalities), measured by the corrected length of the mean vector of doubled angles ( $r\text{-corr CW} > 0 + r\text{-corr CCW} > 0 + r\text{-corr combined} > 0$ ; Schneider and Dreyer et al., 2014, unpublished; see chapter 3.4.2. *Data analysis of rotational stimuli*). Dr. Arndt Meyer and I considered a scenario in which retinal ganglion cells with small positive  $r\text{-corr}$  values in one direction of a turning polarizer might tend to possess a comparably small  $r\text{-corr}$  value – or slightly smaller or slightly higher - in the opposite direction and when combined. This assumption given, ganglion cells that showed small  $r\text{-corr}$  values, marginally positive in one direction of a turning polarizer, but slightly negative in the opposite direction of a turning polarizer, would be excluded from the response continuum of highly significantly bimodal responding cells in Schneider and Dreyer et al. (2014, unpublished). These ganglion cell responses would be sorted to the continuum of non-bimodally responding ganglion cells (Schneider and Dreyer et al., 2014, unpublished; Figure 16). By this selection, the probability of ganglion cells with marginally significant bimodal responses would be reduced, and thereby biasing the left flank of the Gaussian distribution of putatively e-vector-encoding ganglion cells. This selection might have led to the separate response continua observed by Schneider and Dreyer et al. (2014, unpublished; see Figure 16 and compare to Figure 24). A simple example of such a potential sorting bias can be given in a histogram plotting the distribution of  $r\text{-corr}$  values recorded by Dr. Arndt Meyer and me (Table 1), binned in 0.1 intervals (Figure 24). Plotting two distributions, where either all cells with  $r\text{-corr} > 0$  in at least 1 direction of turning a polarizer (see Table 1,  $n = 42$ ; Figure 24) were plotted, or only the selected cells with  $r\text{-corr} > 0$  in all three modalities (see Table 1,  $n = 25$ ; Figure 24) were plotted, resulted in the elimination of all  $r\text{-corr}$  values  $< 0.1$  (positive  $r\text{-corr}$  values close to zero in at least one turning direction of a polarizer) in the latter distribution (Figure 24).



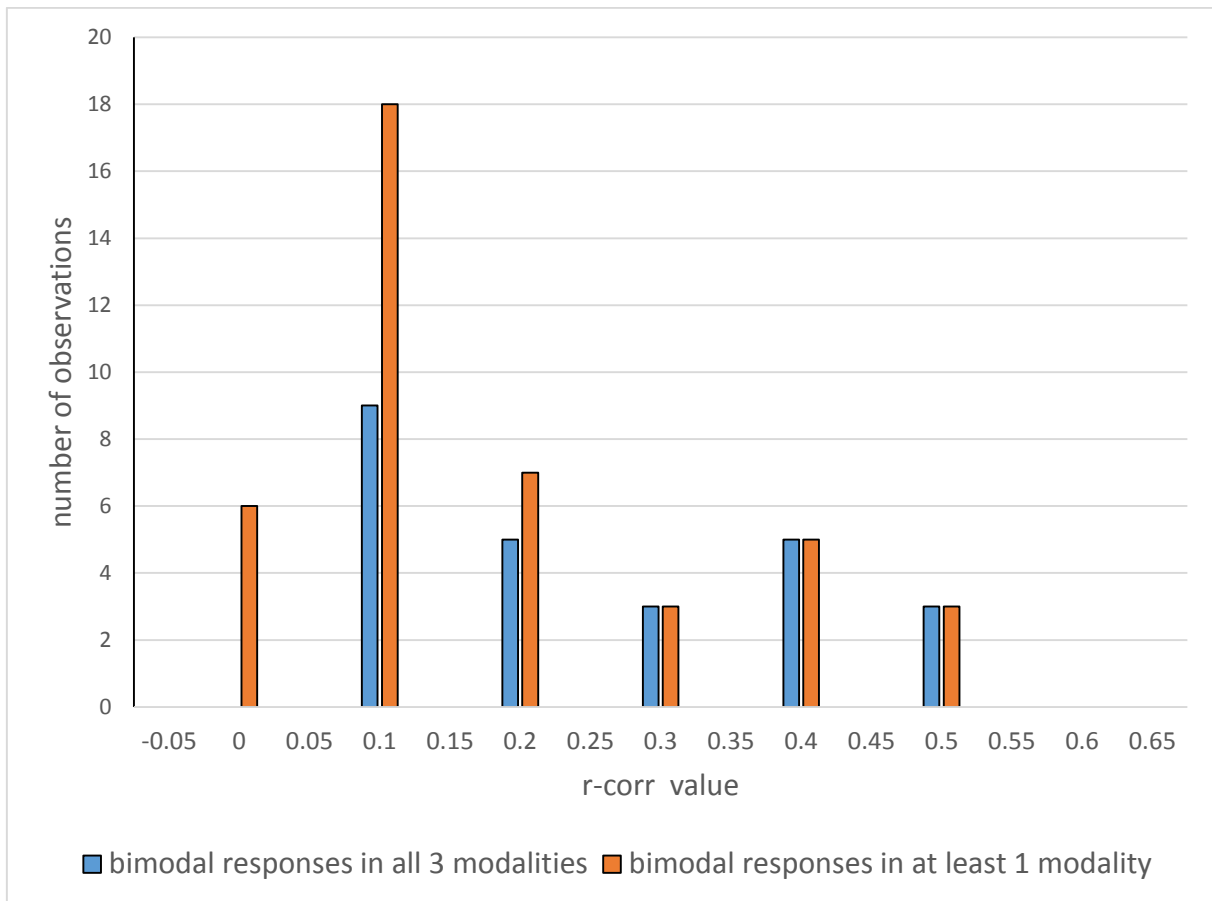


**Figure 24: Selection criteria eliminate the smallest r-corr values.** A histogram of the distribution of r-corr values recorded by Dr. Arndt Meyer and me (Table 1), binned in 0.1 intervals. Orange bars: r-corr values of cells that showed bimodal responses in at least one direction of turning a polarizer (n = 42; see Table 1). Blue bars: r-corr values of cells that showed bimodal responses in both directions of turning a polarizer and combined (n = 25; see Table 1). Note that all ganglion cells with r-corr values below +0.05 and half (9 out of 18) ganglion cells with r-corr values between 0.05 and 0.15 were eliminated by selection in the blue distribution, leading to a biased left flank of the distribution.

(VI) The anticipatory “paradox” polarization response is not paradox and not exclusively indicative for polarization sensitivity:

The e-vector angle at which a polarization sensitive cell maximally responds to linearly polarized light ( $\Phi_{\max}$ ) has been reported to depend on the direction of turning a polarizer in insects (Sakura et al., 2008; Träger and Homberg, 2011; c.f. Schneider and Dreyer et al., 2014, unpublished). The  $\Phi_{\max}$  in clockwise turns was observed to occur earlier, i.e. at lower angles, as compared to counterclockwise turns (depicted in Figure 25). This phenomenon has been termed a “predictive” or “paradox” polarization response because the opposite, i.e. a slightly delayed response would be expected due to latencies between photoreceptor stimulation and ganglion cell response (Sakura et al., 2008; Träger and Homberg, 2011; c.f. Schneider and Dreyer et al., 2014, unpublished). Since this phenomenon has been reported in insect polarization sensitive cells (Sakura et al., 2008; Träger and Homberg, 2011; c.f. Schneider and

Dreyer et al., 2014, unpublished) as well as in the experiments of Schneider and Dreyer et al. (2014, unpublished), it was considered an additional indicator for true polarization sensitivity by the original authors (Schneider and Dreyer et al., 2014, unpublished).

*An explanation for a direction-dependent  $\Phi_{max}$  in polarization sensitive cells:*

The primary perceptual prerequisite for sensitivity to polarized light is a high dichroic ratio on photoreceptor level. The dichroic ratios measured in insect rhabdomers averaged around 10:1, which corresponds to an axial alignment of the long axis of photosensitive molecules with  $\sim 34^\circ$  axial deviation (Snyder & Laughlin, 1975; depicted in Figure 25, A, black lines). Cells with lower dichroic ratios (i.e. < 10:1) possess an even higher axial deviation in their photopigment alignment (i.e. >  $34^\circ$ ; Snyder & Laughlin, 1975). Given that photosensitive molecules in cells with high dichroic ratios ( $\sim 10:1$ , Snyder & Laughlin, 1975) were reported to be aligned with a certain angular deviation, this range of alignment angles might lead to a range of e-vector angles that maximally excite a cell (Figure 25, A and B, window of maximal absorption). As an example, a photoreceptor cell that has its molecules aligned in the  $90/270^\circ$  plane  $\pm 17^\circ$  (high dichroic ratio = 10:1, angular deviation =  $34^\circ$ ; Figure 25, A, black lines) would be maximally excited at e-vector angles between  $73-107^\circ$  and  $253-287^\circ$  (Figure 25). Assuming we stimulate with polarized light and rotate the polarizer, upon a clockwise rotation the maximal light absorption would occur at  $73^\circ/253^\circ$  (Figure 25, A and B, purple circles). Upon a counterclockwise rotation on the other hand, maximal light absorption would occur at  $107^\circ/283^\circ$  (Figure 25, A and B, orange circles). Consequently, the  $\Phi_{max}$  is different depending on the direction of rotation, with a higher  $\Phi_{max}$  value for counterclockwise (i.e. a presumably later response) than clockwise turns (i.e. a presumably earlier response). This is my attempt to explain the “paradox” response reported in polarization sensitive cells in insects (Sakura et al., 2008; Träger and Homberg, 2011; c.f. Schneider and Dreyer et al., 2014, unpublished). To conclude my argument, this phenomenon would be based on true cellular dichroism, i.e. polarization sensitivity, but would not be based on any “anticipation” or “prediction” of the e-vector by the cell, but in this scenario on the imperfect photopigment alignment in a biological system, expressed as its dichroic ratio, that results in a window of acceptance for e-vector angles maximally exciting the cell.

*Why a direction-dependent  $\Phi_{max}$  might not be indicative of true polarization sensitivity:*

Retinal ganglion cells in vertebrates collect the graded potentials of hundreds of

photoreceptors in their receptive field (Masland, 2001; Sanes and Masland, 2015) and ganglion cells respond in form of action potentials when a certain membrane threshold is crossed (all-or-nothing response; Masland, 2001; Sanes and Masland, 2015; see sketch in Figure 26, A).

A consequence of dichroic molecule alignment in polarization-sensitive photoreceptors is that e-vectors oriented in parallel to this alignment lead to highest absorption, perpendicular e-vectors lead to lowest absorption, and 45° oriented e-vectors lead to intermediate absorption. A 360° rotation of the e-vector angle of polarized light would consequently result in a sinusoidal excitation curve with two intensity peaks ( $\Phi_{\max}$ ) and two intensity dips ( $\Phi_{\max} \pm 90^\circ$ ) for the polarization sensitive photoreceptor (see sketch in Figure 25, B). A very comparable sinusoidal intensity curve would be perceived by non-polarization-sensitive photoreceptors stimulated with a regular sinusoidal light intensity change. In both cases, the retinal ganglion cell would respond bimodally, with a preferred response timing (comparable to  $\Phi_{\max}$ ) at the perceived light intensity where the all-or-nothing membrane potential threshold was crossed (depicted in Figures 26, A and B). It is important to note two things: First, the membrane potential threshold resulting in action potentials of a ganglion cell would be crossed when a sufficiently high number of photoreceptors were maximally excited (all-or-nothing response; Masland, 2001; Sanes and Masland, 2015). In other words, if the peak intensity of a sinusoidal intensity change was sufficiently high, the ganglion cell response would not occur at the peak intensity of the sinus, but as soon as the threshold would be crossed (depicted in Figure 26, A and B). Second, by definition, the differential e-vector reflections off surfaces would be dependent on the e-vector angle of incident light, i.e. the dips and peaks in light intensity caused by a light reflection artifact during the rotation of a polarizer can be assigned precisely to perpendicular e-vector angles.

Let us assume a scenario in which the light intensity changes of 75% presented in the recording session in this chapter subsection IV would have been caused by an e-vector-dependent reflection artifact (depicted in Figure 26, C and D). In this scenario, e-vector angles of 90°/270° would be assigned to the dips in light intensity when rotating a polarizer, e-vector angles of 0°/180° would be assigned to peaks in light intensity upon rotation of a polarizer. Following this assumption, I was able to assign each spike time during the 75% intensity change to a hypothetical e-vector angle that would correlate to that intensity caused by a perfect reflection artifact during the turn of a polarizer (the same was done in the contrast controls

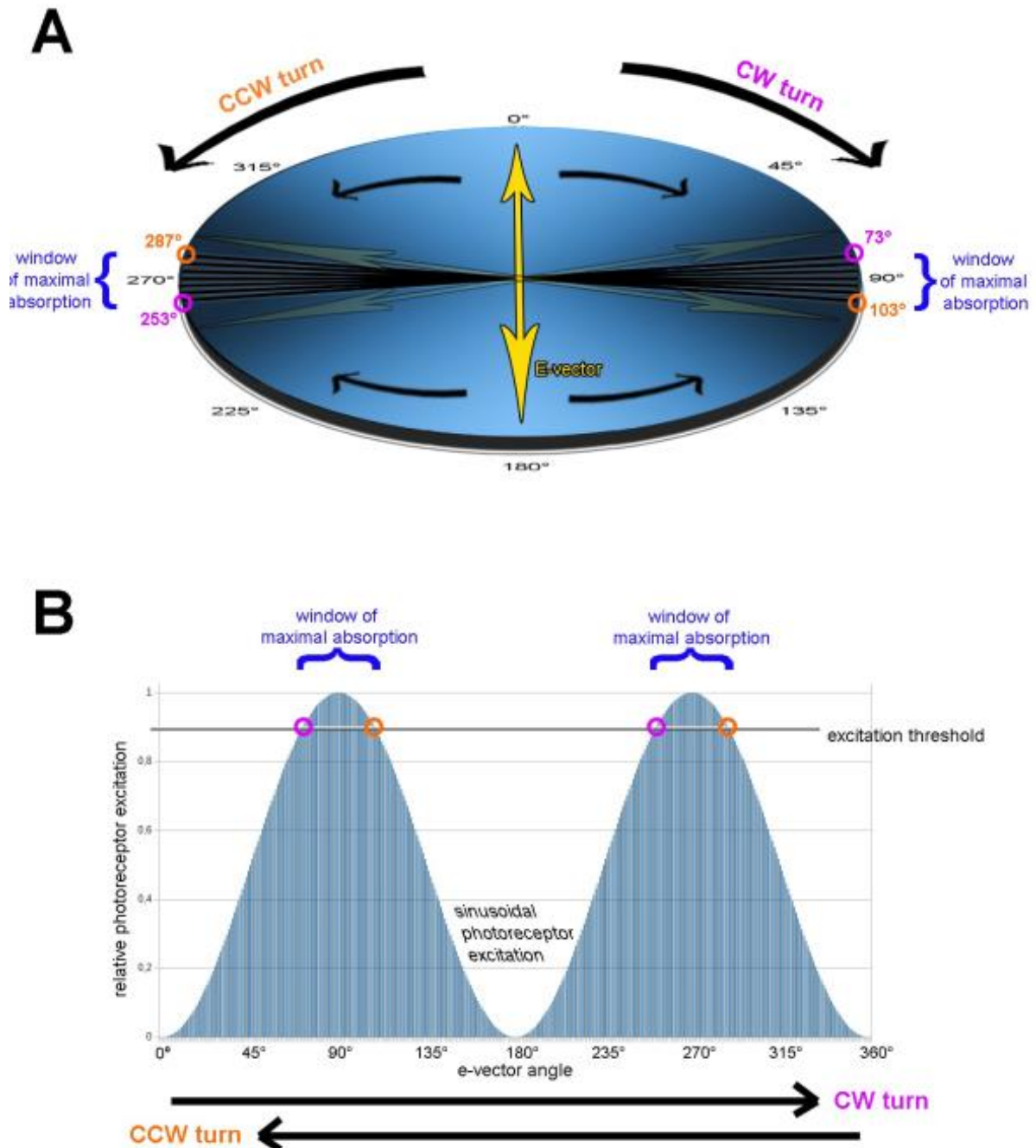


**Figure 25: Illustration of a potential explanation for the direction-dependent  $\Phi_{\max}$  in polarization sensitive cells.** A) Schematic illustration of photosensitive molecule alignment in highly dichroic photoreceptor cells. B) Schematic illustration of the relative photoexcitation in a highly dichroic photoreceptor cell according to the e-vector angle of rotating linearly polarized light.

The axial alignment of photosensitive molecules in polarization sensitive photoreceptors (black lines in (A)) is expressed by the dichroic ratio (highest values measured in insects, ranging around 10:1, and  $\pm 17^\circ$  angular deviation). This deviation might lead to a range of e-vector angles that maximally excite the cell (window of maximal absorption in (A and B)). As an example, we assume that a highly dichroic photoreceptor cell with photosensitive molecules aligned in the  $90/270^\circ \pm 17^\circ$  (dichroic ratio = 10:1, black lines) was stimulated with light sent through a linear polarizer. The cell would be maximally excited at e-vector angles between  $73\text{--}107^\circ$  and  $253\text{--}287^\circ$  (window of maximal absorption in A and B) and least excited at e-vector angles between  $343\text{--}17^\circ$  and  $163\text{--}197^\circ$ . Assuming we rotate a polarizer, upon a clockwise rotation the maximal excitation of the cell would occur at  $73^\circ/253^\circ$  (A and B). Upon a counterclockwise rotation, the maximal excitation would be reached at  $107^\circ/287^\circ$  (A and B). Consequently, the  $\Phi_{\max}$  would be depending on the direction of rotation with a higher  $\Phi_{\max}$  value (i.e. presumably later responses) for counterclockwise turns than clockwise turns (i.e. presumably earlier responses).

for bimodal responses to a 2.5% intensity change in Schneider and Dreyer et al., 2014, unpublished; see chapter 3.4.2 *Control experiments in the original study by Schneider and Dreyer et al. (2014, unpublished)*. During this “simulated reflection artifact” caused by turning of a polarizer in opposing directions, the intensity threshold that led to a ganglion cell response was crossed at lower angles for CW and higher angles for CCW turns (compare Figure 26, C vs. D). Dr. Arndt Meyer and I suggest that an artificial intensity change caused by differential e-vector reflections could in theory mimic the “direction-dependent polarization response” and therefore we suggested, that observations of this phenomenon are not indicative of true polarization sensitivity (Figure 26).

### **3.4.5. Concluding remarks**

To conclude with a synergy of the above documented: Dr. Arndt Meyer and I observed retinal damage (Figure 21, A and C) in form of fractured pigment epithelium, torn photoreceptors that were pushed down towards the ganglion cell layer (Figure 21 C), photoreceptor tilt towards the transverse axis (Figure 17), weak overall contrast sensitivity in most recordings (Figure 21, C and Figure 22), cellular stress in the retinal tissue observable in spreading depression events, and the potential presence of reflection artifacts originating at the electrode array (Figure 21, A and B). In the face of these observations, we cannot be sure if the bimodal responses to the turn of a polarizer in Schneider and Dreyer et al. (2014, unpublished) and our own experiments originate in true polarization sensitivity of the visual system of domestic chicken or in some or some other artifacts described above. We were however able to demonstrate how much effort can be needed to unravel the potential sources of reflection artifacts and potentially introduced artificial polarization sensitivity upon the stimulation with linearly polarized light. We hope that future studies can take our insights into account and that our demonstration of unforeseen sources for light artifacts and pitfalls in apparently well-designed approaches might help to design novel methods to finally prove or disprove polarization sensitivity in birds.

I explicitly want to state here that the efforts and thought put into the approach designed by my former colleagues were excellent. In fact, the design of the original study was beyond comparison in avian research on polarization sensitivity regarding the amount of consideration and care that has been put into a light stimulation protocol, in control experiments against light reflection artifacts and in the fully automated double-blinded data analysis (see chapter 3.4.2.). There was much to like about the techniques chosen by the

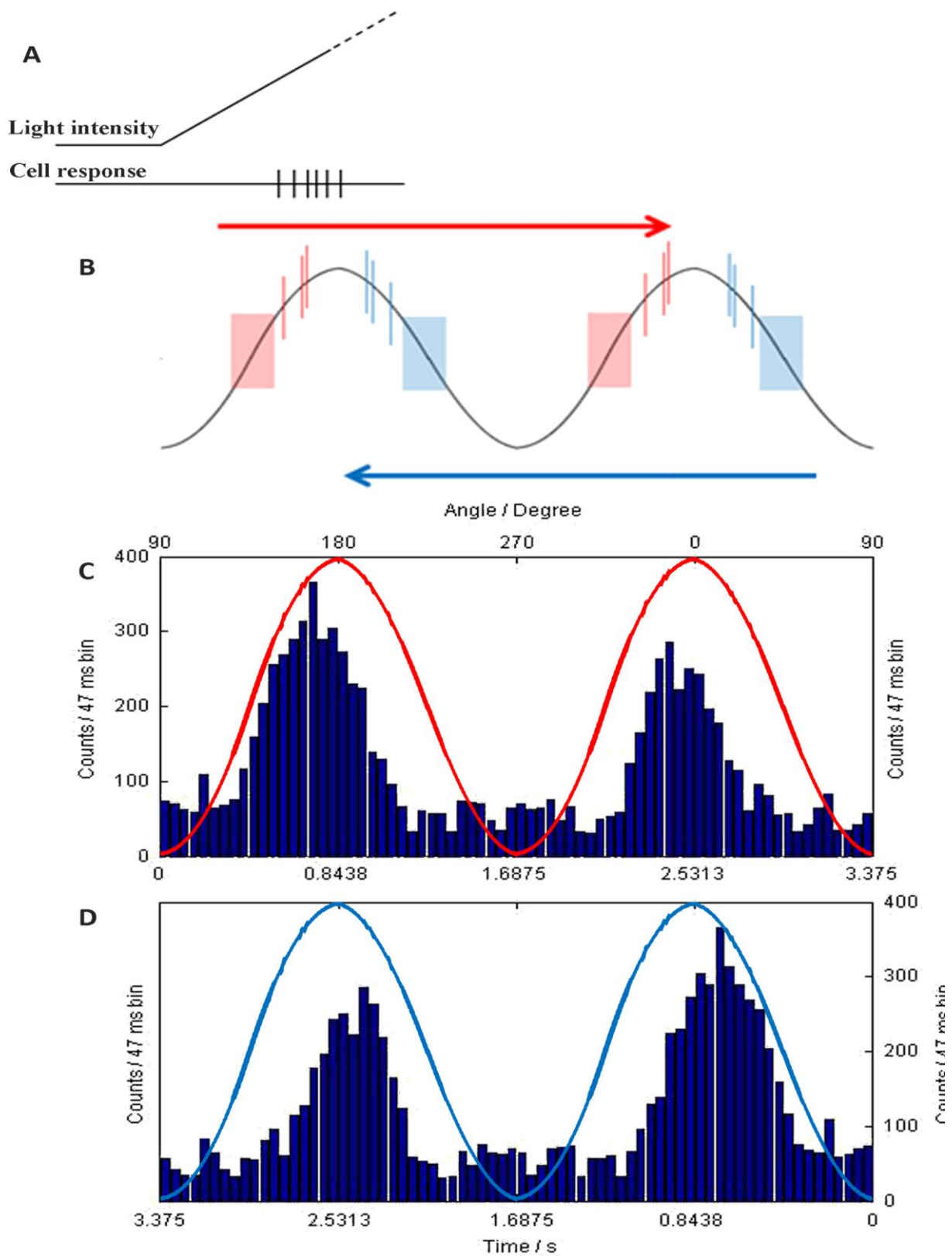


**Figure 26: Theoretical and experimental explanation for a direction-dependent  $\Phi_{\max}$  in retinal ganglion cells to artificial reflection artifacts upon the rotation of a polarizer.** A) Retinal ganglion cells respond in form of action potentials as soon the membrane threshold for an all-or-nothing response was crossed, irrespective of the peak intensity. B) Differential reflections of linearly polarized light produce a sinusoidal light intensity change upon the rotation of a polarizer. If the polarizer was turned clockwise (CW turn, depicted in red), the photoreceptors of a ganglion cell would be maximally excited by the slopes left of the peak intensity of the sinusoidal light intensity change (red squares), followed by ganglion cell responses with a slight processing time delay (red bars). If the polarizer was turned counterclockwise (CCW turn, depicted in blue), the photoreceptors of a ganglion cell

would be maximally excited by the slopes right of the peak intensity of the sinusoidal light intensity change (blue squares), followed by ganglion cell responses with a slight processing time delay (blue bars). C) and D) Experimental scenario mimicking a sinusoidal light intensity change caused by perfect differential reflections of the e-vector of polarized light that could in theory lead to a direction-dependent ganglion cell response angle. C) A 75% light intensity sinus was interpreted as a clockwise rotation of the e-vector of linearly polarized light that caused differential reflections. D) The same 75% light intensity sinus was interpreted as a counterclockwise rotation of the e-vector of linearly polarized light that caused differential reflections identical to the CW scenario. The ganglion cell responded bimodally with lower  $\Phi_{\max}$  (i.e. at presumably earlier angles) in clockwise turns and higher  $\Phi_{\max}$  (i.e. at presumably later angles) in counterclockwise turns. Note that the stimulation did not include the actual rotation of a polarizer but is an interpretation of e-vector-associated light intensity levels according to a putative differential reflection artifact.

original authors and not many more viable approaches come to mind (examples given in the next paragraph of this chapter). Basically all critical flaws of the original study that Dr. Arndt Meyer and I revealed - and that made a claim for unambiguous evidence for polarization sensitivity in an avian visual system, processed by the recorded ganglion cell responses, impossible - were associated with the damage to the tissue caused by the applied retinal dissection methods (see chapter 3.4.4, II) and by the unmonitored potential tilt of photoreceptor outer segments (see chapter 3.4.4, I) in the original study. In my opinion, these problems could potentially be eliminated by the following (potentially expensive) modifications to the methods:

a) The shielding function of an intact pigment epithelium and the preservation of the structural integrity of the photoreceptor outer segments could be guaranteed, if the retinal pieces would not be separated from the eye cup during retinal preparation by the delicate measures including cellulose tissue, adhesion and then pulling the retina - hopefully attached to the pigment epithelium - from the eye cup (see chapter 3.4.2 *retinal dissection*). Instead, I suggest a solution to introduce the multi-electrode array through the intact eye cup of retinal pieces, i.e. entering the electrodes into the tissue from the photoreceptor side to record from the ganglion cell layer, without detaching the retinal network from the sclera. The eye cup - especially the sclera - is rough and would cause damage or even break the fragile tips of the electrodes. A custom-built dummy array, resembling the multi-electrode array in size and dimensions, could be mounted in the micromanipulator arm and used to create 10 x 10 pointy openings by potentially extremely sharp tips (e.g. diamond tips), applied heat or by an applied acid that locally cut/burnt/dissolved the scleral tissue. The depth of incision can be well-controlled by a 3-axis micromanipulator arm and by visual monitoring through a high-resolution stereoscope. Replacing the dummy array by the multi-electrode array, the fragile electrodes could now be carefully driven into the retina through the pre-opened tunnels to

record from an intact retinal network. The established dissection protocol (chapter 3.4.2. *Retinal preparation*) would be followed until the incisions were made to obtain retinal pieces, then a retinal piece would be transferred to the bath chamber, weighed down and kept in place by the rhomboid frame and supported with oxygenated Ringer's solution, before applying the new strategy involving a dummy array.

b) The light stimulation could be adjusted to full-spectrum white light including UV light. My experiment in chapter 3.4.4. *IV* should be systematically tested, to demonstrate if the responsiveness and contrast sensitivity in retinal ganglion cells can be repeatedly enhanced as indicated by my modifications to the light stimulation protocol, i.e. cycles of lights ON and lights OFF, instead of permanent illumination. Furthermore, stimulation of ganglion cells close to the edges of the retinal pieces should be avoided. Damage to the photoreceptor outer segments and to the pigment epithelium were unavoidable at the edges of retinal pieces where the incisions were made. On the other hand, a full field beam that illuminated the whole retinal piece was an important measure to avoid false-positive responses. As a solution, I would suggest a concentric double beam that was projected onto the retina. The center beam would be polarized and adjusted in diameter to illuminate the retinal piece excluding the edges. The concentric exterior beam would be unpolarized, would extend the outline of the retinal piece for full-field light stimulation and match the illumination level of the polarized center beam. Admittedly, it would not be trivial to install, measure and to maintain such a double-beam stimulation.

As mentioned above, not many other physiological approaches to answer the question of polarization sensitivity in birds in any invasive method exist. Translucent plate arrays are commercially available that could be placed into the light path to record from ganglion cells, i.e. without penetrating the retina from the photoreceptor side to record from retinal ganglion cells. However, these arrays are not designed to be used in the context of polarization experiments. The built-in plexiglass and electric wiring inside the array might affect the polarization properties of incoming light, which might lead to reflection artifacts and thereby bias the outcome of a study conducted with semi-translucent arrays. Recordings from the optic nerve would in principle require minute mechanical damage to the retinal network and even allow recording from the "whole" optical apparatus. However, it bears the disadvantage of far less controllable light environments to exclude reflection artifacts from (parts of) the optical apparatus (Voz Hzn et al., 1995; personal communication with Prof. Dr. Henrik



Mouritsen about his experience at Prof. Dr. Frost's lab). Viable techniques that might be fit to find the alleged polarization-sensitive photoreceptor(s) in birds might not involve electrophysiological approaches, but histological and imaging techniques. Calcium imaging techniques come to mind that monitor cell activity upon stimulation with polarized light. Classically, a series of ultramicroscopic sections using diamond blades on a microtome, cutting sections in micron thickness and evaluating alignment of photopigment in a transmission electron microscope could lead to good ultrastructural results for an optical basis of polarization sensitivity in bird photoreceptors. However, these techniques can be extremely time consuming and are commonly speaking like the search for the needle in the hay.

### **3.5. Seen in a different light - No evidence for polarization vision in songbirds in a novel behavioral approach**

As summarized in chapter 3.3. and chapter 3.4. in this thesis, conclusive evidence for polarized light sensitivity in orientation tasks (summarized in chapter 3.3. in this thesis) and in physiological approaches (Coemans et al., 1990; Vos Hzn et al., 1995; own results presented in chapter 3.4. in this thesis) is very critically prone to artificial light intensity changes.

Tests for polarization vision on the other hand can be conducted in well controlled indoor environments (Foster et al., 2018), where the ability of the animal to extrapolate information delivered by polarization contrast can give direct information about a prevailing (multi-dimensional; Labhart, 2016) polarization sensitive system. These approaches can be used to prove a superior level of polarized light processing: the ability to distinguish objects or segregate visual surroundings merely by the distribution of light polarization properties, i.e. polarization vision. The benefit of these experimental paradigms is that the light environment can be very carefully controlled for secondary cues, a wide range of control experiments can be performed, and a positive performance of the model animal can directly indicate a biological use of polarized light (Foster et al., 2018). The downside is that negative results do not directly exclude the capability of the tested animal species to perceive polarized light per se, but only allow for the conclusion that the tested animal is not able to use the information contained in polarized light in this particular task or setup.

Not many of such studies have been performed with birds as a model animal so far. However, all of them used operant conditioning approaches and all well-controlled approaches against light artifacts have exclusively produced negative results (Coemans et al., 1990, 1994b;

Greenwood et al., 2003; Melgar et al., 2015). Pigeons were unable to discriminate the orientation of the e-vector in overhead illumination in two different operant conditioning approaches (Coemans et al., 1990, 1994), migratory starlings and non-migratory quail were unable to discriminate objects that differed in e-vector patterns (Greenwood et al., 2003), zebra finches were unable to discriminate objects and stimuli presented in polarization contrast on manipulated LCD monitor screens (Melgar et al., 2015). The latter study combined operant conditioning paradigms with a by now well-established method for demonstrating polarization contrast vision in various animal models (Foster et al., 2018).

Towards the end of my PhD, I had the opportunity to establish and use the rather novel approach of using manipulated LCD monitor screens to test polarization vision in a behavioral essay in birds.

*The absence of evidence is not the evidence of absence*

Carl Sagan, 1997

### **3.5.1. Introduction**

The visual scenery in natural environments is rich in sources of polarized light. Differential scattering of light in the atmosphere (Wehner, 1976), and light reflections off smooth dielectric surfaces like bodies of water (Horváth, 2014), and basically all smooth surfaces, like stones, leafs and tree branches (Horváth and Hegedüs, 2014) lead to natural partial polarization of light (Horváth, 2014). The biological use of these phenomena in animals sensitive to polarized light (for review see Labhart, 2016) is believed to be used from orientation (underwater: Marshall and Cronin, 2014; on land: Wehner, 1976; reviewed in Horváth and Varjú, 2004), contrast enhancement (Lin and Yemelyanov, 2006) and improved prey detection (Shashar et al., 2000), to camouflage and camouflage breaking (Jordan et al., 2012) and secret communication channels (Cronin et al., 2003).

In birds, polarization sensitivity has been repeatedly reported to be linked to the detection of skylight polarization patterns used in orientation and to the calibration process of their compass systems (for review, see Muheim, 2011; Åkesson, 2014; but see chapter 3.3. in this thesis). Besides the potential use of polarized light detection in orientation behavior, the visual system of migratory passerine birds is optimized for fast image processing in flight, high visual acuity and tetra chromatic color vision matching the requirements of the chromatically and

contrast rich environments they inhabit (Hart and Hunt, 2007). Living underneath shrubs and trees, the surfaces of leaves, smooth tree branches and wet logs produce a mosaic of polarization degrees and angles parallel to the respective reflective surfaces (Wehner, 1976; Horváth, 2014). The integrative processing of polarization contrast, i.e. the capability of the visual system to segregate the visual scenery based on the differences in e-vector orientations, i.e. the sensory capability of polarization vision, would certainly augment the visual specializations of birds necessary for fast flight or foraging in such obstacle rich terrains.

In commercially available LCD monitor screens, the image content is presented in luminance contrast by exploiting the anisotropic properties of crystals. The background illumination in the monitor is linearly polarized and sent through a layer of liquid crystals (Figure 27, A). Upon electric field induction, the orientation of these crystals can be rotated pixel-wise. According to the orientation angle of the crystals in each pixel, the e-vector angle of the emitted polarized light is rotated accordingly (Figure 27, A). A second linear polarizer is mounted in the front of the screen with the plane of polarization oriented perpendicular to the linear polarizer in the back. This arrangement of crossed polarizing filters in commercially available LCD monitor screens filters the light coming from the background illumination LED lighting, i.e. a black screen results even with full background illumination. Only upon the pixel-wise electric induction in the liquid crystal layer that rotates the liquid crystal orientation, and therein the plane of polarization, light can pass the front polarizer. Therefore, the brightness of each pixel is controlled by the induced rotation angle of the liquid crystals, resulting in sharp images on LCD monitor screens. If the front polarizer would now be removed (Figure 27, A), the technically intended intensity contrast as a means of pixel-wise e-vector axis orientation persists but is only visible to a polarization contrast sensitive observer. For the unaided human eye, a uniformly white screen appears. Using this method, several invertebrate species have been demonstrated to possess polarization vision, by presenting dynamic images on the screen in polarization contrast (i.e. images and image sequences presented with the front polarizing filter removed) that trigger behavioral responses in the polarization sensitive animal, e.g. crayfish (Glantz and Schroeter, 2006), cephalopods (Pignatelli et al., 2011), mantis shrimp (How et al., 2014; for recent review see Foster et al., 2018). In the only study using this method in birds so far, the authors combined the presentation of static images and patterns with an operant conditioning approach to reward birds if they learned to recognize different patterns in polarization contrast (Melgar et al., 2015). Zebra finches in that study were

unsuccessfully trained to recognize any kind of pattern or object presented in polarization contrast on manipulated LCD monitor screens (Melgar et al., 2015).

To assess whether birds possess polarization contrast perception, I tested three passerine bird species for optic flow processing in both dynamic luminance contrast (using intact screens) and dynamic polarization contrast (using manipulated screens with the front polarizers removed) in a virtual arena comprised of four reversely manipulated LCD monitor screens. I used biologically relevant stimuli, an apparently fast approaching object (looming stimulus) to trigger escape behavior in the tested birds and moving gratings to evoke saccadic head movements (optomotor responses, OMR) as a form of reflex-like image stabilization behaviors in response to global visual motion. These are established methods for assessment of visual circuitry, acuity and function in birds (Gianni, 1988; Eckmeier & Bishof, 2008; Xiao & Frost, 2009), but also for investigating polarization vision in several animal species (Foster et al., 2018). The advantage of using these stimuli is that they lead to strong, reliably evoked, innate responses that do not need to be trained or conditioned when presented in luminance contrast. When presented in polarization contrast upon removal of the front polarizers of the LCD monitor screens, I expected comparable behavioral responses to responses in luminance contrast, if the birds were able to detect contrast based on differential e-vector angle distributions, i.e. if birds possess polarization vision.

### **3.5.2. Material and Methods**

#### Experimental Animals

I used 25 wild-caught adult European robins *Erithacus rubecula*, 7 wild-caught adult Eurasian blackcaps *Sylvia atricapilla*, and 21 faculty-bred Zebra finches *Taeniopygia guttata* of mixed sex and age. All experiments were performed between Feb – Aug 2017 in daytime between 8am and 7pm. Procedures were in accordance to the local and national guidelines for the use of animals in research and were approved by the Animal Care and Use Committees of the Lower Saxony State Office for Consumer Protection and Food Safety (LAVES), Oldenburg, Germany. (33.9-42502-04-13/1065)

#### Experimental Setup

Four 29" LCD computer monitors (ACER Predator GN26 BDK6000L, 144 Hz frame rate) were arranged in a square arena (Figure 27, B). Wooden plates were mounted as floor and roof of the experimental arena. To reduce unwanted light reflections inside the arena, all surfaces

except the screens were covered with textured, roughened white tapestry (recommended by Coemans et al., 1990; Coemans et al., 1994). The screens were covered by commercially available anti-reflective foil. Attaching this foil to the front of the screens allowed me to drastically reduce the reflections of polarization stimuli from one screen off other screens and therein avoiding the effects of differential reflection properties of polarized light (see chapter 3.1. in this thesis) that would make the stimuli in polarization contrast visible to the unaided eye. A custom-made wooden cage (~20 cm x 20 cm x 25 cm) spanned by coarse nets was placed in the center of the arena. A small perch made of wood (8 cm wide, 5 cm above the floor) was placed in the center of the cage to allow the tested birds to perch (Figure 27, B). A

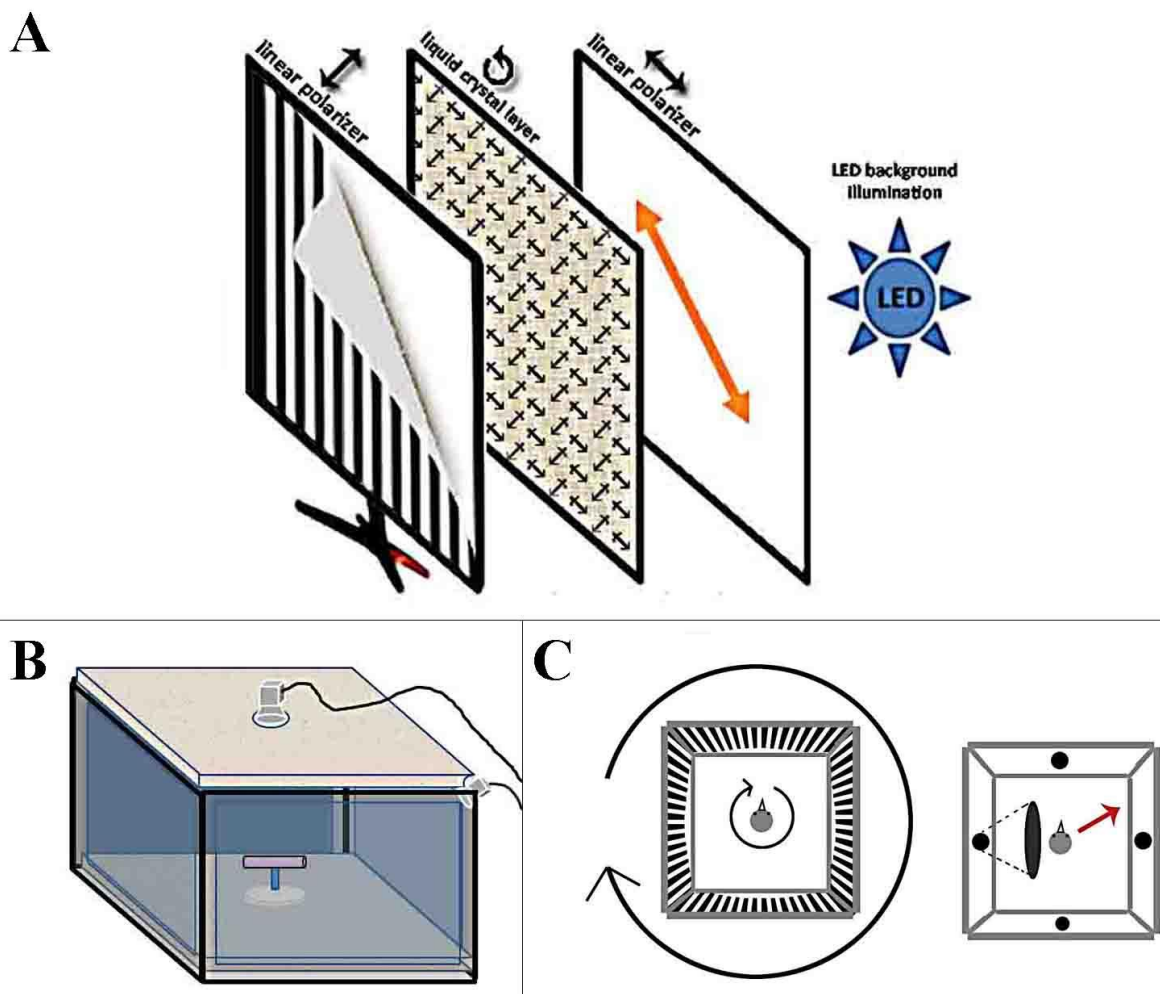


**Figure 27: Presentation of dynamic polarization contrast on modified LCD monitors.** A) Sketch of the principle components of an LCD monitor that allows for presentation of visual stimuli in polarization contrast. From right to left: LED background illumination, background polarizer with plane of polarization at  $315^\circ$ , liquid crystal layer, front polarizer with crossed plane of polarization with respect to the background polarizer, at  $45^\circ$ . Removal of the front polarizer, as depicted (far left), results in a white screen for the unaided human eye, but image presentation in polarization contrast for animals that possess a polarization sensitive visual system. B) Arrangement of 4 LCD screens in a square arena for 3D visual stimulation, top view and side view camera for documenting behavioral responses. C) Left: presentation of moving gratings that appear to rotate around the bird to trigger an optomotor response. Right: Looming stimulus to trigger escape behaviors in the birds.

round opening was cut into the center of the wooden roof plate to fit a VIS-IR camera for top-view monitoring of the tested bird's behavior. A smaller camera was mounted in one top corner of the arena to monitor the stimulus presentation. Synchronous video recording was achieved by a commercially available digital recorder system (Syngetics Digital recorder) connected to one further, separate computer screen. The four LCD monitors were connected to an NVIDIA GeForce 1070 GTX graphics card to guarantee a high resolution, well-buffered, synchronized video output at rates of stable 120 frames per second across four screens. A description of all components and their assembly can be found on the external hard drive linked to this thesis here "Toshiba:\RawData Chapter 3.5\Anleitung zum Versuchsaufbau des LCD Monitor Setups.docx". All visual stimulation protocols were controlled and executed by custom-written functions in MatLab<sup>®</sup> (MathWorks, 2016b). A virtual arena stimulation software was obtained from OpenEtho<sup>®</sup> with kind courtesy of Friedrich Kretschmer (Kretschmer et al., 2015), and implemented into my MatLab<sup>®</sup> routine.

### Visual Stimulation in luminance contrast

#### *Moving gratings:*

I presented a vertical grating of black and white bars as a rotating virtual cylinder across the four screens (virtual radius: 52 cm, height 28 cm; Figure 27, C) for 60 seconds into one direction, clockwise or counterclockwise, followed by a 5-10 second pause in which white screens were presented, followed by a 60 seconds interval of rotation into the opposite direction. The starting direction was alternated from individual to individual. Preliminary tests in a trial-and-error approach resulted in consistent saccadic head movements in all three bird species tested at a spatial frequency of 0.4 cycles per degree (136 black bars on white background per 360°) at an angular velocity of 20 degrees per second (18 seconds for 360°). The birds tested in this preliminary phase were not considered in the analysis of the here presented results. In dedicated rounds of testing (see section *Testing trials in consecutive rounds*), I presented moving gratings in lowered luminance contrast by discretely increasing gray values in the "black" bars to determine a potential lowered contrast threshold for evoking head saccades. This step was important to evaluate whether a potential absence of responses in polarization contrast could be explained by a minimum contrast of the moving gratings necessary to evoke optomotor responses in birds. Intensity contrast in this round of testing was set to 100%, 50%, 38%, 13% or 5%, respectively. I chose to test an individual bird in either increasing or decreasing order of contrast steps in this round. This however resulted in

unbiased data between contrast steps, because I ended the round of trials for an individual bird, after clear responses were recognizable in an increasing contrast ladder, i.e. when clear responses were observable at 10% I did not continue testing the 25%, 50% and 100% contrast trials. The original video recordings can be found on the external hard drive linked to this thesis here “Toshiba:\RawData Chapter 3.5\Video Record Files\”.

#### *Looming stimulus:*

I played back a Matlab<sup>®</sup>-computed video file of sequential image frames (frame rate: 120 Hz). A black disk (initial diameter 5 cm) on white background, centered on all four screens and initially stationary for 5 seconds, exponentially expanded rapidly to 75% of screen height (final diameter 25 cm) to give the impression of a fast approaching object. This expansion repeated three times without interruption while duration changed from 0.5 seconds to 1 second and to 1.5 seconds, respectively (Figure 27, C). Equivalent to the trials in moving gratings, in dedicated rounds I tested the birds in luminance contrast steps of 100%, 50%, 38%, 13% and 5%. The original video recordings can be found on the external hard drive linked to this thesis here “Toshiba:\RawData Chapter 3.5\Video Record Files\”.

#### Visual Stimulation in polarization contrast

When using the method of modified LCD monitors (Glantz & Schroeter, 2006; Pignatelli et al., 2011; How et al., 2014), the image content on the screen can be presented in luminance contrast on intact screens or in polarization contrast upon removal of the front polarizers of the screen. I reversibly removed the front polarizers of the LCD screens, i.e. I was able to restore the “normal” properties of the screens after manipulation for stimulation in polarization contrast. Thereby, I was able to test and retest any group of birds in reversible testing order (either luminance contrast after polarization contrast presentation or vice versa).

#### Luminance measurements

I measured the absolute irradiance of the screens with a portable spectrometer (Ocean optics, Dunedin, FL, USA, USB4000-UV-VIS). While sampling irradiance measurements, I set the illumination intensity using a white background on the four, intact screens to 50 LUX. I saved this setting to be used for the testing trials in luminance contrast. The removal of the front polarizer increased the overall illumination intensity due to the transmission properties of linear polarizing filters. To achieve matching illumination levels of a white background on

intact screens, I adjusted the background illumination settings on the screens and saved it for the testing trials in polarization contrast with manipulated screens (round 4 with birds tested in 6 consecutive rounds; round 1 with naïve birds; see below in section *Testing paradigm in consecutive rounds*). Stimulus presentation on intact screens, i.e. presentation of a black and white grating, reduced the overall illumination intensity compared to white screens, while illumination intensity did not change for the unaided eye during stimulus presentation on manipulated screens. Therefore, I tested birds in polarization contrast with adjusted background illumination to match the intensity of a full contrast grating on intact screens in round 5 for birds tested in 6 consecutive rounds (see below in section *Testing paradigm in consecutive rounds*). Thereby, I was able to detect whether there was an effect of illumination dependency on the behavioral responses of the birds tested in consecutive rounds in polarization contrast.

### Polarimetry

Equipping a portable spectrometer (Ocean optics, Dunedin, FL, USA, USB4000-UV-VIS) with a linear polarizer (Edmund Optics, Barrington, NJ, USA; Ultra Broadband Wire Grid Polarizer, catalogue #68-750), I measured a degree of polarization of 96% on intact screens. The averaged polarization contrast with removed front polarizers was measured to be 70%. The installation of anti-reflective foil – necessary to reduce reflections of polarized light from one screen on the smooth glass surface of another screen – reduced the averaged polarization contrast to 62.6% (Figure 28). The spectral composition of the emitted light (400-700nm) was unaffected by LCD screen manipulations, intensity levels and luminance contrast levels.

### Testing paradigm in consecutive rounds

In the beginning of each round, birds were placed individually into the center of the testing arena and were given 15 min of acclimatization to the arena with white screens prior to the first trial.

#### *Moving gratings:*

Having no prior experience in testing songbirds in dynamic visual stimuli, and being unaware of the potential differences in optomotor responses of the tested birds in polarization contrast as compared to luminance contrast, I aimed to include as many control conditions as possible against possible factors that might influence the results of my experiments in this first approach.



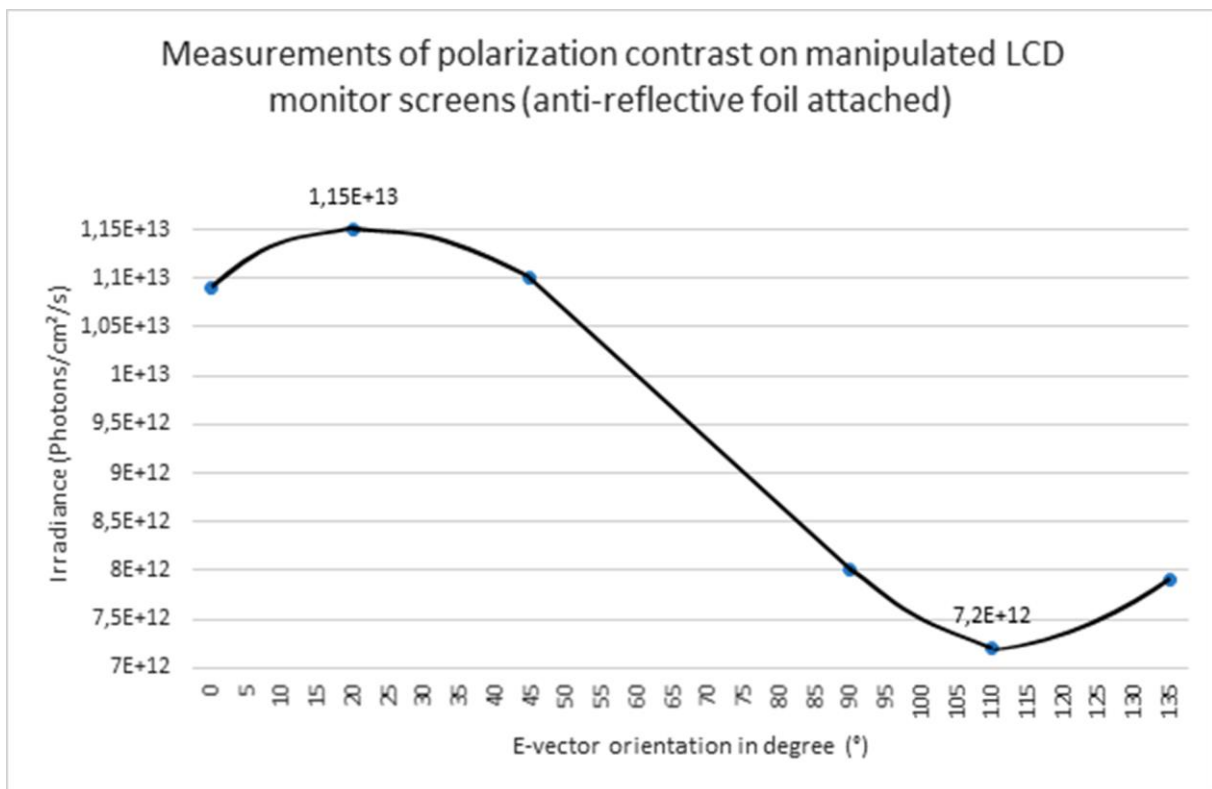


**Figure 28: Measurement of polarization contrast on manipulated LCD monitor screens with the anti-reflective foil attached.** A portable spectrometer (Ocean optics, Dunedin, FL, USA, USB4000-UV-VIS) equipped with a linear polarizer (Edmund Optics, Barrington, NJ, USA; Ultra Broadband Wire Grid Polarizer, catalogue #68-750) was used to measure the degree of polarization to be at 62.6% with removed front polarizers and an anti-reflective foil attached.

15 European robins and 13 Zebra finches were tested in 6 consecutive rounds with an interval of at least 1-2 days:

- Round 1, 2 and 6: All birds were tested in full luminescence contrast to assess the species-specific response frequency and to test for potential attenuation of response frequencies in consecutive rounds.
- Round 3: The birds of each species were separated into two groups. This was done at random without paying attention to performance in prior rounds or bird ID. One group was tested in trials in luminance contrast steps of 100%, 50%, 38%, 13% and 5% luminescence contrast (as described in the section *Visual Stimulation in luminance contrast* in this chapter). The parallel group was tested in full polarization contrast. Unfortunately, I did not test all birds of a species in all contrast steps which led to unbalanced data, Zebra finches were only tested in contrast steps of 100%, 50% and 38%, making the following statistical evaluation of contrast dependency of optomotor responses more complicated and less reliable as necessary.
- Round 4: All birds were tested in full polarization contrast, with illumination levels matching

white, intact screens. Unfortunately, due to data loss, the video recordings of one day were lost before they could be properly analyzed and could not be recovered. The lost video data relate to tests with half of the European robins tested in Round 4. To deal with this misfortune in the following analysis I modified the applied statistical tests in the same way as necessary for the unbalanced data in contrast step trials (see section *Statistical analysis* in this chapter).

- Round 5: All birds were tested in polarization contrast with overall illumination levels reduced to match full luminance contrast on intact screens.

Additionally, 10 European robins, 8 Zebra finches and 7 Blackcaps, all naïve to the setup were separately tested in 2 consecutive rounds, starting with the presentation in polarization contrast, followed by presentation in luminance contrast, to assess if a reversed order of contrast condition presentation might affect the response frequencies:

- naïve Round 1: All birds were tested in full polarization contrast, with illumination levels matching white, intact screens.

- naïve Round 2: All birds were tested in full luminescence contrast after reinstallation of the front polarizers of the screens. Additionally, birds of the naïve groups were tested in contrast steps of 50%, 38%, 13% and 5% to assess the contrast dependency of optomotor responses in these birds, comparable to round 3 in birds tested in 6 consecutive rounds.

- Blackcaps Round 0: To obtain preliminary data on optomotor responses in luminance contrast and contrast steps in Blackcaps that were not previously tested in 6 consecutive rounds, I tested 5 additional Blackcaps in round 0 prior to testing the 7 Blackcaps in naïve rounds 1 and 2.

#### *Looming stimulus:*

At the end of each round after stimulation with moving gratings trials, each bird was presented with a looming stimulus (see section *Visual Stimulation in luminance contrast* in this chapter), according to the preset contrast conditions (luminance or polarization) of the respective round as described above. Looming stimulus was repeated in contrast step trials of 100%, 50% and 38% in rounds 3 and naïve round 2. As in the moving grating trials with lowered contrast steps, I tested in either increasing or decreasing contrast steps per individual and stopped testing further contrast steps in an increasing series when a bird did show strong escape behavior at a low contrast step. This lead to unbalanced data on group level as in the moving grating experiments.

## Data collection

### *Optomotor responses (OMR) to moving gratings:*

Data collection was done blinded by three independent observers. For blinded analysis, only videos of the top view camera were used, excluding a view of the presented stimulus. All videos were cut to identical length of 59 seconds, excluding 0.5 seconds before stimulus onset and after stimulus offset, respectively, in order to ensure that the observer had no knowledge of the contrast condition, round, bird ID and no view of the stimulus. For every 59 second stimulus presentation, the number of head saccades was counted, defined as the consecutive pair of a swaying head movement that was roughly correlated to angular velocity and directionality of the stimulus, followed by a fast “resetting” head movement. Since the birds were free to either perch or roam inside the net cage, viewing angles of the moving gratings stimulus could vary. The resulting OMR responses could thereby vary in head tracking velocity depending on the distance to the observed part of the screens, i.e. higher head saccade frequency with smaller amplitude would result at narrower viewing angles to the stimulus (at close distances to the observed part of the screen), and lower head saccade frequency with higher amplitude would result at greater viewing angles to the stimulus (at farther distances to the observed part of the screen). Additionally, our birds produced “head saccade-like” voluntary head movements while visually exploring the arena in absence of any stimulus during acclimatization, but also during stimulation. Especially in zebra finches and blackcaps, numerous stimulus-unrelated head scanning movements biased the OMR count during the stimulation period. Especially for stimulation in polarization contrast, these arbitrary head movements could influence the results of data collection, since stimulus-related small-amplitude head movements (e.g. at narrow viewing angles close to the observed part of the screen) and voluntary stimulus-unrelated head scans could easily be misinterpreted. To carefully exclude this uncertainty, three independent, blinded observers were analyzing each video of each testing trial twice, counting even the slightest swaying head movements in one direction and a second time counting head movements in the opposite direction, without knowing the actually presented stimulus direction (or contrast mode, i.e. luminance- or polarization contrast, round, contrast step, or bird ID). After unblinding of the results, these response counts were resolved in “responses” (number of responses counted per observer in the actual stimulus direction) and “null responses” (number of responses counted per observer in the opposite direction of the actual stimulus). Additionally, the voluntary head

movements for one minute (minute 08:00 - minute 08:59) during the acclimatization prior to testing, where no stimulus was presented, were counted in the same blinded manner as described above. Thereby, I was able to quantify an individual baseline for voluntary, stimulus-unrelated head movements for each bird in both CW and CCW directions. The videos for determining a baseline activity during 59 seconds of acclimatization were randomly mixed into the pool of all videos for blinded analysis.

#### *Escape behavior to a looming stimulus:*

After preliminary tests, escape behavior was defined as a sudden flight response at the onset of or during the presentation of a looming stimulus. A behavior was considered as a flight response if it clearly indicated the bird's awareness of the stimulus and its interpretation as a threat, i.e. flying away (often observed in a zig-zag pattern because the stimulus was presented on all four screens, i.e. coming from all sides) and behaviors that included a rapid change of location, e.g. ducking down from the perch, hopping to either side. The presence or absence of this strong response was not subjected to potential observer bias. Therefore, responses were analyzed only by myself.

#### Statistical analysis

##### *Optomotor responses to moving gratings:*

The median and  $\frac{1}{4}$  -  $\frac{3}{4}$  quartiles were calculated for each round and each bird species, separated for stimulus direction (CW and CCW) and response type (responses in stimulus direction or responses into null direction). Furthermore, the median and  $\frac{1}{4}$  -  $\frac{3}{4}$  quartiles were calculated for the baseline of each species (responses in CW and CCW direction during 59 seconds in acclimatization with no stimulus presented), separated for the groups testes in 6 consecutive rounds or in two consecutive rounds.

To test for differences in clockwise (CW) and counterclockwise (CCW) response frequencies, I used an ANOVA type III, Wald Chi-square test, of the Generalized Linear Mixed Model for "negative binomial" distribution fit by maximum likelihood (Laplace Approximation; R: packages "Matrix", "lme4", "car" with contrasts option <"contr.sum", "contr.poly"> for unbalanced data) based on data from all trials in 100% luminance contrast (round 1, 2, 6 and naïve round 2), for each species separately and separated for responses and null responses, with the individual bird and observer set as random effects (Formula: Responses ~ Direction + (1 | BirdID) + (1 | Observer), data=subset(species, Contrast=="100" & Stimulus=="Luminance")

& ResponseType=="stim dir" or "Null"). The reason why one should use the GLMM with negative binomial distribution is that (a) the original data are count data hence they do not follow normal distribution, (b) repeated measures from the same individuals were compared which can be averaged in this model by setting random effects.

To test whether there was attenuation of the response frequencies in the birds tested in round 1, round 2 and round 6 in six consecutive rounds, I used the pairwise comparison in a non-parametric paired Wilcoxon Signed-Rank Test. This test should be used for comparison of two samples if errors do not follow normal distribution. In case of an observed attenuation effect, I compared the stimulus-correlated responses in that round to null responses in that round and to the determined baseline response frequencies of the species using pairwise comparison in a non-parametric paired Wilcoxon Signed-Rank Test.

To test whether there were differences in response frequencies between round 1 of birds tested in 6 consecutive rounds and naïve round 2 of birds tested in two consecutive rounds with presentation in polarization contrast first, I used a pairwise two-sample Permutation Test (package "rcompanion") to compensate for different sample sizes.

To analyze the differences in the response frequencies between trials in 100%, 50%, 38%, 13% and 5% luminescence contrast steps - pooled for birds tested in round 3 and naïve round 2 - I used a pairwise two-sample Permutation Test (package "rcompanion") to compensate for unbalanced data. In case of an observed effect of lower contrast steps on response frequencies, I compared the responses in the lowest contrast step to null responses in that contrast step, using a non-parametric paired Wilcoxon Signed-Rank Test, and I compared the responses in lowest contrast step to baseline response frequencies of the species using a pairwise two-sample Permutation Test (package "rcompanion").

To compare response frequencies in polarization contrast trials in birds tested in 6 consecutive rounds and birds in 2 consecutive rounds, I used a non-parametric paired Wilcoxon Signed-Rank Test, if sample sizes were identical and a pairwise two-sample Permutation Test (package "rcompanion") in case of different sample sizes.

To compare response frequencies in luminance contrast with responses in polarization contrast - in the case that neither attenuation nor contrast steps in luminance contrast critically affected the response frequencies compared to null responses or baseline, i.e. if in any round or contrast step, responses were significantly above chance level (baseline activity) and significantly higher than null responses - I used an ANOVA type III, Wald Chi-square test,

of the Generalized Linear Mixed Model for “negative binomial” distribution fit by maximum likelihood (Laplace Approximation; R: packages “Matrix”, “lme4”, “car” with contrasts option <“contr.sum”, “contr.poly”> for unbalanced data) based on all data excluding baseline responses for each species separately, with the individual bird, observer, round, contrast step, order (i.e. birds tested in six consecutive rounds or naïve birds) and stimulus direction set as random effects (Formula: Responses ~ Stimulus\*ResponseType + (1|BirdID) + (1|Observer) + (1|Round) + (1|Contrast) + (1|Order) + (1|Direction), data=subset(species, Stimulus!="Baseline"). The comparison of all data separated for luminance contrast or polarization contrast were compared to the calculated baseline activity by using a pairwise two-sample Permutation Test (package “rcompanion”). The plain R-script modules used for the statistical analysis can be found on the external hard drive linked to this thesis here “Toshiba:\RawData Chapter 3.5\OMR R statistics samples.R”.

#### *Escape behavior to a looming stimulus:*

To evaluate behavioral responses to looming stimuli, I applied a Yes/No categorization to whether a bird did show escape behavior in response to the looming stimulus or not. For each round, separated for stimuli presented in luminance contrast or polarization contrast and for contrast step, the number of birds that responded with an escape behavior was documented. Here, a strong and natural effect of repeated presentation on the presence or absence of a response was predicted in birds tested in 6 consecutive rounds. Consequently, I assumed a-priori that a reduction of birds showing escape behavior in round 2, 3 and 6 or a complete absence of escape behavior in polarization contrast in round 3, 4 and 5 could be explained by response attenuation after repeated presentation rather than the inability of birds to perceive polarized light. Therefore, focus should be laid on the results of the naïve group, where attenuation cannot influence the presence or absence of escape behavior to stimuli in polarization contrast.

#### **3.5.3. Results**

A total of 25 European robins, 22 Zebra finches and 12 Blackcaps were tested for optomotor responses to moving gratings and for escape behavior to a looming stimulus in both luminescence contrast and polarization contrast.

### Moving gratings

There was no significant difference between the amount of responses in 100% contrast in CW and CCW experiments in luminance contrast (stimulus-correlated: Blackcaps, CW: median = 55.0 +-22.5/70.5 (1st/3rd quartile), Blackcaps, CCW: median = 58.0 +-26.0/77.0; European robins, CW: median = 25.50 +-13.0/38.0, European robins, CCW: median = 25.0 +-13.0/40.0; Zebra finches, CW: median = 50.50 +-37.25/66.0, Zebra finches, CCW: median = 58.0 +-36.0/78.0; null direction: Blackcaps, CW: median = 5.0 +-2.0/6.5 (1st/3rd quartile), Blackcaps, CCW: median = 6.0 +-4.0/8.50; European robins, CW: median = 1.0 +-0.0/4.0, European robins, CCW: median = 1.0 +-0.0/4.50; Zebra finches, CW: median = 8.0 +-8.0/16.0, Zebra finches, CCW: median = 9.0 +-3.0/17.0; Figure 29) in any of the three bird species (ANOVA, type III, of the GLMM, CW versus CCW, stimulus-correlated responses: Blackcaps,  $p = 0.289$ ; European robins,  $p = 0.552$ ; Zebra finches,  $p = 0.207$ ; null responses: Blackcaps,  $p = 0.314$ ; European robins,  $p = 0.328$ ; Zebra finches,  $p = 0.202$ ; Figure 29). Therefore, stimulus direction was considered a random effect in the following statistical comparisons.

#### *Baseline activity during acclimatization:*

Spontaneous head movement characteristics of European robins were significantly different from Zebra finches and Blackcaps. Robins did show significantly lower numbers of

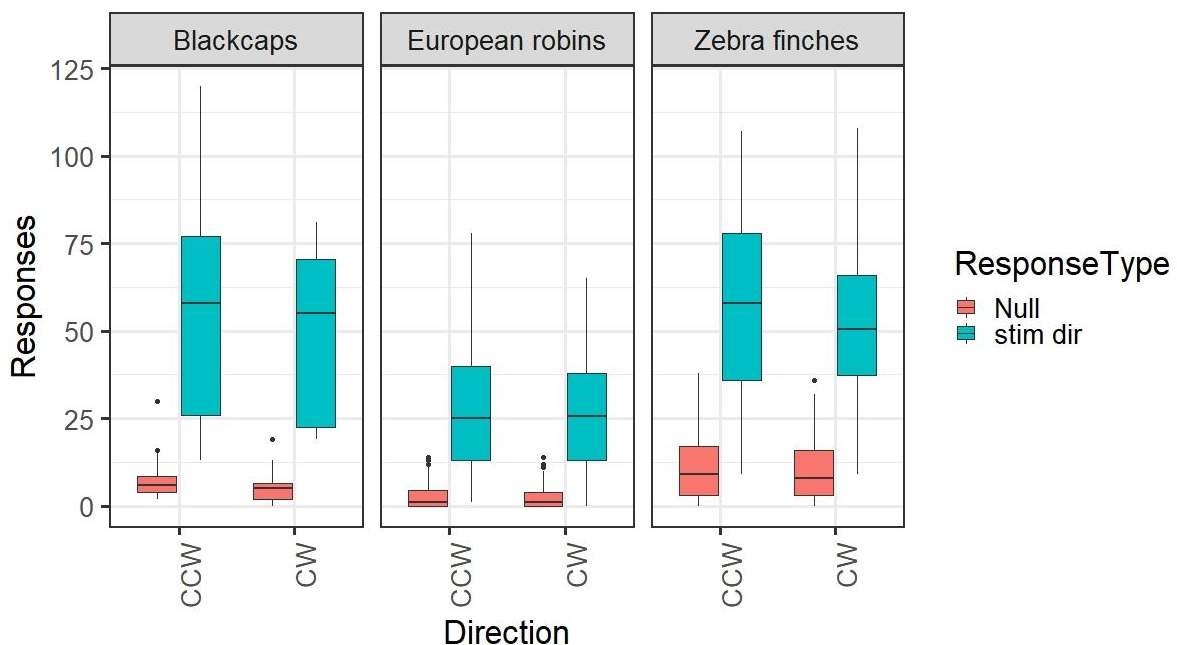


**Figure 29: No differences between CW and CCW stimulation was observed.** There were no significant differences in all three songbird species between the response frequencies in 100% contrast in CW and CCW experiments in luminance contrast, neither in stimulus direction nor in null direction (ANOVA (type III) of the GLMM, stimulus-correlated: Blackcaps,  $p = 0.289$ ; European robins,  $p = 0.552$ ; Zebra finches,  $p = 0.207$ ; null responses: Blackcaps,  $p = 0.314$ ; European robins,  $p = 0.328$ ; Zebra finches,  $p = 0.202$ ).

spontaneous head movements during acclimatization (Baseline, European robins:  $n = 25$ , median =  $6.0 \pm 2.25/12.0$  (1st/3rd quartile)) than Zebra finches (Baseline, Zebra finches:  $n = 22$ , median =  $16.0 \pm 5.75/22.0$ ; pairwise two-sample Permutation Test, Baseline, European robins vs. zebra finches,  $p = 1.996e-09$ ) and Blackcaps (Baseline:  $n = 12$ , median =  $16.50 \pm 3.0/24.0$ ; pairwise two-sample Permutation Test, Baseline, European robins vs. Blackcaps,  $p = 9.253e-08$ ), but not between Zebra finches and Blackcaps (pairwise two-sample Permutation Test, Baseline, Zebra finches vs. Blackcaps,  $p = 0.7848$ ).

*Response frequencies in 100% luminance contrast:*

The trials in 100% luminance contrast in round 1 of birds tested in 6 consecutive rounds resulted in median response frequencies in stimulus direction of  $48.50 \pm 37.0/59.0$  (1st/3rd quartile) in Zebra finches ( $n = 14$ ; Table 2; Figure 30) and  $31.0 \pm 21.0/39.0$  in European robins ( $n = 15$ ; Table 2; Figure 30) and median response frequencies in null direction of  $8.0 \pm 2/14$  in Zebra finches ( $n = 14$ ; Table 2; Figure 30) and  $0.0 \pm 0.0/3.0$  in European robins ( $n = 15$ ; Table 2; Figure 30). For comparison, preliminarily tested Blackcaps in round 0 ( $n = 5$ ; Table 2) showed median response frequencies in stimulus direction of  $52.0 \pm 24/67$  and mean response frequencies in null direction of  $5.0 \pm 3/7$ . In accordance with the spontaneous response characteristics during acclimatization, response frequencies during the first round in 100% luminance contrast were significantly lower in European robins than in Zebra finches (pairwise two-sample Permutation Test, stimulus-correlated: European robins vs. Zebra finches,  $p = 1.022e-11$ ; null responses: European robins vs. Zebra finches,  $p = 5.511e-12$ ) and in Blackcaps (pairwise two-sample Permutation Test, stimulus-correlated: European robins vs. Blackcaps,  $p = 1.797e-05$ ; null responses: European robins vs. Blackcaps,  $p = 1.373e-07$ ), but no statistical difference between Zebra finches and Blackcaps was found (pairwise two-sample Permutation Test, stimulus-correlated: Zebra finches vs. Blackcaps,  $p = 0.9143$ ; null responses: Zebra finches vs. Blackcaps,  $p = 0.08187$ ).



**Table 2: Numerical results of the optomotor responses to moving gratings in Zebra finches, European robins and Blackcaps.** The raw data including response counts from three observers can be found in the Appendix Table 1. The full data table including all responses separated by stimulus direction in digital form, all original videos documenting the behavior and the basic script formula for statistics used in R can be found on the hard drive linked to this thesis here “Toshiba:\RawData Chapter 3.5\Results of Optomotor Responses.xmlx”.

Species	Round	Contrast	Stimulus	Testing order	Response type	# individuals	median Responses	1st quartile	3rd quartile
Zebra finches	1	100	Luminance	LumPol	stim dir	14	48.50	37.00	59.00
Zebra finches	2	100	Luminance	LumPol	stim dir	14	56.00	45.75	66.00
Zebra finches	3	100	Luminance	LumPol	stim dir	1	66.0	50.5	68.0
Zebra finches	3	50	Luminance	LumPol	stim dir	2	60.00	50.00	69.25
Zebra finches	3	38	Luminance	LumPol	stim dir	6	55.50	39.50	61.25
Zebra finches	6	100	Luminance	LumPol	stim dir	14	56.50	20.00	85.25
Zebra finches	3	100	Polarization	LumPol	stim dir	8	23.00	15.75	28.00
Zebra finches	4	100	Polarization	LumPol	stim dir	14	17.50	9.75	24.00
Zebra finches	5	100	Polarization	LumPol	stim dir	14	13.00	7.25	19.00
Zebra finches	1	100	Polarization	PolLum	stim dir	8	16.50	11.50	23.00
Zebra finches	2	100	Polarization	PolLum	stim dir	8	79.00	19.75	87.00
Zebra finches	1	100	Luminance	LumPol	null	14	8.000	2.000	14.000
Zebra finches	2	100	Luminance	LumPol	null	14	9.000	2.000	15.000
Zebra finches	3	100	Luminance	LumPol	null	1	11	7,5	13
Zebra finches	3	50	Luminance	LumPol	null	2	10.000	2.000	12.750
Zebra finches	3	38	Luminance	LumPol	null	6	7.50	4.75	13.25
Zebra finches	6	100	Luminance	LumPol	null	14	7.00	3.75	23.25
Zebra finches	3	100	Polarization	LumPol	null	8	25.50	20.50	30.25
Zebra finches	4	100	Polarization	LumPol	null	14	20.00	12.00	27.00
Zebra finches	5	100	Polarization	LumPol	null	14	14.00	6.75	20.00
Zebra finches	1	100	Polarization	PolLum	null	8	17.50	10.75	26.50
Zebra finches	2	100	Polarization	PolLum	null	8	8.50	5.00	21.25
Zebra finches	Baseline	Baseline	Baseline	LumPol	Baseline	14	18.00	6.75	23.25
Zebra finches	Baseline	Baseline	Baseline	PolLum	Baseline	8	13.00	4.00	20.25
European robins	1	100	Luminance	LumPol	stim dir	15	31.0	21.0	39.0
European robins	2	100	Luminance	LumPol	stim dir	15	24.00	12.00	38.75
European robins	3	100	Luminance	LumPol	stim dir	4	18.00	15.00	25.00
European robins	3	50	Luminance	LumPol	stim dir	6	21.00	16.75	35.50
European robins	3	38	Luminance	LumPol	stim dir	8	15.50	10.75	22.75
European robins	3	13	Luminance	LumPol	stim dir	3	10.00	4.00	15.00
European robins	3	5	Luminance	LumPol	stim dir	3	8.00	6.00	23.50
European robins	6	100	Luminance	LumPol	stim dir	15	20.00	7.25	48.00
European robins	3	100	Polarization	LumPol	stim dir	7	3.000	2.000	5.750
European robins	4	100	Polarization	LumPol	stim dir	8	6.000	3.000	8.000
European robins	5	100	Polarization	LumPol	stim dir	15	4.000	1.000	7.750
European robins	1	100	Polarization	PolLum	stim dir	10	3.000	0.750	5.000
European robins	2	100	Polarization	PolLum	stim dir	10	23.50	14.50	36.25

European robins	2	13	Polarization	PolLum	stim dir	10	12.00	5.00	24.00
European robins	2	5	Polarization	PolLum	stim dir	10	11.00	2.50	18.00
European robins	1	100	Luminance	LumPol	Null	15	0.000	0.000	3.000
European robins	2	100	Luminance	LumPol	Null	15	1.000	0.000	4.000
European robins	3	100	Luminance	LumPol	Null	4	1.000	0.000	5.000
European robins	3	50	Luminance	LumPol	Null	6	0.0	0.0	5.0
European robins	3	38	Luminance	LumPol	Null	8	2.000	0.000	5.000
European robins	3	13	Luminance	LumPol	Null	3	3.000	1.500	3.500
European robins	3	5	Luminance	LumPol	Null	3	3.000	2.500	4.500
European robins	6	100	Luminance	LumPol	Null	15	1.000	0.000	7.750
European robins	3	100	Polarization	LumPol	Null	7	3.000	0.250	6.750
European robins	4	100	Polarization	LumPol	Null	8	5.0	2.0	8.0
European robins	5	100	Polarization	LumPol	Null	15	3.500	1.000	8.000
European robins	1	100	Polarization	PolLum	Null	10	4.000	1.000	9.750
European robins	2	100	Polarization	PolLum	Null	10	3.500	1.000	6.000
European robins	2	13	Polarization	PolLum	Null	10	4.000	0.000	6.000
European robins	2	5	Polarization	PolLum	Null	10	3.500	0.000	7.000
European robins	Baseline	Baseline	Baseline	LumPol	Baseline	15	6.000	3.000	11.750
European robins	Baseline	Baseline	Baseline	PolLum	Baseline	10	5.000	2.000	13.000
Blackcaps	0	100	Luminance	LumPol	stim dir	5	52.00	24.00	67.00
Blackcaps	0	50	Luminance	LumPol	stim dir	2	36.50	25.75	39.75
Blackcaps	0	38	Luminance	LumPol	stim dir	5	35	18	49
Blackcaps	0	13	Luminance	LumPol	stim dir	4	37.00	15.75	41.00
Blackcaps	0	5	Luminance	LumPol	stim dir	4	31.0	13.5	36.0
Blackcaps	2	100	Luminance	PolLum	stim dir	7	63.00	27.00	81.00
Blackcaps	2	13	Luminance	PolLum	stim dir	4	59.00	28.75	96.00
Blackcaps	2	5	Luminance	PolLum	stim dir	7	43.00	28.50	54.50
Blackcaps	1	100	Polarization	PolLum	stim dir	7	7.00	3.00	13.50
Blackcaps	0	100	Luminance	LumPol	Null	5	5.00	3.00	7.00
Blackcaps	0	50	Luminance	LumPol	Null	2	8.00	6.50	10.25
Blackcaps	0	38	Luminance	LumPol	Null	5	6.000	4.000	11.000
Blackcaps	0	13	Luminance	LumPol	Null	4	5.00	4.75	10.00
Blackcaps	0	5	Luminance	LumPol	Null	4	7.500	4.000	13.000
Blackcaps	2	100	Luminance	PolLum	Null	7	6.000	4.000	9.000
Blackcaps	2	13	Luminance	PolLum	Null	4	8.0	5.5	13.0
Blackcaps	2	5	Luminance	PolLum	Null	7	7.000	4.000	10.000
Blackcaps	1	100	Polarization	PolLum	Null	7	11.00	3.75	23.25
Blackcaps	Baseline	Baseline	Baseline	LumPol	Baseline	5	15.00	0.25	21.00
Blackcaps	Baseline	Baseline	Baseline	PolLum	Baseline	7	18.00	8.00	25.00

*Attenuation of response frequencies in 100% luminance contrast in birds tested in 6 consecutive rounds:*

There was no significant attenuation effect in response frequencies in Zebra finches in 100% luminance contrast round 2 (stimulus-correlated, median = 56.0 +-45.75/66.0 (1st/3rd quartile); null responses, median = 9.0 +-2.0/15.0; Table 2; Figure 30) and round 6 (stimulus-correlated, median = 56.5 +-20.0/85.25; null responses, median = 7.0 +-3.75/23.25; Table 2; Figure 30) when compared to round 1 (Wilcoxon Signed-Rank Test, Zebra finches, stimulus-correlated: round 2 vs. round 1,  $p = 0.0702$ ; round 6 vs. round 1:  $p = 0.2591$ ; null responses: round 2 vs. round 1,  $p = 0.760$ ; round 6 vs. round 1:  $p = 0.126$ ; Table 2; Figure 30). Response frequencies were even slightly higher in round two than round 1.

There was a noticeable attenuation of response frequencies in European robins in 100% luminance contrast round 2 (stimulus-correlated, median = 24.0 +-12.0/38.75 (1st/3rd quartile); null responses, median = 1.0 +-0.0/4.0; Table 2; Figure 30) and round 6 (stimulus-correlated, median = 20.0 +-7.25/48.0; null responses, median = 1.0 +-0.0/7.75; Table 2; Figure 30) when compared to round 1 (Wilcoxon Signed-Rank Test, European robins, stimulus-correlated: round 2 vs. round 1,  $p = 0.16190$ ; round 6 vs. round 1:  $p = 0.00586$ ; null responses: round 2 vs. round 1:  $p = 0.0241$ ; round 6 vs. round 1:  $p = 2.50e-07$ ; Figure 30).

However, response frequencies in round 6 of European robins in 100% luminance contrast in stimulus direction were significantly higher than responses in null direction in the same round (Wilcoxon Signed-Rank Test, European robins, round 6: responses vs. null responses,  $p < 2.2e-16$ ; Figure 30), and significantly different from baseline activity (Wilcoxon Signed-Rank Test, European robins: stimulus-correlated responses round 6 vs. baseline responses of European robins tested in 6 consecutive rounds,  $p = 6.146e-15$ ; Figure 30). Therefore, I considered the attenuation effect in European robins as not dramatic and the factor round was considered a random effect in the final comparison of luminance vs- polarization contrast.

*Contrast thresholds in reduced luminance contrast steps:*

In Zebra finches, there was no significant reduction of response frequencies in testing trials in lowered luminance contrast steps when compared to 100% contrast (pairwise two-sample permutation tests, Zebra finches, round 3: 100% ( $n = 1$ ) vs. 50% ( $n = 2$ ),  $p = 0.8051$ ; 100% ( $n = 1$ ) vs. 38% ( $n = 6$ ),  $p = 0.5823$ ; Table 2; Figure 31). However, I missed to test an adequate number of individuals and to test this species in contrast steps lower than 38%. Therefore, the result of the evaluation of a potential contrast threshold cannot be called profound.

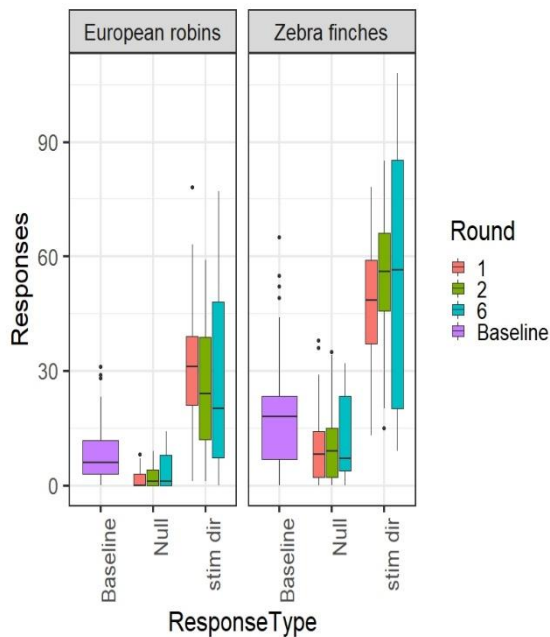


**Figure 30: Response frequencies in birds tested in 6 consecutive rounds in 100% luminance contrast.** There was no significant attenuation effect on stimulus-correlated response frequencies in Zebra finches (Wilcoxon Signed-Rank Test: round 2 vs. round 1,  $p = 0.0702$ ; round 6 vs. round 1:  $p = 0.2591$ ), but in European robins (Wilcoxon Signed-Rank Test, European robins, stimulus-correlated: round 2 vs. round 1,  $p = 0.16190$ ; round 6 vs. round 1:  $p = 0.00586$ ). However, response frequencies in round 6 were significantly different from null responses (Wilcoxon Signed-Rank Test,  $p < 2.2e-16$ ) and from baseline activity (Wilcoxon Signed-Rank Test,  $p = 6.146e-15$ ).

In European robins, there was a significant reduction of response frequencies when tested in lowered luminance contrast of 38%, 13% and 5%, but no significant reduction when tested in 50% (pairwise two-sample permutation test, European robins, pooled data from round 3 and naïve round 2: 100% ( $n = 14$ ) vs. 50% ( $n = 6$ ),  $p = 0.7424$ ; 100% ( $n = 14$ ) vs. 38% ( $n = 8$ ),  $p = 0.002443$ ; 100% ( $n = 14$ ) vs. 13% ( $n = 13$ ),  $p = 2.544e-05$ ; 100% ( $n = 14$ ) vs. 5% ( $n = 13$ ),  $p = 8.786e-07$ ; Figure 31). However, stimulus-correlated response frequencies in 5% contrast were significantly different from null responses in 5% contrast (Wilcoxon Signed-Rank Test, European robins, responses in 5% contrast step vs. null responses in 5% contrast step:  $p < 1.88e-06$ ; Figure 31), and significantly different from baseline activity (pairwise two-sample permutation test, European robins, responses in 5% contrast step ( $n = 13$ ) vs. baseline activity ( $n = 25$ ),  $p = 0.00629$ ; Figure 31). Therefore, I considered the effect of reduced luminance contrast on response frequencies in European robins as not dramatic and the factor contrast step was considered a random effect in the final comparison of luminance vs- polarization contrast.

In Blackcaps, there was a reduction of response frequencies when tested in lowered luminance contrast of 5% and 38%, but not in 50% and 13%, when compared to 100% contrast (pairwise two-sample permutation tests, Blackcaps, pooled data from round 0 and naïve round 2: 100% ( $n = 12$ ) vs. 50% ( $n = 2$ ),  $p = 0.1075$ ; 100% ( $n = 12$ ) vs. 38% ( $n = 5$ ),  $p = 0.004323$ ; 100% ( $n = 12$ ) vs. 13% ( $n = 8$ ),  $p = 0.244$ ; 100% ( $n = 12$ ) vs. 5% ( $n = 11$ ),  $p = 0.02373$ ; Figure 31). However, stimulus-correlated response frequencies in 5% contrast step were significantly

higher than null responses in 5% contrast step (Wilcoxon Signed-Rank Test, Blackcaps, responses in 5% contrast step vs. null responses in 5% contrast step:  $p = 2.447e-10$ ; Figure 31) and significantly different from baseline activity (pairwise two-sample permutation tests, Blackcaps, responses in 5% contrast step ( $n = 11$ ) vs. baseline activity ( $n = 12$ ),  $p = 2.117e-08$ ; Figure 31). Therefore, I considered the effect of reduced luminance contrast on response frequencies in Blackcaps as not dramatic and the factor contrast step was considered a random effect in the final comparison of luminance vs- polarization contrast.

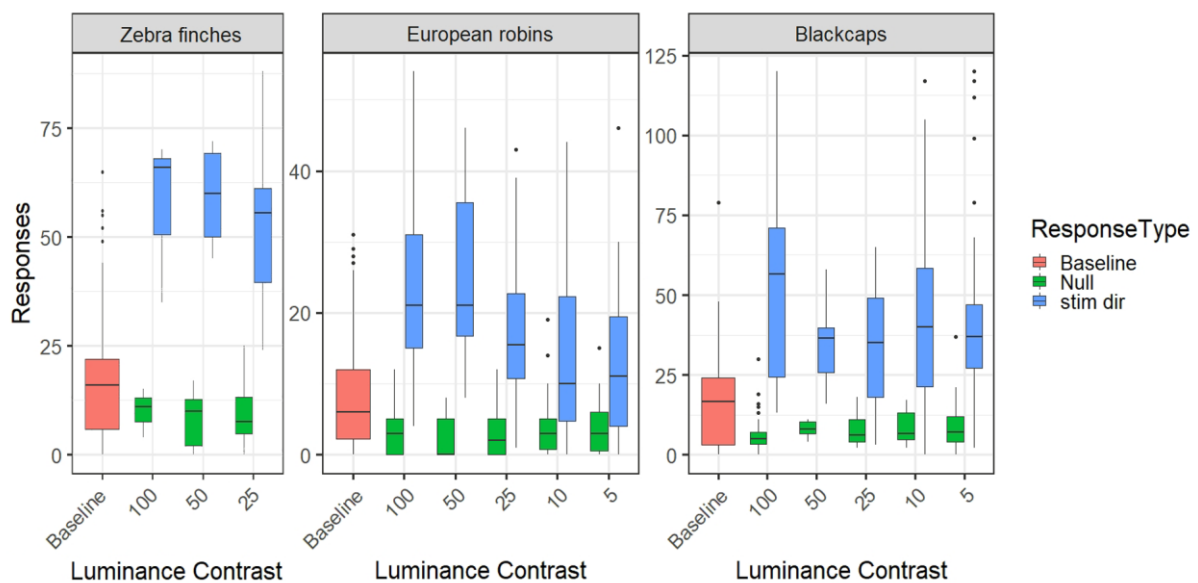


**Figure 31: Response frequencies in birds tested in lowered luminance contrast steps.** In Zebra finches, there was no significant reduction of response frequencies in lowered contrast steps when compared to 100% luminance contrast in round 3 (50%,  $n = 2$ ,  $p = 0.8051$ ; 38%,  $n = 6$ ,  $p = 0.5823$ ). However, I missed to test an adequate number of individuals and to test this species in contrast steps lower than 38%. In European robins and in Blackcaps, there was a reduction of response frequencies in lowered luminance contrast when compared to 100% luminance contrast of round 3 and naïve round 2 (Robins) and round 0 and naïve round 2 (Blackcaps) (pairwise two-sample permutation test: European robins, 50%,  $n = 6$ ,  $p = 0.7424$ ; 38%,  $n = 8$ ,  $p = 0.002443$ ; 13%,  $n = 13$ ,  $p = 2.544e-05$ ; 5%,  $n = 13$ ,  $p = 8.786e-07$ ; Blackcaps, 50%,  $n = 2$ ,  $p = 0.1075$ ; 38%,  $n = 5$ ,  $p = 0.004323$ ; 13%,  $n = 8$ ,  $p = 0.244$ ; 5%,  $n = 11$ ,  $p = 0.02373$ ). However, in the lowest contrast step (5%), stimulus-correlated response frequencies were significantly different from null responses (Wilcoxon Signed-Rank Test, European robins,  $p < 1.88e-06$ ; Blackcaps,  $p = 2.447e-10$ ) and from baseline activity (pairwise two-sample permutation test, European robins,  $p = 0.00629$ ; Blackcaps,  $p = 2.117e-08$ ).

*No significant differences in response frequencies in polarization contrast:*

There were no statistical differences in response frequencies of European robins between consecutive rounds in polarization contrast, and only slight differences between the two groups tested in reversed order of contrast presentation (European robins: pairwise two-sample permutation test: Round 3 vs. 4,  $p = 0.2295$ ; Round 3 vs. 5,  $p = 0.3158$ ; Round 4 vs. 5,  $p = 0.9362$ ; Round 3 vs. naïve round 1,  $p = 0.4161$ ; Round 4 vs. naïve round 1,  $p = 0.01348$ ; Round 5 vs. naïve round 1,  $p = 0.0549$ ; see Table 2 for sample sizes and medians; Figure 32).

There were slightly reduced response frequencies of Zebra finches between consecutive rounds in polarization contrast, but no differences between the two groups of birds tested in reversed order of contrast presentation (Zebra finches: pairwise two-sample permutation test: Round 3 vs. 4,  $p = 0.08802$ ; Round 3 vs. 5,  $p = 0.01401$ ; Round 4 vs. 5,  $p = 0.1792$ ; Round 3 vs. naïve round 1,  $p = 0.07335$ ; Round 4 vs. naïve round 1,  $p = 0.6979$ ; Round 5 vs. naïve round 1,  $p = 0.4481$ ; see Table 2 for sample sizes and medians; Figure 32).

In all three species, stimulus-correlated responses and null responses were indistinguishable in all rounds in polarization contrast, except for slightly elevated null responses in European robins in naïve round 1 and in Zebra finches in Round 3 (Wilcoxon Signed-Rank Test, responses vs. null responses in polarization contrast: European robins: Round 3,  $p = 0.6137$ ; Round 4,  $p = 0.5601$ ; Round 5,  $p = 0.7623$ ; Round 1 naïve,  $p = 0.04609$ ; Zebra finches: Round 3,  $p = 0.03373$ ; Round 4,  $p = 0.1056$ ; Round 5,  $p = 0.5727$ ; Round 1 naïve,  $p = 0.3015$ ; Black caps: Round 1 naïve,  $p = 0.0895$ ; see Table 2 for sample sizes and medians; Figure 31)

Compared to spontaneous head movements during acclimatization time, response frequencies in stimulus direction in polarization contrast were never significantly above, and in principle not distinguishable from baseline level (pairwise two-sample permutation test: Baseline activity vs. responses in stimulus direction in polarization contrast: European robins: Round 3,  $p = 0.006876$ ; Round 4,  $p = 0.0783$ ; Round 5,  $p = 0.04568$ ; Round 1 naïve,  $p = 7.431e-05$ ; Zebra finches: Round 3,  $p = 0.08759$ ; Round 4,  $p = 0.7791$ ; Round 5,  $p = 0.3179$ ; Round 1 naïve,  $p = 0.0825$ ; Black caps: Round 1 naïve,  $p = 0.02329$ ; see Table 2 for sample sizes and medians; Figure 30). In European robins in round 3 and round 5 and in Blackcaps round 1 naïve, response frequencies in polarization contrast were slightly lower than spontaneous head movements.

#### *Combined analysis:*

As elaborated in the preceding statistical evaluations, neither repeated stimulus presentation in consecutive rounds (factor round), nor the order of stimulus presentation (first testing trial presented in luminance contrast or in polarization contrast; factor order), nor the direction of stimulus rotation (CW or CCW; factor direction), nor the contrast step (100% or 50% or 38% or 13% or 5%; factor contrast) had a crucial effect on the response frequencies in luminance contrast. Furthermore, the overall light intensity, i.e. matching illumination levels of white intact screens (round 4 and round naïve1) or matching illumination levels of a full contrast black/white grating on intact screens (round 5), did not have an effect on the response

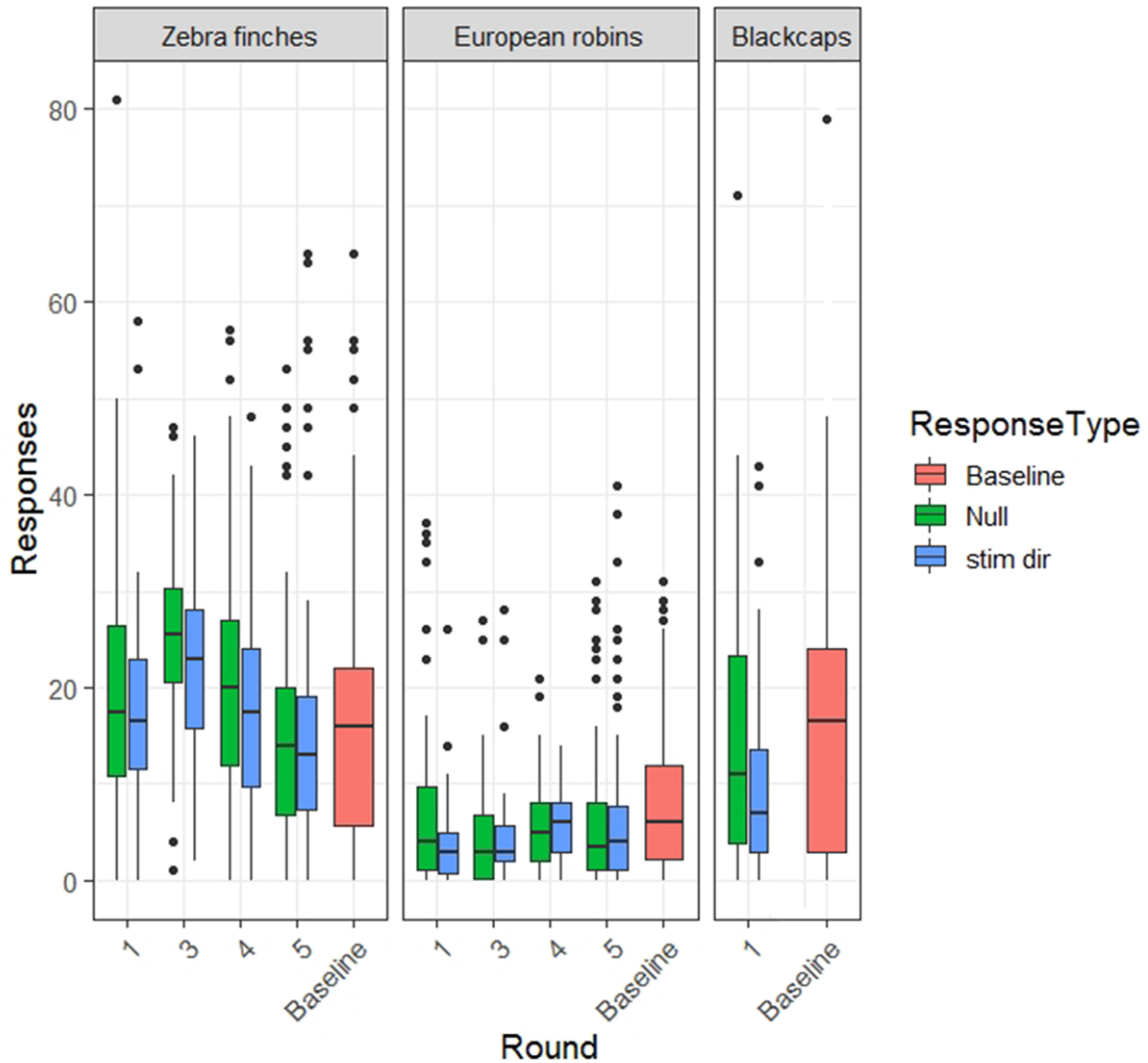


**Figure 32: Response frequencies in birds tested consecutive rounds in full polarization contrast.** In all three species, stimulus-correlated responses and null responses were statistically indistinguishable in all rounds in polarization contrast, except for slightly elevated null responses in European robins in naïve round 1 and in Zebra finches in Round 3 (Wilcoxon Signed-Rank Test, responses vs. null responses in polarization contrast: European robins: Round 3,  $p = 0.6137$ ; Round 4,  $p = 0.5601$ ; Round 5,  $p = 0.7623$ ; naïve Round 1,  $p = 0.04609$ ; Zebra finches: Round 3,  $p = 0.03373$ ; Round 4,  $p = 0.1056$ ; Round 5,  $p = 0.5727$ ; naïve Round 1,  $p = 0.3015$ ; Black caps: naïve Round 1,  $p = 0.0895$ ; see Table 2 for sample sizes and medians). Response frequencies in polarization contrast were never significantly above and in principle not distinguishable from baseline activity in all three species (pairwise two-sample permutation test: European robins: Round 3,  $p = 0.006876$ ; Round 4,  $p = 0.0783$ ; Round 5,  $p = 0.04568$ ; Round 1 naïve,  $p = 7.431e-05$ ; Zebra finches: Round 3,  $p = 0.08759$ ; Round 4,  $p = 0.7791$ ; Round 5,  $p = 0.3179$ ; Round 1 naïve,  $p = 0.0825$ ; Black caps: Round 1 naïve,  $p = 0.02329$ ; see Table 2 for sample sizes and medians).

frequencies in polarization contrast. Therefore, I used the median response frequencies pooled for all trials in polarization contrast or luminance contrast, respectively, for a combined analysis of whether there were general differences in responses to moving gratings presented in polarization contrast and in luminance contrast.

In luminance contrast, median response frequencies in stimulus direction (Zebra finches,  $n = 345$ , median =  $55.0 \pm 38.0/70.0$  (1<sup>st</sup>/3<sup>rd</sup> quartile); European robins,  $n = 510$ , median =  $20.0 \pm$

11.0/34.0; Blackcaps, n = 153, median = 41.0 +-24.0/58.0; Figure 33) were highly significantly different from median response frequencies in null direction (Zebra finches, n = 345; median = 8.0 +-3.0/16.0 (1<sup>st</sup>/3<sup>rd</sup> quartile); European robins, n = 510; median = 2.0 +-0.0/5.0; Blackcaps, n = 153; median = 6.0 +-4.0/11.0; ANOVA of the GLMM: Zebra finches, p < 2e-16; European robins, p < 2.2e-16; Blackcaps, p < 2.2e-16; Figure 33).

Median stimulus-correlated response frequencies in luminance contrast were highly significantly different from median response frequencies in polarization contrast in stimulus direction (ANOVA of the GLMM: Zebra finches, p < 2e-16; European robins, p < 2.2e-16; Blackcaps, p < 2.2e-16; Figure 33).

In polarization contrast, responses in stimulus direction (Zebra finches, n = 264; median = 16.0 +-9.0/24.0 (1<sup>st</sup>/3<sup>rd</sup> quartile); European robins, n = 240; median = 4.0 +-2.0/7.0; Blackcaps, n = 42; median = 7.0 +-3.0/13.50; Figure 33) were not distinguishable or not highly significant different from null responses (Zebra finches, n = 264; median = 18.0 +-12.0/26.0 (1<sup>st</sup>/3<sup>rd</sup> quartile); European robins, n = 240; median = 4.0 +-1.0/8.0; Blackcaps, n = 42; median = 11.0 +-3.75/23.25; Wilcoxon Signed-Rank Test, responses vs. null responses in polarization contrast: Zebra finches, p = 0.009534; European robins, p = 0.2475; Blackcaps, p = 0.0895; Figure 33). Furthermore, responses frequencies in polarization contrast in stimulus direction were not distinguishable or significantly below baseline activity (Zebra finches baseline, n = 132; median = 16.0 +-5.75/22.0 (1<sup>st</sup>/3<sup>rd</sup> quartile); European robins baseline, n = 150; median = 6.0 +-2.25/12.0; Blackcaps baseline, n = 72; median = 16.50 +-3.0/24.0; pairwise two-sample permutation test: Baseline vs. responses in stimulus direction in polarization contrast: Zebra finches, p = 0.1906; European robins, p = 5.759e-05; Blackcaps, p = 0.02329; Figure 33).



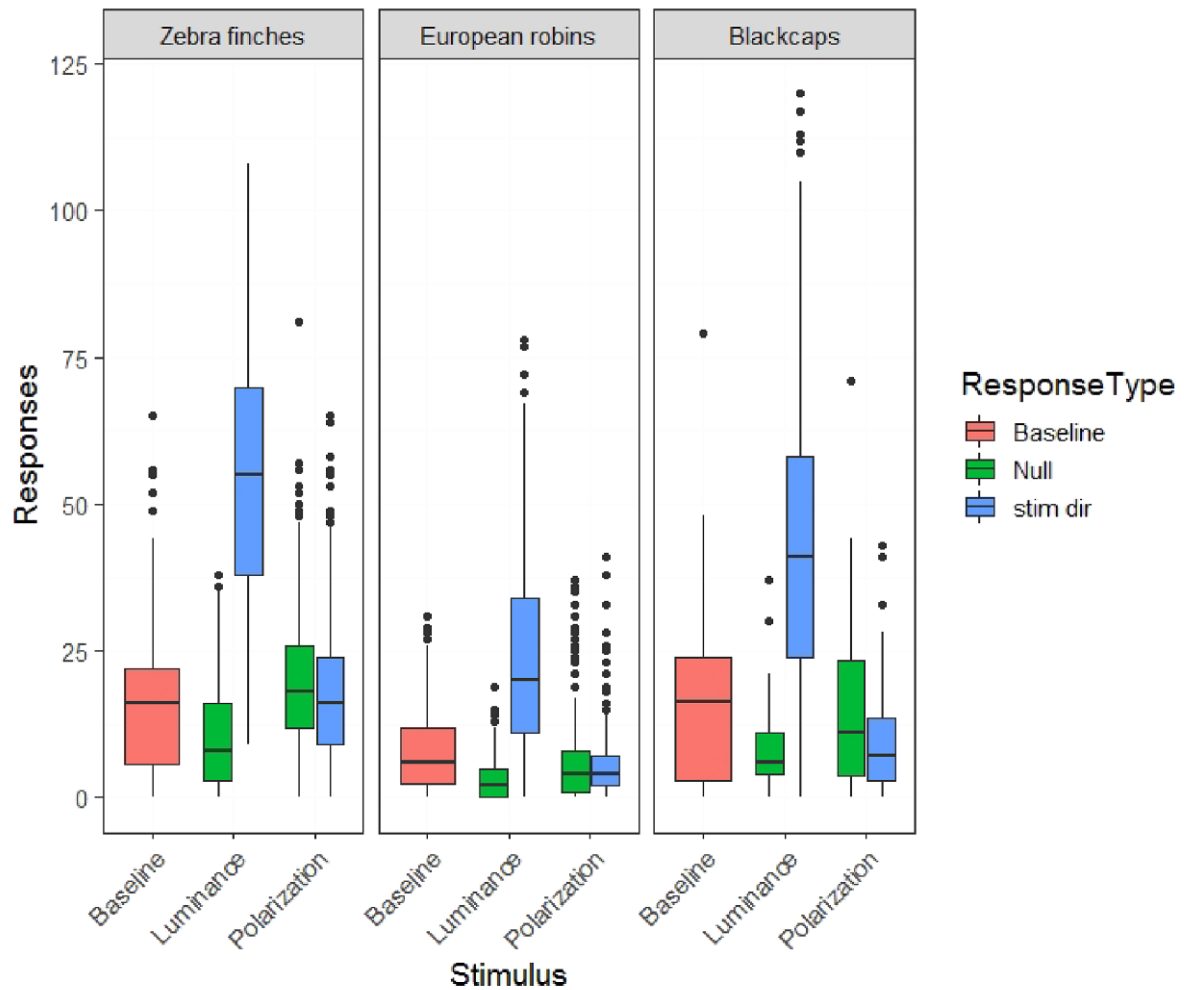


**Figure 33: Response frequencies combined for all rounds, separated for polarization contrast versus luminance contrast and response type.** Median stimulus-correlated response frequencies in luminance contrast were highly significantly different from median response frequencies in polarization contrast in stimulus direction (ANOVA type III of the GLMM: Zebra finches,  $p < 2e-16$ ; European robins,  $p < 2.2e-16$ ; Blackcaps,  $p < 2.2e-16$ ). In polarization contrast, responses in stimulus direction were not distinguishable or not highly significant different from null responses (Wilcoxon Signed-Rank Test: Zebra finches,  $p = 0.009534$ ; European robins,  $p = 0.2475$ ; Blackcaps,  $p = 0.0895$ ). Furthermore, responses frequencies in polarization contrast in stimulus direction were not distinguishable or slightly below baseline activity (pairwise two-sample permutation test: Zebra finches,  $p = 0.1906$ ; European robins,  $p = 5.759e-05$ ; Blackcaps,  $p = 0.02329$ ).

### Looming stimulus

To assess the ability of songbirds to detect contrast based on differential e-vector angle distributions, i.e. if birds possess polarization vision, I presented in total 22 Zebra finches, 25 European robins and 12 Blackcaps to a looming stimulus in polarization contrast, in luminance contrast and in lowered contrast steps in luminance contrast. 14 Zebra finches and 15 European robins were tested in 6 consecutive rounds, an additional 8 Zebra finches, 10 European robins and 7 Blackcaps were tested in two rounds starting with presentation in polarization contrast. To assess a potential contrast threshold in Blackcaps for which I had no

prior data from 6 consecutive rounds, an additional 5 Blackcaps were tested in contrast steps in luminance contrast round 0.

Birds of all three species naïve to the setup and the stimuli, i.e. Blackcaps tested in round 0, Zebra finches and European robins tested in round 1, were exposed to a looming stimulus in 100% luminance contrast, I observed strong escape behavior away from the “incoming” black dots (Blackcaps: 2/4, Zebra finches: 14/14, European robins: 14/15; see Table 3). As expected, a strong attenuation effect seemed to affect the percentage of observed escape behaviors in consecutive rounds in 100% luminance contrast (round 2: Zebra finches, 7/14; European robins: 10/15; round 3: Zebra finches, 0/3; European robins: 2/6; see Table 3). In all rounds with stimulus presentation in polarization contrast, no response was observed (round 3, 4 and 5; see Table 3). However, it is noteworthy that strong escape behavior was observed in round 6, after the manipulation of the screens was reversed and stimuli were presented in 100% luminance contrast (round 6: Zebra finches, 7/7; European robins: 9/15; see Table 3). The testing trials in lowered contrast steps in luminance contrast resulted in low numbers of observed escape behavior (50%: Zebra finches, 0/2; European robins: 1/7; Blackcaps, 1/1; 38%: Zebra finches, 3/6; European robins: 4/14; Blackcaps, 4/9; 13%: Blackcaps, 1/2; 5%: European robins: 1/8; Blackcaps, 1/10; see Table 3). Note that the testing in contrast steps was unbalanced and I missed to test Zebra finches in contrast steps lower than 38%. However, it is noteworthy that even in the lowest contrast steps, some birds are able to show strong escape behavior to a looming stimulus in luminance contrast (Zebra finches, 38%, 3/6; European robins, 5%, 1/8; Blackcaps, 5%, 1/10, see Table 3).

No response was observed in any bird and in any round when the looming stimulus was presented in polarization contrast (round 3, 4 and 5 in Zebra finches and European robins; see Table 3; naïve round 1 in Zebra finches, European robins and Blackcaps; see Table 3 and Figure 34, No response, Polarization). Birds tested in 2 rounds starting with polarization contrast did not show responses in polarization contrast (Figure 34; see Table 3), but did show escape behavior in luminance contrast (Zebra finches, 8/8; European robins: 7/10; Blackcaps, 7/7; Figure 34, Escape behavior, Luminance).

**Table 3: Summary table of observed escape behavior to a looming stimulus.**

Species	# Individuals	Round	Contrast	Stimulus	Testing order	Escape behavior	No response
Zebra finches	8	<b>1</b>	100	Polarization	PolLum	0	8
Zebra finches	8	<b>2</b>	100	Luminance	PolLum	8	0
Zebra finches	14	<b>1</b>	100	Luminance	LumPol	14	0
Zebra finches	14	<b>2</b>	100	Luminance	LumPol	7	7
Zebra finches	3	<b>3</b>	100	Luminance	LumPol	0	3
Zebra finches	8	<b>3</b>	100	Polarization	LumPol	0	8
Zebra finches	14	<b>4</b>	100	Polarization	LumPol	0	14
Zebra finches	14	<b>5</b>	100	Polarization	LumPol	0	14
Zebra finches	14	<b>6</b>	100	Luminance	LumPol	7	7
Zebra finches	2	3	50	Luminance	LumPol	0	2
Zebra finches	6	3	38	Luminance	LumPol	3	3
European robins	10	<b>1</b>	100	Polarization	PolLum	0	10
European robins	10	<b>2</b>	100	Luminance	PolLum	7	3
European robins	15	<b>1</b>	100	Luminance	LumPol	14	1
European robins	15	<b>2</b>	100	Luminance	LumPol	10	5
European robins	6	<b>3</b>	100	Luminance	LumPol	2	4
European robins	7	<b>3</b>	100	Polarization	LumPol	0	7
European robins	15	<b>4</b>	100	Polarization	LumPol	0	15
European robins	15	<b>5</b>	100	Polarization	LumPol	0	15
European robins	15	<b>6</b>	100	Luminance	LumPol	9	6
European robins	7	3	50	Luminance	LumPol	1	6
European robins	14	3 & naive 2	38	Luminance	LumPol	4	10
European robins	8	2	5	Luminance	PolLum	1	7
Blackcaps	7	<b>1</b>	100	Polarization	PolLum	0	7
Blackcaps	7	<b>2</b>	100	Luminance	PolLum	7	0
Blackcaps	4	0	100	Luminance	LumPol	2	2
Blackcaps	1	0	50	Luminance	LumPol	1	0
Blackcaps	9	0	38	Luminance	LumPol	4	5
Blackcaps	2	0 & naive 2	13	Luminance	LumPol	1	1
Blackcaps	10	0 & naive 2	5	Luminance	LumPol	1	9

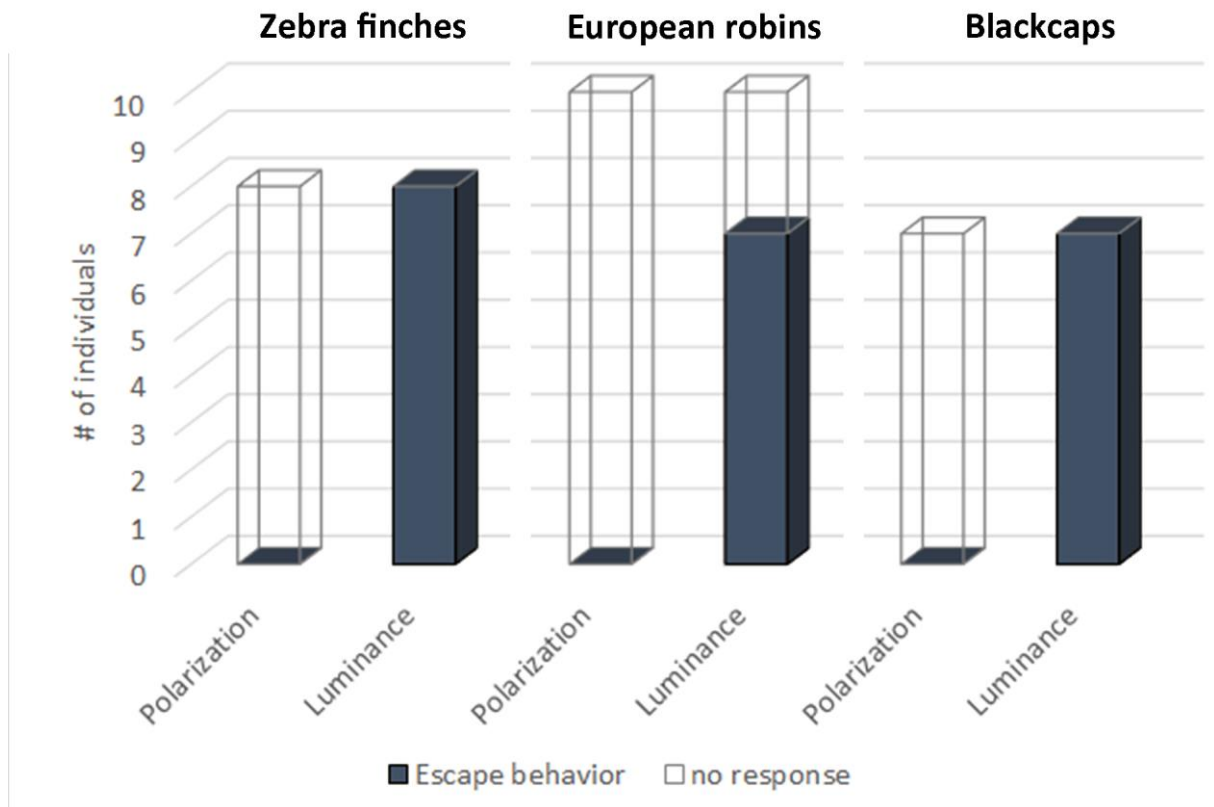


**Figure 34: Observed escape behavior in birds tested in two consecutive rounds starting with polarization contrast.** None of the tested birds did show a response to a looming stimulus in polarization contrast (Polarization, no response, hollow bars; see Table 3). In all three bird species, I observed strong escape behavior in the following round in luminance contrast (Luminance, Escape behavior, dark blue bars; Zebra finches, 8/8; European robins, 7/10, Blackcaps, 7/7).

### 3.5.4. Discussion

The here presented study was designed to bridge a knowledge gap in avian polarization vision research by obtaining results unbiased by light reflection artifacts and by using the presentation of biologically relevant dynamic stimuli on manipulated LCD monitors. The readily evoked, innate behaviors used as readout additionally avoided the potential biases of conditioning paradigms.

The sensitivity to linearly polarized light in birds has been independently suggested in many orientation experiments which provided access to natural or manipulated celestial polarization patterns (for reviews see Åkesson, 2014; Muheim, 2011). Nevertheless, strongly contradictory results have been reported when avian polarization sensitivity was tested in laboratory-based approaches. Kreithon & Keeton (1974) succeeded in raising the heart rate of conditioned birds in response to a rotating polarizer, and Delius et al. (1976) succeeded in training birds to choose the correct arm of a plus maze in response to the orientation of overhead polarized light. Replication attempts of these experiments in similar setups, but

eliminating potential light artifacts repeatedly produced negative results (Coemans et al., 1990 + 1994; Hzn Vos et al., 1995). In another study, birds of different species and ecology could not distinguish between different e-vector orientations reflected from objects to receive a food reward (Greenwood et al., 2003) and the most recent study found that Zebra finches were unable to discriminate the presence or absence of a range of polarization contrasted images on either one of two manipulated LCD screens to receive a reward (Melgar et al., 2015). It is however possible that conditioning paradigms fail to evoke behavioral responses to polarization stimuli, because the coding of sensory stimuli can change dramatically as a function of behavioral relevance (Wagener & Nieder, 2016).

The method employing LCD monitors to present dynamic polarization contrast has already been demonstrated as adequate in several aquatic invertebrate species (Glantz and Schroeter, 2006; Pignatelli et al., 2011; How et al., 2014), but not in fish (Pignatelli et al., 2011). This is the first study that used untrained stereotypic responses in three passerine bird species as a readout to ecologically relevant visual tasks, i.e. image stabilization upon global visual motion and predator or object avoidance. The advantage of our approach is that I was able to present birds with dynamic polarization contrast in form of moving image sequences without producing any potentially biasing secondary cues (light intensity artifacts).

When presented in polarization contrast upon removal of the front polarizers of the screens, we would expect comparable behavioral responses in form of optomotor responses (OMR) to moving gratings and escape behavior to a looming stimulus as compared to presentation in luminance contrast, if the birds were able to detect contrast based on differential e-vector angle distributions, i.e. if birds possess polarization vision.

However, response frequencies to the polarization contrasted moving gratings were not above baseline activity level, whereas even lowest contrast steps in luminance contrast and repeated testing in consecutive rounds in luminance contrast evoked response frequencies significantly higher than baseline activity, i.e. a potential eliminating effect of a minimum contrast threshold or attenuation of the response frequencies over repeated testing could not explain the absence of significantly distinguishable responses in polarization contrast between responses in stimulus direction vs. null responses and vs. baseline activity. Furthermore I documented the absence of escape behavior as a response to a looming stimulus presented in polarization contrast whereas even in the lowest contrast steps tested and after repeated

testing some birds were still able to respond with strong escape behavior to a looming stimulus in luminance contrast.

My results contradict earlier positive evidence (Kreithen & Keeton, 1974; Delius et al., 1976) and are in agreement with all previous indications that birds do not possess polarization vision (Montgomery and Heinemann, 1952; Coemans et al., 1990+1994; Vos Hzn et al., 1995; Greenwood et al., 2003; Melgar et al., 2015).

Nevertheless, it is possible that the putative neuronal processing and integration of information mediated through polarized light is limited to very specific visual tasks in birds and other vertebrates (e.g. limited to behavioral contexts like e.g. orientation by skylight polarization patterns) and cannot be extrapolated to other ecologically relevant visual tasks. Therefore, birds might perceive the dynamic polarization contrast presented in my experiments, but this information would potentially not be integrated into neuronal circuits processing motion detection or object recognition, leading to the absence of the expected reflex-like responses to stimuli presented in polarization contrast in my experiments.

In many invertebrate species, polarization sensitivity is linked to UV sensitive photoreceptors (for review see Labhart, 2016). In fish (excluding anchovies; Novales Flamarique and Harosi, 2002), polarization sensitivity is suggested to be linked to interactions between UV- and double cones (Novales Flamarique et al., 1998). In birds however, the current hypotheses involve (a) internal reflections in double cones (Young and Martin, 1984) which absorb primarily between 520-580 nm or (b) membrane-bound scaffolds that lead to high intracellular opsin alignment on a microscopic level (Kroeger et al 2003). The spectral range for maximal excitation of avian double cones was well covered in my experiments. However, the possibility that the mechanism of polarization sensitivity in birds strongly relies on cones that are sensitive to UV light cannot be excluded. Birds are tetra-chromates with a spectral range from approximately 350-700 nm (Hunt, 2009). Due to technical properties of LCD screens, I was not able to stimulate outside a spectral range of 400 – 700 nm in my experiments. If a polarization sensitive processing pathway in the avian visual system was based on internal reflections from avian double cones on to UV cones (Novales Flamarique et al., 1998; Kram et al., 2010; see chapter 3.2. in this thesis; Figure 10 D), a modification of the LCD monitor background illumination to include UV light would be beneficial, because it would include optimal excitation of all potentially polarization-sensitive photoreceptor types (i.e. optimally stimulate UV cones; Foster et al., 2018). However, the absorption spectrum of avian

UV cones (peaking at 370 or 410 nm; Hunt, 2009) reaches broadly into the spectral range that I used in the present study (400-700 nm). Therefore, my experiments should have at least weakly included UV cones and therein a potential polarization-sensitive system that depended on double cone - UV cone interactions.

A critical remark has to be made about the unbiased testing paradigm in my experiments. I initially designed my experiments to answer a simple question: are optomotor responses and escape behavior present or absent when birds were tested in polarization contrast? I decided that an observed response in a low contrast step would suffice for answering that question, so I accepted the resulting unbiased representation of testing trials in all possible contrast steps, i.e. 100%, 50%, 38%, 13% and 5%. Due to only marginal knowledge about the thereby arising problems in statistical analysis, I did not comprehend that this decision would have the consequence of an unnecessarily inconvenient handling of the statistical evaluation and a limited comparability of groups with different sample sizes. Fortunately, the differences between trials in luminance contrast versus polarization contrast and between responses in stimulus direction versus null direction were strong. Nevertheless, the unbalanced group sizes unnecessarily diminished the reliability of the results to some extent. I suggest, that before publication of this study, a repetition of the trials in lowered contrast steps was made with balanced sample size in all contrast steps and optimally a larger total sample size.

To conclude, this study indicates that there is no involvement of putative polarization sensitive photoreceptors in two specific visual tasks basic to vertebrate retinal processing. Combined with findings of other groups that showed negative evidence in experiments conditioning birds to distinguish different e-vectors, birds might not possess polarization vision, at least in visual tasks that involve motion detection. Until no further evidence for an anatomical basis in the bird retina was raised, the question of polarization sensitivity in birds remains an unsolved mystery in bird vision, following the traditional aphorism “the absence of evidence is not the evidence of absence” (Carl Sagan, 1997).

## 4. Conclusions and Outlook

My PhD thesis successfully advanced the knowledge about compass orientation in coral reef fish homing in a side project that has been published in an international journal (chapter 2 in this thesis). In my main project on avian polarization sensitivity, I critically dissected earlier claims of evidence for a polarization sensitive visual pathway in extracellular electrophysiological recordings from avian retinal ganglion cells upon stimulation with rotating linearly polarized light (chapter 3.4. in this thesis). Furthermore, I presented three songbird species to dynamic visual stimuli in luminance contrast and in polarization contrast to answer the question whether birds possess polarization vision.

Three major findings can be taken from my work on compass orientation in coral reef fish larvae and on the polarization sensitivity in bird:

***(1) Coral reef fish larvae can use a magnetic compass to orient at night (chapter 2 in this thesis).***

We investigated the homing strategies of a coral reef fish species that is known to passively disperse for comparably large distances. To find back to a reef over longer distances after dispersal, global orientation cues are needed that reliably function in overcast and turbulent conditions as well as at night, when other visual cues are unavailable. First, we were able to replicate evidence for sun compass orientation during the day (Mouritsen et al., 2013). In a second step, we experimentally demonstrate the first evidence that coral reef fish larvae can use the geomagnetic field for compass orientation at night, in the absence of any celestial cues. This work has been published prior to release of this thesis in the renowned journal *Current Biology* (Bottesch et al., 2016).

The search for the magnetic sensor in vertebrates is focusing on two major hypotheses, namely magnetite-based and light-dependent magnetoreception based on a radical-pair mechanism. Due to our findings, coral reef fish are now known to possess a magnetic compass. Future studies could investigate the sensory basis of coral reef fish magnetoreception following established experimental paradigms like pulsing experiments, i.e. identifying a magnetite-based mechanism, or like experiments including electromagnetic noise or wavelength-filtered ambient lighting, i.e. identifying a light-dependent radical-pair-based mechanism. Furthermore, it would be very interesting to find out if these fish possess an inclination compass like other vertebrates. Performing a vertical flip experiment as done by



Wiltschko and Wiltschko (1972) could hint towards parallels in the magnetic compasses of birds and coral reef fish larvae. Since there is evidence for sun compass orientation during daytime and now for a magnetic compass that works at night, it would be very interesting to investigate if these reef fish larvae might possess a sensitivity for polarized light (Berenshtein et al., 2014) that might aid larval orientation during the twilight period. Furthermore, olfactory, auditory and visual imprinting (e.g. Gerlach et al., 2007, olfactory imprinting, for review see Leis et al., 2011) has been demonstrated to play a crucial role in coral reef fish homing, but it remains unknown to what extent coral reef fish larvae might imprint on geomagnetic field values at their home reef.

This interesting field basically just opened up and many fascinating revelations about the actual mechanisms and complexity of coral reef fish (magnetic) orientation might be just around the corner.

***(2) No unambiguous evidence for retinal ganglion cells that encode the e-vector of polarized light in chicken (*Gallus gallus*; chapter 3.4. in this thesis)***

We investigated the sensory capabilities of birds to perceive and/or process polarized light information on the level of retinal ganglion cells using multi-electrode extracellular recordings. Former colleagues of mine demonstrated that retinal ganglion cells responded bimodal in extracellular recordings upon light stimulation with a rotating polarizing filter in the light path (Schneider and Dreyer et al., 2014, unpublished; chapter 3.4. in this thesis). After strict analysis criteria and well-controlled light stimulation against possible light reflection artifacts in the light stimulation protocol, their study claimed the first evidence for true polarization sensitivity processed by retinal ganglion cells in birds. However, in the present state of our own results from replication experiments and follow-up investigations, we can neither deny nor confirm this visual capacity. Dr. Arndt Meyer and I convincingly demonstrated in our experiments that invasive approaches like the one used here (chapter 3.4. in this thesis; Schneider and Dreyer et al., 2014, unpublished) do not possess the power to reveal unambiguous results on the polarization sensitivity, since the structural integrity of the retina cannot be preserved. Consequently, there is no guarantee for physiological health of the tissue (lowered cell sensitivity and responsiveness), unaltered geometric order (photoreceptor tilt) and preservation of optical properties (visual shielding function of the pigment epithelium). We were however able to demonstrate how very difficult it might be and how much effort could be needed to rule out reflection artifacts and potential artificial

polarization sensitivity upon the stimulation with linearly polarized light, when using electrophysiological methods. For future studies on physiological responses to polarized light, I would recommend to refrain from invasive methods that include the potential disruption of the retinal network and the introduction of recording equipment into the light path. However, the here applied stimulation protocol and recording equipment are already the most promising in terms of control for light reflection artifacts as compared to translucent flat-arrays, electroretinogram recordings or recordings from the optic nerve upon stimulation of the whole optical apparatus (see chapter 3.4.5. in this thesis). Calcium imaging techniques and *in-vivo* fluorescence microscopy approaches do not require introduction of recording devices into the retinal network, but rely on the visualization of cell activity. These techniques could be a valid alternative in future approaches on polarization sensitivity in retinal networks of birds. Classically, evidence for a basis of polarization sensitivity in photoreceptor cells resulted from systematic ultra-structural investigations for the properties of cellular dichroism and/or photopigment alignment in vertebrate photoreceptor outer segments (e.g. Novales Flamarique and Harosi, 2002; Roberts et al., 2004; Roberts and Needham, 2007) or in insect ommatidia (for review see e.g. Cronin and Marshall, 2014; Labhart, 2016). To my knowledge, no such systematic study focusing on bird photoreceptors has been published so far. I would recommend the use of microspectrophotometric equipment to systematically evaluate avian photoreceptor dichroic ratios. I would recommend the use of transmission electron microscopy techniques to systematically search for highly aligned structures in photoreceptor outer segments and inner segments. Or as an alternative using the experimental approach discussed in chapter 3.4, I recommend the alteration of the retinal dissection protocol in ways described in chapter 3.4.5., in short to use a dummy array that can penetrate the sclera and pre-open a gateway for the multi-electrode array. In this way, retinal damage could probably be minimized to an acceptable level and simultaneously the intriguing experimental approach used by Schneider and Dreyer et al. (2014, unpublished) could be continued to be used in a promising experiment to prove or disprove polarized light sensitivity in birds.

I hope that future studies on physiological responses to polarized light stimuli can take the insights on the manifold sources for potential light reflection artifacts gathered from the work by Dr. Arndt Meyers, Dr. David Dreyer, Dr. Nils-Lasse Schneider, Prof. Dr. Henrik Mouritsen and me into account and that the question of polarization sensitivity in birds will soon find a satisfying answer.

### ***(3) No evidence for polarization vision in songbirds (chapter 3.5. in this thesis)***

Conditioning of birds to polarization stimuli (Melgar et al., 2015), training birds to detect different polarization-based properties in objects (Greenwood et al., 2003), or conditioning to rotating polarizers (Montgomery and Heinemann, 1952), all these former approaches resulted in negative data on polarization vision in birds. In very short time, I established an experimental setup and stimulation protocol in my working group that would not rely on conditioning or training for a behavioral readout, and that would not be affected by unintendedly introduced light artifacts. I adopted the technique of LCD monitor manipulation (Glantz and Schroeter, 2006) for investigating the visual capability of polarization vision in birds. In a virtual arena using four LCD monitor screens, I was able to trigger stable optomotor responses (OMR) in birds to moving gratings presented in luminance contrast on intact screens. Furthermore, I was able to trigger strong escape behavior in birds presented with a looming stimulus mimicking a very fast approaching object in luminance contrast. Upon removal of the polarizing sheets from the front of the screens, these stimuli were presented in polarization contrast which in turn was only visible to animals that possess the sensory basis to detect polarized light. However, in polarization contrast no comparable response was triggered in the tested birds of three different songbird species. The optomotor responses (OMR) were not distinguishable from baseline activity and no response to a looming stimulus was ever observed when tested in polarization contrast.

My results led to the conclusion that songbirds might not possess polarization vision and that it is rather likely that polarization sensitivity does not exist in the tested songbird species. Nevertheless, the triggered behaviors are to some extent cognitively processed. Polarization sensitive retinal pathways and/or processing brain areas might not be integrated in these tasks. In other words, the information might be processed by an indeed present polarization sensitive visual system but the extracted information cannot be extrapolated to the sensorimotor and cognitive circuits underlying the behavioral tasks of image stabilization (moving gratings) and escape behavior (looming stimulus).

In conclusion, my PhD thesis revealed interesting findings on the existence of a magnetic compass in coral reef fish larvae and on the question whether polarization sensitivity in birds exists.

#### **4.1. Closing the lid – A novel optical property of the third eye lid in birds and its implications for a potential polarization sensor**

Although focus in research on polarized light in behavioral contexts was mainly based on linearly polarized light and its potential biological use as an orientation cue in birds, I will shortly present the phenomenon of circular polarization of light.

First, light waves travelling through optically dense media can be slowed down for the time of transmission. In optically dense anisotropic media, e.g. calcite crystals or chiral biological molecules like carotenoids (Chiou et al., 2012), such a wave retardation does occur only in one particular vibrational plane, called the *slow axis* of the medium (Figure 35, A). Light waves propagating with e-vector orientations perpendicular to the slow axis (called the *fast axis of the medium*; Figure 35, A) are not slowed down. Second, the electric fields produced by separate electromagnetic waves that propagate into the same direction add up to one single vector (Figure 35, B, top). Therefore, an observable e-vector orientation of linearly polarized light in a 45° angle can simultaneously be expressed as the added vectors of two perpendicularly propagating e-vectors at 90° and 0°, with synchronized phases (Figure 35, B, top). If a phase shift of a ¼ wave length occurs in one of the perpendicularly propagating linearly polarized rays (Figure 35, B, top), circular polarization results (Figure 35, B, bottom). The observed summed e-vector now rotates around the direction of propagation with a particular handedness, i.e. right-handed or left-handed, depending on which of the two perpendicular e-vectors was phase shifted (Figure 35, A). Note that the resulting e-vector is propagating circularly, but the principle e-vectors are still perpendicularly plane polarized (Figure 35, B, bottom). Reversely, such a phase shift in already circularly polarized light consequently results in linear polarized light (1/4 wave shift; Figure 35, A) or circularly polarized light of reversed handedness (1/2 wave shift, for example in a transmitting medium of doubled thickness). All intermediate states of phase shifts are referred to as elliptically polarized light. Third, chiral molecules in right-handed conformation (e.g. D-Glucose) absorb left-handed circularly polarized light and transmit right-handed circularly polarized light.

Migratory birds travel huge distances every year with astonishing precision. Their sensory system is fine-tuned to orientation cues like the geomagnetic field, the sun and the stars. However, whether birds use skylight polarization for navigation remains a sensory mystery. Whilst there is much useful directional information available from the pattern of polarized

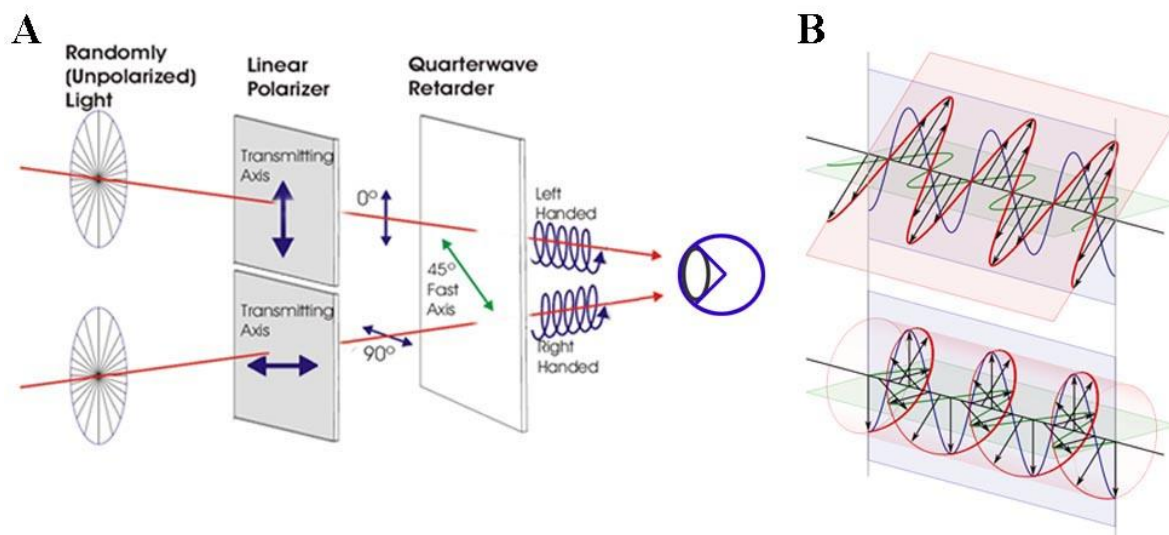


**Figure 35: Wave retardation can lead to a conversion from linearly polarized to circularly polarized light, and vice versa.** A) From left to right: Unpolarized light is passing a linear polarization filter. After that, all transmitted light has an e-vector orientation propagating in parallel o the transmission axis of the linear polarizer. When passed through a  $\frac{1}{4}$  wave retarder plate with its fast axis oriented in  $45^\circ$  to the e-vector orientation, circularly polarized light results. The handedness of the circular propagation of light waves is depending on which of the two perpendicularly propagating, phase locked waves is retarded, i.e. passing the slow axis of the retarder plate. B) The electric fields of two perpendicularly propagating, phase-locked waves of linearly polarized light add up (green and blue wave, top in B) to a result in a summed electric field vector (observable e-vector) with intermediate orientation. The circular propagation of the e-vector is illustrated in the bottom drawing. In this case, the green wave was retarded during transition through a quarter-wave retarder, resulting in left-handed circularly polarized light. Modified from [www.ledinside.com](http://www.ledinside.com)

light in the sky, photoreceptors that are sensitive to the plane of polarized light – as readily found in polarization sensitive insects or fish – have not been identified in birds.

I have discovered a so far undescribed optical property of the avian nictitating membrane and this extra-retinal structure might confer avian polarization sensitivity.

The nictitating membrane (NM) is a translucent third eye lid of birds under voluntarily control. Extra-ocular structures like the NM have been overlooked as putative mediators in polarized light detection. During my PhD, I have found evidence that the NM in songbirds and domestic chicken is highly birefringent which suggested a new hypothesis for polarized light detection. Birefringence is the optical property of optically dense anisotropic media described above. The NM modulates the properties of polarized light that travels through the tissue on its way to the retina. I observed that

- Wave retardation in the NM converts incident linearly polarized light into circular polarized light (CPL). The handedness of the CPL can reverse with the incident e-vector orientation.
- Depending on the e-vector orientation of incident linearly polarized light, the spectral composition of light is shifted distinctly, either filtered to the UV/blue spectral range or

towards the yellow/orange. This spectral shift that is depending on the e-vector angle of incident linearly polarized light can excite two different populations of avian photoreceptors, i.e. UV cones and double cones, depending on the e-vector or incident polarized light.

Two hypotheses arose based on my findings: It is possible that distinct planes of polarization might appear as distinct colors to birds, when light travels through the voluntarily closed NM, i.e. being spectrally shifted before reaching the retina. The beauty of this polarization sensitivity mechanism lies in its voluntary 'on demand' character, which could also explain the reported restriction of behavioral responses to polarized light in birds to precise ecological circumstances. Furthermore, the current hypotheses on a UV- / double cone dependency of PS could be met by my hypothesis, since distinctively these photoreceptor types would be maximally excited by the spectral shift caused by the NM. A second hypothesis includes the oil droplets in the avian retina. These spectral filters in the avian photoreceptors contain high amounts of carotenoids, which in turn possess polarization-active anisotropic properties (Chiou et al., 2012). A precise interplay between first circular polarization of linearly polarized light through the NM and a subsequent absorption or transmission in the chiral carotenoid in the oil droplets, respectively depending on the handedness of circularly polarized light (which in turn depends on the e-vector orientation of light incident to the NM).

For first experimental investigation of the role of the NM in visual processing in birds, I would suggest precise microspectrophotometry (MSP) measurements of the chromatic properties of the spectral shift caused by the NM. Extractions from oil droplets could be investigated for polarization properties and a potentially given interplay between anisotropic modulation of the vibrational properties in the NM and photoreceptor oil droplets could be measured.

My findings, combined with systematic testing using the above-mentioned methods, could have the potential to revolutionize understanding of bird polarization sensitivity. I am looking forward to investigating the implications of this fascinating phenomenon for avian visual behavior and navigational systems in birds in my future scientific career.

## 5. Own contributions

I worked in two main projects during my PhD concerning the ability to detect polarized light information in birds. In a side project, I investigated whether coral reef fish larvae possess a magnetic compass that might help them return to their natal reef. The side project led to the paper “A magnetic compass that might help coral reef fish larvae return to their natal reef”, Bottesch et al. (2016), published in *Current Biology*. The following authors contributed to this work: Prof. Dr. Henrik Mouritsen (HM), Prof. Dr. Michael J. Kingsford (MK), Dr. Andreas Bally (AB), Maurits Halbach (MH), Prof. Dr. Gabriele Gerlach (GG) and Michael Bottesch (MB). HM, GG and MB planned and designed the experimental setup. MB, MH, GG and AB performed the experiments at the One Tree Island research station, Capricorn bunker reef group, Australia. MB, AB and MH measured the magnetic field values on a daily basis and set the appropriate coil adjustments for magnetic stimulation. MB and MH analyzed the videos for orientation behavior. GG, AB and MB performed the sun compass experiments during the day. MB did the statistical analysis of the orientation data. MB wrote the original manuscript, HM, GG, MK and MB revised and compressed the text to meet correspondence requirements.

In the project “Are retinal ganglion cells encoding the e-vector axis of linearly polarized light in birds?” the following coworkers contributed to the study: Prof. Dr. Henrik Mouritsen (HM), Dr. Nils-Lasse Schneider (NLS), Dr. David Dreyer (DD), Dr. Arndt Meyer (AM) and Michael Bottesch. HM, NLS and DD designed and planned the original experiments. DD and NLS built up the light stimulation. NLS compiled custom-written MatLab<sup>®</sup> scripts to execute and monitor the light stimulation and to statistically analyze and plot the recorded data for bimodal firing patterns in a fully automated protocol. NLS plotted the data compressed in the submitted manuscript figures. DD performed the experiments of the original study, in total 25000 units recorded. At the time of submission of the original manuscript, DD graduated and NLS left the university to quit his scientific career. I joined the project mainly for handling potential reviewers’ critique and conducting additional experiments to assure the validity of the data collected by DD and NLS. I was soon joined by AM, who boosted our progress by his fine skills in confocal imaging and his brilliant out-of-the-box way of thinking. MB and AM performed recordings and analysis of retinal preparations in the identical way as DD and NLS. MB and AM elaborated a set of post-recording controls for investigating the structural integrity of the retina and photoreceptor layer of the analyzed tissues. AM made fine intensity

measurements at the level of the multi-electrode array. MB changed specific parameters of the stimulation protocol by modifying the scripts of the original MatLab<sup>®</sup> routines. MB performed additional unsystematic experiments to test for low contrast sensitivity and potential effects that enhance the number of ganglion cells that bimodally respond to the turn of a polarizer in a single recording. AM and MB elaborated a sensory explanation for the so-called “paradox polarization response”.

The project “Seen in a different light – No evidence for polarization vision in songbirds in a novel behavioral approach”, the following coworkers contributed to the study: Prof. Dr. Henrik Mouritsen (HM), Dr. Friedrich Kretschmer (FK), Saskia Hinze (SH), Jens Lake (JL), Julia Forst (JF), Dmitry Kobylkov (DM) and Michael Bottesch (MB). MB and HM planned the study. MB designed and established the LCD monitor setup. MB pre-tested viable stimuli and chose the stimulation parameters to elicit optomotor responses (OMR) and escape behavior in three songbird species. FK provided the custom-written software to create a three-dimensional arena with four screens arranged in a square. FK also assisted in choosing the compatible components for well-buffered, high-resolution display of the moving grating cylinder across four screens. MB designed the controls to lowered luminance contrast. MB and HM elaborated the treatment sequence. MB, SH, JL and JF analyzed and quantified the optomotor responses to moving gratings. MB did the blinding and unblinding of raw data for independent, blinded evaluation. MB statistically analyzed the results, guided by the experience of DK. MB plotted the results. HM and MB discussed the main argument delivered by the results. MB wrote a manuscript that was revised by MB, DK and HM.



## 6. References

- Able, K.P. (1980). Mechanisms of orientation, navigation and homing. In: Gauthreaux, S.A. (ed.). *Animal migration, orientation and navigation*. Springer, Berlin. pp 283–373.
- Able, K.P. (1982). Skylight polarization patterns at dusk influence migratory orientation in birds. *Nature*, 299, 550–551.
- Able, K.P. (1989). Skylight polarization patterns and the orientation of migratory birds. *J. Exp. Bio.*, 141, 241–256.
- Able, K.P. (1991). Common Themes and Variations in Animal Orientation Systems. *Amer. Zool.*, 31, 157–167.
- Able, K.P., and Able, M.A. (1990a). Calibration of the magnetic compass of a migratory bird by celestial rotation. *Nature*, 347, 378–380.
- Able, K.P., and Able, M.A. (1990b). Ontogeny of migratory orientation in the Savannah sparrow, *Passerculus sandwichensis*: calibration of the magnetic compass. *Anim. Behav.*, 39, 905–913.
- Able, K.P., and Able, M.A. (1990c). Ontogeny of migratory orientation in the Savannah sparrow, *Passerculus sandwichensis*: mechanisms at sunset. *Anim. Behav.*, 39, 1189–1198.
- Able, K.P., and Able, M.A. (1993). Daytime calibration of magnetic orientation in a migratory bird requires a view of skylight polarization. *Nature*, 364, 523–525.
- Able, K.P., and Able, M.A. (1995a). Interactions in the flexible orientation system of a migratory bird. *Nature*, 375, 230–232.
- Able, K.P., and Able, M.A. (1995b). Manipulations of polarized skylight calibrate magnetic orientation in a migratory bird. *J. Comp. Physiol. A*, 177, 351–356.
- Able, K.P., and Able, M.A. (1996). The flexible migratory orientation system of the Savannah sparrow (*Passerculus sandwichensis*). *J. Exp. Biol.*, 199, 3–8.
- Able, K.P., and Able, M.A. (1997). Development of sunset orientation in a migratory bird: no calibration by the magnetic field. *Anim. Behav.*, 53, 363–368.
- Able, K.P., and Bingman, V.P. (1987). The development of orientation and navigation behavior in birds. *Q. Rev. Biol.*, 62, 1–29.
- Adler, H.E. (1963). Sensory factors in migration. *Anim. Behav.*, 11, 566–577.

- Åkesson, S. (2014). The Ecology of Polarisation Vision in Birds. In: Horváth, G. (ed.). *Polarized Light and Polarization Vision in Animal Sciences. Springer Heidelberg New York*. pp 275–292.
- Åkesson, S., and Bianco, G. (2017). Route simulations, compass mechanisms and long-distance migration flights in birds. *J. Comp. Physiol. A*, 203, 475–490.
- Åkesson, S., Morin, J., Muheim, R., and Ottosson, U. (2001). Avian orientation at steep angles of inclination: experiments with migratory white-crowned sparrows at the magnetic North Pole. *Proc. R. Soc. Lond. B Biol. Sci.*, 268, 1907–1913.
- Åkesson, S., Odin, C., Hegedüs, R., Ilieva, M., Sjöholm, C., et al. (2015). Testing avian compass calibration: comparative experiments with diurnal and nocturnal passerine migrants in South Sweden. *The Company of Biologists*, 4, 35–47.
- Alert, B., Michalik, A., Helduser, S., Mouritsen, H., and Güntürkün, O. (2015a). Perceptual Strategies of Pigeons to Detect a Rotational Centre – A Hint for Star Compass Learning?. *PLoS ONE*, 10, 3, e0119919.
- Alert, B., Michalik, A., Thiele, N., Bottesch, M., and Mouritsen, H. (2015b). Re-calibration of the magnetic compass in hand-raised European robins (*Erithacus rubecula*). *Scientific Reports*, 5, 14323.
- Atema, J. (1988). Distribution of chemical stimuli. In: Atema, J., Fay, R.R., Popper, A.N., and Tavolga, W.N. (eds.). *Sensory Biology of Aquatic Organisms*. Springer Berlin. pp 29–56.
- Batschelet, E. (1981). *Circular Statistics*. Biology, London: Academic Press, 371pp.
- Beck, W. (1984). The influence of the earth magnetic field to the migratory behavior of Pied Flycatchers (*Ficedula hypoleuca Pallas*). In: Varjú, D. and Schnitzler, H.-U. (eds.). *Localization and orientation in biology and engineering*. Springer Berlin. pp 357–359.
- Beck, W., and Wiltschko, W. (1988). Magnetic factors control the migratory direction of pied flycatchers (*Ficedula hypoleuca Pallas*). *Acta XIX Congress of International Ornithology*.
- Begon, M., Townsend, C.A., and Harper, J.L. (2005). *Ecology: From Individuals to Ecosystems*. Wiley-Blackwell, 4th Edition.
- Berenshtein, I., Kiflawi, M., Shashar, N., Wieler, U., Agiv, H., et al. (2014). Polarized Light Sensitivity and Orientation in Coral Reef Fish Post-Larvae. *PLoS One*, 9, 2, e88468.
- Berthold, P. (1991). Spatiotemporal programmes and genetics of orientation. In: Berthold, P. (ed.). *Orientation in Birds*. Birkhäuser Basel. pp. 86–105.
- Berthold, P. (2001). *Bird migration: a general survey*. Oxford University Press.

- Berthold, P., Helbig, A.J., Mohr, G. and Querner, U. (1992). Rapid microevolution of migratory behaviour in a wild bird species. *Nature*, 360, 668–670.
- Bingman, V.P. (1984). Night sky orientation of migratory pied flycatchers raised in different magnetic fields. *Behav. Ecol. Sociobiol.*, 15, 77–80.
- Bingman, V.P. (1987). Earth's magnetism and the nocturnal orientation of migratory European robins. *Auk*, 104, 523–525.
- Blaser, N., Guskov, S.I., Meskenaite, V., Kanevskiy, V.A., and Lipp, H.-P. (2013). Altered orientation and flight parts of pigeons reared on gravity anomalies: a GPS tracking study, *PLoS One*, 8, 10, e77102.
- Blaser, N., Guskov, S.I., Entin, V.A., Wolfer, D.P., Kanevskiy, V.A., et al. (2014). Gravity anomalies without geomagnetic disturbances interfere with pigeon homing – a GPS tracking study. *J. Exp. Biol.*, 217, 22, 4057–4067.
- Bolte, P., Bleibaum, F., Einwich, A., Günther, A., Liedvogel, M., et al. (2016). Localisation of the putative magnetoreceptor cryptochrome 1b in the retinae of migratory birds and homing pigeons. *PLoS One*, 11, e0147819.
- Bottesch, M., Gerlach, G., Halbach, M., Bally, A., Kingsford, M., and Mouritsen, H. (2016). A magnetic compass that might help coral reef fish larvae return to their natal reef. *Current Biology*, 26, 24 pR1266–R1267.
- Born, M., and Wolf, E. (1999). Principles of optics. *Cambridge University Press*, 7th Edition.
- Browman, H.I., Skiftesvik, A.B., and Kuhn, P. (2006). The relationship between ultraviolet and polarized light and growth rate in the early larval stages of turbot (*Scophthalmus maximus*), Atlantic cod (*Gadus morhua*) and Atlantic herring (*Clupea harengus*) reared in intensive culture conditions. *Aquaculture*, 256, 296–301.
- Brothers, J., and Lohmann, K. (2015). Evidence for Geomagnetic Imprinting and Magnetic Navigation in the Natal Homing of Sea Turtles. *Curr. Biol.*, 25, 3, 392–396.
- Brothers, E.B., Williams, D.M., and Sale P.F. (1983). Length of larval life in twelve families of fishes at “One Tree Lagoon”, Great Barrier Reef, Australia. *Mar. Biol.*, 76, 319–324.
- Burda, H., Marhold, S., Westenberger, T., Wiltschko, R., and Wiltschko, W. (1990). Magnetic compass orientation in the subterranean rodent, *Cryptomys hottentottus* (Bathyergidae). *Experientia*, 46, 528–530.
- Chen, Y., and Naito, J. (2009). Morphological Properties of Chick Retinal Ganglion Cells in relation to their central projections. *J. Comp. Neurol.*, 514, 117–130.

- Chernetsov, N. (2015). Avian compass systems: Do all migratory species possess all three? *J. Avian Biol.*, 46, 001–002.
- Chernetsov, N. (2016). Orientation and Navigation of Migrating Birds. *Biology Bulletin*, 43, 8, 788–803.
- Chernetsov, N., Kishkinev, D., Kosarev, V., and Bolshakov, C.V. (2011). Not all songbirds calibrate their magnetic compass from twilight cues: a telemetry study. *J. Exp. Biol.*, 214, 2540–2543.
- Chernetsov, N., Pakhomov, A., Davydov, A., Cellarius, F., and Mouritsen, H. (2020). No evidence for the use of magnetic declination for migratory navigation in two songbird species. *PLoS One*, 15, 4, e0232136.
- Chernetsov, N., Pakhomov, A., Kobylkov, D., Kishkinev, D., Holland, R. A., et al. (2017). Migratory Eurasian Reed Warblers Can Use Magnetic Declination to Solve the Longitude Problem. *Curr. Biol.*, 27, 17, 2647–2651.
- Chiou, T., Kleinlogel, S., Cronin, T., Caldwell, R., Loeffler, B. et al. (2008). Circular Polarization Vision in a Stomatopod Crustacean. *Curr. Biol.*, 18, 6, 429–434.
- Chiou, T., Place, A.R., Caldwell, R.L., Marshall, N.J., and Cronin, T.W. (2012). A novel function for a carotenoid: astaxanthin used as a polarizer for visual signalling in a mantis shrimp. *J. Exp. Biol.*, 215, 584–589.
- Cochran, W.W., Mouritsen, H., and Wikelski, M. (2004). Migrating Songbirds Recalibrate Their Magnetic Compass Daily from Twilight Cues. *Science*, 304, 5669, 405–408.
- Coemans, M.A.J.M., Vos Hzn, J.J., and Nuboer, J.F.W. (1990). No Evidence for Polarization Sensitivity in the Pigeon. *Naturwissenschaften*, 77, 138–142.
- Coemans, M.A.J.M., Vos Hzn, J.J., and Nuboer, J.F.W. (1994a). The Relation Between Celestial Colour Gradients and the Position of the Sun, with Regard to the Sun Compass. *Vis. Res.*, 34, pp 1461–1470.
- Coemans, M.A.J.M., Vos Hzn, J.J., and Nuboer, J.F.W. (1994b). The Orientation of the E-Vector of Linearly Polarized Light Does Not Affect the Behaviour of the Pigeon *Columba Livia*. *J. Exp. Biol.*, 191, 107–123.
- Cronin, T.W., Caldwell, R., and Marshall, J. (2001). Sensory adaptation: Tunable colour vision in a mantis shrimp. *Nature*, 411, 547–548.
- Cronin, T.W., and Marshall, J. (2011). Patterns and properties of polarized light in air and water. *Phil. Trans. R. Soc. B*, 366, 619–626.

- Cronin, T.W., Shashar, N., Caldwell, R., Marshall, J., Cheroske, A., et al. (2003). Polarization Vision and Its Role in Biological Signaling. *Integr. Comp. Biol.*, 43, 549–558.
- Dacke, M. (2014). Polarized light orientation in ball-rolling dung beetles. In: Horváth, G. (ed.). *Polarized Light and Polarization Vision in Animal Sciences*. Springer Heidelberg New York. pp 27–40.
- Darwin, C. (1871). The descent of man, and selection in relation to sex. 2nd Vol., *J. Murray, London*, 1st Edition. pp 423–475.
- Demaine, C., and Semm, P. (1985). The avian pineal as an independent magnetic sensor. *Neurosci. Lett.*, 2, 119–122.
- Delius, J.D., Perchard, R.J., and Emmerton, J. (1976). Polarized Light Discrimination by Pigeons and an Electroretinographic Correlate. *J. Comp. Physiol. Psy.*, 90, 6, 560–571.
- DeRosa, C., and Taylor, D.H. (1978). Sun-Compass Orientation in the Painted Turtle, *Chrysemys picta* (Reptilia, Testudines, Testudinidae). *J. Herpet.*, 12, 25–28.
- Deutschlander, M.E., Phillips, J.B., and Borland, S.C. (1999). The case for light-dependent magnetic orientation in animals. *J. Exp. Biol.*, 202, 891–908.
- Edelman, N.B., Fritz, T., Nimpf, S., Pichler, P., Lauwers, M., et al. (2015). No evidence for intracellular magnetite in putative vertebrate magnetoreceptors identified by magnetic screening. *PNAS*, 112, 1, 262–267.
- Emlen, S.T. (1967a). Migratory orientation in the indigo bunting, *Passerina cyanea*: Part I: Evidence for use of celestial cues. *Auk*, 84, 309–342.
- Emlen, S.T. (1967b). Migratory orientation in the indigo bunting, *Passerina cyanea*: Part II: Mechanism of celestial orientation. *Auk*, 84, 463–489.
- Emlen, S.T. (1969). The development of migratory orientation in young indigo buntings. *Living Bird*, 8, 113–126.
- Emlen, S.T. (1970). Celestial rotation: its importance in the development of migratory orientation. *Science*, 170, 1198–1201.
- Emlen, S.T. (1972). The ontogenetic development of orientation capabilities. In: Galler, S.R. (ed.). *Animal orientation and navigation*. Washington. pp 191–210.
- Emlen, S.T. (1975). The stellar-orientation system of migratory bird. *Sci. Am.*, 233, 102–111.
- Engels, S., Schneider, N.-L., Lefeldt, N., Hein, C.M., Zapka, M., et al. (2014). Anthropogenic electromagnetic noise disrupts magnetic compass orientation in a migratory bird. *Nature*, 509, 353–356.

- Ferguson, D.E. (1971). The sensory basis of orientation in amphibians. *Ann. New York Acad. Sci.*, 188, 30–36.
- Ferguson, D.E., and Landreth, H.F. (1966). Celestial orientation of Fowler's toad, *Bufo fowleri*. *Behaviour*, 26, 105–123.
- Ferguson, D.E., McKeown, J.P., Bosarge, O.S., and Landreth, H.F. (1968). Sun-Compass Orientation of Bullfrogs. *Copeia*, 2, 230.
- Fisher, R., Bellwood, D.R., and Job, S.D. (2000). Development of swimming abilities in reef fish larvae. *Mar. Ecol. Prog. Ser.*, 202, 163–173.
- Fisher, R., and Leis, J.M. (2009). Swimming performance in larval fishes: from escaping predators to the potential for long distance migration. In: Domenici, P., and Kapoor, B.G. (eds.). *Fish locomotion: an etho-ecological approach. Science Publishers Enfield*. pp 333–73.
- Fluharty, S.L., Taylor, D.H., and Barrett, W.G. (1976). Sun-Compass Orientation in the Meadow Vole, *Microtus pennsylvanicus*. *J. Mammal.*, 57.
- Fleissner, G., Holtkamp-Rotzler, E., Hanzlik, M., Winklhofer, M., Fleissner, G., et al. (2003). Ultrastructural analysis of a putative magnetoreceptor in the beak of homing pigeons. *J. Comp. Neurol.*, 458, 350–360.
- Foster, J., Temple, E.S., How, M., Daly, I., Sharkey, C., et al. (2018). Polarisation vision: overcoming challenges of working with a property of light we barely see. *The Science of Nature*, 105, 27.
- Förschler, M., del Val, E., and Bairlein, F. (2010). Extraordinary high natal philopatry in a migratory passerine. *J. Ornithol.*, 151, 745–748.
- Fromme, H.G. (1961). Untersuchungen über das Orientierungsvermögen nächtlich ziehender Kleinvögel (*Erithacus rubecula*, *Sylvia communis*). *Ethology*, 18, 2, 205–220.
- Gagliardo, A. (2013). Forty years of olfactory navigation in birds. *J. Exp. Biol.*, 216, 2165–2171.
- Gagliardo, A., Ioalè, P., Savini, M., and Wild, J.M. (2006). Having the nerve to home: trigeminal magnetoreceptor versus olfactory mediation of homing in pigeons, *J. Exp. Biol.*, 209, 15, 2888–2892.
- Gegenfurtner, K.R., and Kiper, D.C. (2003). Color vision. *Annual Review of Neuroscience*, 26, 1, 181–206.
- Gerlach, G., Atema, J., Kingsford, M.J., Black, K.P., and Miller-Sims, V. (2007). Smelling home can prevent dispersal of reef fish larvae. *PNAS*, 104, 3, 858–863.

- Gill, R.E., Douglas, D.C., Handel, C.M., Tibbitts, T.L., Hufford, G., et al. (2014). Hemispheric-scale wind selection facilitates bar-tailed godwit circum-migration of the Pacific. *Animal Behaviour*, 90, 117–130.
- Glantz, R.M., and Schroeter, J.P. (2006). Polarization contrast and motion detection. *J. Comp. Physiol. A*, 192, 905–914.
- Goodyear, C.P., and Ferguson, D.E. (1969). Sun-compass orientation in mosquitofish, *Gambusia affinis*. *Animal Behavior*, 17, 636–640.
- Gould, J. (2008). Animal Navigation: The Evolution of Magnetic Orientation. *Curr. Biol.*, 18, 11, 482–484.
- Greenwood, P.J. (1980). Mating systems, philopatry and dispersal in birds and mammals. *Animal Behaviour*, 28, 4, 1140–1162.
- Greenwood, P.J., and Harvey, P.H. (1982). The natal and breeding dispersal of birds. *Annu. Rev. Ecol. Syst.*, 13, 1–21.
- Gudmundsson, G.A., and Alerstam, T. (1998). Optimal map projections for analysing long-distance migration routes. *J Avian Biol*, 29, 597–605
- Greenwood, V.J., Smith, E.L., Church, S.C., and Partridge, J.C. (2003). Behavioural investigation of polarisation sensitivity in the Japanese quail (*Coturnix coturnix japonica*) and the European starling (*Sturnus vulgaris*). *J. Exp. Biol.*, 206, 18, 3201–3210.
- Griffin, D.R. (1952). Bird navigation. *Biol. Rev.*, 27, 359–390.
- Grimes, C.B., and Kingsford, M.J. (1996). How do riverine plumes of different sizes influence fish larvae: Do they enhance recruitment? *Mar. Freshwat. Res.*, 47, 191–208.
- Guillory, K.S., and Normann, R.A. (1999). A 100-channel system for real time detection and storage of extracellular spike waveforms. *J. Neurosci. Methods.*, 91, 21–29.
- Giunchi, D., Vanni, L., Baldaccini, N. E., Spina, F., and Biondi, F. (2015). New cue-conflict experiments suggest a leading role of visual cues in the migratory orientation of Pied Flycatchers *Ficedula hypoleuca*. *J. Ornithol.*, 156, 1, 113–121.
- Günther, A., Einwich, A., Sjulstok, E., Feederle, R., Bolte, P., et al. (2018). Double-Cone Localization and Seasonal Expression Pattern Suggest a Role in Magnetoreception for European Robin Cryptochrome 4. *Curr. Biol.*, 28,2, 211–223.
- Gwinner, E. (1996). Circadian and circannual programmes in avian migration. *J. Exp. Biol.*, 199, 39–48.

- Hagstrum, J.T., (2000). Infrasound and the avian navigational map, *J. Exp. Biol.*, 203, 7, 1103–1111.
- Hagstrum, J.T. (2001). Infrasound and the avian navigational map, *J. Navigat.*, 54, 3, 377–391.
- Hagstrum, J.T. (2013). Atmospheric propagation modeling indicates homing pigeons use loft-specific infrasonic ‘map’ cues, *J. Exp. Biol.*, 216, 4, 687–699.
- Hawryshyn, C.W. (2010). Ultraviolet polarization vision and visually guided behavior in fishes. *Brain Behav. Evol.*, 75, 186–194.
- Heinze, S. (2014). Polarized-Light Processing in Insect Brains: Recent Insights from the Desert Locust, the Monarch Butterfly, the Cricket, and the Fruit Fly. In: Horváth, G. (ed.). *Polarized Light and Polarization Vision in Animal Sciences*. Springer Heidelberg New York. pp. 61–112.
- Helbig, A. (1990). Depolarization of natural skylight disrupts orientation of an avian nocturnal migrant. *Experientia*, 46, 755–758.
- Helbig, A. (1991). Dusk orientation of migratory European robins, *Erithacus rubecula*: the role of sun-related directional information. *Anita. Behav.*, 41, 313–322.
- Helbig, A.J. (1996). Genetic basis, mode of inheritance and evolutionary changes of migratory directions in palaeartic warblers (Aves: Sylviidae). *J. Exp. Biol.*, 199, 49–55.
- Helbig, A.J., and Wiltschko, W. (1989). The Skylight Polarization Patterns at Dusk Affect the Orientation Behavior of Blackcaps, *Sylvia atricapilla*. *Naturwissenschaften*, 76, 227–229.
- Hein, C.M., Zapka, M., Heyers, D., Kutschbauch, S., Schneider, N.L. and Mouritsen, H. (2010). Night-migratory garden warblers can orient with their magnetic compass using the left, the right or both eyes. *J R Soc Interface*, 7, Suppl 2, S227-33.
- Hein, C.M., Engels, S., Kishkinev, D. and Mouritsen, H. (2011). Robins have a magnetic compass in both eyes. *Nature*, 471, 7340, E11–2, E12–3.
- Heyers, D., Elbers, D., Bulte, M., Bairlein, F., and Mouritsen, H. (2017). The magnetic map sense and its use in fine-tuning the migration programme of birds. *J. Comp. Physiol. A*, 203, 491–497.
- Heyers, D., Manns, M., Luksch, H., Güntükün, O., and Mouritsen, H. (2007). A Visual Pathway Links Brain Structures Active during Magnetic Compass Orientation in Migratory Birds. *PLoS One*, 9, e937.



- Heyers, D., Zapka, M., Hoffmeister, M., Wild, M.J., and Mouritsen, H. (2010). Magnetic field changes activate the trigeminal brainstem complex in a migratory bird. *PNAS*, 107, 20, 9394–9399.
- Hiscock, H.G., Mouritsen, H., Manolopoulos, D.E., and Hore, P.J. (2017). Disruption of magnetic compass orientation in migratory birds by radiofrequency electromagnetic fields. *Biophys. J*, 113, 1475–1484.
- Hodson, R.B. (2000). Magnetoreception in the short-tailed stingray, *Dasyatis brevicaudata* (Doctoral dissertation, *ResearchSpace@ Auckland*).
- Hoffmann, K. (1953). Die Einrechnung der Sonnenwanderung bei der Richtungsweisung des sonnenlos aufgezogenen Stares. *Naturwissenschaften*, 40, 4, 148–148.
- Holland, R.A. (2014). True navigation in birds: from quantum physics to global migration. *J. Zool.*, 293, 1, 1–15.
- Holland, R., Thorup, K., Vonhoff, M., Cochran, W., and Wikelski, M. (2006). Bat orientation using Earth's magnetic field. *Nature*, 444, 702.
- Hore, P.J., and Mouritsen, H. (2016). The Radical-Pair Mechanism of Magnetoreception. *Annu. Rev. Biophys.*, 45, 299–344.
- Horváth, G. (2014). Polarization Patterns of Freshwater Bodies with Biological Implications. In: Horváth, G. (ed.). *Polarized Light and Polarization Vision in Animal Sciences*. Springer Heidelberg New York. pp 333–344.
- Horváth, G., and Csabai, Z. (2014). Polarization Vision of Aquatic Insects. In: Horváth, G. (ed.). *Polarized Light and Polarization Vision in Animal Sciences*. Springer Heidelberg New York. pp 113–146.
- Horváth, G., and Hegedüs, R. (2014). Polarization Characteristics of Forest Canopies with Biological Implications. In: Horváth, G. (ed.). *Polarized Light and Polarization Vision in Animal Sciences*. Springer Heidelberg New York. pp 345–366.
- Horváth, G. & Varjú, D. (2004). *Polarized Light in Animal Vision: Polarization Patterns in Nature*. Springer Heidelberg New York.
- How, M.J., Porter, M.L., Radford, A.N., Feller, K.D., Temple, S.E., et al. (2014). Out of the blue: the evolution of horizontally polarized signals in Haptosquilla (Crustacea, Stomatopoda, Protosquillidae). *J. Exp. Biol.*, 217, 3425–3431.

- Hunt, D.M., Carvalho, L.S., Cowing, J.A., & Davies, W.L. (2009). Evolution and spectral tuning of visual pigments in birds and mammals. *Phil. Trans. R. Soc. B: Biol. Sci.*, 364, 2941–2955.
- Imboden, C., Imboden, D. (1972). Formel für Orthodrome und Loxodrome bei der Berechnung von Richtung und Distanz zwischen Beringungs- und Wiederfundort. *Vogelwarte*, 26, 336–346.
- Jones, G.P., Almany, G.R., Russ, G.R., Sale, P.F., Steneck, R.S., et al. (2009). Larval retention and connectivity among populations of corals and reef fishes: History, advances and challenges. *Coral Reefs*, 28, 2, 307–325.
- Jordan, T.M., Partridge, J.C., & Roberts, N.W. (2012). Non-polarizing broadband multilayer reflectors in fish. *Nat. Photonics*, 6, 759–763.
- Kalmijn, A. J. (1981). Biophysics of Geomagnetic Field Detection. *IEEE Transactions on Magnetism*, 17, 1, 1113–1124.
- Kaufman, L., Ebersole, J., Beets, J., & McIvor, C.C. (1992). A key phase in the recruitment dynamics of coral reef fishes: post-settlement transition. *Environ. Biol. Fishes*, 34, 109–118.
- Kingsford, M.J. (2001). Diel patterns of arrival of reef fish to a coral reef: One Tree Island, Great Barrier Reef. *Marine Biology*, 138, 853–868.
- Kingsford, M., Leis, J., Shanks, A., Lindeman, C.K., Morgan, S., et al. (2002). Sensory environments, larval abilities and local self-recruitment. *Bulletin of Marine Science*, 70, S1, 309–340.
- Kishkinev, D., Chernetsov, N., Heyers, D., & Mouritsen, H. (2013). Migratory Reed Warblers Need Intact Trigeminal Nerves to Correct for a 1,000 km Eastward Displacement. *PLoS One*, 8, 6, e65847.
- Kirschvink, J.L., Walker, M.M., & Diebel, C.E. (2001). Magnetite-based magnetoreception. *Curr. Opinion Neurobiol.*, 11, 462–467.
- Kobytkov, D., Schwarze, S., Michalik, B., Winklhofer, M., Mouritsen, H., & Heyers, D. (2020). A newly identified trigeminal brain pathway in a night-migratory bird could be dedicated to transmitting magnetic map information. *Proc. R. Soc. B.*, 287, 20192788.
- Kobytkov, D., Wynn, J., Winklhofer, M., Chetverikova, R., Xu, J., et al. (2019). Electromagnetic 0.1–100 kHz noise does not disrupt orientation in a night-migrating songbird implying a spin coherence lifetime of less than 10  $\mu$ s. *J R Soc Interface*, 16, 161, 20190716.

- Komolkin, A.V., Kupriyanov, P., Chudin, A., Bojarinova, J., Kavokin, K., et al. (2017). Theoretically possible spatial accuracy of geomagnetic maps used by migrating animals. *J. R. Soc. Interface*, 14, 20161002.
- Konôpková, Z., McWilliams, R.S., Gómez-Pérez, N., & Goncharov, A.F. (2016). Direct measurement of thermal conductivity in solid iron at planetary core conditions. *Nature*, 534, 99–101.
- Kavokin, K., Chernetsov, N., Pakhomov, A., Bojarinova, J., Kobylkov, D., & Namozov, B. (2014). Magnetic orientation of garden warblers (*Sylvia borin*) under 1.4 MHz radiofrequency magnetic field. *J. R. Soc. Interface*, 11, 20140451.
- Kram, Y.A., Mantey, S., & Corbo, J.C. (2010). Avian Cone Photoreceptors Tile the Retina as Five Independent, Self-Organizing Mosaics. *PLoS One*, 5, 2, e8992.
- Kramer, G. (1949). Über Richtungstendenzen bei der nächtlichen Zugunruhe gekäfigter Vögel. In: Mayr, E., & Stresemann, E. (eds.). Ornithologie als biologische Wissenschaft. *Carl Winter Universitätsverlag Heidelberg*.
- Kramer, G. (1950). Orientierte Zugaktivität gekäfigter Singvögel. *Naturwissenschaften*, 37, 8, 188.
- Kramer, G. (1952). Experiments on bird orientation. *Ibis*, 94, 2, 265–285.
- Kramer, G. (1953). Wird die Sonnenhöhe bei der Heimfindeorientierung verwertet? *J. Ornithol.*, 94, 201–219.
- Kramer, G. (1957). Experiments on bird orientation and their interpretation. *Ibis*, 99, 196–227.
- Krenz, J.D. (2018). Use of sun compass orientation during natal dispersal in Blanding's turtles: in situ field experiments with clock-shifting and disruption of magnetoreception. *Behav. Ecol. Sociobiol.*, 72, 177.
- Kreithen, M.L., & Keeton, W.T. (1974). Detection of Polarized Light by the Homing Pigeon, *Columba livia*. *J. Comp. Physiol.*, 89, 83–92.
- Kretschmer, F., Kretschmer, V., Kunze, V.P., & Kretzberg, J. (2013). OMR-Arena: Automated Measurement and Stimulation System to Determine Mouse Visual Thresholds Based on Optomotor Responses, *PLoS One*, 8, 11, e78058.
- Kroeger, K., Pflieger, K.D.G., & Eidne, K.A. (2003) G-protein-coupled receptor oligomerization in neuroendocrine pathways. *Front. Neuroendocrinol.*, 24, 254–278.
- Labhart, T. (2016). Can invertebrates see the e-vector of polarization as a separate modality of light? *J. Exp. Biol.*, 219, 3844–3856.

- Larkin, T., & Keeton, W.T. (1978). An apparent lunar rhythm in the day-to-day variations in initial bearings of homing pigeons. In: Schmidt-Koenig, K., & Keeton, W.T. (eds.). *Animal Migration, Navigation and Homing*. Springer Berlin. pp 92–106.
- Lauwers, M., Pichler, P., Edelman, N.B., Resch, G.P., Ushakova, L., et al. (2013). An Iron-Rich Organelle in the Cuticular Plate of Avian Hair Cells. *Curr. Biol.*, 23, 924–929.
- Lefeldt, N., Dreyer, D., Steenken, F., Schneider, N.-L., & Mouritsen, H. (2014). Migratory blackcaps tested in Emlen funnels can orient at 85 but not at 88 degrees magnetic inclination. *J. Exp. Biol.*, 218, 206–211.
- Leis, J.M., and Carson-Ewart, B.M. (2003). Orientation of pelagic larvae of coral-reef fishes in the ocean. *Mar. Ecol. Prog. Ser.*, 252, 239–53.
- Leis, J.M., Siebeck, U., & Dixson, D. (2011). How Nemo Finds Home: The Neuroecology of Dispersal and of Population Connectivity in Larvae of Marine Fishes. *Integr. Comp. Biol.*, 51, 5, 826–843.
- Leis, J.M., Siebeck, U.E., Hay, A.C., Paris, C.B., Chateau, O., et al. (2015). In situ orientation of fish larvae can vary among regions. *Mar. Ecol. Prog. Ser.*, 537, 191–203.
- Leis, J.M., Wright, K.J., & Johnson, R.N. (2007). Behaviour that influences dispersal and connectivity in the small, young larvae a reef fish. *Mar. Biol.*, 153, 103–117.
- Liedvogel, M., Maeda, K., Henbest, K., Schleicher, E., Simon, T., et al. (2007). Chemical magnetoreception: bird cryptochrome 1a is excited by blue light and forms long-lived radical-pairs. *PLoS ONE*, 2, e1106.
- Liem, K.F., & Walker, W.F. (2001). *Functional anatomy of the vertebrates: An evolutionary perspective*. Fort Worth: Harcourt College Publishers.
- Lin, S., Yemelyanov, K.M. (2006). Separation and contrast enhancement of overlapping cast shadow components using polarization. *Opt. Express*, 14, 7099–7107.
- Liu, X. & Chernetsov, N. (2012). Avian orientation: multi-cue integration and calibration of compass systems. *Chinese Birds*, 3, 1–8.
- Lohmann, K. (1991). Magnetic orientation by hatchling loggerhead sea turtles (*Caretta caretta*). *J. Exp. Biol.*, 155, 37–49.
- Lohmann, K.J., Hester, J.T. & Lohmann, C.M.F. (1999). Long-distance navigation in sea turtles. *Ethol. Ecol. Evol.*, 11, 1–23.
- Lohmann, K.J., & Lohmann, C.M.F. (1993). A Light-Independent Magnetic Compass in the Leatherback Sea Turtle. *Biol. Bull.*, 185, 149–151.

- Lohmann, K.J., Lohmann, C.M.F., Ehrhart, L.M., Bagley, D.A. & Swing, T. (2004). Geomagnetic map used in sea-turtle navigation. *Nature*, 428, 909–910.
- Lohmann, K.J., Lohmann, C.M.F., & Putman, N.F. (2007). Magnetic maps in animals: nature's GPS. *J. Exp. Biol.*, 210, 3697–3705.
- Marshall, J. & Cronin, T. (2014). Polarization Vision of Crustaceans, In: Horváth, G. (ed.). Polarized Light and Polarization Vision in Animal Sciences. *Springer Heidelberg New York*. pp 171–216.
- Marshall, J., Cronin, T.W., & Kleinlogel, S. (2007). Stomatopod eye structure and function: A review. *Arthropod Structure & Development*, 36, 4, 420–448.
- Masland, R.H. (2001). The fundamental plan of the retina. *Nature Neuroscience*, 4, 9, 877–886.
- Melgar, J., Lind, O., & Muheim, R. (2015). No response to linear polarization cues in operant conditioning experiments with zebra finches. *J. Exp. Biol.*, 218, 13, 2049–2054.
- Merkel, F.W. & Fromme, H.G. (1958). Untersuchungen über das Orientierungsvermögen nächtlich ziehender Rotkehlchen (*Erithacus rubecula*). *Naturwissenschaften*, 45, 499–500.
- Meyer-Rochow, V.B. (2014a). Polarization Sensitivity in Amphibians. In: Horváth, G. (ed.). Polarized Light and Polarization Vision in Animal Sciences. *Springer Heidelberg New York*. pp 249–264.
- Meyer-Rochow, V.B. (2014b). Polarization Sensitivity in Reptiles. In: Horváth, G. (ed.). Polarized Light and Polarization Vision in Animal Sciences. *Springer Heidelberg New York*. pp 265–274.
- Michalik, A., Alert, B., Engels, S., Lefeldt, N., & Mouritsen, H. (2013). Star compass learning: how long does it take? *J. Ornithol.*, 155, 1, 225–234.
- Molteno, T.C.A., & Kennedy, W.L. (2009). Navigation by Induction-Based Magnetoreception in Elasmobranch Fishes. *J. Biophys. (Hindawi Publishing Corporation: Online)*, 2009, 380976.
- Montgomery, K.C., & Heinemann, E.G. (1952). Concerning the Ability of Homing Pigeons to Discriminate Patterns of Polarized Light. *Science*, 116, 454–457.
- Moore, F. (1978). Sunset and the orientation of a nocturnal migrant bird. *Nature*, 274, 154–156.
- Moore, F.R. (1986). Sunrise, Skylight Polarization, and the Early Morning Orientation of Night-Migrating Warblers. *Condor*, 88, 493–498.

- Moore, F.R., & Phillips, J.B. (1988). Sunset, skylight polarization and the migratory orientation of yellow-rumped warblers, *Dendroica coronata*. *Animal Behaviour*, 36, 6, 1770–1778.
- Mouritsen, H. (1998). Modelling migration: the clock-and-compass model can explain the distribution of ringing recoveries. *Animal Behaviour*, 56, 899–907.
- Mouritsen, H. (2015). Magnetoreception in birds and its use for long-distance migration. In: Scanes, C.G. (ed.). *Sturkie's Avian Physiology*. Amsterdam: Elsevier Academic Press. pp 113–133.
- Mouritsen, H. (2018). Long-distance navigation and magnetoreception in migratory animals. *Nature*, 558, 50–59.
- Mouritsen, H., Atema, J., Kingsford, M.J., and Gerlach, G. (2013). Sun Compass Orientation Helps Coral Reef Fish Larvae Return to Their Natal Reef. *PLoS One*, 8, 6, e66039.
- Mouritsen, H., Derbyshire, R., Stalleicken, J., Mouritsen, O.O., Frost, B.J., et al. (2013b). An experimental displacement and over 50 years of tag-recoveries show that monarch butterflies are not true navigators. *Proc Nat Acad Sci USA*, 110, 7348-7353.
- Mouritsen, H., Heyers, D., & Güntürkün, O. (2016). The neural basis of long-distance navigation in birds. *Annu. Rev. Physiol.*, 78, 133–54.
- Mouritsen, H., & Hore, P.J. (2012). The magnetic retina: light-dependent and trigeminal magnetoreception in migratory birds. *Curr. Neurobiol.*, 22, 343–352.
- Mouritsen, H., Janssen-Bienhold, U., Liedvogel, M., Feenders, G., Stalleicken, J., et al. (2004). Cryptochromes and neuronal-activity markers colocalize in the retina of migratory birds during magnetic orientation. *Proc. Natl Acad. Sci. USA*, 101, 14, 294–299.
- Mouritsen, H., & Larsen, O.N. (2002). Migrating songbirds tested in computer-controlled Emlen funnels use stellar cues for a time-independent compass. *J. Exp. Biol.*, 204, 3855–3865.
- Muheim, R. (2011). Behavioural and physiological mechanisms of polarized light sensitivity in birds. *Phil. Trans. R. Soc. B*, 366, 763–771.
- Muheim, R., Åkesson, S. and Alerstam, T. (2003). Compass orientation and possible migration routes of passerine birds at high Arctic latitudes. *Oikos*, 103, 341–349.
- Muheim, R., Moore, F.R., & Phillips, J.B. (2006). Calibration of magnetic and celestial compass cues in migratory birds – a review of cue-conflict experiments. *J. Exp. Biol.*, 209, 2–17.

- Muheim, R., Phillips, J.B., & Deutschlander, M.E. (2009). White-throated sparrows calibrate their magnetic compass by polarized light cues during both autumn and spring migration. *J. Exp. Biol.*, 212, 3466–3472.
- Muheim, R., Sjöberg, S., & Pinzon-Rodriguez, A. (2016). Polarized light modulates light-dependent magnetic compass orientation in birds. *PNAS*, 113, 6, 1654–1659.
- Muheim, R., Akkesson, S., & Phillips, J.B. (2007). Magnetic compass of migratory Savannah sparrows is calibrated by skylight polarization at sunrise and sunset. *J. Ornithol.*, 148, 485–494.
- Munro, U., & Wiltschko, R. (1995). The role of skylight polarization in the orientation of a day-migrating bird species. *J. Comp. Phys. A*, 177, 357–362.
- Mussi, M., Haimberger, T.J. & Hawryshyn, C.W. (2005). Behavioural discrimination of polarized light in the damselfish *Chromis viridis* (family Pomacentridae). *J. Exp. Biol.*, 208, 3037–3046.
- Myklatun, A., Lauri, A., Eder, S.H.K., Cappetta, M., Shcherbakov, D., et al. (2018). Zebrafish and medaka offer insights into the neurobehavioral correlates of vertebrate magnetoreception. *Nature Communications*. 9, 802.
- Naisbett-Jones, L.C., Putman, N.F., Scanlan, M.M., Noakes, D.L.G., and Lohmann, K.J. (2020). Magnetoreception in Fishes: The Effect of Magnetic Pulses on Orientation of Juvenile Pacific Salmon. *J. Exp. Biol.*, 18, 223, 10, jeb222091.
- Nedergaard, M., Cooper, A.J., & Goldman, S.A. (1995). Gap Junctions Are Required for the Propagation of Spreading Depression. *J. Neurobiol.*, 28, 4, 433–444.
- Newton, I. (2008). *The Migration Ecology of Birds*. Academic Press, Elsevier, London.
- Niessner, C., Denzau, S., Gross, J.C., Peichl, L., Bischof, H.J., et al. (2011). Avian ultraviolet/violet cones identified as probable magnetoreceptors. *PLoS ONE*, 6, e20091.
- Niessner, C., Gross, J.C., Denzau, S., Peichl, L., Fleissner, G., et al. (2016). Seasonally changing cryptochrome 1b expression in the retinal ganglion cells of a migrating passerine bird. *PLoS One*, 11, e0150377.
- Novales Flamarique, I., & Hárosi, F.I. (2002). Visual pigments and dichroism of anchovy cones: a model system for polarization detection. *Visual Neuroscience*, 19, 4, 467–73.
- Novales Flamarique, I., Hawryshyn, C.W., and Hárosi, F.I. (1998). Double-cone internal reflection as a basis for polarization detection in fish. *J. Opt. Soc. Am. A*, 15, 349–358.

- O'Connor, J., and Muheim, R. (2017). Pre-settlement coral-reef fish larvae respond to magnetic field changes during the day. *J. Exp. Biol.*, 220, 2874-2877.
- O'Neill, P. (2013). Magnetoreception and baroreception in birds. *Dev. Growth Diff*, 55, 188–197.
- Pakhomov, A., Anashina, A., & Chernetsov, N. (2017). Further evidence of a time-independent stellar compass in a night-migrating songbird. *Behav. Ecol. Sociobiol.*, 71, 48.
- Pakhomov, A., Anashina, A., Heyers, D., & Kobylkov, D. (2018). Magnetic map navigation in a migratory songbird requires trigeminal input. *Sci. Rep.*, 8, 11975.
- Pakhomov, A., Bojarinova, J., Cherbunin, R., Chetverikova, R., Grigoryev, P.S. et al. (2017). Very weak oscillating magnetic field disrupts the magnetic compass of songbird migrants. *J. R. Soc. Interface*, 14, 20170364.
- Papi, F., Fiore, L., Fiaschi, V., and Benvenuti, S. (1971). The influence of olfactory nerve section on the homing capacity of carrier pigeons. *Monitore Zoologico Italiano N.S.*, 5, 265–267.
- Papi, F., Fiore, L., Fiaschi, V., and Benvenuti, S. (1972). Olfaction and homing in pigeons, *Monitore Zoologico Italiano N.S.*, 6, 85–95.
- Paris, C.B., & Cowen, R.K. (2004). Direct evidence of a biophysical retention mechanism for coral reef fish larvae. *Limnol. Oceanogr.*, 49, 6, 1964–1979.
- Paulin, M.G. (1995). Electroreception and the compass sense of sharks. *J. Theor. Biol.*, 174, 325–339.
- Pennycuik, C.J. (1960). The physical basis of astro-navigation in birds: theoretical considerations. *J. Exp. Biol.*, 37, 573–593.
- Perdeck, A.C. (1958). Two types of orientation in migrating starlings, *Sturnus vulgaris L.*, and chaffinches, *Fringilla coelebs L.*, as revealed by displacement experiments. *ARDEA*, 1, 2.
- Phillips, J.B., & Borland, S.C. (1992a). Behavioural evidence for use of a light-dependent magnetoreception mechanism by a vertebrate. *Nature*, 359, 142–144.
- Phillips, J.B. and Borland, S.C. (1992b). Magnetic compass orientation is eliminated under near-infrared light in the eastern red-spotted newt *Notophthalmus viridescens*. *Anim. Behav.*, 44, 796–797.
- Pignatelli, V., Temple, S.E., Chiou, T., Roberts, N.W., Collin, S.P., et al. (2011). Behavioural relevance of polarization sensitivity as a target detection mechanism in cephalopods and fishes. *Phil. Trans. R. Soc. B*, 366, 734–741.



- Pritchard, D.J., Scott, R.D., Healy, S.D., & Hurly, A.T. (2016). Wild rufous hummingbirds use local landmarks to return to rewarded locations. *Behav. Proc.*, 122, 59–66.
- Putman, N.F., Endres, C.S., Lohmann, C.M.F., and Lohmann, K.J. (2011). Longitude Perception and Bicoordinate Magnetic Maps in Sea Turtles. *Curr. Biol.*, 21, 463–466.
- Putman, N.F., Lohmann, K.J., Putman, E.M., Quinn, T.P., Klimley, A.P., et al. (2013). Evidence for Geomagnetic Imprinting as a Homing Mechanism in Pacific Salmon. *Curr. Biol.*, 23, 4, 312–316.
- Putman, N.F., Scanlan, M.M., Billman, E.J., O’Neil, J.P., Couture, R.B. et al. (2014). An Inherited Magnetic Map Guides Ocean Navigation in Juvenile Pacific Salmon. *Curr. Biol.*, 24, 446–450.
- Putman, N.F., Verley, P., Endres, C.S., & Lohmann, K.J. (2015). Magnetic navigation behavior and the oceanic ecology of young loggerhead sea turtles. *J. Exp. Biol.*, 218, 1044–1050.
- Putman, N.F., Williams, C.R., Gallagher, E.P., and Dittman, A.H. (2020). A sense of place: pink salmon use a magnetic map for orientation. *J Exp Biol.*, 223, 4, jeb218735.
- Quinn, T.P. (1980). Evidence for Celestial and Magnetic Compass Orientation in Lake Migrating Sockeye Salmon Fry. *J. Comp. Physiol*, 137, 243–248.
- Rajchard, J. (2009). Ultraviolet (UV) light perception by birds: a review. *Veterinarni Medicina*, 54, 8, 351–359.
- Ramsden, S.D., Anderson, L., Mussi, M., Kamermans, M., & Hawryshyn, C.W. (2008). Retinal processing and opponent mechanisms mediating ultraviolet polarization sensitivity in rainbow trout (*Oncorhynchus mykiss*). *J. Exp. Biol.*, 211, 1376–1385.
- Ritz, T., Adem, S., & Schulten, K. (2000). A model for photoreceptor-based magnetoreception in birds. *J. Biophys.*, 78, 707–718.
- Ritz, T., Ahmad, M., Mouritsen, H., Wiltschko, R., & Wiltschko, W. (2010). Photoreceptor-based magnetoreception: optimal design of receptor molecules, cells, and neuronal processing. *J. R. Soc. Interface*, 7, S135–146.
- Ritz, T., Thalau, P., Phillips, J.B., Wiltschko, R., & Wiltschko, W. (2004). Resonance effects indicate a radical-pair mechanism for avian magnetic compass. *Nature*, 429, 177–80.
- Ritz, T., Wiltschko, R., Hore, P.J., Rodgers, C.T., Stapput, K., et al. (2009). Magnetic compass of birds is based on a molecule with optimal directional sensitivity. *Biophys. J*, 96, 3451–3457.

- Roberts, N.W. (2014). Polarisation Vision of Fishes. In: Horváth, G. (ed.). Polarized Light and Polarization Vision in Animal Sciences. *Springer Heidelberg New York*. pp 225–248.
- Roberts, N.W., Gleeson, H.F., Temple, S.E., Haimberger, T.J., & Hawryshyn, C.W. (2004). Differences in the optical properties of vertebrate photoreceptor classes leading to axial polarization sensitivity. *J. Opt. Soc. Am. A*, 21, 335–345.
- Roberts, N.W., & Needham, M.G. (2007). A mechanism of polarized light sensitivity in cone photoreceptors of the goldfish *Carassius auratus*. *J. Biophys.*, 93, 3241–3248.
- Sandberg, R. (1991). Sunset orientation of robins, *Erithacus rubecula*, with different fields of sky vision. *Behav Ecol Sociobiol*, 28, 77–83.
- Sanes, J.R., & Masland, R.H. (2015). The Types of Retinal Ganglion Cells : Current Status and Implications for Neuronal Classification. *Annu. Rev. Neurosci.*, 38, 221–246.
- Sauer, E.G.F. (1957). Astronavigatorische Orientierung einer unter künstlichem Sternenhimmel verfrachteten Klappergrasmücke, *Sylvia c. curruca* (L.). *Naturwissenschaften*, 44, 71.
- Sauer, E.G.F. (1961). Further studies on the stellar orientation of nocturnally migrating birds. *Psychol. Forsch.*, 26, 224–244.
- Sauer, E.G.F., & Emlen, S.T. (1971). Celestial rotation and stellar orientation in migratory warblers. *Science*, 173, 459–461.
- Sauer, E.G.F., & Sauer, E.M. (1960). Star navigation of nocturnal migrating birds - The 1958 planetarium experiments. *Cold Spring Harb. Symp. Quant. Biol.*, 25, 463–473.
- Schmidt-Koenig, K (1958). Der Einfluß experimentell veränderter Zeitschätzung auf das Heimfindevermögen bei Brieftauben. *Naturwissenschaften*, 45, 47.
- Schmidt-Koenig, K. (1961). Die Sonne als Kompaß im Heim-Orientierungssystem der Brieftauben1. *Zeitschrift Für Tierpsychologie*, 18, 2, 221–241.
- Schulten, K., Swenberg, C.E. & Weller, A. (1978). Biomagnetic sensory mechanism based on magnetic coherent electron-spin motion. *Z Phys Chem*, 111, 1–5.
- Schwarze, S., Schneider, N.-L., Reichl, T., Dreyer, D., Lefeldt, N., et al. (2016a). Weak broadband electromagnetic fields are more disruptive to magnetic compass orientation in a night-migratory songbird (*Erithacus rubecula*) than strong narrow-band fields. *Front. Behav. Neurosci.*, 10, 55.

- Schwarze, S., Steenken, F., Thiele, N., Kobylkov, D., Lefeldt, et al. (2016b). Migratory blackcaps can use their magnetic compass at 5 degrees inclination, but are completely random at 0 degrees inclination. *Sci. Rep.*, 6, 33805.
- Semm, P., Schneider, T. & Vollrath, L. (1980). Effects of an earth-strength magnetic field on electrical activity of pineal cells. *Nature*, 288, 607–608.
- Shashar, N., Hagan, R., Boal, J.G., & Hanlon, R.T. (2000). Cuttlefish use polarization sensitivity in predation on silvery fish. *Vis Res*, 40, 71–75.
- Shashar, N. (2014). Polarization Vision in Cephalopods. In: Horváth, G. (ed.). *Polarized Light and Polarization Vision in Animal Sciences*. Springer Heidelberg New York. pp 217–224.
- Shaw, J., Boyd, A., House, M., Woodward, R., Mathes, F. et al. (2015). Magnetic particle-mediated magnetoreception. *J. R. Soc. Interface*, 12, 20150499.
- Shima, J., Noonburg, E., Swearer, S., Alonzo, H.S., & Osenberg, C. (2017). Born at the right time? A conceptual framework linking reproduction, development, and settlement in reef fish. *Ecology*, 99.
- Skiles, D.D. (1985). The geomagnetic field, its nature, history, and biological relevance. In: Kirschvink, J.L., Jones, D.S., & MacFadden, B.J. (eds). *Magnetite biomineralization and magnetoreception in organisms. A new biomagnetism*, Plenum Press, New York. pp 43–102.
- Snyder, A.W. (1973). Polarisation sensitivity of individual retinula cells. *J. Comp. Physiol.*, 83, 331–360.
- Snyder, A.W., & Laughlin, S.B. (1975). Dichroism and absorption by photoreceptors. *J. Comp. Physiol.*, 100, 101–116.
- Sponaugle, S., Cowen, R.K., Shanks, A., Morgan, S.G., Leis, J.M., et al. (2002). Predicting self-recruitment in marine populations: Biophysical correlates and mechanisms. *Bull. Mar. Sci.*, 70, 1, 341–375.
- Temple, S.E., Pignatelli, V., Cook, T., How, M.J., Chiou, T.-H., et al. (2012). Polarization vision in a cuttlefish. *Curr. Biol.*, 22, 4, R121–R122.
- Thalau, P., Ritz, T., Burda, H., Wegner, R.E. & Wiltschko, R. (2006). The magnetic compass mechanisms of birds and rodents are based on different physical principles. *J. R. Soc. Interface*, 3, 583–587.

- Treiber, C.D., Salzer, M.C., Riegler, J., Edelman, N., Sugar, C. et al. (2012). Clusters of iron-rich cells in the upper beak of pigeons are macrophages not magnetosensitive neurons. *Nature*, 484, 367–370.
- Taylor, D.H., & Adler, K. (1973). Spatial orientation by salamanders using plane-polarized light. *Science*, 181, 4096, 285–287.
- Taylor, D.H., & Adler, K. (1978). The pineal body: site of extraocular perception of celestial cues for orientation in the tiger salamander (*Ambystoma tigrinum*). *J. Comp. Physiol. A*, 124, 357–361.
- Van Harreveld, A. (1978). Two mechanisms for spreading depression in the chicken retina. *J. Neurobiol.*, 9, 419–431.
- Vaney, D.I., Sivyer, B., & Taylor, W.R. (2012). Direction selectivity in the retina: symmetry and asymmetry in structure and function. *Nature Reviews. Neuroscience*, 133, 194–208.
- Viehmann, W. (1982). Interrelation of Magnetic Compass, Star Orientation, and the Sun in the Orientation of Blackcaps and Robins. In: Papi, F., & Wallraff, H.G. (eds.). Avian Navigation. *Proceedings in Life Sciences. Springer, Berlin, Heidelberg*. pp 59–67.
- Vos Hzn, J.J., Coemans, M.A.J.M. & Nuboer, J.F.W. (1995). No evidence for polarization sensitivity in the pigeon electroretinogram. *J. Exp. Biol.*, 198, 325–335.
- Wallraff, H.G. (1960). Does celestial navigation exist in animals? *Cold Spring Harb. Symp. Quant. Biol.*, 25, 451–461.
- Wallraff, H.G. (1974). Das Navigationssystem der Vögel: Ein theoretischer Beitrag zur Analyse ungeklärter Orientierungsleistungen. *München: R. Oldenbourg Verlag*.
- Wallraff, H.G. (2003). Zur olfaktorischen Navigation der Vögel. *J. Ornithol.*, 144, 1–32.
- Wallraff, H.G., & Andreae, M.O. (2000). Spatial gradients in ratios of atmospheric trace gases: a study stimulated by experiments on bird navigation. *Tellus*, 52B, 1138–1157.
- Walker, M.M., Diebel, C.E., & Kirschvink, J.L. (2003). Detection and use of the earth's magnetic field by aquatic vertebrates. In: Proceedings of Sensory Processing in Aquatic Environments (SPA '03). *Springer, New York*. pp 53–74.
- Wehner, R. (1976). Polarized-light navigation by insects. *Sci Am*, 235, 106–115.
- Wehner, R. (2001). Polarization vision – A uniform sensory capacity? *J. Exp. Biol.*, 204, 2589–2596.

- Weindler, P., Beck, W., Liepa, V., & Wiltschko, W. (1995). Development of migratory orientation in Pied Flycatchers in different magnetic inclinations. *Anim. Behav.*, 49, 227–234.
- Wellington, W.G. (1974). Bumblebee Ocelli and Navigation at Dusk. *Science*, 183
- Wiltschko, W. (1968). Über den Einfluß statischer Magnetfelder auf die Zugorientierung der Rotkehlchen (*Erithacus rubecula*). *Z. Tierpsychol.*, 25, 537–558.
- Wiltschko, W., Daum, P., Fergenbauer-Kimmel, A., & Wiltschko, R. (1987). The development of the star compass in garden warblers, *Sylvia borin*. *Ethology*, 74, 4, 285–292.
- Wiltschko, W., Munro, U., Ford, H. & Wiltschko, R. (1993). Red-light disrupts magnetic orientation of migratory birds. *Nature*, 364, 525–527.
- Wiltschko, W., Munro, U., Ford, H., & Wiltschko, R. (2009). Avian orientation: the pulse effect is mediated by the magnetite receptors in the upper beak. *Proc. R. Soc. B*, 276, 2227–2232.
- Wiltschko, R., Stapput, K., Thalau, P., & Wiltschko, W. (2010). Directional orientation of birds by the magnetic field under different light conditions. *J. R. Soc. Interface*, 7, S163–S177.
- Wiltschko, W., & Gwinner, E. (1974). Evidence for an innate magnetic compass in garden warblers. *Naturwissenschaften*, 61, 406–406.
- Wiltschko, W., & Wiltschko, R. (1972). Magnetic compass of European robins. *Science*, 176, 62–64.
- Wiltschko, W., & Wiltschko, R. (1974). Bird orientation under different sky sectors. *Z. Tierpsychol.*, 35, 536–542.
- Wiltschko, W., & Wiltschko, R. (1975a). The interaction of stars and magnetic field in the orientation of night migrating birds. I. Autumn experiments with European Warblers (gen. *Sylvia*). *Z. Tierpsychol.*, 37, 337–355.
- Wiltschko, W., & Wiltschko, R. (1975b). The interaction of stars and magnetic field in the orientation of night migrating birds. II. Spring experiments with European Robins (*Erithacus rubecula*). *Z. Tierpsychol.* 39, 265–282.
- Wiltschko, R., and Wiltschko, W. (1978). Relative importance of stars and the magnetic field for the accuracy of orientation in night-migrating birds. *Oikos*, 30, 195–206.
- Wiltschko, R. & Wiltschko, W. (1995c). *Magnetic Orientation in Animals*. Springer-Verlag, Berlin.

- Wiltschko, W., & Wiltschko, R. (1976). Interrelation of magnetic compass and star orientation on night-migrating birds. *J. Comp. Physiol. A.*, 109, 91–99.
- Wiltschko, R., & Wiltschko, W. (1988a). Einfluß von Windexposition auf das Orientierungsverhalten von Brieftauben. *Verh. Dtsch. Zool. Ges.*, 236–237.
- Wiltschko, W., & Wiltschko, R. (1988b). Die Orientierung von Zugvögeln: Magnetfeld und Himmelsfaktoren wirken zusammen. *J. Ornithol.*, 129, 265–286.
- Wiltschko, R., & Wiltschko, W. (1989). Pigeon homing: Olfactory orientation- a paradox. *Behav. Ecol. Sociobiol.*, 24, 163–173.
- Wiltschko, W., & Wiltschko, R. (1990). Magnetic orientation and celestial cues in migratory orientation. *Experientia*, 46, 342–352.
- Wiltschko, W., & Wiltschko, R. (2007). Magnetoreception in birds: two receptors for two different tasks. *J. Ornithol.*, 148, S61–S76.
- Wiltschko, R., & Wiltschko, W. (2013). The magnetite-based receptors in the beak of birds and their role in avian navigation. *J. Comp. Physiol. A*, 199, 89–98.
- Wiltschko, W., Wiltschko, R., & Keeton, W.T. (1976). Effects of a “permanent” clock-shift on the orientation of young homing pigeons. *Behav. Ecol. Sociobiol.*, 1, 3, 229–243.
- Winklhofer, M., & Kirschvink, J.L. (2010). A quantitative assessment of torque-transducer models for magnetoreception. *J. R. Soc. Interface*, 7, S273–289.
- Wittemyer, G., Getz, W.M., Vollrath, F., & Douglas-Hamilton, I. (2007). Social dominance, seasonal movements, and spatial segregation in African elephants: a contribution to conservation behavior. *Behav. Ecol. Sociobiol.*, 61, 12, 1919–1931.
- Wu, H., Scholten, A., Einwich, A., Mouritsen, H., & Koch, K.W. (2020). Protein-protein interaction of the putative magnetoreceptor cryptochrome 4 expressed in the avian retina. *Sci Rep.*, 10, 1, 7364.
- Xiao, Q. & Frost, B. (2009). Looming responses of telencephalic neurons in the pigeon are modulated by optic flow. *Brain Research*, 1305, 40-46.
- Zapka, M., Heyers, D., Hein, C.M., Engels, S., Schneider, N.-L., et al. (2009). Visual but not trigeminal mediation of magnetic compass information in a migratory bird. *Nature*, 461, 1274–1278.
- Zapka, M., Heyers, D., Liedvogel, M., Jarvis, E. D., & Mouritsen, H. (2010). Night-time neuronal activation of Cluster N in a day- and night-migrating songbird. *Eur. J. Neurosci.*, 32, 619–624.

Zeil, J., Ribi, W.A., & Narendra, A. (2014). Polarisation Vision in Ants, Bees and Wasps. In: Horváth, G. (ed.). Polarized Light and Polarization Vision in Animal Sciences. *Springer Heidelberg New York*, 41–60.

## Appendix

**Appendix Table 1: Raw data of the experiments in chapter 3.5 *Moving Gratings* including response counts from three observers.** Due to file size and to save paper, a full data table including all responses separated by stimulus direction in digital form, a sample of original videos documenting the behavior, the basic script formula for statistics used in R and the stimulation functions that were custom-written in Matlab®, can be provided via cloud on demand.

Species	Observer	Round	Contrast	Stimulus	Testing order	Response type	# individuals	median Responses	1st quartile	3rd quartile
Zebra finches	Observer1	1	100	Luminance	LumPol	stim dir	14	38,0	28,8	45,8
Zebra finches	Observer1	2	100	Luminance	LumPol	stim dir	14	51,0	43,8	60,3
Zebra finches	Observer1	3	100	Luminance	LumPol	stim dir	1	35,0	35,0	35,0
Zebra finches	Observer1	3	50	Luminance	LumPol	stim dir	2	51,0	50,0	52,0
Zebra finches	Observer1	3	38	Luminance	LumPol	stim dir	6	51,0	31,8	57,3
Zebra finches	Observer1	3	100	Polarization	LumPol	stim dir	8	27,5	23,0	29,0
Zebra finches	Observer1	4	100	Polarization	LumPol	stim dir	14	19,5	13,8	23,0
Zebra finches	Observer1	5	100	Polarization	LumPol	stim dir	14	15,5	12,8	19,0
Zebra finches	Observer1	6	100	Luminance	LumPol	stim dir	14	56,5	49,5	72,0
Zebra finches	Observer1	1	100	Polarization	PolLum	stim dir	8	18,5	15,8	23,0
Zebra finches	Observer1	2	100	Luminance	PolLum	stim dir	8	83,5	63,8	93,3
Zebra finches	Observer2	1	100	Luminance	LumPol	stim dir	14	57,5	46,3	62,5
Zebra finches	Observer2	2	100	Luminance	LumPol	stim dir	14	60,5	48,8	74,5
Zebra finches	Observer2	3	100	Luminance	LumPol	stim dir	1	70,0	70,0	70,0
Zebra finches	Observer2	3	50	Luminance	LumPol	stim dir	2	71,0	70,5	71,5
Zebra finches	Observer2	3	38	Luminance	LumPol	stim dir	6	61,5	41,8	70,3
Zebra finches	Observer2	3	100	Polarization	LumPol	stim dir	8	11,0	7,0	20,0
Zebra finches	Observer2	4	100	Polarization	LumPol	stim dir	14	15,5	8,8	29,0
Zebra finches	Observer2	5	100	Polarization	LumPol	stim dir	14	18,0	12,8	43,3
Zebra finches	Observer2	6	100	Luminance	LumPol	stim dir	14	89,0	85,0	94,3
Zebra finches	Observer2	1	100	Polarization	PolLum	stim dir	8	15,5	12,0	23,5
Zebra finches	Observer2	2	100	Luminance	PolLum	stim dir	8	86,0	81,8	89,5
Zebra finches	Observer3	1	100	Luminance	LumPol	stim dir	14	49,5	42,0	58,3
Zebra finches	Observer3	2	100	Luminance	LumPol	stim dir	14	54,5	48,0	61,5
Zebra finches	Observer3	3	100	Luminance	LumPol	stim dir	1	66,0	66,0	66,0
Zebra finches	Observer3	3	50	Luminance	LumPol	stim dir	2	56,0	50,5	61,5
Zebra finches	Observer3	3	38	Luminance	LumPol	stim dir	6	52,5	43,8	59,0
Zebra finches	Observer3	3	100	Polarization	LumPol	stim dir	8	23,0	19,8	27,5
Zebra finches	Observer3	4	100	Polarization	LumPol	stim dir	14	15,5	5,3	28,0
Zebra finches	Observer3	5	100	Polarization	LumPol	stim dir	14	3,0	1,8	8,3
Zebra finches	Observer3	6	100	Luminance	LumPol	stim dir	14	15,0	11,0	20,0
Zebra finches	Observer3	1	100	Polarization	PolLum	stim dir	8	10,5	1,5	24,0
Zebra finches	Observer3	2	100	Luminance	PolLum	stim dir	8	18,0	15,8	19,3
Zebra finches	Observer1	1	100	Luminance	LumPol	null	14	1,0	0,0	2,0
Zebra finches	Observer1	2	100	Luminance	LumPol	null	14	1,5	0,8	4,0
Zebra finches	Observer1	3	100	Luminance	LumPol	null	1	11,0	11,0	11,0
Zebra finches	Observer1	3	50	Luminance	LumPol	null	2	6,0	3,0	9,0



Zebra finches	Observer1	3	38	Luminance	LumPol	null	6	3,5	1,0	5,0
Zebra finches	Observer1	3	100	Polarization	LumPol	null	8	25,0	22,5	29,3
Zebra finches	Observer1	4	100	Polarization	LumPol	null	14	15,5	12,8	21,0
Zebra finches	Observer1	5	100	Polarization	LumPol	null	14	16,0	14,0	21,0
Zebra finches	Observer1	6	100	Luminance	LumPol	null	14	6,0	4,0	9,0
Zebra finches	Observer1	1	100	Polarization	PolLum	null	8	17,0	14,5	21,0
Zebra finches	Observer1	2	100	Luminance	PolLum	null	8	8,5	6,5	11,0
Zebra finches	Observer2	1	100	Luminance	LumPol	null	14	10,5	8,5	12,3
Zebra finches	Observer2	2	100	Luminance	LumPol	null	14	12,0	10,0	15,3
Zebra finches	Observer2	3	100	Luminance	LumPol	null	1	15,0	15,0	15,0
Zebra finches	Observer2	3	50	Luminance	LumPol	null	2	10,5	9,3	11,8
Zebra finches	Observer2	3	38	Luminance	LumPol	null	6	11,5	9,8	14,5
Zebra finches	Observer2	3	100	Polarization	LumPol	null	8	24,5	18,8	34,0
Zebra finches	Observer2	4	100	Polarization	LumPol	null	14	23,5	12,8	33,8
Zebra finches	Observer2	5	100	Polarization	LumPol	null	14	17,5	13,0	29,3
Zebra finches	Observer2	6	100	Luminance	LumPol	null	14	26,0	23,8	28,3
Zebra finches	Observer2	1	100	Polarization	PolLum	null	8	22,0	13,5	35,0
Zebra finches	Observer2	2	100	Luminance	PolLum	null	8	24,5	21,8	28,0
Zebra finches	Observer3	1	100	Luminance	LumPol	null	14	14,5	7,5	24,0
Zebra finches	Observer3	2	100	Luminance	LumPol	null	14	13,5	4,5	21,3
Zebra finches	Observer3	3	100	Luminance	LumPol	null	1	4,0	4,0	4,0
Zebra finches	Observer3	3	50	Luminance	LumPol	null	2	8,5	4,3	12,8
Zebra finches	Observer3	3	38	Luminance	LumPol	null	6	13,0	6,0	15,3
Zebra finches	Observer3	3	100	Polarization	LumPol	null	8	26,0	15,8	31,5
Zebra finches	Observer3	4	100	Polarization	LumPol	null	14	24,0	12,0	36,0
Zebra finches	Observer3	5	100	Polarization	LumPol	null	14	3,0	2,0	7,8
Zebra finches	Observer3	6	100	Luminance	LumPol	null	14	3,0	2,0	5,0
Zebra finches	Observer3	1	100	Polarization	PolLum	null	8	11,5	5,8	26,5
Zebra finches	Observer3	2	100	Luminance	PolLum	null	8	4,0	3,8	5,0
Zebra finches	Observer1	Baseline	Baseline	Baseline	LumPol	Baseline	14	22,5	20,0	26,3
Zebra finches	Observer2	Baseline	Baseline	Baseline	LumPol	Baseline	14	20,0	15,0	24,0
Zebra finches	Observer3	Baseline	Baseline	Baseline	LumPol	Baseline	14	4,0	0,8	8,0
Zebra finches	Observer1	Baseline	Baseline	Baseline	PolLum	Baseline	8	19,5	14,5	23,3
Zebra finches	Observer2	Baseline	Baseline	Baseline	PolLum	Baseline	8	14,5	8,8	19,5
Zebra finches	Observer3	Baseline	Baseline	Baseline	PolLum	Baseline	8	1,0	0,0	4,0
European robins	Observer1	1	100	Luminance	LumPol	stim dir	15	26,0	18,3	33,8
European robins	Observer1	2	100	Luminance	LumPol	stim dir	15	17,0	8,8	36,5
European robins	Observer1	3	100	Luminance	LumPol	stim dir	4	17,0	16,0	19,0
European robins	Observer1	3	50	Luminance	LumPol	stim dir	6	19,0	15,0	36,0
European robins	Observer1	3	38	Luminance	LumPol	stim dir	8	11,5	2,8	13,5
European robins	Observer1	3	13	Luminance	LumPol	stim dir	3	9,0	8,0	10,0
European robins	Observer1	3	5	Luminance	LumPol	stim dir	3	8,0	7,0	8,0
European robins	Observer1	3	100	Polarization	LumPol	stim dir	7	4,5	3,0	7,0
European robins	Observer1	4	100	Polarization	LumPol	stim dir	6	8,0	5,8	10,0
European robins	Observer1	5	100	Polarization	LumPol	stim dir	15	3,0	2,0	4,0
European robins	Observer1	6	100	Luminance	LumPol	stim dir	15	18,0	9,0	26,8
European robins	Observer1	1	100	Polarization	PolLum	stim dir	10	4,0	2,8	5,3

European robins	Observer1	2	100	Luminance	PolLum	stim dir	10	16,5	11,8	23,3
European robins	Observer1	2	13	Luminance	PolLum	stim dir	10	12,0	9,0	17,5
European robins	Observer1	2	5	Luminance	PolLum	stim dir	10	12,0	7,0	14,0
European robins	Observer2	1	100	Luminance	LumPol	stim dir	15	38,0	33,0	45,0
European robins	Observer2	2	100	Luminance	LumPol	stim dir	15	34,0	23,3	43,8
European robins	Observer2	3	100	Luminance	LumPol	stim dir	4	26,0	23,0	30,5
European robins	Observer2	3	50	Luminance	LumPol	stim dir	6	24,5	17,8	37,8
European robins	Observer2	3	38	Luminance	LumPol	stim dir	8	18,5	0,0	5,0
European robins	Observer2	3	13	Luminance	LumPol	stim dir	3	0,0	0,0	0,0
European robins	Observer2	3	5	Luminance	LumPol	stim dir	3	23,0	5,0	24,0
European robins	Observer2	3	100	Polarization	LumPol	stim dir	7	3,0	2,0	4,8
European robins	Observer2	4	100	Polarization	LumPol	stim dir	8	5,0	3,0	8,3
European robins	Observer2	5	100	Polarization	LumPol	stim dir	15	9,0	7,3	18,8
European robins	Observer2	6	100	Luminance	LumPol	stim dir	15	52,5	48,0	63,8
European robins	Observer2	1	100	Polarization	PolLum	stim dir	10	4,0	2,8	7,0
European robins	Observer2	2	100	Luminance	PolLum	stim dir	10	39,0	30,3	48,3
European robins	Observer2	2	13	Luminance	PolLum	stim dir	10	15,0	3,5	25,5
European robins	Observer2	2	5	Luminance	PolLum	stim dir	10	12,5	6,5	24,8
European robins	Observer3	1	100	Luminance	LumPol	stim dir	15	27,5	19,5	33,5
European robins	Observer3	2	100	Luminance	LumPol	stim dir	15	21,5	12,0	34,3
European robins	Observer3	3	100	Luminance	LumPol	stim dir	4	15,0	14,0	18,0
European robins	Observer3	3	50	Luminance	LumPol	stim dir	6	21,5	16,8	27,3
European robins	Observer3	3	38	Luminance	LumPol	stim dir	8	19,0	14,8	29,3
European robins	Observer3	3	13	Luminance	LumPol	stim dir	3	1,0	0,0	10,0
European robins	Observer3	3	5	Luminance	LumPol	stim dir	3	14,0	8,0	26,0
European robins	Observer3	3	100	Polarization	LumPol	stim dir	7	0,5	0,0	3,8
European robins	Observer3	4	100	Polarization	LumPol	stim dir	8	5,0	2,5	7,0
European robins	Observer3	5	100	Polarization	LumPol	stim dir	15	0,0	0,0	1,8
European robins	Observer3	6	100	Luminance	LumPol	stim dir	15	7,0	4,0	11,8
European robins	Observer3	1	100	Polarization	PolLum	stim dir	10	0,0	0,0	0,5
European robins	Observer3	2	100	Luminance	PolLum	stim dir	10	18,0	16,5	28,5
European robins	Observer3	2	13	Luminance	PolLum	stim dir	10	11,0	4,5	26,0
European robins	Observer3	2	5	Luminance	PolLum	stim dir	10	0,0	0,0	19,0
European robins	Observer1	1	100	Luminance	LumPol	Null	15	0,0	0,0	0,0
European robins	Observer1	2	100	Luminance	LumPol	Null	15	0,0	0,0	0,0
European robins	Observer1	3	100	Luminance	LumPol	Null	4	0,0	0,0	0,0
European robins	Observer1	3	50	Luminance	LumPol	Null	6	0,0	0,0	0,0
European robins	Observer1	3	38	Luminance	LumPol	Null	8	0,0	0,0	1,3
European robins	Observer1	3	13	Luminance	LumPol	Null	3	3,0	2,0	3,0
European robins	Observer1	3	5	Luminance	LumPol	Null	3	3,0	3,0	3,0
European robins	Observer1	3	100	Polarization	LumPol	Null	7	4,0	3,0	6,8
European robins	Observer1	4	100	Polarization	LumPol	Null	6	6,0	4,0	7,0
European robins	Observer1	5	100	Polarization	LumPol	Null	15	3,0	1,0	5,0
European robins	Observer1	6	100	Luminance	LumPol	Null	15	0,0	0,0	0,0
European robins	Observer1	1	100	Polarization	PolLum	Null	10	4,5	3,8	5,3
European robins	Observer1	2	100	Luminance	PolLum	Null	10	3,0	1,8	4,0
European robins	Observer1	2	13	Luminance	PolLum	Null	10	3,0	3,0	4,5
European robins	Observer1	2	5	Luminance	PolLum	Null	10	4,0	3,0	6,3
European robins	Observer2	1	100	Luminance	LumPol	Null	15	3,5	3,0	5,0

European robins	Observer2	2	100	Luminance	LumPol	Null	15	4,0	3,0	5,0
European robins	Observer2	3	100	Luminance	LumPol	Null	4	5,0	4,5	6,5
European robins	Observer2	3	50	Luminance	LumPol	Null	6	5,5	4,8	6,0
European robins	Observer2	3	38	Luminance	LumPol	Null	8	5,5	4,0	8,0
European robins	Observer2	3	13	Luminance	LumPol	Null	3	5,0	3,0	5,0
European robins	Observer2	3	5	Luminance	LumPol	Null	3	5,0	4,0	6,0
European robins	Observer2	3	100	Polarization	LumPol	Null	7	4,0	1,3	11,5
European robins	Observer2	4	100	Polarization	LumPol	Null	8	11,5	2,8	13,5
European robins	Observer2	5	100	Polarization	LumPol	Null	15	12,5	7,3	23,8
European robins	Observer2	6	100	Luminance	LumPol	Null	15	9,0	8,0	11,8
European robins	Observer2	1	100	Polarization	PolLum	Null	10	4,0	1,0	15,5
European robins	Observer2	2	100	Luminance	PolLum	Null	10	6,5	4,8	8,3
European robins	Observer2	2	13	Luminance	PolLum	Null	10	5,0	4,5	7,0
European robins	Observer2	2	5	Luminance	PolLum	Null	10	6,5	3,8	8,3
European robins	Observer3	1	100	Luminance	LumPol	Null	15	0,0	0,0	0,0
European robins	Observer3	2	100	Luminance	LumPol	Null	15	1,0	0,0	4,0
European robins	Observer3	3	100	Luminance	LumPol	Null	4	1,0	0,5	4,5
European robins	Observer3	3	50	Luminance	LumPol	Null	6	0,0	0,0	4,3
European robins	Observer3	3	38	Luminance	LumPol	Null	8	1,0	0,0	4,0
European robins	Observer3	3	13	Luminance	LumPol	Null	3	0,0	0,0	2,0
European robins	Observer3	3	5	Luminance	LumPol	Null	3	2,0	0,0	4,0
European robins	Observer3	3	100	Polarization	LumPol	Null	7	0,0	0,0	4,0
European robins	Observer3	4	100	Polarization	LumPol	Null	8	2,5	1,0	5,3
European robins	Observer3	5	100	Polarization	LumPol	Null	15	0,0	0,0	1,0
European robins	Observer3	6	100	Luminance	LumPol	Null	15	1,0	0,0	3,0
European robins	Observer3	1	100	Polarization	PolLum	Null	10	1,0	0,0	12,0
European robins	Observer3	2	100	Luminance	PolLum	Null	10	0,0	0,0	1,3
European robins	Observer3	2	13	Luminance	PolLum	Null	10	0,0	0,0	0,0
European robins	Observer3	2	5	Luminance	PolLum	Null	10	0,0	0,0	0,0
European robins	Observer1	Baseline	Baseline	Baseline	LumPol	Baseline	15	6,0	5,0	6,8
European robins	Observer2	Baseline	Baseline	Baseline	LumPol	Baseline	15	16,5	12,0	22,0
European robins	Observer3	Baseline	Baseline	Baseline	LumPol	Baseline	15	1,5	0,0	3,0
European robins	Observer1	Baseline	Baseline	Baseline	PolLum	Baseline	10	3,5	1,8	5,0
European robins	Observer2	Baseline	Baseline	Baseline	PolLum	Baseline	10	14,5	7,8	23,3
European robins	Observer3	Baseline	Baseline	Baseline	PolLum	Baseline	10	2,5	1,5	11,5
Blackcaps	Observer1	1	100	Polarization	PolLum	stim dir	7	12,5	8,3	16,5
Blackcaps	Observer1	2	100	Luminance	PolLum	stim dir	7	63,0	58,5	73,5
Blackcaps	Observer1	2	13	Luminance	PolLum	stim dir	4	59,0	56,8	60,5
Blackcaps	Observer1	2	5	Luminance	PolLum	stim dir	7	42,5	33,8	46,5
Blackcaps	Observer1	0	100	Luminance	LumPol	stim dir	5	64,0	45,0	71,0
Blackcaps	Observer1	0	50	Luminance	LumPol	stim dir	2	39,5	39,3	39,8
Blackcaps	Observer1	0	38	Luminance	LumPol	stim dir	5	41,0	32,5	49,5
Blackcaps	Observer1	0	13	Luminance	LumPol	stim dir	4	40,0	37,3	41,3
Blackcaps	Observer1	0	5	Luminance	LumPol	stim dir	4	32,0	30,3	35,3
Blackcaps	Observer2	1	100	Polarization	PolLum	stim dir	7	8,0	6,0	19,0
Blackcaps	Observer2	2	100	Luminance	PolLum	stim dir	7	99,0	78,5	111,5
Blackcaps	Observer2	2	13	Luminance	PolLum	stim dir	4	102,0	98,0	108,0

Blackcaps	Observer2	2	5	Luminance	PolLum	stim dir	7	67,5	48,5	99,0
Blackcaps	Observer2	0	100	Luminance	LumPol	stim dir	5	62,0	56,5	68,5
Blackcaps	Observer2	0	50	Luminance	LumPol	stim dir	2	46,0	40,0	52,0
Blackcaps	Observer2	0	38	Luminance	LumPol	stim dir	5	49,0	43,5	49,5
Blackcaps	Observer2	0	13	Luminance	LumPol	stim dir	4	40,0	38,0	44,0
Blackcaps	Observer2	0	5	Luminance	LumPol	stim dir	4	38,5	35,5	40,8
Blackcaps	Observer3	1	100	Polarization	PolLum	stim dir	6	2,5	1,0	3,3
Blackcaps	Observer3	2	100	Luminance	PolLum	stim dir	7	22,0	18,0	25,5
Blackcaps	Observer3	2	13	Luminance	PolLum	stim dir	4	20,5	18,5	24,3
Blackcaps	Observer3	2	5	Luminance	PolLum	stim dir	7	13,0	8,0	20,5
Blackcaps	Observer3	0	100	Luminance	LumPol	stim dir	5	21,0	19,0	22,5
Blackcaps	Observer3	0	50	Luminance	LumPol	stim dir	2	19,5	17,8	21,3
Blackcaps	Observer3	0	38	Luminance	LumPol	stim dir	5	15,0	13,0	17,0
Blackcaps	Observer3	0	13	Luminance	LumPol	stim dir	4	10,5	6,8	13,3
Blackcaps	Observer3	0	5	Luminance	LumPol	stim dir	4	8,5	6,5	9,8
Blackcaps	Observer1	1	100	Polarization	PolLum	Null	7	14,5	10,0	17,0
Blackcaps	Observer1	2	100	Luminance	PolLum	Null	7	4,0	4,0	5,0
Blackcaps	Observer1	2	13	Luminance	PolLum	Null	4	10,0	6,8	13,0
Blackcaps	Observer1	2	5	Luminance	PolLum	Null	7	7,5	5,3	10,3
Blackcaps	Observer1	0	100	Luminance	LumPol	Null	5	7,0	5,5	14,5
Blackcaps	Observer1	0	50	Luminance	LumPol	Null	2	11,0	11,0	11,0
Blackcaps	Observer1	0	38	Luminance	LumPol	Null	5	15,0	11,5	16,0
Blackcaps	Observer1	0	13	Luminance	LumPol	Null	4	14,0	12,0	15,5
Blackcaps	Observer1	0	5	Luminance	LumPol	Null	4	14,0	13,3	14,0
Blackcaps	Observer2	1	100	Polarization	PolLum	Null	7	26,5	4,5	41,0
Blackcaps	Observer2	2	100	Luminance	PolLum	Null	7	11,0	9,0	13,0
Blackcaps	Observer2	2	13	Luminance	PolLum	Null	4	11,5	9,8	13,5
Blackcaps	Observer2	2	5	Luminance	PolLum	Null	7	8,0	6,3	14,5
Blackcaps	Observer2	0	100	Luminance	LumPol	Null	5	5,0	4,0	5,5
Blackcaps	Observer2	0	50	Luminance	LumPol	Null	2	8,0	8,0	8,0
Blackcaps	Observer2	0	38	Luminance	LumPol	Null	5	6,0	4,5	6,5
Blackcaps	Observer2	0	13	Luminance	LumPol	Null	4	5,0	5,0	5,5
Blackcaps	Observer2	0	5	Luminance	LumPol	Null	4	7,5	4,8	8,8
Blackcaps	Observer3	1	100	Polarization	PolLum	Null	6	2,0	1,0	4,5
Blackcaps	Observer3	2	100	Luminance	PolLum	Null	7	5,0	3,5	6,0
Blackcaps	Observer3	2	13	Luminance	PolLum	Null	4	4,0	3,5	4,5
Blackcaps	Observer3	2	5	Luminance	PolLum	Null	7	2,0	1,0	4,0
Blackcaps	Observer3	0	100	Luminance	LumPol	Null	5	3,0	2,0	3,5
Blackcaps	Observer3	0	50	Luminance	LumPol	Null	2	5,0	4,5	5,5
Blackcaps	Observer3	0	38	Luminance	LumPol	Null	5	3,0	3,0	4,0
Blackcaps	Observer3	0	13	Luminance	LumPol	Null	4	3,5	2,8	4,3
Blackcaps	Observer3	0	5	Luminance	LumPol	Null	4	3,0	2,3	4,5
Blackcaps	Observer1	Baseline	Baseline	Baseline	LumPol	Baseline	5	20,5	14,8	23,3
Blackcaps	Observer2	Baseline	Baseline	Baseline	LumPol	Baseline	5	16,5	0,0	22,5
Blackcaps	Observer3	Baseline	Baseline	Baseline	LumPol	Baseline	5	2,0	0,0	7,0
Blackcaps	Observer1	Baseline	Baseline	Baseline	PolLum	Baseline	7	22,0	17,0	24,8
Blackcaps	Observer2	Baseline	Baseline	Baseline	PolLum	Baseline	7	24,5	19,0	33,0
Blackcaps	Observer3	Baseline	Baseline	Baseline	PolLum	Baseline	7	2,0	0,3	7,8

## Scientific Curriculum Vitae

### Employment History

- 2019 - date                    **GIS Specialist**  
IBL Umweltplanung GmbH  
Environmental planning office, Oldenburg
- Geographic information systems (GIS), ArcPy scripting
  - Bat identification and monitoring
  - Semi-automated multispectral image classification
- 2013 - 2017                    **Research Fellow**  
Animal Navigation group, Prof. Dr. Henrik Mouritsen  
Institute of Biology and Environmental Science, University Oldenburg
- Established a 3D virtual arena using LCD monitor screens and coding in MatLab<sup>®</sup>
  - Found first evidence for geomagnetic compass orientation in coral reef fish larvae
  - Gave tutorials on Amira<sup>®</sup> 3D reconstruction software and MatLab<sup>®</sup> Graphical User Interface Applications
- 2012 -2013                    **Course Supervisor**  
Department II Neurobiology, LMU Munich
- Practical Course: "Comparative Anatomy and Evolution of Vertebrates"
  - Supervision of dissections. Acquisition and preparation of class material
- 2011                                **Bird Migration Helper**  
Project Waldrappteam.at, Austria/Slovenia/Italy
- Human-led migration of hand-raised Ibis *Geronticus eremita* to their winter habitat in Tuscany, Italy
  - Project Supervisor: Dr. Johannes Fritz
- 2009                                **Course Supervisor**  
Department I Systematic Biology, LMU Munich
- Field Trip: "Marine Biology of the Wadden Sea" at the Alfred Wegener Institute for Polar and Marine Research, Sylt, Germany
  - Supervision of field experiments and species classification

### Advanced Training

- 2018                                **Professional in GIS**  
*Fachanwender Geoinformationssysteme mit ArcGIS*  
WBS Training, Germany
- Advanced data processing, analysis and cartography in ArcGIS 10.5 and QGIS 2.8, Model Builder-based processing, Geodatabase Management,

- WebMapping, Remote Sensing, ArcPy scripting
- Self-organized geodata acquisition and validation

## Education

2013 - date

### PhD student

Institute of Biology and Environmental Science, University Oldenburg

- associated member in Research Training Group „Molecular Basis of Biological Systems“

2008 - 2011

### Studies of Biological Sciences

Ludwig-Maximilian University Munich

- graduated with Diploma (first class degree; Majors: Neurobiology and Ecology)

## Publications

- **Bottesch M.**, Gerlach G., Halbach M., Bally A., Kingsford M. & Mouritsen H. (2016) "A magnetic compass that might help coral reef fish larvae return to their natal reef". **Current Biology** 26, 24 pR1266–R1267.
- Alert B., Michalik A., Thiele N., **Bottesch M.** & Mouritsen H. (2015) "Re-calibration of the magnetic compass in hand-raised European robins (*Erithacus rubecula*)."  
**Scientific Reports**, 5:14323

## Conference Contributions

Feb 2018

### Invited seminar talk at the

Centre of Integrative Ecology (CIE), Deakin University, Australia

- Title: "Magnetic fish babies and polarization sensitivity in birds"

Sep 2017

### Invited seminar talk at the

Max Planck Institute for Neurobiology, Martinsried, Germany

- Title: "To see or not to see – Polarization sensitivity in birds"

July 2017

### Oral Presentation at the

35th International Ethological Conference (IEC) "Behaviour 2017", Estoril, Portugal

- Title: "A magnetic compass that might help coral reef fish larvae return to their natal reef"

Dez 2016

### Oral Presentation at the

International Meeting of The Association for the Study of Animal Behaviour (ASAB) "Winter Meeting", London, England

- Title: "Magnetic compass orientation in coral reef fish larvae"

Oct 2011

### Poster Presentation at the

National Meeting of the German Zoological Society (DZG), Munich, Germany

- Title: “3D Morphology of the Stomatopod Visual System”

### Research Grants and Prizes

- |      |  |
|------|--|
| 2017 | <b>Conference Travel Grant</b><br>Association for the Study of Animal Behaviour (ASAB)                                       |
| 2014 | <b>2nd prize winner of the „4th Science Slam Oldenburg“</b><br>transfer of complex scientific knowledge to general audiences |

### Special Skills

#### *IT:*

ArcGIS<sup>®</sup> 10.5, QGIS<sup>®</sup> 3.2, (basics in Python<sup>®</sup>, SQL<sup>®</sup>, R<sup>®</sup> and VBScript<sup>®</sup>)  
MatLab<sup>®</sup> 2016b (Toolbox: Circular Statistics, Data Acquisition, Computer Vision System, Image Processing)  
Adobe Photoshop CS5<sup>®</sup>, ImageJ/Fiji<sup>®</sup>, Amira6<sup>®</sup> – 3D Visualizations  
Oriana<sup>®</sup> 4 for Circular Statistics  
Microsoft Office (Word<sup>®</sup>, Excel<sup>®</sup>, Powerpoint<sup>®</sup>), LibreOffice<sup>®</sup>

#### *Imaging:*

CLSM, TEM, SEM, Light microscopy, DIC optic, POL optic

#### *Physiological and histological methods:*

Electrophysiology, extracellular micro-electrode array (MEA) recordings  
Photospectrometry, Polarimetry  
Basic Immunohistochemistry

#### *Behavioral tests:*

Optomotor response in a virtual arena  
Orientation experiments in magnetic coils, artificial stars test chambers, outdoor setups  
Hand-raising of birds, testing social communication of zebra finches equipped with ultra-light microphones

#### *Model animals:*

songbird species, domestic chicken, coral reef fish larvae, mantis shrimp, mice

### Volunteer Work

2014 – 2018                      **Organizing Committee Member and on-stage Host**

“Science Slam Oldenburg”, Oldenburg

- Creating a public platform for knowledge transfer and science communication

2016

**Organizing Committee Member**

3-day-Workshop: „Career Opportunities in Science and Industry“

- invitation and preparation of guest speakers, bookings, social program planning

2012 - 2013

**Active Member**, Rehab Republic e.V., Munich

- Public work for global resource sustainability

2009

**Intern**, EarthLink e.V. Munich

- Educational work on environmental policy and development aid
- Quantitative and Qualitative Expert Interviews, Database Maintenance
- Representation at a Symposium



## Danksagung

Zunächst möchte ich mich bei meinem Doktorvater Henrik Mouritsen dafür bedanken, dass er mir die Arbeit an dieser Doktorarbeit ermöglicht hat, dafür, dass er mich in das spannende Feld der Vogelnavigation eingeführt hat, welches er mit sichtbarer Begeisterung und größtem internationalen Erfolg maßgeblich gestaltet und vermittelt, und dafür, dass er stets darum bemüht war, meine Arbeit zu finanzieren und mein Engagement zu unterstützen. Besonders dankbar bin ich für sein Vertrauen in meine wissenschaftlichen Fähigkeiten, welches er mir besonders im Zuge meiner Forschungsreisen nach Australien entgegengebracht hat.

Allergrößter Dank gilt Prof. Gabriele Gerlach, welche mich maßgeblich in meiner wissenschaftlichen Denke geprägt hat, mich wiederholt auf den sprichwörtlichen Hosenboden zurücksetzen konnte und mir sowohl mit professionellem, geradezu freundschaftlichem und immer gut gemeintem Rat stets zur Seite stand. Die Erfahrungen auf OTI, die ich ohne Dich, Mike und Andreas nie gesammelt hätte, werde ich nie vergessen und für immer in bester Erinnerung halten. Es ist so klasse, dass es Dich und Professor\*Innen wie Dich gibt. Danke.

Der nächste Dank wird schwer. Danke Arndt. Meine Gedanken sind noch sehr oft bei Dir und der gemeinsamen Zeit, die wir hatten. Ich hatte nie einen Kollegen wie Dich, den ich sowohl wegen seiner überragenden wissenschaftlichen Fähigkeiten, aber noch viel viel mehr wegen unserer Verbindungen als Musiker, Musikliebhaber und Semi-Nerds so sehr schätzte. Unseren Jam mit Andi werd ich nicht vergessen! Es gibt nicht viele Menschen, die sich über ein Jahr in eine dunkle Kabine sperren könnten, um trotz aller beruflichen Erschwernisse als dickere Freunde als vorher raus ans Licht zu kommen (Du in nerdiger Brille zur Dunkeladaptation und ich mit nem Campinghocker auf nen Schnack im Gras). Scheiße, Arndt, du fehlst! Hätte Dich gerne bei meiner Verteidigung... und überhaupt hier! Das Diskussionsthema Onkelz hatten wir ja öfter, aber hier haben sie nen Punkt getroffen: Nur die Besten sterben jung. Yours truly...

Neben Arndt und Gabi gab es eine weitere ultrawichtige Person, ohne die das Ganze im Leben nix geworden wäre: Beate, Du bist wirklich die beste Seele wo gibt! Wie unentwegt Du (nicht nur für mich!) eine Quelle an Trost, Hilfe, Ratschlag, organisatorischer Vermittlung und an Inspiration warst und bist, und was Du einfach für eine wundervolle Person bist, ist unglaublich. „Dank gilt nur Beate Grünberg...“ you know ;)

Liebe GKler, liebe AGler, Forscherkollegen und Freunde: Die abwechslungsreiche und inspirierende Zeit mit euch hat mich mitunter sehr geprägt, bewegt und zu dem gemacht was in den letzten Jahren aus mir geworden ist. Wenn man sich unter Freunden fühlt, kriegt man einfach so allerhand gebacken. Ich danke Tina, Fina, Kristin, Jasmin, Janina, Stefan, Dana, Dominik, Beena und Emil, Marco, Mitya, David, Florian, Bianka, Andreas, Nadine, Margrit, Peter, Karin Dedek, Michael Winklhofer, Karl-Wilhelm Koch, Nina, Rea, Mike Kingsford und Mark, Rachel Muheim, Dima, Nikita, Peter, Richard, Andy, Bally, Maurits, Laura, Simon, Max, Ela und allen anderen Menschen aus der AG Neurosensorik, aus dem Graduiertenkolleg, die ich auf Forschungsreisen und Tagungen oder durch meine Tätigkeit an der Universität Oldenburg im norddeutschen Exil kennenlernen konnte, welche ich jetzt aber leider nicht namentlich genannt habe. Last but not-at-all-least: Bibi, der besten Rätselbüro-Kollegin, Freundin, Dream-Team ScienceSlam Co-Moderatorin, und Tanzpartnerin der Welt. An alle: Es waren bunte und aufregende Zeiten.

Ganz vielen lieben Dank möchte ich auch meinen Geschwistern Julia, Marianne, Stefan, sowie SchwagerInnen Andi, Seba und Eva und meiner ganzen Familie entgegenbringen. Ihr gebt mir Halt und begleitet mich trotz ekelhaft weiter Distanz. Ich hab euch alle sehr lieb. Das gleiche gilt für Jana und Raíssa... You were big and will stay in my heart forever. Danke Jana für Deine Liebe! Muitos obrigados e saudades a nossa aventura increível, Raíó!

So, un jetzt mog i a Bier, zwoa Schnaps, drei Jahr Urlaub und mei Ruah.

## Erklärung gemäß § 11 der Promotionsordnung

Hiermit erkläre ich gemäß § 11 Abs. 2 der Promotionsordnung der Fakultät V vom 21.03.2013, dass

(i) ich die Dissertation selbstständig verfasst habe und dass die benutzten Hilfsmittel vollständig angegeben sind,

(ii) ein Teil dieser Dissertation, genauer Kapitel 2 „Magnetic compass orientation in coral reef fish larvae“, bereits unter dem Titel "A magnetic compass that might help coral reef fish larvae return to their natal reef" in der renommierten internationalen Zeitschrift *Current Biology* vorveröffentlicht wurde. Die ist im Text ausdrücklich gekennzeichnet. Folgende Publikationsliste füge ich hiermit bei:

**Bottesch M.**, Gerlach G., Halbach M., Bally A., Kingsford M. & Mouritsen H. (2016) "A magnetic compass that might help coral reef fish larvae return to their natal reef". *Current Biology* 26, 24 pR1266–R1267.

Des Weiteren erkläre ich hiermit gemäß § 11 Abs. 2 der Promotionsordnung der Fakultät V vom 21.03.2013, dass

(iii) die Dissertation weder in ihrer Gesamtheit noch in Teilen einer anderen wissenschaftlichen Hochschule zur Begutachtung in einem Promotionsverfahren vorliegt oder vorgelegen hat,

(iv) gegebenenfalls der Grad eines Doktors der Naturwissenschaften verliehen werden soll,

(v) die Leitlinien guter wissenschaftlicher Praxis an der Carl von Ossietzky Universität Oldenburg befolgt worden sind, und

(vi) im Zusammenhang mit dem Promotionsvorhaben keine kommerziellen Vermittlungs- oder Beratungsdienste (Promotionsberatung) in Anspruch genommen worden sind.

Meine Namensvorschläge für die Zweitgutachterinnen oder Zweitgutachter sind

- Prof. Dr. Michael Winklhofer,
- Prof. Dr. Gabriele Gerlach,
- Prof. Dr. Karl-Wilhelm Koch.

Oldenburg, den 18.02.2021

Michael Bottesch, Dipl.-Biol.